UNIVERSITY OF BIRMINGHAM

SUSPENDED SEDIMENT DYNAMICS DURING STORM EVENTS IN URBAN CATCHMENTS

(RIVER TAME: WEST MIDLANDS, UK)

by

ISAAC ALBERT AIDOO

A Thesis submitted to

The University of Birmingham

for the degree of

DOCTOR OF PHILOSOPHY

School of Geography, Earth and Environmental Sciences

The University of Birmingham

November 2014

Abstract

The study of urban catchment's suspended sediment dynamics during storm events was undertaken by using continuously monitored, high resolution turbidity, ammonia, rainfall and flow data from EA UK. Review of literature revealed that turbidity dynamics during storm events are not systematically characterised leading to gaps in our process understanding, with short time periods used and with most of them formed on single gauges in urban environments. The study thus aimed at contributing knowledge and novel methods to improve understanding with the specific objectives of characterising the events hydrologically, assessing them and their seasonal variability to examine their influence on the turbidity patterns, and also to evaluate the spatial scale effect on turbidity.

The event characterisation resulted in the development of novel, robust, universally adaptable quantification of hydrological events selection and classification criteria. These enabled events to be classified as single, double and multiple flow peaks, which revealed that the double and multiple flow peak events together constituted more than 40 and 60% of the total events for the respective studied smaller and larger sub-catchments. Thus, the analyses of only single events which hitherto were mostly the case, could have resulted in missing key dynamics involving these double and multiple flow peak events. While single and double peak events did not show any significant effect, multiple events showed significant increases in rate of change and availability of

turbidity as shown in the increased gradients and intercepts of the turbidity attributes-discharge and ammonia attributes regression lines. Events hysteresis analyses showed more anticlockwise than clockwise events in the studied catchment, a finding contrary to most published works of more clockwise events for rivers. A pattern of the number of anticlockwise events decreasing while the clockwise and coinciding events increased from single to multiple events was also observed. Also, more than a third of total events had more turbidity peaks than discharge peaks per event, a situation linked mostly with effluent spillage and was more frequent for higher intensity rain storms.

Seasonally, the peak, range, total time and rate of rise and recession of discharge, as well event time, ammonia peak and total, rainfall total and turbidity-discharge peaks lag times among others all showed significant effects on turbidity attributes mostly in summer and autumn. Out of these were inferred the significant effects of the catchment's high urban extent and effluent spillage mostly in summer and autumn. All seasons but spring with more anticlockwise than clockwise events were also associated with more low flows. Winter had the highest anticlockwise events, possibly because of its wider areal rain event extent, high number of low flows as well as more distal runoff sources.

The spatial scale study showed a flipping behaviour in event type distribution with more single events in the smaller and more multiple events in the larger catchments as well as in clockwise – anticlockwise events distribution with more anticlockwise in the smaller and more clockwise events in the larger catchment.

Acknowledgement

I thank my supervisors Prof. David Hannah and Dr. Nicholas Kettridge for their enormous support, guidance, motivation and immeasurable patience they offered me.

A big thank you also goes to the Environment Agency for the river flow, quality and rainfall data provided me, with a special one to Dr. Sarah Hainie for her prompt assistance.

My heart-felt appreciation is expressed for the immense assistance, motivation, advise, moral support and encouragement received from colleagues in the School of Geography and Environmental Sciences, especially from Room 325, both in the Water Sciences and Environmental Health Research Groups, and from elsewhere which all hugely contributed to how far I have reached.

I thank Ghana Government for sponsoring me through the Ghana Educational Trust Fund (GETFund), and to my institution Ho Polytechnic, Ghana, I say thank you for offering me the opportunity of study leave for further studies.

Last but not the least, I express my profound gratitude to my wife and children for the sacrifice, patience, spiritual and moral support offered and for their understanding for me to leave them alone for the studies.

Table of Contents

List of Figures

List of Tables

CHAPTER 1 INTRODUCTION

1.1 Chapter Introduction

Suspended sediment dynamics in urban rivers has a critical impact on human and aquatic life. Urbanisation leads to increase in population and building densities, which result in numerous associated environmental and hydrological impacts including deteriorated receiving water quality with the subsequent pollution control problems (Andjelkovic, 2001; Goodwin et al., 2003). Impacts of increased suspended sediment concentrations (SSC) include causing plants, invertebrates, and insects in the channel bed to be moved out of position, painful reaction in fish gills, death, blockage of gravel passages for spawning and reduce movement of light through water (Taylor and Owens, 2009). SSC also cause decline in quality of habitat and weakened biota strength (Collins et al., 2011b). Runoff increases and transports urban sediment, with trace and other contaminants attached, through streams into water bodies (Walling et al., 2003; De Carlo et al., 2004; Owens et al., 2005; Horowitz et al., 2007; Horowitz et al., 2008; Horowitz, 2009; Devereux et al., 2010; Horowitz et al., 2012). Increased flow leads to increased sediment transport, with time of transport affected by amount of stored sediment (Brakebill et al., 2010). The transport of sediment and its associated contaminants is an important pathway in the geochemical cycle, (Doomen et al., 2008).

Understanding key processes involved in headwaters' fine sediment delivery downstream is of high importance (Duvert et al., 2010). Worldwide, managers of land and water resources are extremely worried about two main environmental

challenges of increasing soil erosion rate and transport of fine sediment to rivers (Duvert et al., 2010). Delivery of fine sediment results in harsh effects downstream: channel bed sediment build-up can result in increased flooding, reduced reservoir storage, and reduced aquatic habitat quality through high turbidity and picking up of attached pollutants (Duvert et al., 2010). Such characteristics as slope and morphology make upstream catchments key sources for the preparation and supply of fine sediment to downstream catchments (Duvert et al., 2010). There is still a limited understanding of drivers of suspended sediment dynamics during rain events although there have been some studies in this field (Lawler et al., 2006; López-Tarazón et al., 2009). This is mainly due to technical difficulties that are associated with direct measurement of suspended sediment concentrations (SSC) and the calculation of accompanying sediment loads as often as needed (Lopez-Tarazon et al., 2009).

Turbidity, as a measured water optical characteristics, has been widely used for suspended sediment monitoring (Rasmussen et al., 2009). Surface water turbidity values are convincingly associated with suspended sediment concentration (SSC) and are found as cheap, successful pointer of SSC and water quality (Lewis, 2002; Rasmussen et al., 2009). Compared to discrete sample collection, SSC and sediment discharge values are obtained at the interval of water discharge measurements, irrespective of flow conditions (Gray and Gartner, 2009). River flow-sediment properties whose in-situ measurements are hard, risky and costly to undertake as often as needed, are done by using turbidity data to obtain enough characteristics of their spatio-

temporal changes (Gray et al., 2010). It usually makes it possible to nearly accurately measure and regularly check SSC and suspended sediment load (SSL) for different rivers with different flow-sediment characteristics continuously and even from distal sources (Gray et al., 2010). More information on a catchment's dynamics of suspended sediment can, therefore, be obtained through that of turbidity. However, the relationship between them is site and time specific and limited to specific catchments (Sun et al., 2001). Suspended and dissolved materials such as clay, silt, fine organic materials in the water, among others, drive turbidity (Rasmussen et al., 2009).

Suspended matter is the sediment (which, after filtration, is) retained on a standard filter with pore diameters of 0.45 μm, while dissolved matter (is that which) passes through the filter and respectively referred to as non-filterable and filterable matter (Bartram and Ballance, 1996; Chapman, 1996). Suspended sediment, the mineral component (mostly silt and clay) of the suspended solids, is the sediment found in water column carried by water movement. Suspended sediment concentration is the amount (weight in grammes or milligrammes) per unit volume of water (litres), of the non-filterable sediments retained on a standard filter after filtration of a given sample of total sediment (Bartram and Ballance, 1996; Chapman, 1996).

1.2 Aims

The study aims at outcomes to improve understanding of fluvial turbidity dynamics, controls and processes at smaller headwaters and bigger downstream sub-catchments of an urban river through individual and sequenced storm events.

1.3 Objectives

The specific objectives used to achieve the main aim above are:

1) To characterise events and examine their influence to unravel the interaction of factors influencing the turbidity dynamics

2) To assess inter- and intra-seasonal variability to identify their distribution and examine their influence on the turbidity patterns.

3) To evaluate the scale effect on turbidity dynamics by comparing the upstream and downstream sub-catchments.

4) To identify key controls, processes and drivers to help improve understanding of factors driving the turbidity dynamics in an urban catchment.

1.4 Thesis outline

The thesis comprises seven sections. Chapter 1 outlines the background of the research, aims and objectives. Chapter 2 reviews the research literature of previous studies. It provides information on drivers, controls, processes, temporal and spatial dynamics, various methods and the research gaps for this research. Chapter 3 outlines the research methodology adopted in the subsequent result chapters (4, 5 and 6). The methodology includes characterisation of event selection and classification criteria (event characterisation), study area description and maps, data acquisition and quantity, analytical techniques as well as some basic statistical analysis. Chapter 4 uses characterised events to explore their effect on the turbidity dynamics downstream an urban river. Chapter 5 explores the seasonality of these events downstream an urban river (event seasonality). Chapter 6

compares the urban river headwaters with the downstream sub-catchments to explore the inter-site variations of urban river turbidity dynamics responses to storm events (spatial scale effect). Hypotheses for Chapters 3 to 6 are outlined at the end of the literature background in each chapter. Chapter 7 provides the synthesis, conclusion and gives further research concerns.

CHAPTER 2 LITERATURE REVIEW

2.1 Significance of turbidity

A range of significant impacts of turbidity have been identified, specifically impacting river engineering and ecology. Some of these impacts are given in section 1.1, and highlight the relevance of this study. Engineering impacts include reduced navigability of rivers, infilling of dams and reservoirs (Collins et al., 2011b); increased water treatment cost (Landers, 2010; Collins et al., 2011a), reduced waterway values for flood-control, recreation, stream restoration and contaminated sediment removal (Landers, 2010), channel deposition, decline in channel gradient, shrinkage of river channel, impaired irrigation (Song et al., 2010) and disruption of commercial shipping and recreational boating (Brakebill et al., 2010). Ecological impacts include reduction in such biota and habitat quality as gill choking, blockage of gravel spawning spaces, deprivation of air and burial of fish eggs and larvae (Taylor and Owens, 2009; Collins et al., 2011a); loss of benthic aquatic habitat, changes in photosynthesis and visibility (Landers, 2010); degradation of commercial fisheries, submerged aquatic vegetation, blanketing of benthic organisms and direct effect on benthic communities (Brakebill et al., 2010).

The mobilisation and suspenion of fine sediment can lead to high turbidity, changes in biological and ecological processes of rivers (Schwarzenbach et al., 2010). In particular, the associated reduction in water clarity can limit the availability of photosynthetically active radiation, thus reducing in-stream primary production and associated benthic biota (Brakebill et al., 2010; Devereux et al., 2010). Suspended sediment is a major pollutant in many river

systems (Devereux et al., 2010). Reduced aquatic habitat and biota quality and sediment-attached pollutants result in direct and indirect water quality effects respectively (Goodwin et al., 2003). The environment can be altered by activities of man (Peters, 2009). Changes to surface of the land for industrial, urban and suburban development purposes have resulted in altered water routing and brought about alteration to natural processes (Peters, 2009). Such anthropogenic activities generate pollution which, through such various routes as point and non-point distribution sources, waste disposal and atmospheric deposition, finally gets into water bodies (Peters, 2009). An area's culture, economic and technological level as well as time influence the specific type of contaminants and their delivery mechanism (Peters, 2009). Furthermore, domestic and industrial waste that are discharged into urban rivers without being treated cause water quality challenges (Goodwin et al., 2003). Transport of these contaminants associated with river bottom sediments in small rivers is highly dynamic and exhibits fluctuations in concentrations that are of the same magnitude as for transport associated with suspended particles (Estrany et al., 2011).

2.2 Processes, controls and drivers

2.2.1 Processes and controls

Temporal and spatial variability of turbidity-discharge (Tu-Q) relationships are often high (Carter et al., 2006; Lefrançois et al., 2007; Viglione et al., 2010) for the same river, and depicts variable sediment origins or availability (Lefrançois et al., 2007). The high variability inferred from high scatter in the relationship between turbidity-discharge, could suggest other factors influencing suspended

sediment transport (Hudson, 2003), such as in-channel exhaustion or difference in sediment availability (Rovira and Batalla, 2006), catchment area and flashy flow (Ferrier, 2001). Also, high inter-event variability in turbidity can exist in a catchment due to complex interactions between the sediment production and transport control factors that can be both manmade and natural (Zabaleta et al., 2007).

The nature of turbidity in river systems is often dependent on discharge or energy conditions (Wood, 1977; Ferrier, 2001; Seeger et al., 2004; BaČA, 2008; Duvert et al., 2010; Bizzi and Lerner, 2012), in particular flow velocity exerts a strong control on sediment transport (Seeger et al., 2004). In addition to discharge, seasonality affects concentration (Ferrier, 2001), such that seasons could be regarded as an additional control on turbidity dynamics (Goodwin et al., 2003). Besides discharge, varying sediment source depletion and nourishment influence turbidity, especially through the quantity from upstream sources (Doomen et al., 2008). Upstream areas are mostly considered key sources and contributors of fine sediment preparation and transport to catchments downstream (Duvert et al., 2010). In larger catchments, timing of suspended sediment contributions from various tributaries influence downstream turbidity levels (Doomen et al., 2008), notably, the length of time between successive events, and the time of year (Wood, 1977).

The sediment transport regime of large catchments depends on the sediment quantity the catchment receives, the capability and efficiency of the catchment to transport this material, and the amount of deposition along the river (Asselman et al., 2003). Sediment delivery, availability and exhaustion all

influence rates of sediment transport (BaČA, 2008). Sediment availability is a function of both the sediment already deposited in and that currently supplied to a channel or catchment (Lefrançois et al., 2007), and is high when rain storm events or rainy seasons start and/or after a long time without any sufficient rains (Rovira and Batalla, 2006). The total suspended sediment transported within an event depends on the discharge magnitude, duration and the time position relative to other events (Rovira and Batalla, 2006). Flow peaks with similar magnitude for successive events in series could have varying turbidity accompanying them, sometimes with the secondary flow peaks having reduced turbidity values (Rovira and Batalla, 2006). This shows that in single or multi-peaked events, available sediment for transport could be depleted with time (Rovira and Batalla, 2006). Time in-between events provides the opportunity for bio-physical activities to replenish and increase sediment availability as well (BaČA, 2008).

At the seasonal scale, two phases are used to describe variability of suspended sediment. The first phase, sediment preparation and transfer, is when sediment transfer downstream is less, but sediment is made available in the catchment. The second phase, sediment exhaustion, is when most suspended sediment is transported (Rovira and Batalla, 2006). Seasonal dynamics of sediment availability is evident in being highest and lowest during low and high flow periods respectively (Lefrançois et al., 2007). Availability of sediment and ability of river to transport it, among other factors, determine turbidity (Lefrançois et al., 2007). For the same discharge, turbidity changes with sediment availability (Lefrançois et al., 2007). The ability of a river to transport sediment increases

with increased flow, but if there is low sediment available, then turbidity may decrease. Also, decreased discharge decreases the stream transport capacity, but turbidity may increase if availability of sediment increases (Lefrançois et al., 2007). These phenomena are referred to as supply-limited and transport-limited sediment dynamics respectively (Holden, 2005). As readily available transportable sediment partly determines fine suspended sediment (wash load) transport and deposition, changes in soil erosion that could be caused by climatic change may subsequently affect sediment transport and floodplain deposition rates (Asselman et al., 2003).

Sediment replenishing is mostly through storage or deposition processes. Not all but just a small portion of carried upstream sediment actually reaches the catchment outlet, because of local deposition of sediment within catchment and channel (Cammeraat, 2002; Goodwin et al., 2003; Estrany et al., 2011). Sediment storage or deposition is promoted, among such other factors as low gradient and growing vegetation within the channel (Estrany et al., 2011), by low or decreased discharge, especially during discharge recession (Jansson, 2002; Lefrançois et al., 2007; BaČA, 2008; Estrany et al., 2011; Hupp et al., 2013). Also, the amount of sediment deposition depends not only on the amount of sediment supplied from the drainage basin, but also on its grain size composition, with the coarser sediment contributing the most to the deposition (Xu, 2008). The occurrence of lead and simultaneous peaking events could confirm evidence of temporary in-channel sediment storage, while increased flows could stand in the way of local, in-channel sediment settling (Duvert et al., 2010). In-channel sediment could be picked up and quickly re-deposited in the

upstream reaches due to low energy from low flow and transmission losses (Estrany et al., 2011). However, high energy downstream resulting from tributary contributions and large storm flows could lower sediment deposition (Estrany et al., 2011).

Sediment exhaustion is mostly through flushing of eroded or re-suspended (re-mobilised) processes, mostly under high discharge conditions (Jansson, 2002; BaČA, 2008; Bizzi and Lerner, 2012). Sediment is flushed downstream mostly because influent flows could dominate, increasing the runoff energy (Estrany et al., 2011). Flushing of the drainage system and catchment surfaces in the early stages of runoff from rain events generally leads to high turbidity on the hydrograph's rising limb and, thus, a clockwise hysteresis (de Boer and Campbell, 1989; Hudson, 2003; Lim, 2003; Stubblefield et al., 2007). The cause of this could be the large fine-grained sediment quantities available at the beginning of rainy event/season which can rapidly be transported to the channel resulting in sediment depletion or exhaustion (Jansson, 2002; Goodwin et al., 2003; Hudson, 2003; Lefrançois et al., 2007; Doomen et al., 2008; Smith and Dragovich, 2009). However, if storms occur in close succession, a decrease in concentration due to the exhaustion of sources from prior storms can be observed (Lim, 2003; Rovira and Batalla, 2006). Thus, the key driver of clockwise hysteresis (sediment flushing and depletion), can occur at the diurnal, intra-seasonal (i.e. between successive events), seasonal and decadal time-scales. Intra-seasonal flushing is an indication of sediment exhaustion, where decreasing turbidity response for equivalent discharge events are observed as

each season progressed (Hudson, 2003; Stubblefield et al., 2007; Doomen et al., 2008; Minella et al., 2008).

2.2.2 Drivers

The drivers of turbidity dynamics can be defined and classified differently based on the context. For example, "*any phenomenon that may change the time-averaged state of a flooding system is referred to as a driver*" (Hall et al., 2003), with such typologies as driver sets and source or pathway or receptor drivers used to classify them (Hall et al., 2003; Lane and Thorne, 2004). Catchment runoff in urban environments is controlled by both meteorological drivers, for example rainfall (quantity and spatial distribution), source, and land use patterns, for example urbanisation (imperviousness and storm water drainage systems) (Hall et al., 2003). Fluvial processes represent another driver set, with river morphology and sediment supply as a driver-pathway, dictating storage and conveyance (Hall et al., 2003) to produce marked changes in the volume and timing of delivery of flood water to the drainage network. In small to intermediate scale catchments, basin morphology can control the magnitude and frequency of high flows, and thus influence the supply of sediment from headwater streams as a result of the sensitivity of sediment yield to land management (Lane and Thorne, 2004). Land use change and degradation has been identified as a key control on turbidity dynamics (Ferrier, 2001; Edwards and Withers, 2008; Duvert et al., 2010) with the urbanisation index (Ferrier, 2001; Hall et al., 2003; Edwards and Withers, 2008) and point source pollution (Stanfield and Jackson, 2011). Numerous other factors can influence the quantity, timing and composition of turbidity ranging from hydrological alteration,

hydrological budgets, microbial activity and physical abrasion (Wenger et al., 2009), rain events, snowmelt, winter wash-off and biofilm breakup (Lawler et al., 2006), channel slope and stream power (Bizzi and Lerner, 2012) and acidification (Ferrier, 2001). Examples of microorganisms that influence turbidity and suspended sediment include *E. coli* and faecal coliforms (Bejankiwar, 2009; Huey and Meyer, 2010; Nagy et al., 2012; Goransson et al., 2013). These microorganisms are transported at higher concentrations during storm runoff events (Huey and Meyer, 2010), periods normally associated with high turbidity (Goransson et al., 2013), and are higher for catchments with greater impervious cover (Chelsea Nagy et al., 2012). Increasing urbanisation, measured by impervious cover, increases microbial activity up to a certain level of urban impact (Wenger et al., 2009).

Stream turbidity or runoff mechanisms are controlled by rainfall properties, such as rainfall quantity (Seeger et al., 2004; Zabaleta et al., 2007), frequency (Wood, 1977), storm duration (Wood, 1977; Vivoni et al., 2007) and intensity (Vivoni et al., 2007; Zabaleta et al., 2007). Deposition is prominent in river sediment transport for low flow events, while for high flow events, it is controlled by the erosion or re-mobilisation process (Gao and Puckett, 2012). Smaller events could show storms changing widely spatially and temporally within the catchment (Smith and Dragovich, 2009). Larger scale response to smaller events could be having prevailing influence mainly from contribution of discharge and sediment from smaller areas within the catchment and could be modified by main channel effects, (transmission losses and tributary inputs magnitude and timing), before reaching the catchment outlet (Smith and

Dragovich, 2009). Bigger widespread rain events, mostly in winter, generally display minimal spatial-temporal variability, hence, similar processes operate in smaller tributary catchments simultaneously, with larger catchment response an enlarged scale of similar contributions from tributaries (Smith and Dragovich, 2009). Smaller catchment response to high-magnitude localised storm events, mostly in summer, could have flow large enough for its reduced quantity to get to the bigger basin outlet maintaining a similar pattern (Smith and Dragovich, 2009).

Variety of sources of sediment, fast rate of runoff due to high imperviousness, efficient routing and storage in tanks together complicate an urban system (Goodwin et al., 2003). The situation is made more complex in a catchment by the presence of such works as sewage treatment works (STW) or flood by-pass structures (Goodwin et al., 2003). Water quality is more liable to change due to urban development influence than hydrological or geomorphological influences (Gurnell et al., 2007). Urbanisation leads to changes in land use, water consumption patterns, waste and stormwater flow patterns and associated pollutant loadings (Rose, 2003), all of which can have an impact on the aquatic life in the receiving rivers (Astaraie-Imani et al., 2012). Such products of urban development as impervious surfaces and runoff drainage network construction lead to changes in a catchment's hydrology, sediment and discharge regimes (Gurnell et al., 2007). Surface compaction and imperviousness resulting in increased runoff, as well as efficient runoff routing are some causes of river discharge regime changes (Gurnell et al., 2007). River discharge regime changes relating to urban development is also associated with sediment

delivery and transport changes, with bed and bank erosion being a key sediment source for natural, un-engineered channels (Gurnell et al., 2007).

The impacts of urban imperviousness (i.e. the urban creep) on hydrological systems include high volume rainfall causing more runoff with increasing imperviousness (Gurnell et al., 2007; Astaraie-Imani et al., 2012), decreased lag time between precipitation and peak flow, increased flooding occurrences, hydrograph shape variations such as increased flow peak and reduced peaking time, and decrease in baseflow or low flow discharge due to reduced contributions from ground water (Rose, 2003; Gurnell et al., 2007).

Contaminants from runoff and wastewater (non-point and point sources respectively) influence quality of stream sediment and water (Gurnell et al., 2007). Significant variations in stream properties emanate from the efficient runoff routing as a result of extensive stream channel engineering (Gurnell et al., 2007). Urban suspended sediment, among others, with attached pollutants from surfaces, industrial and domestic waste sources could pose water quality challenges in receiving water bodies into which they are discharged, in some situations (Goodwin et al., 2003). Combined sewer overflows (CSOs) are designed for the discharge of untreated sewage and runoff into water bodies from combined sewer systems (CSSs) when their design capacities are exceeded in periods of large rain events (Goodwin et al., 2003; Estrany et al., 2011). This discharge could at times contain increased levels of fine sediment and organic matter (Goodwin et al., 2003; Estrany et al., 2011). The increased runoff causes CSOs and storm tank overflows which, in turn, lead to the deteriorating river water quality (Astaraie-Imani et al., 2012). Foul sewage and

storm runoff from impervious surfaces including roads lead to increased levels of metals such as lead (Pb) found in CSOs in receiving water bodies (Estrany et al., 2011). Untreated sewage and storm runoff are nowadays carried by separate sewer systems in modern designs although most urban cities still have combined sewer networks (Goodwin et al., 2003). However, water bodies receive effluent from both combined and separate sewer networks through a lot of surface water drains (Goodwin et al., 2003).

2.3 Methods

Although many suspended sediment studies exist, only few have used automated monitoring station data to describe pattern of suspended sediment concentration (Pavanelli and Pagliarani, 2002; Beck, 2005; Lawler, 2005; Lawler et al., 2006; Huang et al., 2007; Duvert et al., 2010). Automatic monitoring of high-resolution data is key for tracking transient and extreme changes in variables, whose characteristics cannot be accounted for by the use of manual, low-resolution monitoring (Lawler et al., 2006). Low-resolution data miss completely some significant details, and substantially underestimates the mean, range, variability and trend of the actual response (Lawler, 2005). High-resolution SSC data measured separately from flow data are needed for the determination of precise river sediment loads in situations where suspended sediment transport is regulated by sediment supply variations upstream (Topping et al., 2007). This high resolution data set allows for the development of insight into key drivers in a catchment's sediment transport (Goodwin et al., 2003). Despite the significance, few studies have used high resolution data.

Few studies in urban catchments have quantified turbidity across multiple events. Turbidity time-series have been used to compute a variety of constituent concentrations that correlate well with SSC, which in turn have been used to compute loads of those constituents (Lawler et al., 2006; Massei et al., 2006; Gray and Gartner, 2009; Rasmussen et al., 2009; Duvert et al., 2010; Gray et al., 2010; Landers and Sturm, 2013). Turbidity is widely used for suspended sediment monitoring (Sun et al., 2001), and described to be the most appropriate proxy technology that can be employed everywhere to estimate SSC (Landers and Sturm, 2013). It has been shown to be a reliable indicator of total suspended solids and such microbial organisms (of size < 0.45 µm) as *Escherichia coli*, *Enterococci* spp., *Cryptosporidium* spp. and *Giardia duodenalis*, and studies have identified variability with land use and river hydrology (Huey and Meyer, 2010). In most cases, river turbidity correlates well with its suspended sediment (Rasmussen et al., 2009); with robust, well recognised correlation seen as cheap but useful signal for SSC and water quality (Lewis, 2002). Continuous SSC-turbidity records have been produced in some studies (Minella et al., 2008), leading to relationships having R^2 (coefficient of determination) values ranging from 0.593 (Choy, 2004) through 0.978 (Gray et al., 2010). R^2, the coefficient of determination, is the proportion of variation in a dependent variable explained by an independent variable. For James Bridge monitoring station on River Tame, SSC-turbidity relationship gave R^2=0.6654 (Lawler et al., 2006). Changes in composition and size of particles as well as the colour of the water can confuse SSC-turbidity relationships, a situation which can negate the advantages of using turbidity measurement to

minimise challenges related to sequential suspended sediment measurement (Gippel, 1995). Water colour impact on turbidity is mostly less than 10% (Gippel, 1995). Although the catchment-specific nature of SSC-turbidity relationships make river suspended particle composition less variable within than between catchments, some discrepancies could be introduced into the relationship by in-storm changes in suspended particle composition (Gippel, 1995). The influence of changes in particle size, that can occur during rain events, on changes in SSC-turbidity relationships may not be excessive except that SSC and particle size are not connected (Gippel, 1995). More often, sufficient correlation in field-measured SSC-turbidity should usually result (Gippel, 1995). However, due to the resolution of limited sampling challenges, the utmost source of error in sediment load calculation, through uninterrupted measurement of SSC, some discrepancies must be permitted (Gippel, 1995). Turbidity-discharge relationships often exhibit hysteresis effects that can be used to classify events, to interpret geomorphological processes, to give the main points regarding the areal spreading of sediment sources or investigate scale effect of sediment transport processes. Further details of each of these are provided below:

(1) Classifying events based on:

A) Rotational pattern of loops as clockwise, anticlockwise, coinciding or simultaneous peaks, figure of eight (F8) and complex loops (Figure 2.1 to Figure 2.3).

B) Trend as positive, negative and null/neutral.

C) Curvature as concave and convex.

D) Combination of curvature and rotational pattern as C3 whose loops are concave and their rotation clockwise and A3 – whose loops are concave and their rotation anti-clockwise.

E) A combination of trend and rotational pattern as loops which are clockwise and at the same time with generally positive and negative trends, explaining the processes of flushing and dilution respectively.

F) Relative peak occurrence as lead – turbidity peak leading discharge peak, lag – turbidity peak lagging discharge peak and co – turbidity and discharge peaking together (Evans and Davies, 1998; Jansson, 2002; Goodwin et al., 2003; Rose, 2003; Seeger et al., 2004; Gao and Pasternack, 2007; Lefrançois et al., 2007; Stubblefield et al., 2007; Doomen et al., 2008; Moravcova et al., 2009; Smith and Dragovich, 2009; Duvert et al., 2010).

(2) Interpreting catchment geomorphic processes.

A) Lead events are caused by (i) remobilisation and transport of in-channel deposited sediments (Walling et al., 1997; Jansson, 2002; Bowes et al., 2005; Gao and Pasternack, 2007; Smith and Dragovich, 2009; Duvert et al., 2010) whose availability is restricted during the event (Lefrançois et al., 2007). (ii) Sediment flushing/entrainment of temporarily stored in-channel sediments and subsequent exhaustion/depletion during rainfall-runoff events (Goodwin et al., 2003; Hudson, 2003; Lefrançois et al., 2007; Stubblefield et al., 2007; BaČA, 2008; Doomen et al., 2008; Duvert et al., 2010). (iii) Reduction in precipitation associated erosion (Smith and Dragovich, 2009).

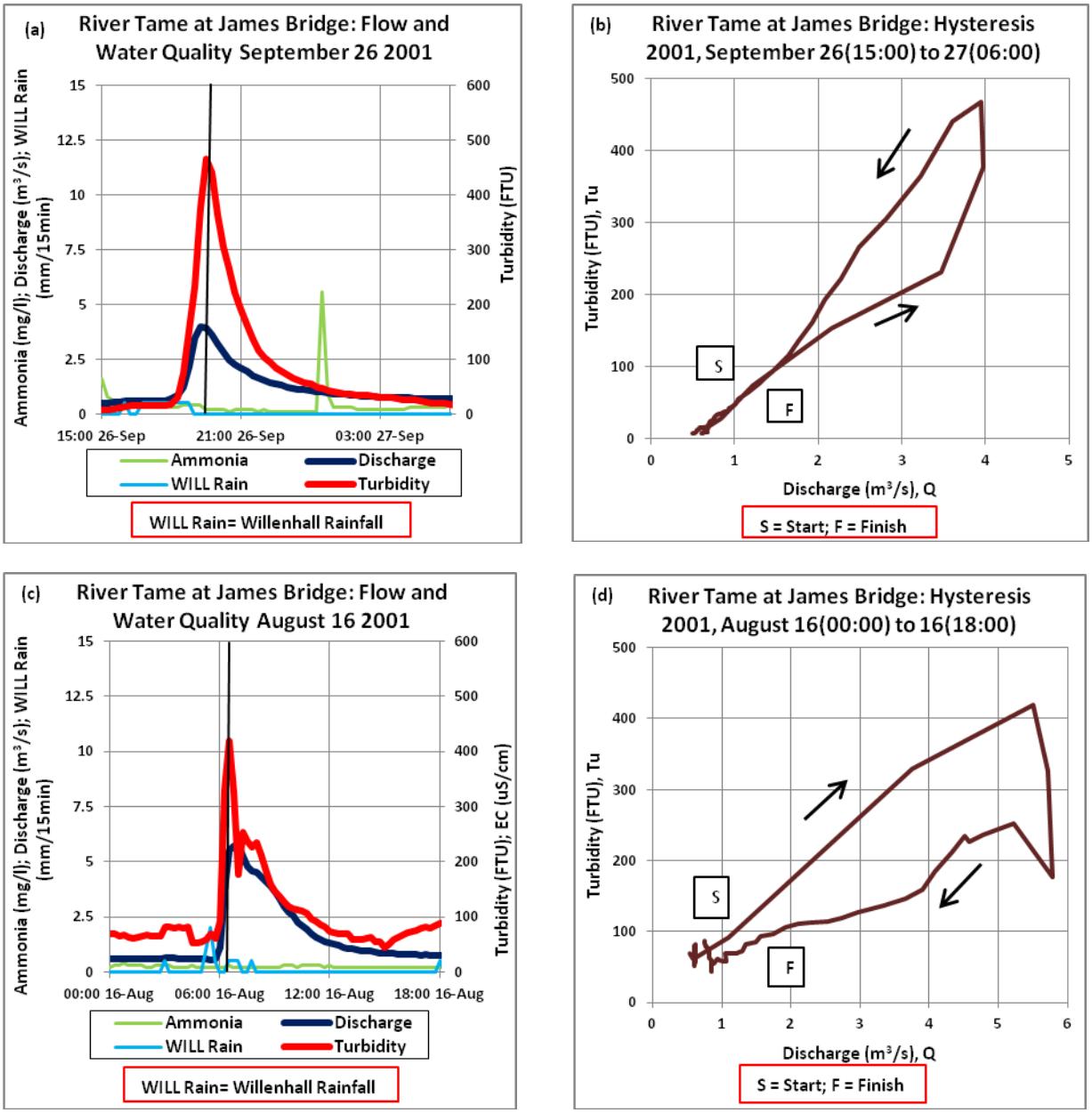

Figure 2.1: Times Series and corresponding Q – Tu hysteresis loops for events on: 26 September 2001 showing (a) turbidity peak lagging discharge peak, (b) anticlockwise loop; 16 August 2001 showing (c) turbidity peak leading discharge peak, (d) clockwise loop. Solid vertical line passes through turbidity peak.

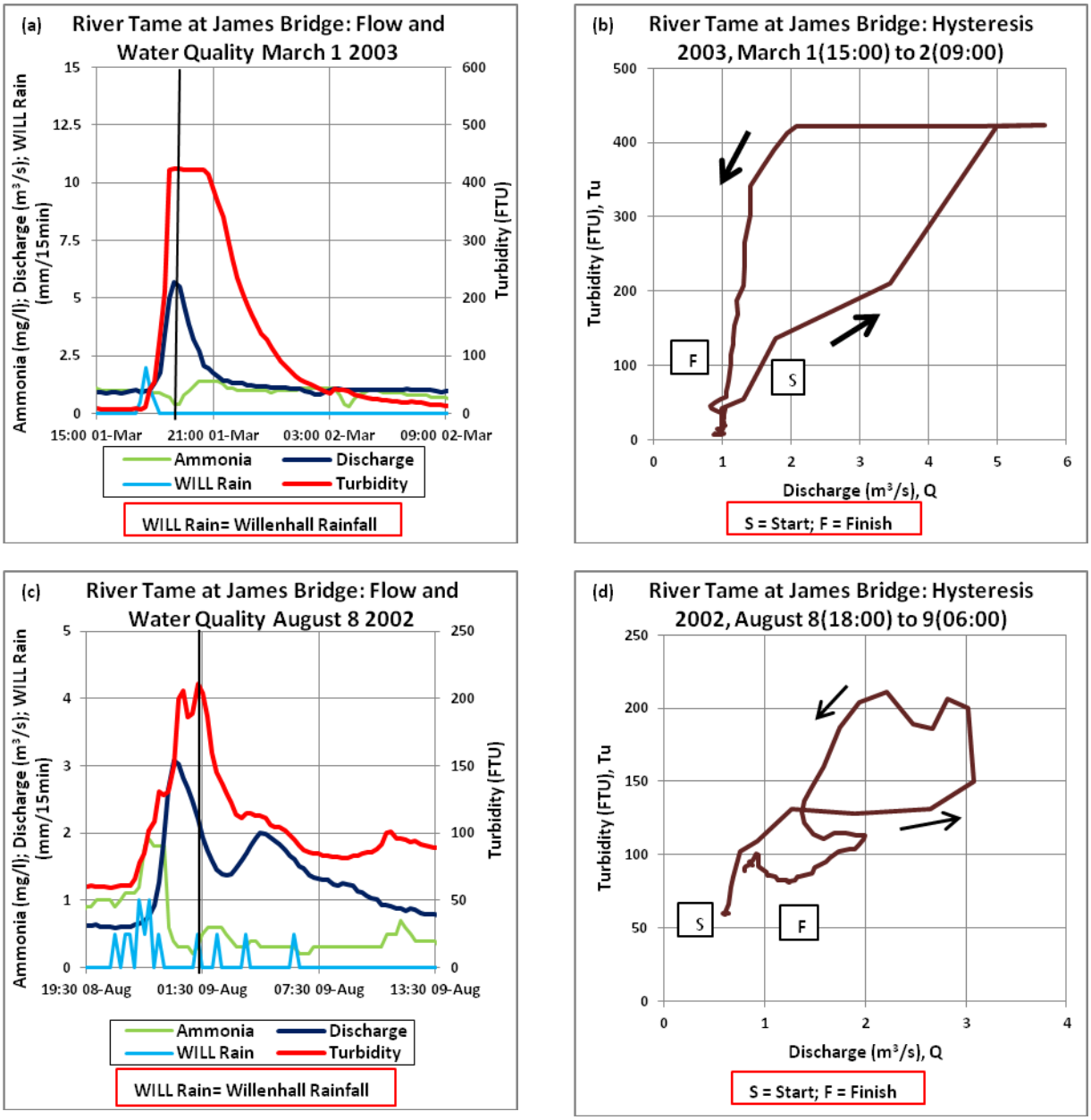

Figure 2.2: Times Series and corresponding Q – Tu hysteresis loops for events on: 1 March 2003 showing (a) discharge and turbidity peaks coinciding, (b) anticlockwise loop; 8 August 2002 showing (c) turbidity peak lagging discharge peak, (d) figure-of-eight (F8) loop. Solid vertical line passes through turbidity peak.

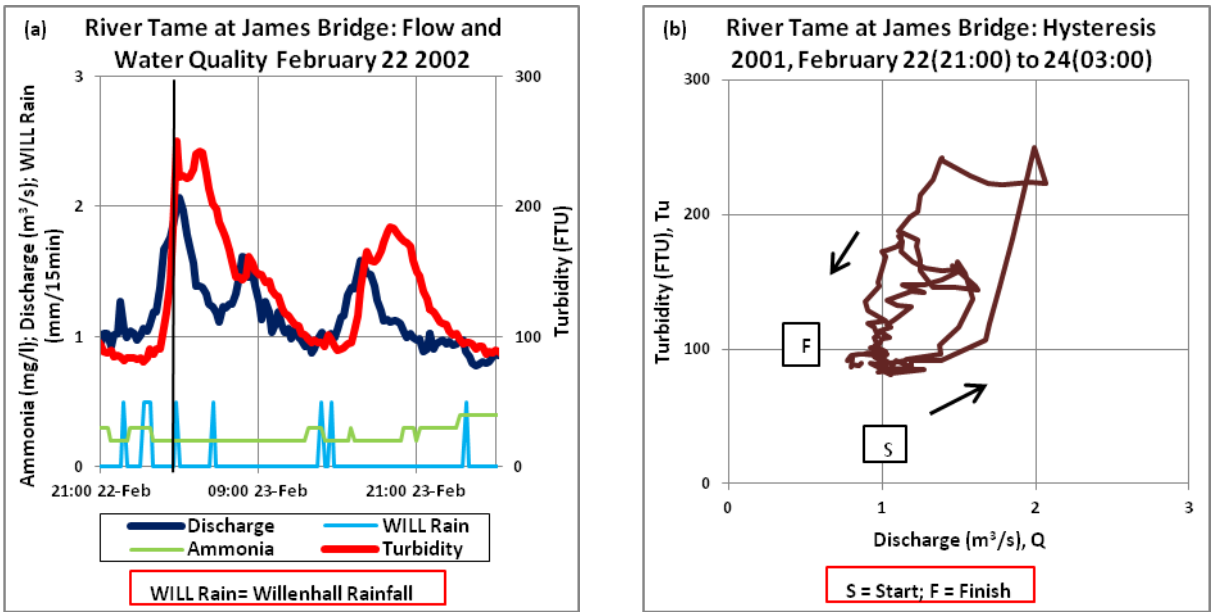

*Figure 2.3: Times Series and corresponding Q – Tu hysteresis loops for events on: 14 November 2002 showing (a) turbidity peak leading discharge peak, (b) complex loop***.** Solid vertical line passes through turbidity peak.

(iv) Dilution with increased base flow during recession or less contaminated flow from downstream or tributaries (Jansson, 2002; Rose, 2003; Lawler et al., 2006; Rovira and Batalla, 2006).

B) Lag events are caused by: (i) Absence of in-channel sediment delivery (Duvert et al., 2010); (ii) Late arrival of external sediment sources due to sediment peaks lagging flow peaks resulting from their different times of travel (Smith and Dragovich, 2009; Duvert et al., 2010) (iii) Biofilm break-up resulting in sediment peak lagging flow peak because the stored sediment is let out late (Lawler et al., 2006; Smith and Dragovich, 2009). (iv) Fine sediment eroded from headwaters or distal sources travelling a long

distance without temporary deposition, or storm runoff providing extra sediment (Asselman et al., 2003; Gao and Pasternack, 2007; Moravcova et al., 2009). (v) Less sediment for transport and lower rate of change in position in channel than in flow (Gao and Pasternack, 2007).

C) Coinciding peaks can be due to a variety of processes (i) Transport (Jansson, 2002) or (ii) re-suspension/entrainment of in-channel sediments (Hudson, 2003).

D) Clockwise with positive trend are caused by flushing during which increasing flow is associated with increasing concentration (Moravcova et al., 2009).

E) Clockwise with negative trend are caused by dilution during which concentration decreases with increasing flow (Moravcova et al., 2009).

(3) Outlining the spatial distribution of sediment sources (Jansson, 2002; Duvert et al., 2010) such as:

A. Distal: upland or upstream or headwaters, tributary input

B. Proximal: In-channel deposits, channel banks and areas close to channel

(4) Investigating the effect of spatial scale (Hudson, 2003).

A. Clockwise/first flush events are often associated with larger catchments.

B. Anticlockwise/anti-first flush events are often associated with smaller catchments.

Turbidity has been found to be related with variables like flow peak, sediment load, initial moisture levels and rainfall intensity (Duvert et al., 2010; Helmreich

et al., 2010). Hence, many studies have used linear regression models to estimate turbidity for a range of such purposes as to:

(1) Describe variability in turbidity conditions. (2) Evaluate turbidity relative to water-quality criteria and water-resource management goals. (3) Compare the turbidity among watersheds. (4) Compute turbidity and stream flow data in riverine systems to estimate SSL delivery to reservoirs. (5) Compute turbidity to study channel morphology and basic process analysis of sediment sources. In addition, (6) Continuous, time-series turbidity data are used to identify sources and timing of sediment transport more accurately than on the basis of periodic sample collection. (7) Computed daily, monthly, seasonal, and annual SSL can be used to assess differences in fluvial-sediment characteristics between basins as a function of hydrologic conditions, contributing drainage area, land use, sediment sources, and human activity (Rasmussen et al., 2009).

2.4 Research gaps

The above review has led to the identification of the following research gaps which form the focus of the result chapters 4 to 6.

1. Turbidity dynamics in storm events are not systematically characterised in the research literature leading to gaps in our process understanding.

Single hydrological events have principally been used to determine turbidity dynamics (Goodwin et al., 2003; Lefrançois et al., 2007; Smith and Dragovich, 2009; Duvert et al., 2010; Stanfield and Jackson, 2011; Gao and Puckett, 2012). These studies described in section 4.2 have different definitions for events. These could result in varying event-based analysis with different event

start/end times, classification and event response dynamics, which in turn could result in less detailed analysis of catchment processes, controls and drivers. Few studies mention multiple discharge peak events. Those that do visually identified them when distinct troughs were observed during continuous rainfall (Smith and Dragovich, 2009). Analysing only single events could possibly be missing key dynamics involving the multiple flow peak events which are mostly not analysed because they are deemed complex (Lefrançois et al., 2007; Moravcova et al., 2009; Talei et al., 2010).

2. Most studies of storm events turbidity dynamics have formed on short time periods (days or weeks); therefore, there is the need to explore seasonal and inter-annual patterns and processes.

Seasonality of the relative contributions of the various nutrient and suspended sediment sources exists (Edwards and Withers, 2008), its variations determining the quantity and quality of water parameters (Yunus and Nakagoshi, 2004) and seasonal assessment of hydrologic responses gives more detailed information regarding erosion, transport and deposition processes (Hannaford and Buys, 2012). Although urbanisation causes increased concentrations of suspended sediment-related constituents such as turbidity with increasing stream flow (Peters, 2009), few studies of urban catchments exist, mostly concentrating on short time periods and for few events. Dry seasons' point source contaminants concentrations increase due to low flow resulting from low rainfall and runoff (Yunus and Nakagoshi, 2004). Discharge as well as associated determinants/attributes changes seasonally. In urbanised basins, wet season runoff increases pollution from diffuse sources.

Previous studies indicated that urban land-use had strong linear relationships with water quality due to point and non-point source pollution (Yunus and Nakagoshi, 2004). Some of these statements could only be ascertained through study of events seasonality.

3. Previous studies have generally focused on single gauges in urban environments; hence, there is a need to assess the importance of space-time patterns of event dynamics.

Scale issue is important in hydrological processes to unravel the dominant processes controlling hydrological response in different catchments (Gao and Puckett, 2012), with runoff generation distribution significantly influenced by catchment scale (Vivoni et al., 2007). Although it is necessary to study the dynamic change of patterns of urban rivers at varying scales of time and space (Yue, 2012) due to the fact that their implicit understanding are fundamental to geomorphology, problems of scale transference are generally overlooked (de Boer and Campbell, 1989), with only few works in this area concentrating on a few variables at a time or at one temporal or spatial scale or in non – urban rivers. Higher scatter and flashier flows are mostly associated with smaller catchment area (Ferrier, 2001). Spatial scale effect can lead to noticeable flow-suspended sediment hysteresis with SSC peak leading or lagging flow peak (Hudson, 2003). In smaller drainage areas, SSC mostly portrays increased responsiveness to proximal sources, but their more homogeneous precipitation can give room for a simpler rainfall, runoff and erosion forces data explanation (Duvert et al., 2010). Sediment concentration would lag discharge peak by an increasing amount with scale if the source of the sediment is located in the most

distal portions of the basin (Hudson, 2003). It is thus important for spatial scale studies to verify some of these research statements.

4. There is a paucity of understanding regarding the key controls, drivers and processes that determine space-time patterns in storm event turbidity dynamics in urban river catchments.

Stream turbidity or runoff mechanisms are controlled by rainfall properties, such as rainfall quantity (Seeger et al., 2004; Zabaleta et al., 2007), frequency (Wood, 1977), storm duration (Wood, 1977; Vivoni et al., 2007) and intensity (Vivoni et al., 2007; Zabaleta et al., 2007). Variety of sources of sediment, fast rate of runoff due to high imperviousness, efficient routing and storage in tanks together complicate an urban system (Goodwin et al., 2003). The situation is made more complex in a catchment by the presence of such works as sewage treatment works (STW) or flood by-pass structures (Goodwin et al., 2003). The nature of turbidity in river systems is often dependent on discharge or energy conditions (Wood, 1977; Ferrier, 2001; Seeger et al., 2004; BaČA, 2008; Duvert et al., 2010; Bizzi and Lerner, 2012), with flow velocity in particular exerting a strong control on sediment transport (Seeger et al., 2004). In addition to discharge, seasonality affects concentration (Ferrier, 2001), such that seasons could be regarded as an additional control on turbidity dynamics (Goodwin et al., 2003). Besides discharge, varying sediment source depletion and nourishment influence turbidity, especially through the quantity from upstream sources. Upstream areas are considered key sources for the preparation and supply of fine sediment to downstream catchments (Duvert et al., 2010). These

and many others could only be explained through such studies to enhance understanding.

2.5 Chapter summary

The significance of general sediment and particularly suspended sediment studies, regarding engineering, ecological and recreation impact, and their relations with anthropogenic activities, mostly in urban environments, has been outlined. The general processes, controls and drivers regarding suspended sediment dynamics, indicating various factors involved, are also discussed. Various methods used in this field have been described. Finally this review has identified a number of research gaps to be addressed in subsequent chapters, and will improve our understanding of processes and controls on SS dynamics in a highly urbanised catchment.

CHAPTER 3 PROJECT METHODOLOGY

3.1 Chapter Introduction

This chapter outlines the methods of data collection and analysis. The overall structure of the thesis is outlined (section 3.2) and the study area characterised (section 3.3). The development of a methodology to systematically identify and characterise turbidity events is subsequently developed (sections 3.4-3.8).

3.2 Overview of research design

The key controls, processes and drivers of urban turbidity dynamics are derived through the assessment of discharge, suspended sediment and ammonia gauge station measurements within the UK's most urbanised catchment. A new approach for systematically analysing and classifying storm events is developed. The approach assesses all events; classical, text book storm events are mostly hand-picked (Lawler et al., 2006). Such idealised events may represent a small portion of storms, with system drivers showing a systematic departure from more complex events that are more representative of catchment hydrological behaviour. The urban catchment which forms the basis for this research is outlined within this chapter, and the systematic storm event classification and quantification procedure defined. This measurement approach is implemented to inform our understanding of catchment dynamics within Chapters 4, 5 and 6. Derivation of the primary controls on urban storm water turbidity dynamics are derived in Chapter 4, assessing whether there is a systematic departure in the functioning of these controls, processes and drivers between different hydrological events which vary in their temporal complexity.

The seasonal variability in the storm water turbidity dynamics are examined within Chapter 5, to evaluate the impact of antecedent conditions on system function, to interrogate the primary processes controlling empirical relationships derived within Chapter 4. The knowledge and understanding derived from Chapters 4 and 5 are applied within Chapter 6 to assess the scalability of such process understanding. Using a novel nested catchment approach, storm events are tracked through the catchment, enabling their attributes to be tracked through space and time. The findings from this research are subsequently synthesised and concluded within Chapter 7. The bases of these chapters are the objectives outlined within Chapter 1 and the research gaps identified through review of relevant studies (Chapter 2). Figure 3.1 shows the research processes in relation to the structure of the thesis.

3.3 Study area

The River Tame catchment provides the focus of this study (Figure 3.2). This catchment was chosen for the study because of its large urban cover needed for the urban context. It covered the smaller headwaters James Bridge and the larger, downstream Water Orton catchments, both needed for the spatial scale effect studies. In other words, the spatial scale effect (smaller, larger), sub-catchments (headwaters, downstream) as well as urban activities associated with, among others, some anthropogenic effects (imperviousness, storm runoff and effluent spillage) were some of the reasons for selecting the River Tame catchment.

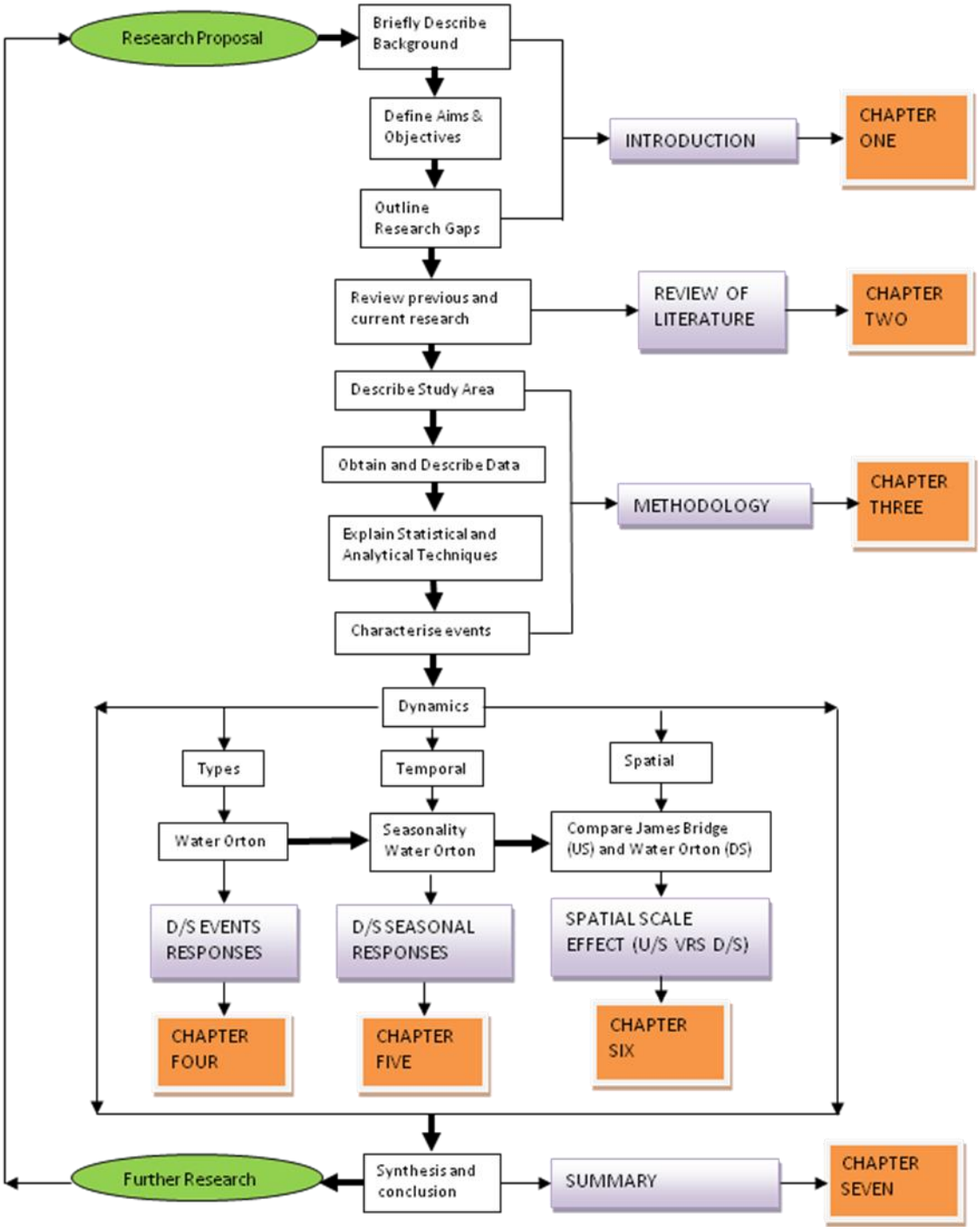

Figure 3.1: Research process parts in relation with the structure of thesis; U/S,D/S = upstream, downstream.

The land cover map for the catchment showing the percentage compositions of the various land uses indicate the following. In addition to the 59.2% urban extent, mountainous, shrubby uncultivated land and marshy ground together make up 0.1%. Also, woodland, arable/horticultural land and grassland make up 4.8%, 3.1% and 13.4% respectively (Figure 3.4) (CEH, 2012). This means vegetation cover in the Water Orton catchment is more than 21%. Figure 3.7 and Figure 3.8 are images of longer and shorter stretches respectively of this downstream catchment. In addition to its meandering nature, it confirms the vegetation cover stated above and seen in Figure 3.9 and Figure 3.10, and also show other urban land uses. Figure 3.9 show the weir at the Water Orton gauging site viewed from its (a) downstream and, (b) upstream ends.

The catchment, with a total area of 1400km^2 (Crabtree et al., 1999), efficiently drains the West Midlands containing Birmingham, UK's second largest city, displaying a relatively flashy hydrograph. It is noted as a catchment which reacts quickly to rain event and having its flow greatly affected by large amount of wastewater discharged into it (Marsh and Hannaford, 2008), producing stream velocities that are exceptionally increased during rain events that they impose ecological challenges (Lawler et al., 2006). Once noted for its fishing, its history has reflected the fast industrial and urban development of West Midlands that included the modification of much of the river channel through such engineering structures as Gabion bank support (Webster et al., 2001; Ellis et al., 2007).

Table 3.1: Catchment characteristics

	Tame	James Bridge	Water Orton
Area (m^2)	1400	57	408
CSOs number	374		
Base flow index			0.61
Urban cover (%)			59.2
Grass-farm-woodland (%)			21.3
Station level (m AOD)		113.3	74.4
Tributaries number		3 (smaller)	7 (4 larger and 3 smaller)
Mean annual rainfall (mm)			725 (1961 - 1990)
Mean annual flow (m^3)			5.39
Peak flow - record (m^3)			128.33 (2006/7)
Peak flow - measured (m^3)		14.7	70.39
Peak flow rank			36
WwTW number		1	4

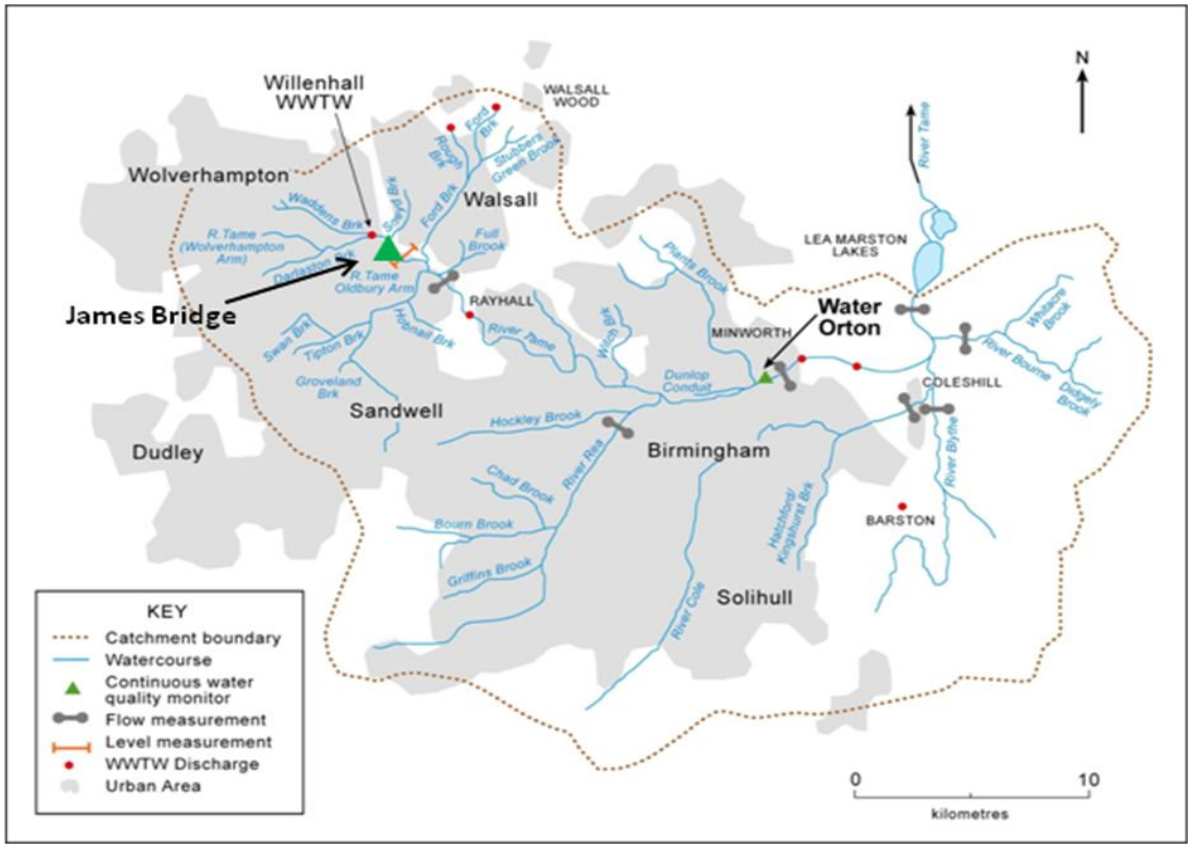

Figure 3.2: River Tame catchment showing the James Bridge and Water Orton monitoring stations

.

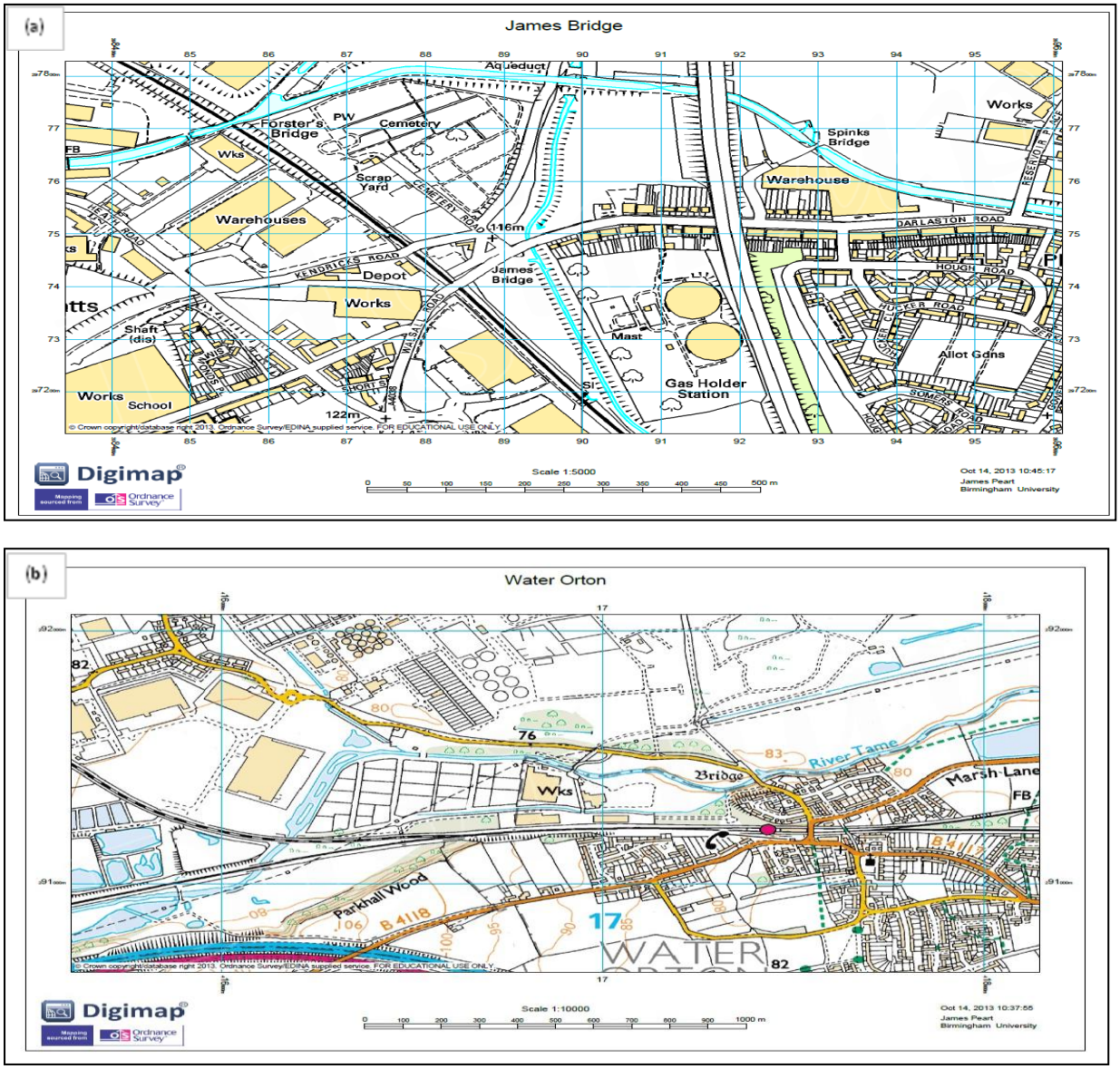

Figure 3.3: The locations of the (a) James Bridge (Easting – 9891; Northing – 9751, and (b) Water Orton (Easting – 1695; Northing - 9150) monitoring stations.

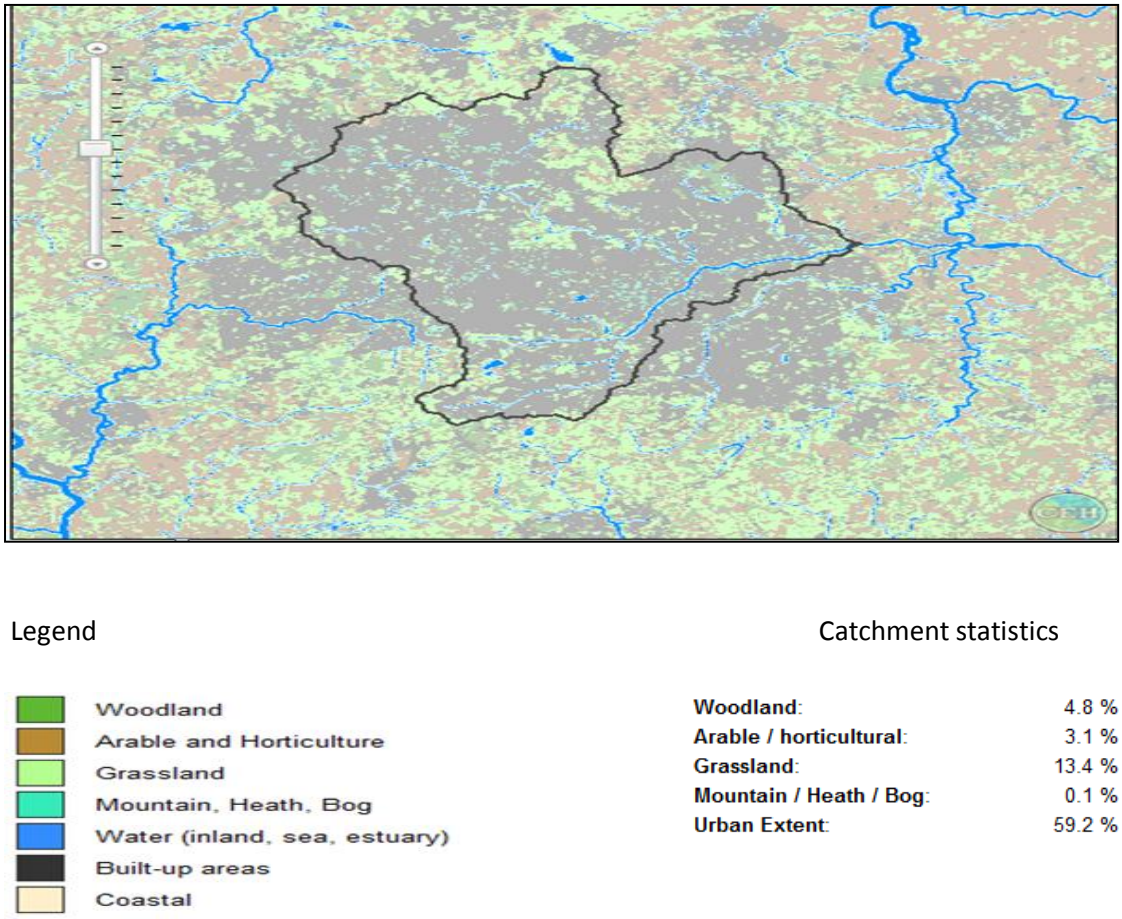

Figure 3.4: Tame catchment land cover map. Source: CEH

The annual rainfall in the River Tame catchment is 650-800mm and its river is 8-12m wide and 0.2-2m deep, and consists both of modified and natural stretches with natural settling of sediment in the channel bed. The headwaters James Bridge catchment could likely be associated with the narrow and deep sections with the broad and shallow sections relating to the downstream Water Orton catchment. The headwaters zones of rivers are noted for their steep

slopes, low number and length of tributaries (Table 3.1), straight and narrow v-shaped valleys (Figure 3.5 and Figure 3.6) and coarser bed channel materials (Gordon et al., 2013). The lowland zones of rivers are also noted for their low slopes (Table 3.1), wide and meandering sections (Figure 3.7 to Figure 3.10), shallow sections, finer channel bed materials and sediment deposition (Gordon et al., 2013).

Substantial wastewater effluent enters the river (Rivett et al., 2011). Severn Trent Water Ltd undertook a programme to improve the standards of River Tame and tributaries between the years 2000 to 2010. According to this programme, there are Combined Sewer Overflows (CSOs) which relieve sewerage systems of increased hydraulic pressure during heavy rains (Tame, 2010). 92 out of 374 CSOs found in the catchment were put under Unsatisfactory Intermittent Discharges (UIDs) which had adverse environmental effects on the receiving water body (Salt, 2009) and which needed to be improved (Tame, 2010).

The Water Orton which is less than 30km downstream the smaller James Bridge headwater sub-catchment, covers a bigger sub-catchment of the River Tame. The catchment has an area of 408km^2 (Marsh and Hannaford, 2008; CEH, 2012), accounting for approximately one third of the total of the River Tame. The catchment and the location of the monitoring stations utilised within this study are shown in Figure 3.2 and Figure 3.3.

Figure 3.5: Image of a stretch of River Tame at James Bridge

Figure 3.6: Image of River Tame crossing the Walsall Road at James Bridge

Figure 3.7: Image of a longer stretch of River Tame at Water Orton

Figure 3.8: Image of a shorter stretch of River Tame at Water Orton

The catchment is almost fully urbanised (Figure 3.4), of moderate relief and solid geology. It has a base flow index of 0.62, mean annual rainfall, runoff, loss of 743mm, 427mm, 316mm respectively, mean and peak flow of 5.49m^3/s and 128.3m^3/s respectively (Marsh and Hannaford, 2008; CEH, 2012). The Water Orton monitoring station is just upstream of Minworth Sewage Treatment Works (STW). In addition to the Willenhall Wastewater Treatment Works (WwTW) upstream James Bridge monitoring station, there are three others upstream Water Orton, two of which drain into Ford Brook, a tributary of River Tame and the other one at Rayhall on the main river stem (Figure 3.2).

The James Bridge catchment is a sub-catchment of the Water Orton. It has an area of 57km^2 and an average altitude of 113.3m A.O.D. The Black Country urban area is the source of the Wolverhampton branch (Rivett et al., 2011), which flows through James Bridge gauging station with Darlaston, Waddens and Sneyd Brooks as tributaries (Figure 3.2). The Bescot station which is 2km downside the James Bridge station has mean annual rainfall, flow (mean and peak) of 712mm, 2.32 and 56.8m^3s^{-1} respectively (Marsh and Hannaford, 2008; CEH, 2012). A major WwTW (Wastewater Treatment Works) is upstream the James Bridge station at Willenhall and three additional WwTWs before Water Orton (Figure 3.2). Table 3.1 is a summary of some basic characteristics for the two studied sub-catchments.

Figure 3.9: The weir of River Tame at Water Orton viewed from (a) downstream end, (b) upstream end and also showing some curved reach.

Figure 3.10: River Tame at Water Orton showing (a) straight and (b) curved reaches.

3.4 Data quantity and quality

Hydrologic parameters (flow and rainfall) and water quality parameters (turbidity and ammonia) were examined. The lack of continuous SSC data necessitated the use of turbidity data for this study, due to the established robust relationships between them. Continuous SSC-turbidity records have been produced in some studies (Minella et al., 2008), leading to relationships having R^2 values ranging from 0.59 (Choy, 2004) through 0.98 (Gray et al., 2010), such as 0.76 (Lenhart et al., 2010), 0.811 (Sun et al., 2001), 0.846 (Choubey, 1992), and 0.93 (Gray and Gartner, 2009). More often, sufficient correlation in field-measured SSC-turbidity usually result (Gippel, 1995).

Automated monitoring high-resolution 15-minutes data were used because they enable the tracking of transient and extreme changes in variables (Lawler et al., 2006), allows knowledge about major catchment sediment transport controls to be presented in stages (Goodwin et al., 2003) and also ensure accurate determination of sediment loads in rivers where changes in the upstream sediment supply regulates the transport of suspended sediment (Topping et al., 2007). The UK Environment Agency (EA) river flow and automatic water quality monitoring and rain gauge stations were the sources for the flow, turbidity, ammonia and rainfall data used. They covered the period from 1 March 2001 to 29 February 2004 (36 continuous months; 12 continuous seasons) for the Water Orton monitoring station. All the data are high resolution 15-minute and instantaneous type for all parameters except rainfall, which is total. The rainfall data measurements were conducted from Frankley rainfall intensity station (UK National Grid Reference SP, [Easting 72, and Northing 8015]) which lies

approximately 20 km upstream of Water Orton, with Tipping Bucket. The other data were obtained from the UK National Grid Reference SP, [Easting 1695, Northing 9150 for turbidity and ammonia, and Easting 1694, Northing 9146 for flow] ("Environment Agency information © Environment Agency and database right"). Elevation (in meters-m) of Frankley and Water Orton are about ~185 and 74 respectively (Google, 2013).

Data for the James Bridge monitoring stations covered the period from 15 March 2001 to 30 November 2003 (33 continuous months; 11 continuous seasons) due to unavailability of quality turbidity data. The rainfall data measurements were conducted from Willenhall tipping bucket rainfall intensity station (UK National Grid Reference SO, [Easting 9786, and Northing 9826]) which lies about 1.5 km upstream of James Bridge. The other data were obtained from the UK National Grid Reference SO, [Easting 9891, Northing 9751 for turbidity and ammonia, and Easting 9892, Northing 9750 for flow] (Environment Agency information © Environment Agency and database right). Elevations of Willenhall and James Bridge are ~140 and 113 m, respectively (Google, 2013). The parameters used were measured by means of automatic continuous monitoring at 15-minutes resolution. Turbidity, discharge and ammonia were recorded as instantaneous measurements.

Formazin Turbidity Unit (FTU), the most commonly used units for turbidity measurement, are associated with absorptiometric methods which use spectrophotometric equipment (Papoutsa and Hadjimitsis, 2013). The method which has formazin as standardisation solution, is used for both scientific and industrial purposes mainly because it combines neutral buoyancy with constant

particle size (Wass et al., 1997), and also because, for a known concentration, they are homogeneous and repeatable (Susfalk et al., 2008). These absorptiometric turbidimeters which are used for water data, use in-situ spectrophotometric equipment calibrated to measure, from a known light source, the transmittance and reflectance, attenuation or loss in its intensity (Bilotta and Brazier, 2008; O'Toole and Diamond, 2008; Liu et al., 2009). These known light sources include light emitting diodes (LEDs) which have such merits as longer lifetime, lower cost and power consumption, smaller sizes, higher brightness among others, over the other sources with breadth of spectral range of 247-1550 nm commercially available (O'Toole and Diamond, 2008). Photodetectors commonly used with LEDs include phototransmitters (PTs), photodiodes (PDs), Light Dependent Resistors (LDRs) and photodiodes arrays. LED and LDR used as source and detector respectively, arranged such that they were in the same plane at 45^{o} with respect to the water surface at an angle of 90^{o} between them is reported (O'Toole and Diamond, 2008). Also reported is a light source of 860 nm wavelength and having a spectral bandwidth of 60 nm, with detector orientation measurement angle of 90^{o}+/-2.5^{o} using formazin polymers as primary standards (Ziegler, 2002). Dilution is permitted in the use of absorptiometric turbidimeters, with the equipment having an aperture angle of 20^{o}-30^{o} and a path length of less than 10 cm. It is calibrated to suit suspended fine silt and smaller size particles (Ziegler, 2002), which could be indicative of turbidity as well as associated constituents (Landers and Sturm, 2013). Commonly used photodetectors coupled with LEDs in such configurations as probe photometers are the PDs, with such merits over the others as extreme

versatility, rapid response and wide linear range (O'Toole and Diamond, 2008). The use of blue LED as a spectroscopic source and PD as a detector using a fibre optic across an optical path and an inlet/outlet in a transducer cell arrangement (40 mm wide and 15 mm high) is reported (O'Toole and Diamond, 2008).

In the study, measurement of turbidity was carried out with a pHOX750M absorptiometric turbidity head (Phoenix Instrumentation Ltd.) connected to an in-line probe within a facility from a 50-mm gap using a visible red LED light source in the instrument, connected to an automatic data acquisition system. The instrument was automatically cleaned 5 times per hour and manually cleaned once a week. Weekly inspections for zero drift and monthly calibrations of endpoint were carried out, using deionised water and 500-FTU (Formazin Turbidity Units) standard turbidity liquid (Lawler et al., 2006).

Data, and the associated storm events, were excluded when turbidity or ammonia values exceeded their maximum levels of detection by the instrumentation (turbidity and ammonia greater than 500FTU and 20mgl^{-1} respectively). Anomalous data, e.g. turbidity values changing over an infinitesimally small time without corresponding changes in flow and/or rainfall values were inspected and discarded.

Data gaps of three or more hours in length were also discarded, whilst data gaps less than three hours were linearly interpolated. The following explains the linear interpolation method of filling data gaps. In an excel row, for example row number 2, data before a gap, the data gap and data after the gap for the variable with gap(s) (e.g. turbidity) are imputed in the first three columns A, B

and C such that the cells A2, B2 and C2 represent data before a gap, the data gap and data after the gap respectively. The next three cells D2, E2, and F2 represent the corresponding data for the variable without gap(s) (e.g. discharge). The missing value in cell B2 is determined using equation (2) which is derived from equation (1) on the bases of simple ratio and proportion.

$$(B2-A2)/(C2-A2) = (E2-D2)/(F2-D2). \quad (1)$$

$$B2 = [(E2-D2)/(F2-D2)*(C2-A2)+A2]. \quad (2)$$

The same principle is used whether the gap is for a single or multiple missing values.

Linear drifts in turbidity were evident throughout and were corrected. Such drifts were assumed to result from the build up of material on the optical sensors that was not adequately removed by the automatic cleaning processes. Figure 3.11(a) is an example of time series showing a drift in turbidity data after the 18th April 2001; the measured turbidity increasing with time. This drift is indicated by the solid purple line. The magnitude of the drift was quantified from regression analysis and subtracted from the storm event. Periods impacted by the storm event with turbidity values above those of base flow conditions were first identified and excluded from the data set Figure 3.11(b)). The linear increase in turbidity with time was calculated for the remaining data through linear regression and subtracted from the entire data set. Figure 3.11(c) is the final time series showing reduced turbidity data after correction. The following explains how the drifts were corrected. The average base turbidity value before the drift was identified as 25 FTU for the example given here. Turbidity values

before and after the drift impact were used to establish a line of best fit with the equation:

y=0.0442x+59.022

This equation was applied to quantify the magnitudes of the drift which were subtracted from turbidity values with the drift. The average base turbidity value before the drift was then added to the resulting differences to obtain the corrected turbidity values.

Ammonia threshold of 2 mg/l (Chapman, 1996), has been used for analysis as a surrogate for pollution from point (WwTWs, STWs and CSOs) and/or non-point (e.g. fertilizer runoff) sources. Turbidity as a source of urban river impairment resulting from suspended sediment and nutrients such as ammonia has been reported (Carpenter et al., 2002). The EA stations are equipped with the Hach NH_4D SC Ammonium Sensor, a multi-parameter probe, which is capable of taking continuous data, with a response time of less than 2 minutes and could measure data in the range of 0.2-1000 mg/l (HACH, 2008). The measuring method uses ion-selective electrodes (ISEs) for ammonium (to detect ammonium ions (NH_4^+) directly as ammonium nitrogen (NH_4-N)) and potassium (to compensate for potential potassium ions (K+) interference), together with a differential pH reference electrode and temperature sensor (for pH and temperature effects) (YSI Inc., 2015; HACH, 2008). Ammonia in water consists of un-ionised ammonia and ammonium ion, relative portions of both of which are highly affected by pH, with their equilibrium also affected by temperature (YSI Inc., 2015).

3.5 Event selection criteria

This section aims at characterising the events by developing criteria for event selection by defining events on the basis of response size threshold, start and end time quantitatively. Hitherto, events were mostly defined qualitatively as those whose hydrographs consist both of the rising and falling limbs (Smith and Dragovich, 2009), which is required to be single-peaked as much as possible to enable the direction of rotation to be defined (Evans and Davies, 1998), with the limits of events defined by minimum discharge between peaks (Zabaleta et al., 2007). It is hypothesised that events could be quantitatively defined and selected.

An event is defined here as a clear observable response in flow to a rain event. From the assessment of 47 events, picked randomly by visual inspection, a threshold discharge of 2.6m^3/s and threshold rate of change in discharge of 0.04m^3/s/h were defined as the event selection criteria. Box and whiskers plots used to help establish the above given thresholds are shown (Figure 3.12).

The event starts where there is a clear rise in either flow or turbidity, whichever comes first. This is defined as the first ≥1% increase per 15 minute in discharge or turbidity after the onset of rainfall, where turbidity or discharge increases progressively afterwards. If discharge or turbidity remains constant or declines after the first exceedance of the 1% threshold, the next ≥1% increase is assessed. An example of the initial event selection criteria are presented within Table 3.2.

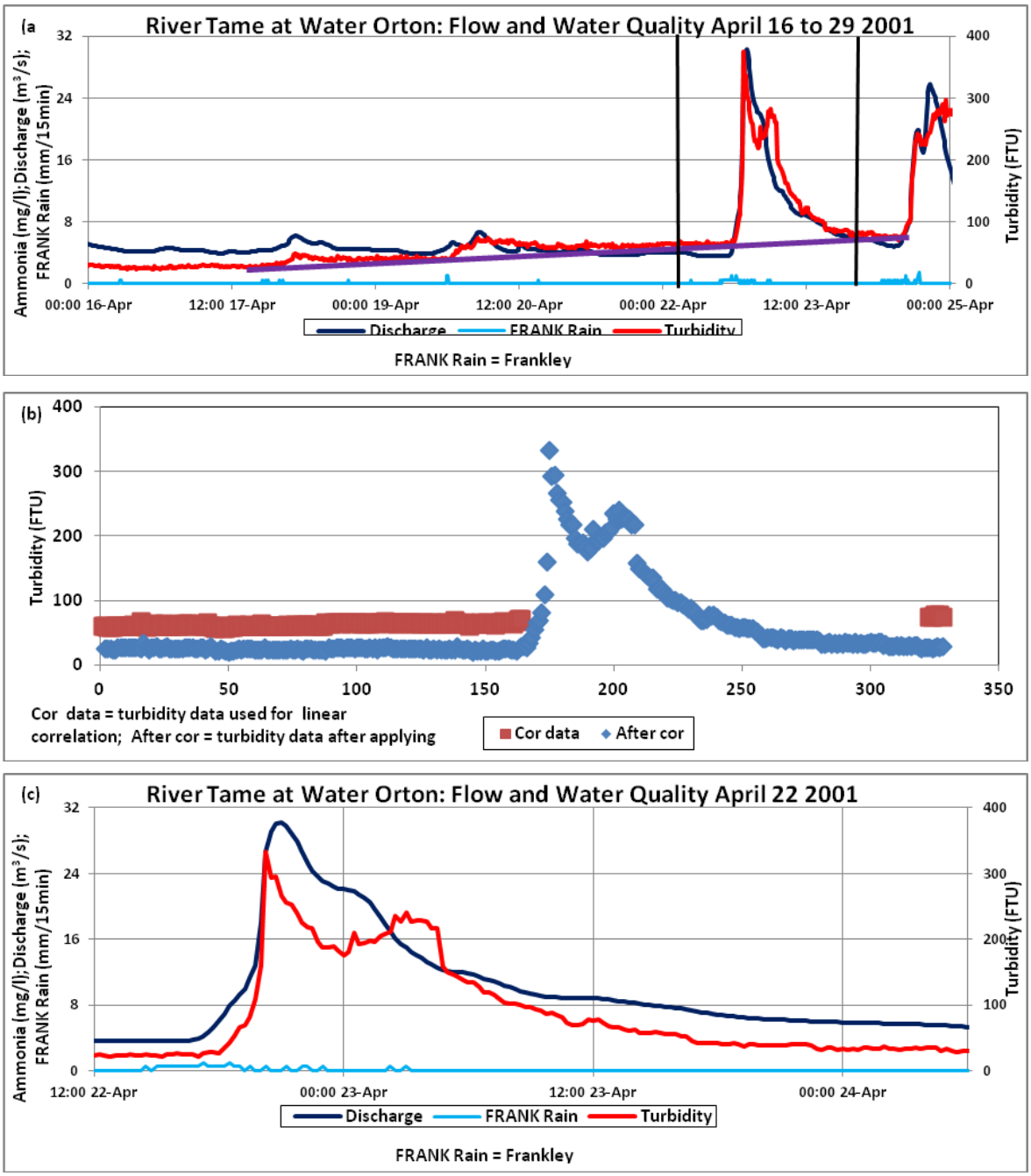

Figure 3.11:(a) time series showing a drift in turbidity data after 18 April as shown by the purple line; (b) turbidity data during correlation; (c) final time series showing turbidity data after correcting drift

The initial rainfall is presented in green. The orange colour indicates the first exceedance of the ≥1% threshold in turbidity and discharge. The event start time is indicated in light blue, representing the first exceedance of the discharge or turbidity threshold. In this example, flow is the first to exceed the threshold, with a discharge of 3.51m^3/s occurring at 12:30. Table 3.3 is an example of how event start time is determined for those in which the first exceedance of ≥1% increase is immediately followed by constant change. The first exceedance of the 1% threshold occurs in the turbidity (indicated in yellow). The increase to 41FTU is followed by another rise to 42FTU, after which the turbidity remains constant. A progressive increase is thus not observed. The next ≥1% increase indicated in orange is taken as the event start time (43FTU occurring at 09:30).

The end of an event should capture the falling limb of both flow and turbidity. Ideally, discharge and turbidity should both recede to their values at the start of the event. However, this is not always achieved either due to a) a longer term increase in turbidity/discharge onto which the storm event is superimposed or b) the onset of an additional storm event before the recession is complete. Therefore, the end of an event is defined as:

1. The point on the falling limb, where both flow and turbidity values are equal or less than that at the event start.
2. If 1 is not achieved, where both falling limb minimum flow and turbidity differ by ≤30% with respect to the equivalent values at event start point on rising limb.

For example, Figure 3.13(a) shows the April 6 2001 event. The horizontal black line passes through event start time with a discharge value of 9.9m^3s^{-1},

intersecting the falling limb at approximately 06:00 on the 7th April. During this time the turbidity increased from 71 FTU at the event start, to its peak value of 430 FTU, before returning to a value of 173 FTU (144% above its start values). Thus the event continues until the turbidity intersects its initial start value which occurs at approximately 12:00 on the 7th April. Figure 3.13(b) also gives an example of the end of an event at the beginning of the next event. The solid vertical line is the end of the 6 April 2001 event as well as the beginning of the 7th April 2001 event. At this time, a rain event has already started, which results in a flow response qualifying it to be a separate event. The above methods developed allowed for the quantitative events definition and selection.

3.6 Classifying events

Multiple flow peaks have previously been defined visually from event hydrographs (Smith and Dragovich, 2009). These are indicated in multi rise events between which there are distinct troughs observed with continuing rainfall. This section aims to classify the storm events identified above quantitatively. It is hypothesised that events could be quantitatively classified. Identified events are classified as either a single peak, double peak or multiple peak events.

1. A single peak event consists of a single flow peak (e.g. Figure 3.13(a)). Single peak events mostly result from a single, but could also result from multiple rainfall events.

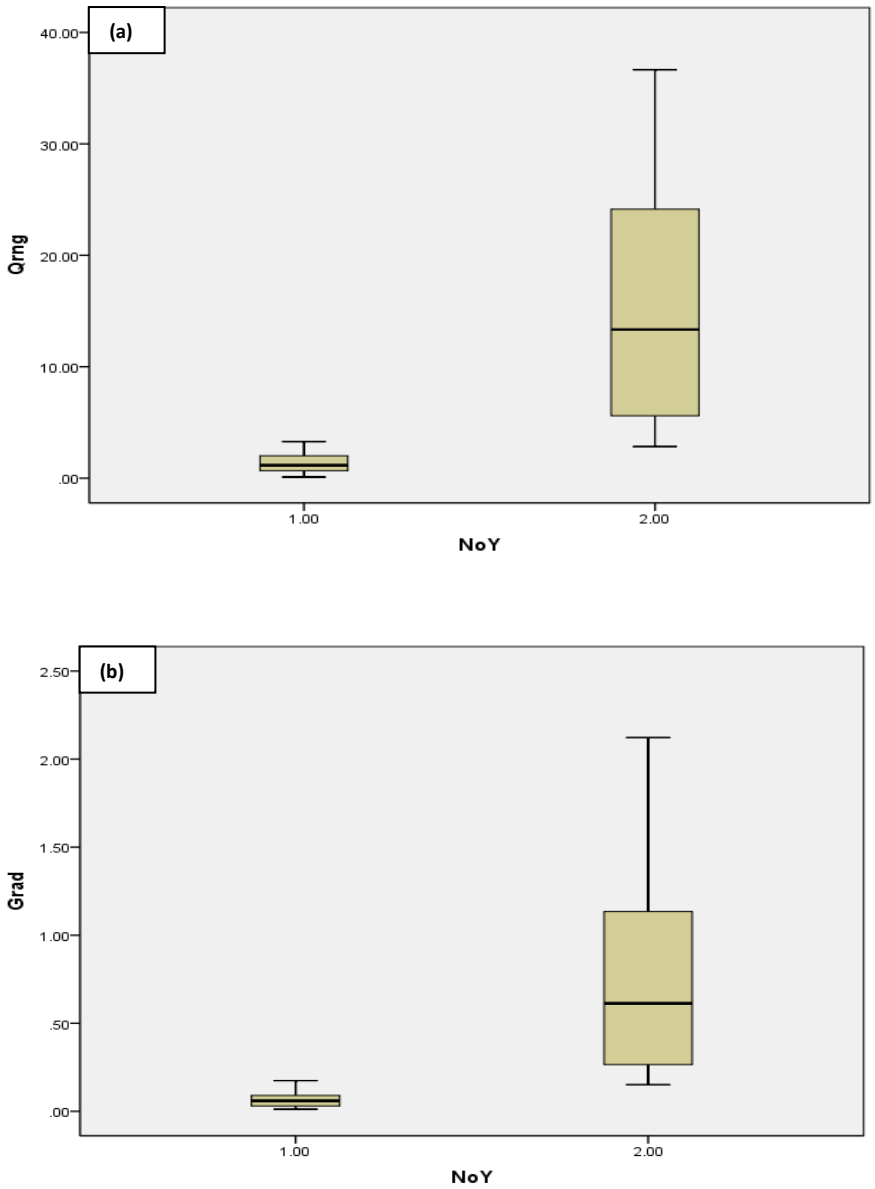

Figure 3.12: Box and whiskers plots for randomly selected low (1) and high (2) flows for (a) range and (b) gradient used for events thresholds.

Table 3.2: Determining event start time for 5 March 2003 event. Orange-First value exceeding the previous value by ≥1%, after which there is a progressive increase in the values; Light blue-Event start time. Green indicates the initial start of rainfall.

			Flow			Turbidity			
Date	**Time**	**Rainfall**	**Value**	**Change**	**% Change**	**Value**	**Change**	**% Change**	**Description**
05/03/2003	05:30	0	3.62	0	0.00	41	-2	-4.65	
05/03/2003	05:45	0.5	3.62	0	0.00	46	5	12.20	**Rain start**
05/03/2003	06:00	0	3.62	0	0.00	43	-3	-6.52	
05/03/2003	06:15	0	3.60	-0.02	-0.55	41	-2	-4.65	
05/03/2003	06:30	0	3.59	-0.01	-0.28	41	0	0.00	
05/03/2003	06:45	0	3.57	-0.02	-0.56	42	1	2.44	
05/03/2003	07:00	0	3.56	-0.01	-0.28	42	0	0.00	
05/03/2003	07:15	0.5	3.54	-0.02	-0.56	40	-2	-4.76	
05/03/2003	07:30	0	3.52	-0.02	-0.56	40	0	0.00	
05/03/2003	07:45	0	3.52	0	0.00	43	3	7.50	
05/03/2003	08:00	0	3.49	-0.03	-0.85	38	-5	-11.63	
05/03/2003	08:15	0.5	3.49	0	0.00	40	2	5.26	
05/03/2003	08:30	0	3.46	-0.03	-0.86	40	0	0.00	
05/03/2003	08:45	0	3.45	-0.01	-0.29	39	-1	-2.50	
05/03/2003	09:00	0	3.45	0	0.00	38	-1	-2.56	
05/03/2003	09:15	0	3.43	-0.02	-0.58	40	2	5.26	
05/03/2003	09:30	0	3.42	-0.01	-0.29	38	-2	-5.00	
05/03/2003	09:45	0	3.42	0	0.00	40	2	5.26	
05/03/2003	10:00	0	3.40	-0.02	-0.58	38	-2	-5.00	
05/03/2003	10:15	0	3.38	-0.02	-0.59	40	2	5.26	
05/03/2003	10:30	0	3.38	0	0.00	40	0	0.00	
05/03/2003	10:45	0	3.38	0	0.00	38	-2	-5.00	
05/03/2003	11:00	0	3.40	0.02	0.59	40	2	5.26	
05/03/2003	11:15	0.5	3.40	0	0.00	39	-1	-2.50	
05/03/2003	11:30	0	3.40	0	0.00	38	-1	-2.56	
05/03/2003	11:45	0.5	3.42	0.02	0.59	44	6	15.79	
05/03/2003	12:00	0	3.43	0.01	0.29	40	-4	-9.09	
05/03/2003	12:15	0	3.45	0.02	0.58	43	3	7.50	
05/03/2003	12:30	0	3.51	0.06	**1.74**	40	-3	-6.98	**>1% increase in discharge and event start**
05/03/2003	12:45	0	3.54	0.03	0.85	38	-2	-5.00	
05/03/2003	13:00	0.5	3.60	0.06	1.69	41	3	7.89	**>1% increase in turbidity**
05/03/2003	13:15	0	3.68	0.08	2.22	42	1	2.44	
05/03/2003	13:30	0	3.73	0.05	1.36	43	1	2.38	
05/03/2003	13:45	0	3.78	0.05	1.34	45	2	4.65	
05/03/2003	14:00	0.5	3.83	0.05	1.32	45	0	0.00	
05/03/2003	14:15	0.5	3.92	0.09	2.35	45	0	0.00	
05/03/2003	14:30	0.5	4.05	0.13	3.32	47	2	4.44	
05/03/2003	14:45	0.5	4.25	0.2	4.94	51	4	8.51	
05/03/2003	15:00	0.5	4.49	0.24	5.65	59	8	15.69	

Table 3.3: Determining event start time for 20 January 2004 event in which first exceedance of ≥1% increase is immediately followed by constant change. Colours are in accordance with Table 4.2. In addition, yellow indicated increase in turbidity or discharge ≥1% that is not followed by a constant increase.

			Flow			Turbidity			
Date	**Time**	**Rainfall**	**Value**	**Change**	**% Change**	**Value**	**Change**	**% Change**	**Description**
20/01/2004	06:00	0	4.17			43			
20/01/2004	06:15	0	4.12	-0.05	-1.20	43	0	0.00	
20/01/2004	06:30	0	4.07	-0.05	-1.21	41	-2	-4.65	
20/01/2004	06:45	0.2	4.02	-0.05	-1.23	41	0	0.00	
20/01/2004	07:00	0	3.99	-0.03	-0.75	42	1	2.44	
20/01/2004	07:15	0	3.97	-0.02	-0.50	41	-1	-2.38	
20/01/2004	07:30	0	3.96	-0.01	-0.25	42	1	2.44	
20/01/2004	07:45	0.2	3.94	-0.02	-0.51	41	-1	-2.38	
20/01/2004	08:00	0	3.94	0	0.00	40	-1	-2.44	
20/01/2004	08:15	0.2	3.94	0	0.00	41	1	2.50	**>1% increase in turbidity**
20/01/2004	08:30	0	3.94	0	0.00	42	1	2.44	**Continued increase**
20/01/2004	08:45	0.2	3.94	0	0.00	42	0	0.00	**Zero increase in turbidity**
20/01/2004	09:00	0	3.92	-0.02	-0.51	43	1	2.38	**>1% increase in turbidity and event start**
20/01/2004	09:15	0	3.94	0.02	0.51	44	1	2.33	
20/01/2004	09:30	0	3.94	0	0.00	46	2	4.55	
20/01/2004	09:45	0	3.96	0.02	0.51	48	2	4.35	
20/01/2004	10:00	0.2	4	0.04	1.01	49	1	2.08	**>1% increase in discharge**
20/01/2004	10:15	0	4.09	0.09	2.25	51	2	4.08	
20/01/2004	10:30	0.2	4.2	0.11	2.69	53	2	3.92	
20/01/2004	10:45	0	4.32	0.12	2.86	56	3	5.66	
20/01/2004	11:00	0.2	4.44	0.12	2.78	57	1	1.79	
20/01/2004	11:15	0	4.57	0.13	2.93	61	4	7.02	
20/01/2004	11:30	0	4.66	0.09	1.97	64	3	4.92	

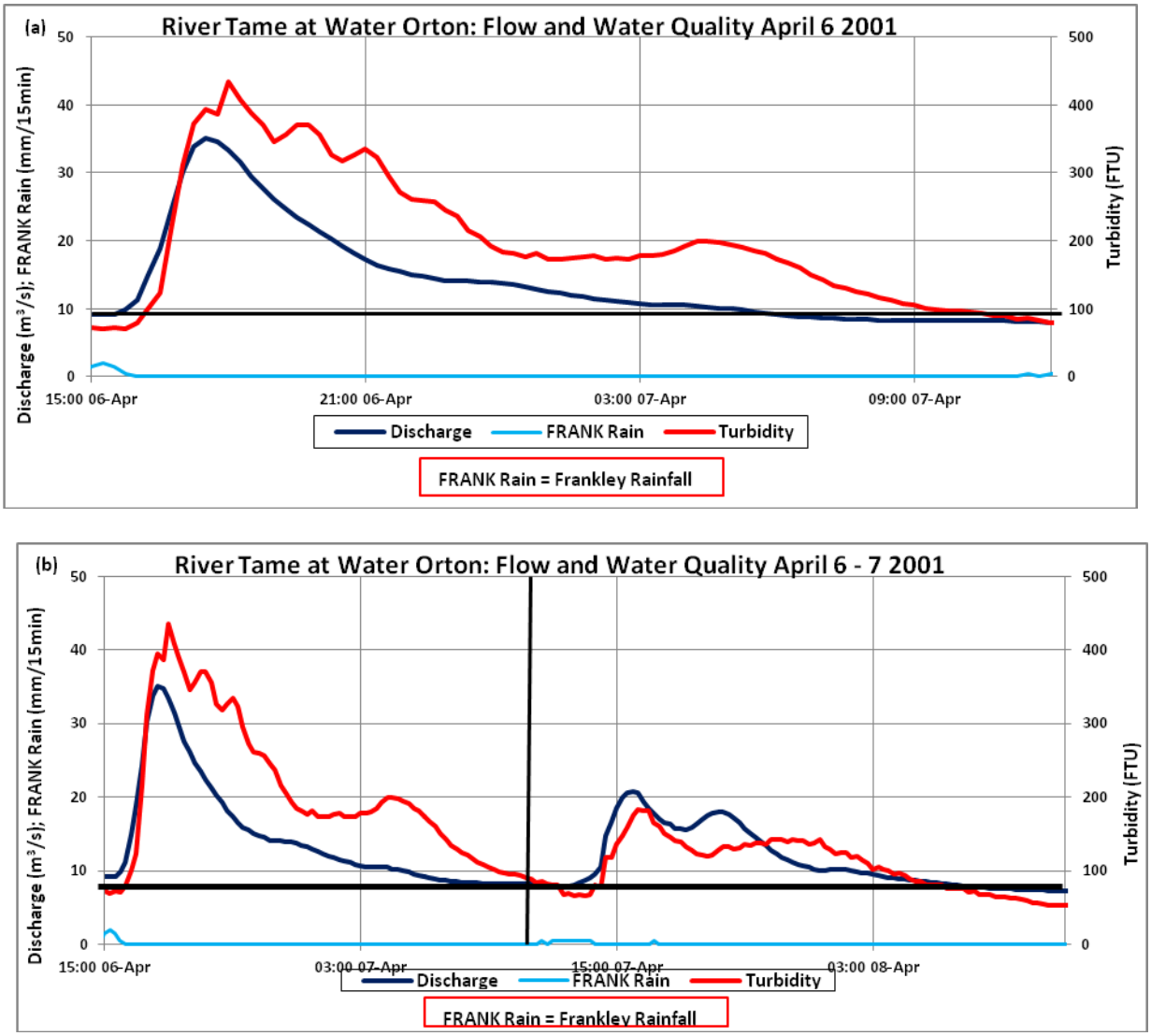

Figure 3.13: Times series ends (a) when both falling limb minimum flow and turbidity differ by ≤30% with respect to rising limb values; horizontal line passes through flow rise start time (b) just before a rain event which results in a flow response of value enough for a new event; vertical line is marking end of April 6 event and beginning of April 7 event.

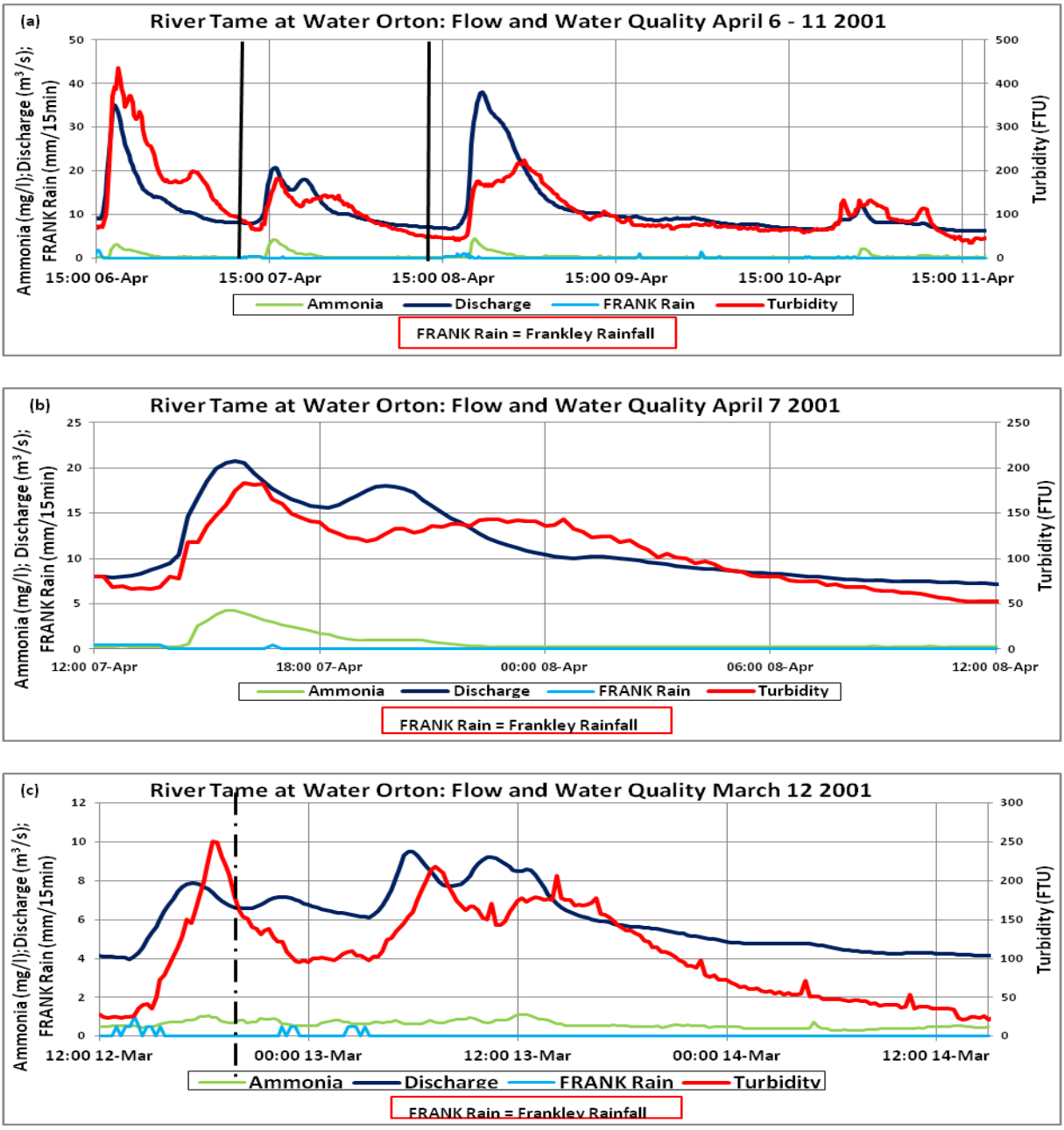

Figure 3.14: Times series showing (a) a sequence of events; (b) double flow peak event); (c) multiple flow peak event.

2. A double peak event has two flow peaks separated by a distinct trough. A trough is defined here as having a flow drop greater than or equal to 10% of the event flow range and a drop/rise time greater than or equal to 5% the event time. Importantly, the trough is not large enough to make either of the two peaks qualify as separate single events (e.g. Figure 3.14(b)).

3. A multiple peak events, which mostly result from multiple rain events, have multiple flow peaks separated by distinct troughs. Such troughs do not make any parts qualify as separate single or double events e.g. Figure 3.14(c).

The above method developed allowed for quantitative events classification.

3.7 Characteristics of event attributes

Numerous attributes are used to describe the characteristics of the storm events in time, in terms of precipitation, discharge, turbidity and ammonia and the interconnections between them. These attributes are defined in

Table *3.4*. Key attributes are also indicated within Figure 3.15. The attributes are quantifying key characteristics of the shape and timing of the storm hydrograph and enabling quantitative comparisons of how these variations in event classification, seasonality and spatial scale modify their response.

3.8 Time series and hysteresis graphs

Hysteresis in the relationship between discharge and turbidity (as discussed in Chapter 2.3) was examined through the analysis of the timing of peak discharge and turbidity. The peak turbidity was identified as lagging, leading or coinciding with the peak discharge (Figure 3.16 a, c, e respectively).

Table 3.4: Definitions of attributes used to characterise storm hydrographs

Attribute	***Definition***	***Equation***
t_{STS}	Starting time of time series	
t_{ETS}	Ending time of time series	
t_o (h)	Rain start time (cumulative time at start of rain from starting time of time series)	
t_c (h)	Rain centroid time (cumulative time at the centroid of rain from starting time of time series)	
t_{eo} (h)	Event start time (cumulative time at start of event from starting time of time series, defined as where there is evident increase in flow/turbidity)	
t_{ee} (h)	Event end time (cumulative time at end of event from starting time of time series)	
t_E (h)	Event time (event end time - event start time)	$t_{ee} - t_{eo}$
t_{ET} (h)	Total event time (event end time - starting time of time series)	$t_{ee} - t_{STS}$
t_r (h)	Event response time (event start time - rain start time)	$t_{eo} - t_o$
Q_{pk} (m^3/s)	Flow peak	
Q_o (m^3/s)	Minimum flow at event start time	
Q_{ee} (m^3/s)	Minimum flow at event end time	
Q_r (m^3/s)	Flow range (flow peak - minimum flow at event start time)	$Q_{pk} - Q_o$
Q_{tot} (m^3/s)	Event total flow	
EFR ($m^3/s/h$)	Event flow rate (Event total flow/event time)	Q_{tot}/t_E
t_{Qpk} (h)	Flow peak time (cumulative time at flow peak from starting time of time series)	
t_{QRL} (h)	Flow rise time (flow peak time - event start time)	$t_{Qpk} - t_{eo}$
t_{QFL} (h)	Flow recession time (event end time - flow peak time)	$t_{ee} - t_{Qpk}$
dQ_{RL} ($m^3/s/h$)	Rate of flow rise (Flow range/flow rise time)	Q_r/t_{QRL}
dQ_{FL} ($m^3/s/h$)	Rate of flow recession (Flow range/flow recession time)	Q_r/t_{QFL}
Lag_{RQ} (h)	Rainfall/flow lag time (Flow peak time - rain centroid time)	$t_{Qpk} - t_c$
Tu_{pk} (FTU)	Turbidity peak	
Tu_o (FTU)	Minimum turbidity at event start time	
Tu_{ee} (FTU)	Minimum turbidity at event end time	
Tu_r (FTU)	Turbidity range (turbidity peak - minimum turbidity at event start time)	$Tu_{pk} - Tu_o$
t_{Tupk} (h)	Turbidity peak time (cumulative time at turbidity peak from starting time of time series)	
t_{TuRL} (h)	Turbidity rise time (turbidity peak time - event start time)	$t_{TuRL} - t_{eo}$
t_{TuFL} (h)	Turbidity recession time (event end time - turbidity peak time)	$t_{ee} - t_{TuFL}$
dTu_{RL} (FTU/h)	Rate of turbidity rise (turbidity range / turbidity rise time)	Tu_r / t_{TuRL}
dTu_{FL} (FTU/h)	Rate of turbidity recession (turbidity range/turbidity recession time)	$Tu_{r\,/}\, t_{TuFL}$
Lag_{TuQ} (h)	Turbidity/flow lag time (flow peak time - turbidity peak time)	$t_{Qpk} - t_{Tupk}$
R_{pk} (mm)	Rainfall peak	
R_{ant} (mm)	24 - hour antecedent rain	
R_{tot} (mm)	Event total rainfall	
ERI (mm/h)	Event rainfall intensity (event total rainfall / event duration)	R_{tot}/t_E
NH_{pk} (mg/l)	Ammonia peak;;	
t_{NHpk} (h)	Ammonia peak time (cumulative time at ammonia peak from starting time of time series)	
Lag_{TuNH}(h)	Turbidity/ammonia lag time (ammonia peak time - turbidity peak time)	$T_{NHpk} - t_{Tupk}$

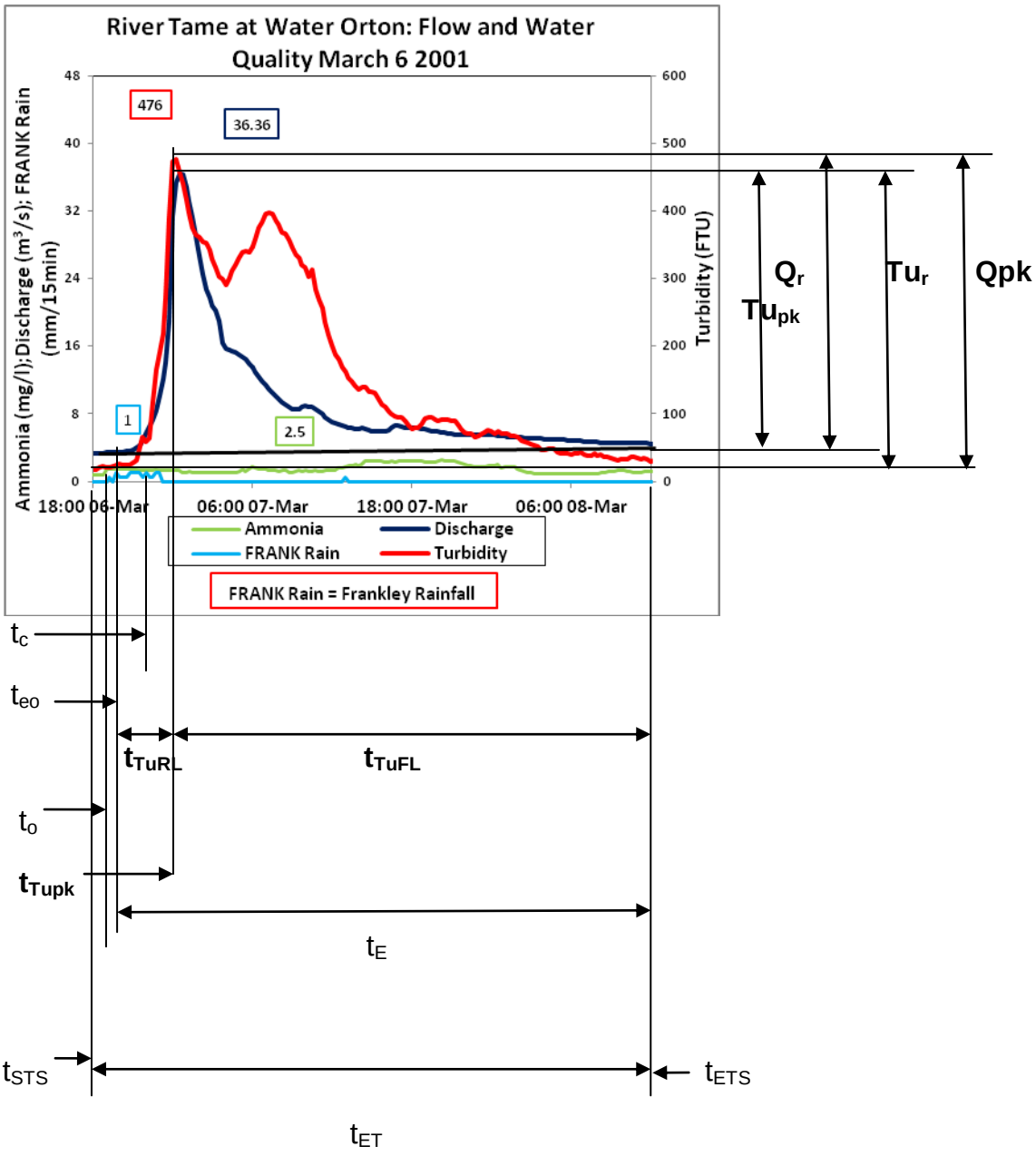

Figure 3.15: Time series of 6 March 2001 event showing some of the terms stated above and calculated in the next worked example. Peaks are in textboxes.

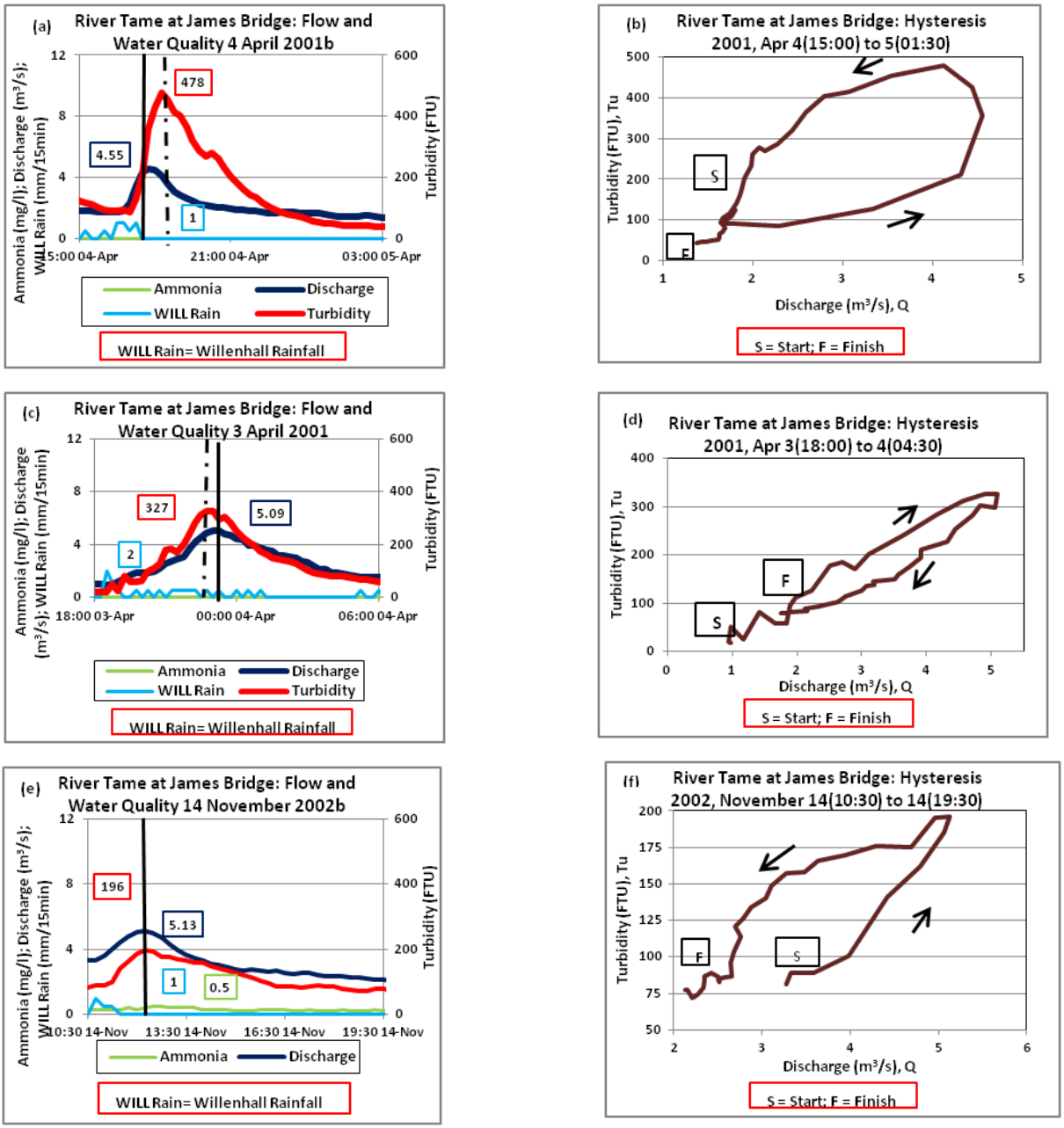

Figure 3.16: Times Series and corresponding Q – Tu hysteresis loops for events on: 4 April 2001 showing (a) turbidity peak lagging discharge peak, (b) simple anticlockwise loop; 3 April 2001 showing (c) turbidity peak leading discharge peak, (d) clockwise loop; 14 November 2002 showing (e) discharge and turbidity peaks coinciding, (f) anticlockwise loop. Peaks are in textboxes.

The strength of the hysteresis is dependent on the time difference between the peaks. For example, within Figure 3.16 a and c, the solid vertical lines pass through discharge peak and the dash vertical lines passes through the turbidity peak. Discharge is seen to lead turbidity in Figure 3.16 a, and lag within Figure 3.16 c. In comparison, the timing of the peak turbidity and discharge coincide within the event depicted within Figure 3.16 e. This classification is in accordance with those already described in previous studies (Duvert et al., 2010). They could also help in classifying the hysteresis loops according to various forms of rotation (clockwise, anti-clockwise, random, and figure-of-eight) (Smith and Dragovich, 2009) and trend (positive and negative) (Moravcova et al., 2009) of the loops (as discussed in Chapter 2.3). However, for simplicity, the storm events are characterised only based on the timing of the peak events. Turbidity, discharge, rainfall and ammonia peak values are differentiated by red, dark blue, blue and light green outline colours respectively throughout the work as seen in Figure 3.15 and Figure 3.16 e.

The shape of the hysteresis loops could not be accurately determined with qualitative, biased, visual characterisation. Whilst the 'textbook' examples presented within Figure 3.16 b, d and f demonstrate clear direction, the assessment of all storm events during the defined study periods highlighted the extreme complexity of the hysteresis pattern that did not fit predefined classifications. Classification of events having a single flow peak with single turbidity peak could easily be done, and thus have been the norm, mostly neglecting the real, more complex double and multiple events. It is hypothesised that complex double and multiple events could be quantitatively

classified. A method has been developed to classify these complex events which use the highest peaks of both turbidity and discharge to determine the lead/lag/co events, which has been used for analysis in Chapter 4. In this method, lead, lag and coinciding events are those in which the highest turbidity peak leads, lags and coincides with the highest discharge peak respectively. The above method developed allowed for quantitative classification of complex events for analysis.

3.9 Chapter summary

The study site used for the subsequent assessment of urban sediment dynamics has been outlined. Further, the development of a systematic approach to define individual storm events and to classify and characterise their form has been outlined. Hysteresis resulting from turbidity peaks leading, lagging or coinciding with discharge peaks has been introduced, including a method for determining the lead lag for the real, complex double and multiple events. In the subsequent chapters, these methodologies will be applied to determine the primary controls on sediment dynamics within urban catchments and their dependence on seasons and scale.

CHAPTER 4 CHARACTERISATION OF EVENTS DOWNSTREAM AN URBAN RIVER CATCHMENT

4.1 Chapter Introduction

This chapter examines turbidity responses to storm events. Events are characterised in accordance with the methodologies outlined in Chapter 3 to identify the controls, processes and drivers of turbidity dynamics. This first results chapter addresses the first research objective outlined in Chapter 1. The chapter consists of six main sections. It is first introduced and a brief literature background provided, leading to the objectives of the chapter. The methodological approach is then outlined. This describes the study area, data (quantity and quality), and quantification of event selection criteria, classification and characteristics. The results section subsequently outlines the findings of the work which are examined within the discussion in the context of the literature.

4.2 Literature background

People living in urban areas in the world is almost half of its population, covering just 10% of the land surface area (Old et al., 2003a). Urban development changes river systems and causes surface water quality degradation from such sources as storm water urban storm runoff, wastewater sewage system (residential and industrial effluents) and diffuse pollutant inputs. Further, the characteristic conditions of catchment hydrology, river flow and sediment are influenced by impervious cover construction, the compaction of

pervious surfaces and storm water drainage systems (storm sewers) that provide the well organised storm runoff removal into river networks (Gurnell et al., 2007). As a result, urban rivers are more flashy (Webster et al., 2001) with steepened flow-duration curves. Runoffs and flow velocities are also increased leading to decreased drainage catchment response time and increased flooding.

Urban rivers' SSC changes rapidly with time mostly increasing when there are high flows (Doomen et al., 2008; Huey and Meyer, 2010). Water quality changes fast and significantly when flows are high, but sluggishly when flows are low or normal (Moravcova et al., 2009). Rain event events are responsible for transporting the greatest part of a year's SS and contaminant loads (Horowitz, 2009). Water quality is the suitability of water for diverse uses which is affected by natural biological, geological, hydrological, meteorological, topographical, aesthetic, and radiological factors (Bartram and Ballance, 1996; Codd, 2000).

In the event-based studies of urban catchments, there is no universal method to identify, select and classify events. Several events-based studies have assigned different definitions to an event based on the study objectives (Goodwin et al., 2003; Merz and Blöschl, 2003; Rovira and Batalla, 2006; Lefrançois et al., 2007; Smith and Dragovich, 2009; Furusho et al., 2010; Talei et al., 2010; Gao and Puckett, 2012) (Table 4.1). While some attempt to give start and end conditions, others give the threshold of hydrologic variable used. These could result in varying event-based analysis with different event start/end

times, classification and event response dynamics, which in turn could result in less detailed analysis of catchment processes, controls and drivers.

Events are characterised by a range of hydrograph shapes. Most event-based studies consider all events together without separating them according to the number of flow peaks. Most studies focus on a single peak event (Jansson, 2002; Lefrançois et al., 2007; Duvert et al., 2010; Furusho et al., 2010). Those studies that do discuss double and/or multiple flow peak events (Rovira and Batalla, 2006; Furusho et al., 2010; Talei et al., 2010) treat them as a succession of peaks that are used, for example, to explain sediment exhaustion within the catchment. When such events are examined, their analysis is severely limited. Notably, peaks and troughs are visually identified within the storm hydrograph. For instance, multiple flow peaks separated by definite troughs resulting from continuous storms were recognised by visual observation and considered separately by Smith and Dragovich (2009).

To examine sediment dynamics, there is a need to quantitatively assess all event types. This requires the development of a quantifiable, universally adaptable working definition for event start and end times, as well as event response size thresholds. Again, the development of a quantifiable classification of events would be needed. It is then important to quantify event selection criteria and event type classification (Chapter 3.6 and 3.6).

This chapter will use this information to infer catchment hydrological processes and the erosion, transport and deposition of sediment at a catchment scale. The following hypotheses are investigated in this regard.

1. Single flow peak events dominate discharge events within urban catchments.
2. Clockwise events occur more frequently in urban river systems.
3. Multiple turbidity peaks can result from a single discharge peak.

4.3 Methodology

4.3.1 Study area

The description of study area, data quantity, quality, events identification, selection and classification, as well as events attributes and characteristics used in this chapter are discussed in chapter 3.3 to 3.8.

4.3.2 Time series and hysteresis loops

Examples of time series of turbidity, discharge, ammonia and rainfall during the study period are presented within Figure 4.1. These are examples of a turbidity peak occurring (a) before, (b) after and (c) with discharge peak. Turbidity-discharge relationships result in hysteresis, some of which are given in Figure 4.2 below as (a) clockwise, (b) anticlockwise, (c) figure-of-eight, and (d) complex or irregular shapes. Hysteresis analysis could explain channel bed-water sediment exchange (Jansson, 2002). Clockwise loops mostly associated with turbidity peak leading discharge peak, could be a result of sediment erosion and transport without net deposition (Jansson, 2002), the availability of which is restricted during the range of discharge events (Lefrançois et al., 2007). Anticlockwise loops mostly associated with turbidity peak lagging discharge peak, could result in net sediment deposition (Jansson, 2002; Lefrançois et al., 2007).

Table 4.1: Classifications of storm events presented within the literature

Event name	*Definition*	*Reference*
Hydrological event	Rising and recession limbs, beginning at when flow rise of over 3l/s per 10min or rise in SSC of over 10mg/l per 10min) and ending at flow and SSC values lower than 3l/s and 10mg/l per 10min	Lefrançois et al., 2007
Storm event	Rain event with enough amount of greater or equal to 5mm and with enough large areal coverage	Stanfield and Jackson, 2011
Flood event	Flow is greater than 3.5m^3/s. Those less considered as base flows.	Furusho et al., 2010
Small and larger events	Events are small if flow is less than 6 m^3/s, and large if more	Gao and Puckett, 2012
Group 1 hydrograph	One peak in rainfall and one peak in runoff	Talei et al., 2010
Group 2 hydrograph	Multiple peaks in rainfall and one peak in runoff	Talei et al., 2010
Group 3 hydrograph	Multiple peaks in rainfall and multiple peaks in runoff	Talei et al., 2010
Flow event	Sampling is made in a way that the hydrograph contains both rising and recession parts	Smith and Dragovich, 2009
Rainfall event	The start and end times are considered to be the first measured rainfall and when SSC get back to near starting values	Goodwin et al., 2003
Long-rain flood	Large spatial extent, large daily rainfall depths, fast to medium runoff response, no extreme rainfalls of short duration	Merz and Blöschl, 2003
Flash flood	Very small spatial extent, small daily rainfall depths and minimum antecedent rainfall, runoff coefficients were 0.5 (relatively dry catchment conditions), short times of concentration	Merz and Blöschl, 2003

Figure-of- eight loops are mostly associated with more turbidity peaks than discharge peaks in a single event and could result from the complex interaction of sediment erosion, deposition or transport throughout the storm event. Complex loops mostly associated with complex rain events (Lefrançois et al., 2007), could also result in sediment erosion, deposition or transport. No hysteresis mostly associated with turbidity peak coinciding with discharge peak, could result in net sediment mobilisation and transport (Jansson, 2002), the availability of which is not restricted during the range of discharge events (Lefrançois et al., 2007).

4.3.3 Analytical techniques

A total of 66 events were characterised and classified in accordance with the protocol developed in Chapter 4. The proportions of single, double and multiple flow peaks were determined and the hysteresis of discharge-turbidity relationship quantified. Attributes were derived for each individual event. Chi-square tests, analysis of variance (ANOVA) and t-tests were applied to assess the significance in the number of event of each event type and the difference in the event attributes between the different event types. The relationship between turbidity attributes and discharge/ammonia attributes were determined through correlation matrix and the characteristics of turbidity-discharge regression relationships tabulated. Lead and lag times for events were analysed to help explain the dynamics of turbidity. Logistic multiple linear regressions were performed between turbidity and the other significantly correlated attributes to identify the influence of event type of the interdependence of event attributes.

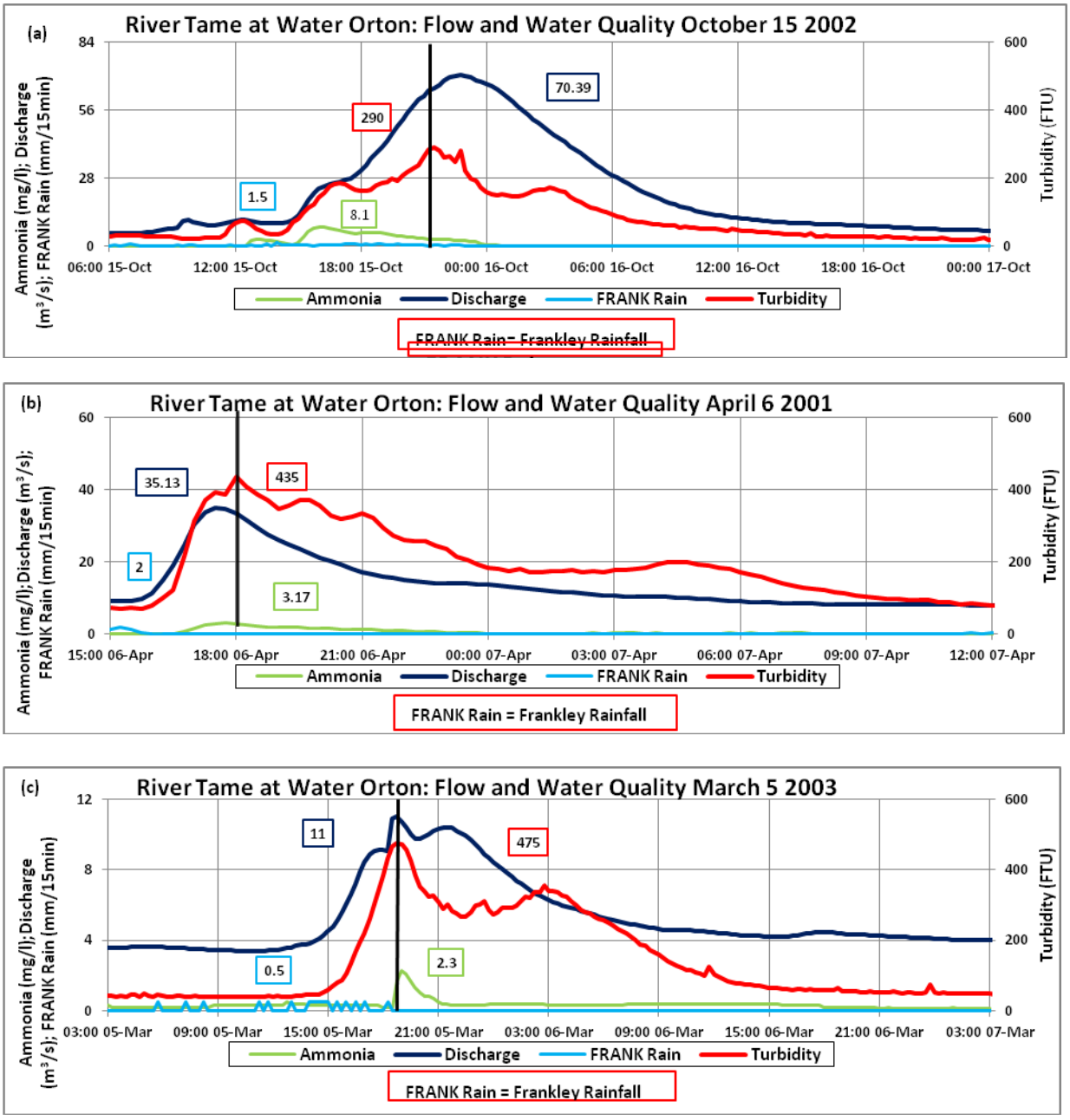

Figure 4.1: Time series showing turbidity peak (in text box with red outline) (a) leading, (b) lagging and (c) coinciding with discharge peak (in text box with deep blue outline). Solid vertical line passes through turbidity peak (in text box with deep blue outline). Rainfall and ammonia peaks are in text boxes with light blue and green outlines respectively.

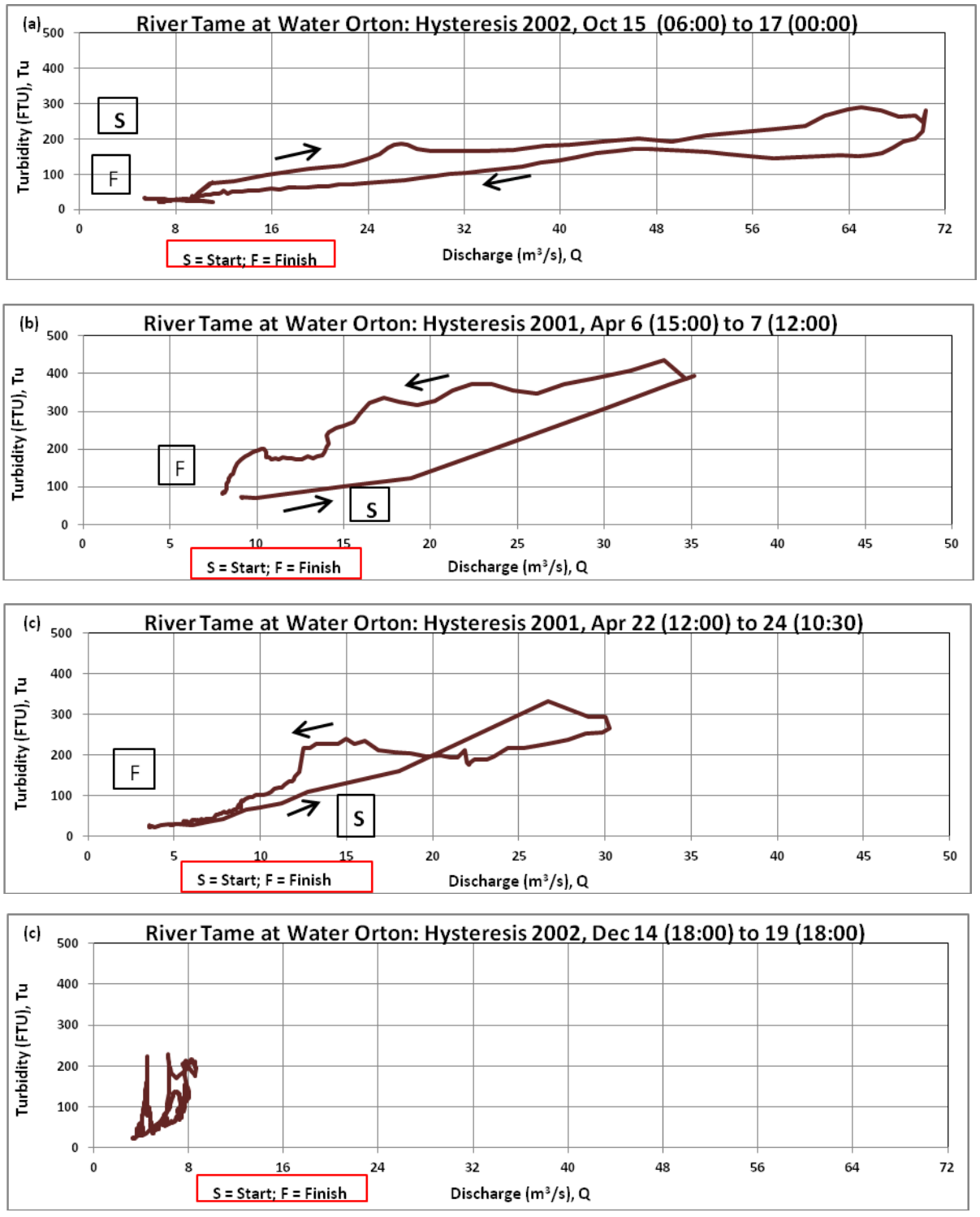

Figure 4.2: Hysteresis types of turbidity versus discharge showing: (a) clockwise; (b) anticlockwise; (c) figure-of-eight; (d) complex patterns.

4.4 Results

4.4.1 Event time series and types

The studied catchment is highly responsive and exhibits a flashy regime. The minimum, maximum and mean times of rise in hours are, for discharge, 1.5, 26, and 6.9 respectively, and for turbidity, 2.5, 30.5 and 8.3 respectively, for single flow peak events. Distributions for the others are also presented (Figure 3.1). Out of the total of 66 events analysed, the largest proportion are double flow peak, accounting for about 44% (29) of events. Multiple flow peak events account for the smallest proportion of events (17%, 11 events). The double and multiple flow peak events together constitute more than 60% of the events (Table 4.2(a), Figure 4.4 (a)).

4.4.2 Discharge characterisation

The means of the attributes event total, peak, range, flow rate, rate of rise and rate of recession show some differences between the single, double and multiple flow peak events. All decrease except the event total discharge which increases (Figure 4.4 (b)). However, analysis of variance indicates no significant difference in the means of all attributes between the three event types (Table 4.2 (b.)).

4.4.3 Turbidity characterisation

Turbidity attributes used include event total, peak, range, rate of rise and rate of recession. Like the discharge, the means of these attributes show some differences within the single, double and multiple flow peak events. Event total turbidity increases, turbidity peak, range and rate of rise show alternating

patterns and rate of recession decrease (Figure 4.4 (c)). However, analysis of variance of these attribute again indicated that there are no significant differences in all attributes between the three event types (Table 4.2 (b)).

4.4.4 Characterisation of rainfall, ammonia and time

Means of total rainfall, total ammonia, event time and event total time increase from single to double to multiple events, while peak rainfall, peak ammonia and event rainfall intensity alternate from single to multiple flow peak events (Figure 4.5). Analysis of variance of the attribute means indicate that there are no significant difference in all attributes between the three event types (Table 4.2 (b)).

4.4.5 Turbidity peak lead/lag/coinciding with discharge peaks for events types

Table 4.3(a) summarises the proportion of lead, lag and coinciding events between single, double and multiple flow peaks. For single flow peak events, the turbidity peak lags the discharge peak in 58% of events (15 events). Turbidity peak leads in 38% of events (10 events). Peaks coinciding occur once (4%), (Table 4.3(a), Figure 4.6(a)). The observed occurrences of turbidity peak leading, lagging and coinciding with discharge peak do not vary significantly between single, double and multiple events from Chi-square tests results (Table 4.3(b)). Note that the lead and coinciding events are combined within this analysis (Table 4.3(c)). From this distribution, the overall show 52 and 42% of events are anticlockwise and clockwise respectively (Table 4.3(a); Figure 4.6). While the number of lag events decreases from maximum with single events to minimum with multiple events, the reverse is the case for both lead and

coinciding peak events, increasing from minimum with single to maximum with multiple events.

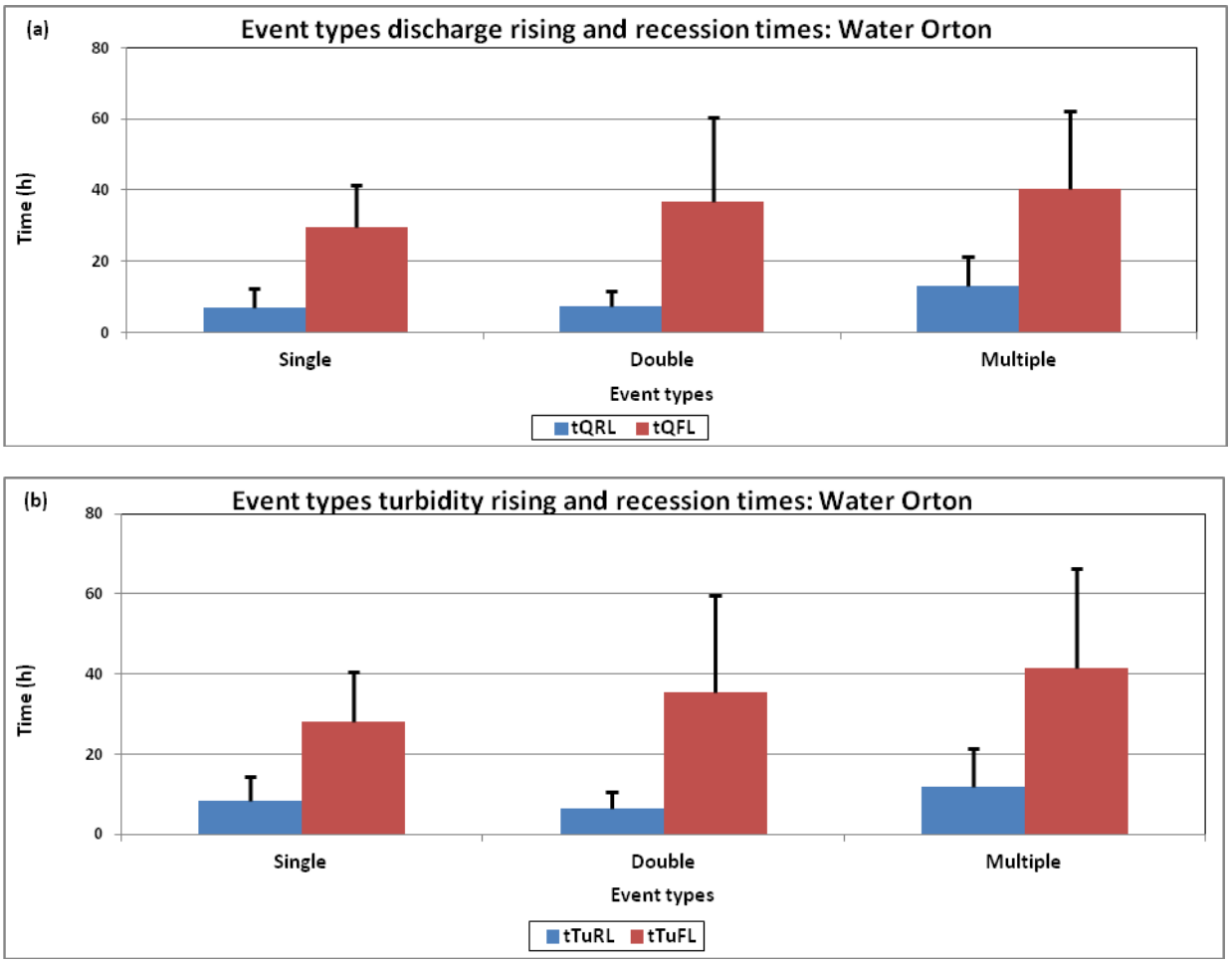

Figure 4.3: Distribution of event type mean rising and recession times for (a) discharge (tQRL and tQFL), (b) turbidity (tTuRL and tTuFL) showing error bars of standard deviation.

Table 4.2: (a) Discharge Event types Distribution; (b) Analysis of Variance for event attributes.

(a) Event	2001	%	2002	%	2003	%	Overall	%
Single	7	31.82	12	46.15	7	39	26	**39.39**
Double	11	50	12	46.15	6	33	29	**43.94**
Multiple	4	18.18	2	7.69	5	28	11	**16.67**
Total	**22**	**100**	**26**	**100**	**18**	**100**	**66**	**100**

(b)		ANOVA (95 % CL)			
			Probability of True		A/R Ho
	Attribute	Sig	Ho	Ha	A IF Ha<95
1	tET	0.066	6.6	93.4	A
2	tQRL	0.062	6.2	93.8	A
3	tE	0.081	8.1	91.9	A
4	Qpk	0.088	8.8	91.2	A
5	Qr	0.122	12.2	87.8	A
6	Tutot	0.181	18.1	81.9	A
7	EFR	0.243	24.3	75.7	A
8	tQFL	0.344	34.4	65.6	A
9	Rtot	0.416	41.6	58.4	A
10	NHtot	0.416	41.6	58.4	A
11	Rpk	0.441	44.1	55.9	A
12	NHpk	0.45	45	55	A
13	Tur	0.797	79.7	20.3	A
14	Tupk	0.844	84.4	15.6	A
15	Qtot	0.881	88.1	11.9	A
16	ERI	0.983	98.3	1.7	A

4.4.6 Distribution of lead and lag times between turbidity and discharge peaks

Figure 4.7 shows the distribution of lag time between turbidity and discharge peaks for (a) single, (b) double, (c) multiple, and (d) overall events. Use of such methods as linear regression for analyses requires that the data or their log-transformed equivalence should be analysed must be normally distributed.

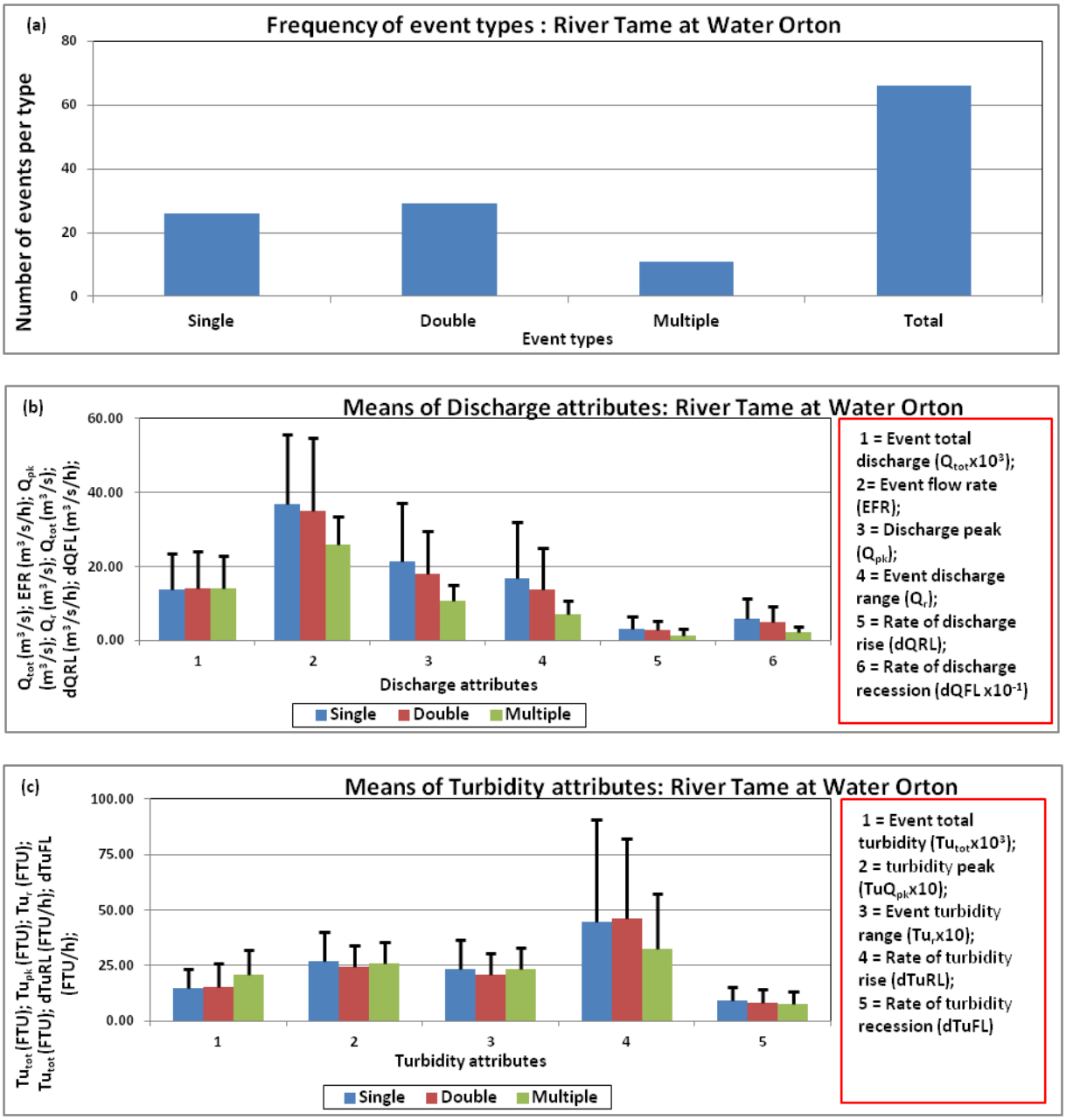

Figure 4.4: (a) Events distribution; (b) means of discharge attributes; (c) means of turbidity attributes within single, double and multiple flow peak events showing error bars of standard deviation.

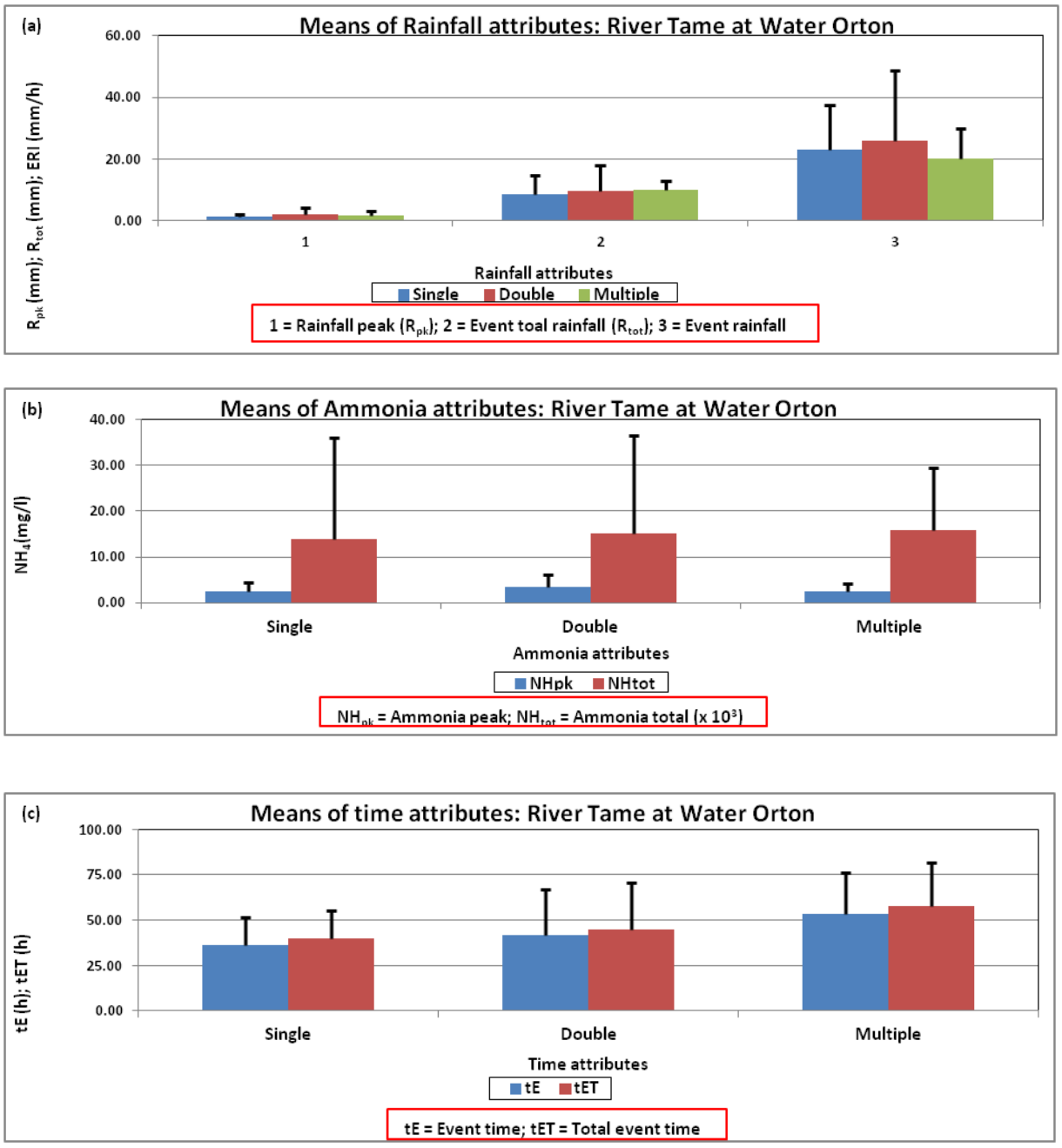

Figure 4.5: Means within single, double and multiple flow peak events of: (a) Rainfall, (b) Ammonia, (c) Time attributes showing error bars of standard deviation.

Table 4.3: (a) Distribution of Tupk Ld/Lg/Co Qpk; Chi-square test (b) with lead, lag and Co separately; and (c) lead/co together and lag events

(a) Event	Lead	%	Lag	%	Co	%	Total	%
Single	10	38	15	58	1	4	26	100
Double	12	41	15	52	2	7	29	100
Multiple	6	55	4	36	1	9	11	100
Total	**28**	**42**	**34**	**52**	**4**	**6**	**66**	**100**

(b)	Value	df	Asymp. Sig. (2-sided)
Pearson Chi-Square	1.578[a]	4	0.813
Likelihood Ratio	1.607	4	0.808
N of Valid Cases	66		

a. 4 cells (44.4%) have expected count less than 5.

(c)	Value	df	Asymp. Sig. (2-sided)
Pearson Chi-Square	1.409[a]	2	0.494
Likelihood Ratio	1.42	2	0.492
N of Valid Cases	66		

a. 0 cells (.0%) have expected count less than 5.

Table 4.4: Skewness test for normal distribution of turbidity-discharge peaks lag times for single, double, multiple flow peak and all events.

	Skewness		
Events	**Statistic**	**Std. Error**	**2xStd. Error**
Single	0.411	0.456	0.912
Double	-0.244	0.434	0.868
Multiple	-0.389	0.689	1.378
All	-0.033	0.295	0.59

One of the ways to check is to draw the normal distribution curve for the data, and if normality is observed, a skewness test, among others, could be used to confirm it. A variable to be approximated by a normal distribution should have the skewness statistic of between -1 and +1, and less than twice its standard error. Table 4.4 gives test values showing that the lag time distribution could be

approximated by a normal distribution for all events and the event types. The overall events distribution gives a strong normal distribution, while the distributions for the event types show some slight skewness. Means of lead and lag times for event types are summarised (Table 4.5 (a); Figure 4.8). Results of t-test between the lead and lag times shows significantly different means between the lead and lag times for the overall events as well as for all the event types (Table 4.5(b)).

4.4.7 Events with more turbidity peaks than discharge peaks

A higher number of turbidity peaks than discharge peaks were observed on numerous occasions throughout the data collection period (Table 4.6(a); Figure 4.9(a) and Figure 4.10). 36% of events demonstrated such a response to rainfall events in total. Thus, the number of turbidity peaks exceeds the number of discharge peaks during one third of events. Further, this response varies between event types. 65% of single events show more than one turbidity peak. In comparison, a greater number of turbidity peaks than discharge peaks are evident in none of the multiple discharge events observed. Thus, the number of turbidity peaks greater than discharge peaks decreases as the complexity (number of discharge peaks) of an event increases (Table 4.6(a); Figure 4.9(a)). Over the entire study period, ammonia peaks greater than or equal to 2 mg/l, an indication of pollution from point and/or non-point sources (Chapman, 1996), were observed within 59% of events (39 events in total).

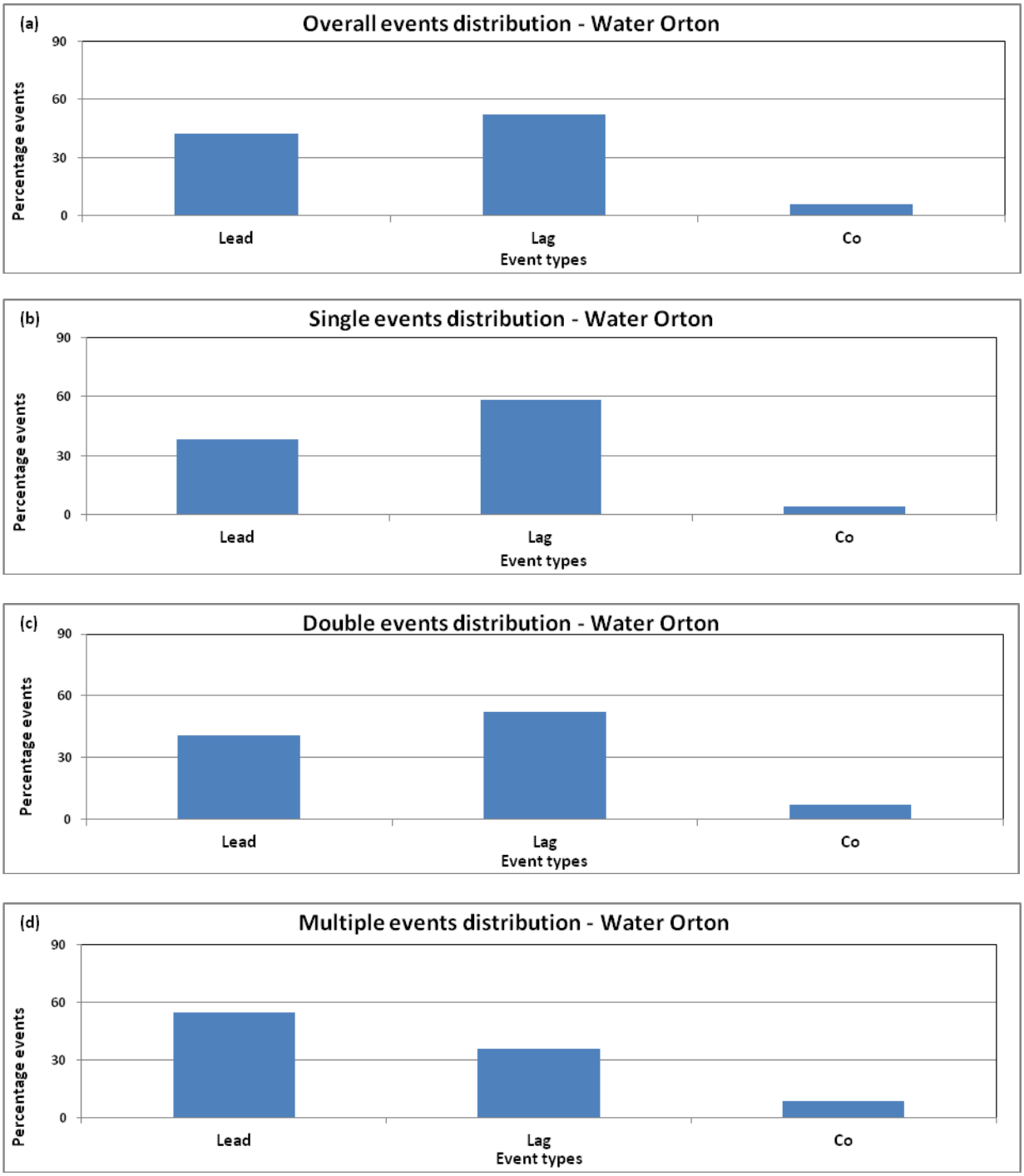

Figure 4.6: Percentage distribution of lead/lag/co events for (a) overall, (b) single, (c) double (d) multiple flow peak events.

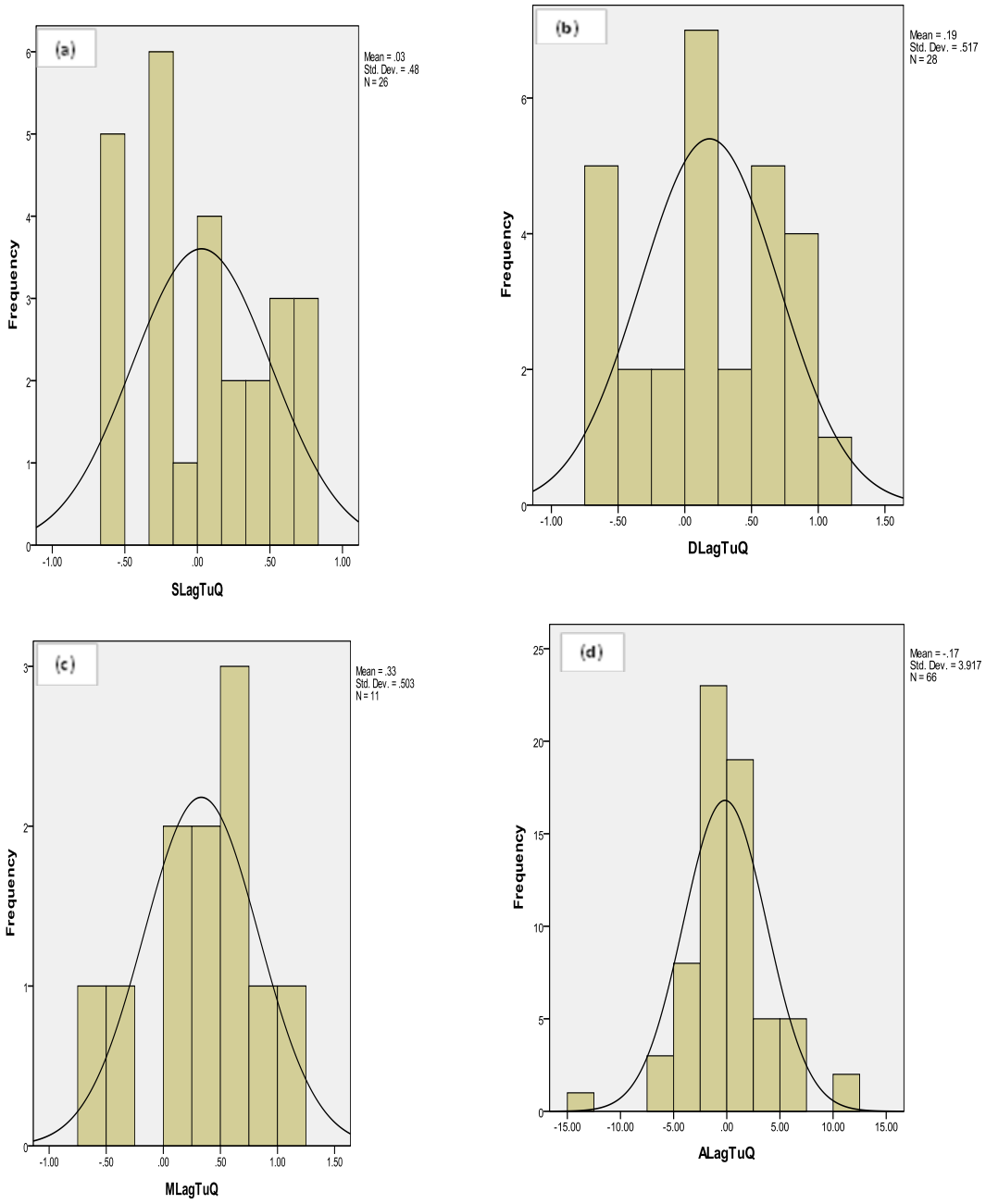

Figure 4.7: Lag time (between turbidity and discharge peaks) distribution for: (a) Single, (b) Double, (c) Multiple, (d) All flow peak events

Table 4.5: (a) Event types mean times for turbidity peaks leading and lagging discharge peaks for all events, (b) Lead/lag time t-test results.

(a) Attribute	Lead time (h)			Lag time (h)		
Event type	**Mean**	**Maximum**	**Minimum**	**Mean**	**Maximum**	**Minimum**
Single	0.6	1.75	0.25	2.75	6.75	0.5
Double	4.39	10	0.25	1.72	5.75	0.25
Multiple	4.25	11.25	0.25	3	4.5	1

(b) Attribute Seasons	LagTuQ Significance
All	<0.001
Single	<0.001
Double	<0.001
Multiple	0.012

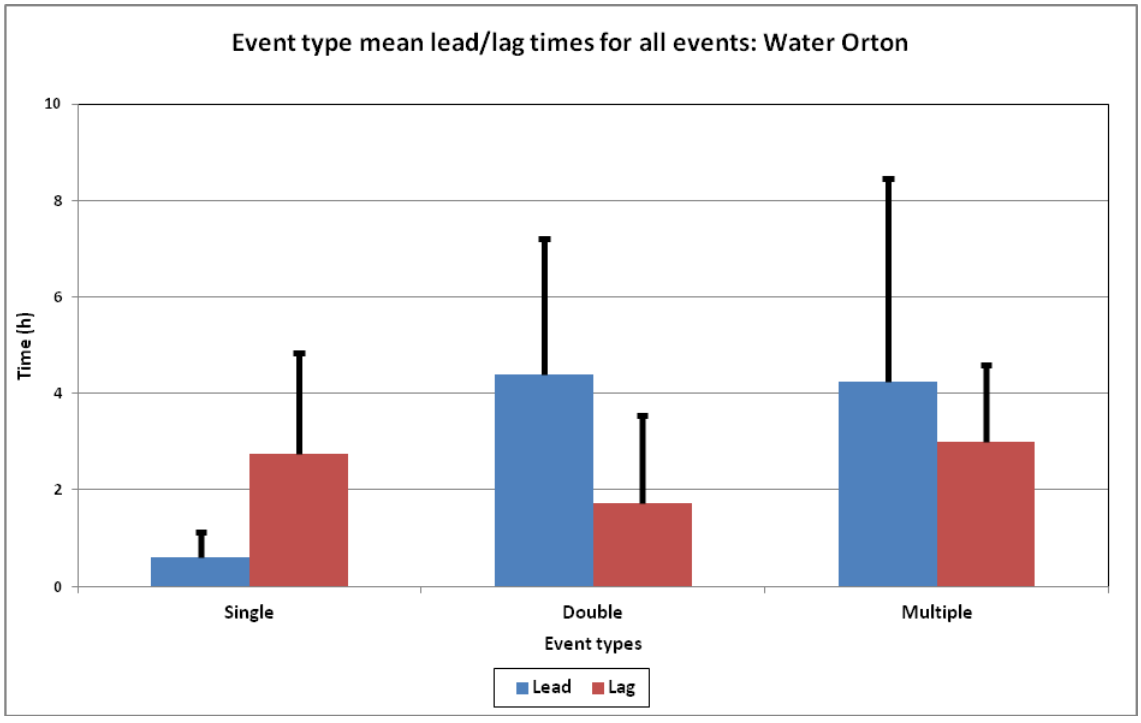

Figure 4.8: Event types mean times for turbidity peaks leading and lagging discharge peaks for all events, with error bars of standard deviation.

Table 4.6: Distribution of events with: (a) differing numbers of turbidity and discharge peaks (Tupk, Qpk); (b) ammonia peak around 2mg/l; (c) more turbidity peaks than discharge peaks and with ammonia peak (NHpk) above/below 2mg/l.

(a)	Events with Tupk ≤ Qpk		Tupk > Qpk		
Event	**No**	**%**	**No**	**%**	**Total**
Single	9	35	17	65	26
Double	22	76	7	24	29
Multiple	11	100	0	0	11
Total	42	64	24	36	66

(b)	Events with NHpk				
Event	**< 2 mg/l**	**%**	**≥ 2 mg/l**	**%**	**Total**
Single	13	50	13	50	26
Double	8	28	21	72	29
Multiple	6	55	5	45	11
Total	27	41	39	59	66

(c)	Events with Tupk > Qpk having NHpk				
Event	**< 2 mg/l**	**%**	**≥ 2 mg/l**	**%**	**Total**
Single	5	29	12	71	17
Double	1	14	6	86	7
Multiple	0	0	0	0	0
Total	6	25	18	75	24

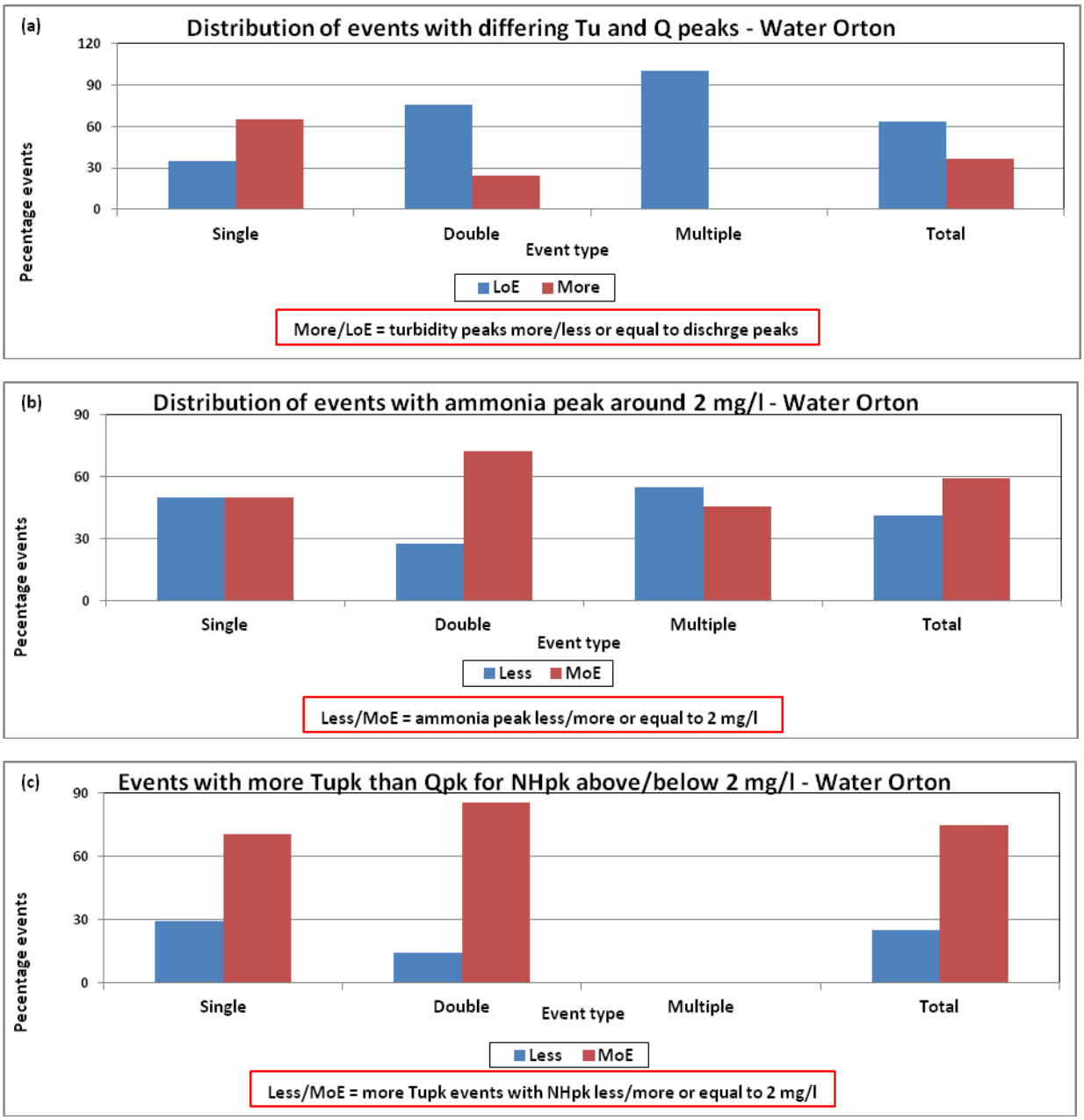

Figure 4.9: Distribution of events with: (a) differing numbers of turbidity and discharge peaks; (b) ammonia peak around 2mg/l; (c) more turbidity peaks than discharge peaks for ammonia peak above/below 2mg/l.

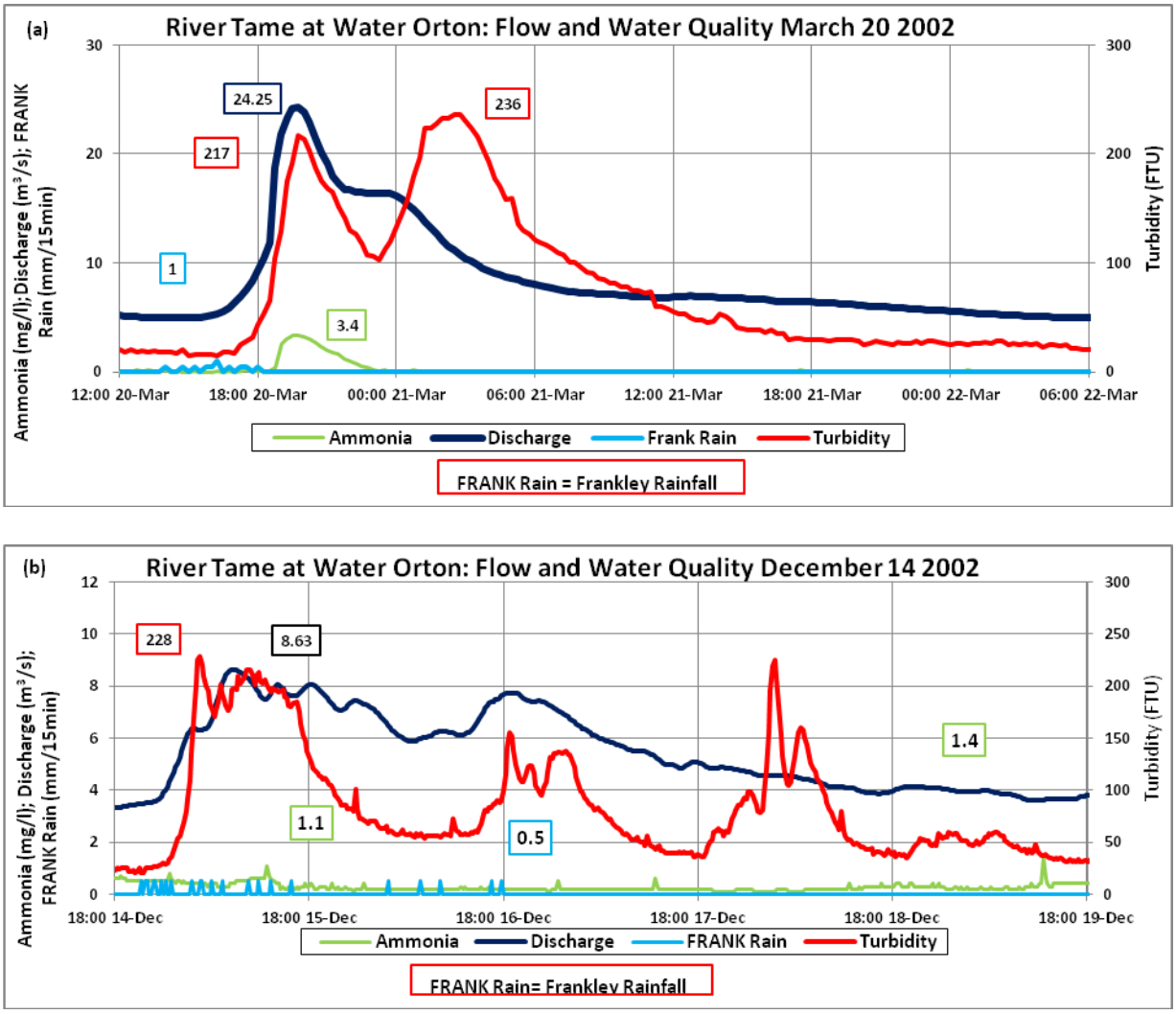

Figure 4.10: Time series for events with more turbidity peaks (in text box with red outline) than discharge peaks (in text box with deep blue outline): (a) single flow peak event with two distinct turbidity peaks, (b) double flow peak event with more than two turbidity peaks. Rainfall and ammonia peaks are in text box with light blue and green outlines respectively.

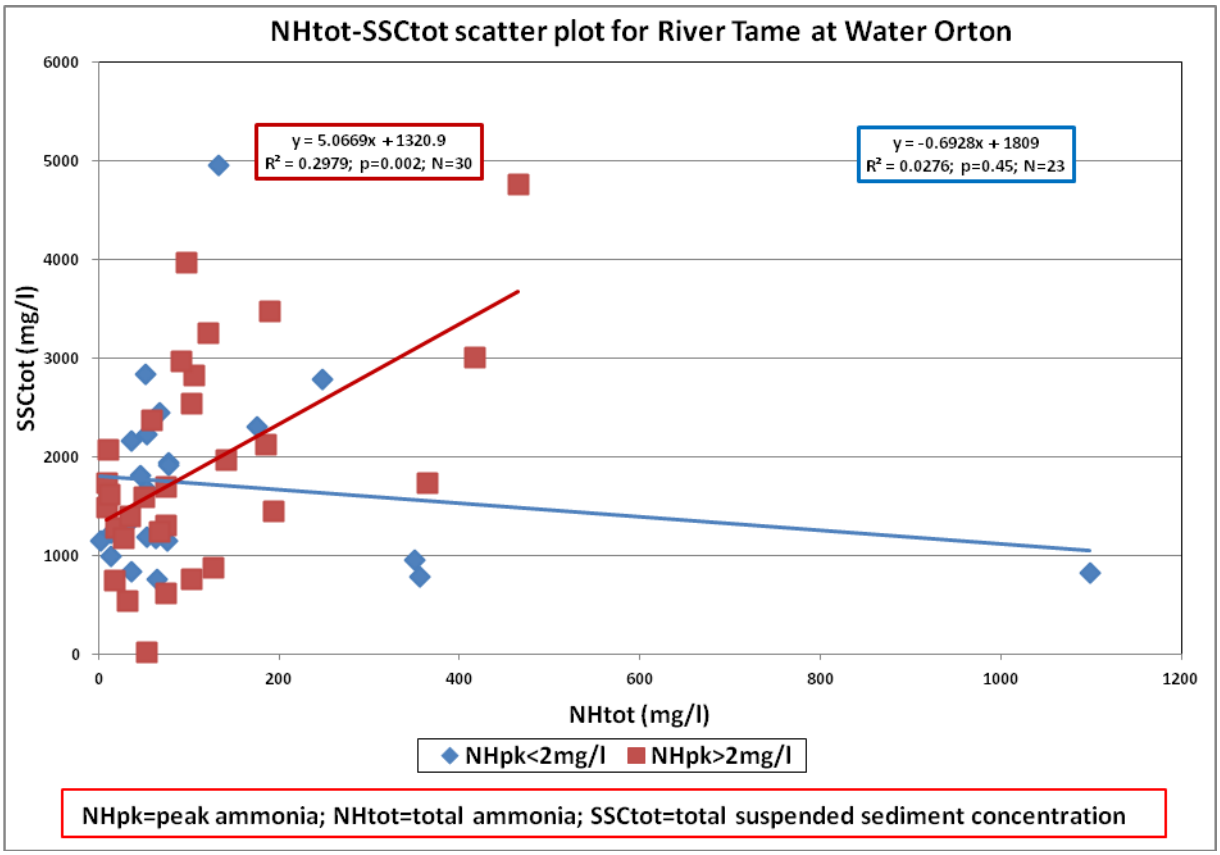

Figure 4.11: Scatter plots of total ammonia and total suspended sediment data above and below peak ammonia threshold of 2mg/l.

Ammonia levels greater than 2mg/l occurred in 75% of double events. In comparison, this threshold was exceeded in only 45% of multiple events (Table 4.6(b); Figure 4.9(b)). The number of events with turbidity peaks greater than discharge peaks with ammonia peaks greater than or equal to 2 mg/l averaged 75 % (18 events). This ranged from a maximum of 86% for double events and 0% multiple discharge peak events (Table 4.6(c); Figure 4.9(c)).

Figure 4.11 shows the correlation between total suspended sediment concentration and total ammonia for data above and below the ammonia peak threshold of 2 mg/l used. While data with ammonia peak above 2 mg/l showed significant correlation (R^2=0.298; p=0.002; N=30), those with ammonia peak below 2 mg/l did not.

4.4.8 Turbidity attributes relationships with other event attributes

The means of event attributes did differ significantly between event types, and Table (a) in Appendix B gives a summary of some basic statistics of the attributes, with Figure 4.14 to Figure 4.16 showing the bar charts with error bars of standard deviations of the attribute mean to show their wide variations.

Turbidity parameters (peak-Tupk, range-Tur and total-Tutot) were all strongly correlated with discharge parameters (peak-Qpk, range-Qr, total-Qtot and event flow rate-EFR), with correlations increasing from the single to multiple for turbidity peak and range. Total turbidity had strongest correlation with total discharge in all event types, with the strongest for double (r=0.86) and weakest for single events (r=0.68) (Table 4.7(a)). The total turbidity gives the strongest correlation and highest explained variance with discharge attributes in all the three event types. The explained variance is highest for the double flow peak events (R^2=0.827), and the lowest for single flow peak events (R^2=0.708), when all significantly correlated attributes are assessed through a single multiple regression model (Table 4.7(b)).

The strength of the relationship between turbidity attributes and discharge range and total (indicated as Best r in Table 4.7(b)) indicates that Q total

accounted for 45.8, 73.1 and 71.4% of total variance for the single, double and multiple flow peak events respectively (Figure 4.12(a) to (c)). In percentage terms, Qr explained 44, 60 and 91% of the variance in the turbidity peak, and 50, 72 and 90% of the variance in the turbidity range. Q total alone accounts for 65, 88 and 93% of total turbidity explained variance. Thus, of all attributes used, Q contributes the highest of explained turbidity variance (R^2) and increases from turbidity peak to total turbidity, and also from single to multiple flow peak events. Three regressions (Figure 4.12), for single, double and multiple events were drawn to compare their respective Tu-Q variations.

The relationship between turbidity and discharge attributes varies between event types. The gradient of the relationship between Tupk, Tur and discharge regression equation is steeper for multiple than single and double events. In comparison, there is strong correspondence in the gradient of the regression relationship between Tutot and discharge for the different event types. However, the intercept of the multiple events is higher than that of single and double events (Figure 4.12(c)).

Multiple flow peak events give the highest rate of change of turbidity with respect to flow (Table 4.8(b)); more than 2 times in Tupk and Tur, and about 1½ times in Tutot regression lines (Table 4.8(c)). Logistic multiple regressions were applied to determine whether the gradient and intercept of the relationship between turbidity and discharge attributes varied significantly with event types (Figure 4.12(a) to (c)). Intercept and gradient components of double and multiple flow peak events (DIn, DGr, MIn, MGr) were introduced as dummies within the turbidity-discharge multiple regression models. R^2 values for the

model outputs 1 and 2 are presented within Table 4.7 and Table 4.8 together with the influence of single, double and multiple flow peak events. The gradient (DGr) or intercept (DIn) of the double flow peak events does not differ significantly from the single flow peak events. However, the gradient of multiple flow peak events (MGr) differ significantly for turbidity peak and range ($p<0.05$ respectively). Further, the intercept of multiple flow peak events (MIn) differed significantly for turbidity total ($p<0.05$) from that of the single and double flow events. The summary of the coefficients and their significance are presented within Table 4.8(a).

The influence of single, double and multiple flow peak events on the linear regression lines of turbidity attributes with the other attributes were also investigated (Table 4.9 and Table 4.10). It revealed that in addition to the discharge attributes, multiple events again had a significantly higher intercept in the relationship between turbidity total and ammonia peak than the single and double events (Table 4.10; Figure 4.13(c)). Regarding all other attributes, no significant differences were found between the event types.

Definitions of attributes used in Table 4.7 to Table 4.10: S, D, M=single, double and multiple flow peak events, In, Gr=intercept, slope/gradient of line of best fit, Tu=turbidity, Q=discharge/flow, R=rainfall, NH=ammonia, pk=peak, r=range, tot=total, ERI=event rainfall intensity, EFR=event flow rate, dQRL=rate of flow rise, dQFL=rate of flow recession, LagRQ=rainfall-flow peaks lag time,tQRL, tQFL= flow rise and flow recession times, tE, tET=event and total event times.

*Table 4.7: (a) r for turbidity attributes relationship with other attributes; (b) R^2 for enter mode multiple regressions and for turbidity-discharge scatter (Best r); (c) Stepwise model output. Note: * Significance at 0.01, others at 0.05 confidence levels. D (double), M (multiple), In (intercept) and Gr (gradient)*

(a)	Tupk			Tur			Tutot		
Single									
No	**Attr**	**r**	**Sig**	**Attr**	**r**	**Sig**	**Attr**	**r**	**Sig**
1	**Qr**	0.5	0.009*	**Qr**	0.487	0.01*	**Qtot**	0.677	<0.001*
2	**NHpk**	0.473	0.015	**NHtot**	0.459	0.02	**tE**	0.641	<0.001*
3	**NHtot**	0.468	0.016	**NHpk**	0.456	0.02	**tET**	0.609	0.001*
4	**Qpk**	0.455	0.019	**Qpk**	0.436	0.03	**tQFL**	0.606	0.001*
5	**dQFL**	0.427	0.029	**dQFL**	0.416	0.04	**Qr**	0.585	0.002*
6	**LagRQ**	-0.405	0.04				**Rtot**	0.57	.002*
7	**dQRL**	0.388	0.05				**Qpk**	0.559	.003*
8							**NHtot**	0.514	.007*
9							**NHpk**	0.508	.009*
10							**tQRL**	0.463	0.017
Double									
1	**EFR**	0.579	0.001*	**Qr**	0.574	.001*	**Qtot**	0.855	<0.001*
2	**Qpk**	0.551	0.002*	**Qpk**	0.557	.002*	**tQFL**	0.729	<0.001*
3	**Qr**	0.548	0.002*	**EFR**	0.543	.002*	**tE**	0.706	<0.001*
4	**Qtot**	0.516	0.004*	**Qtot**	0.542	.002*	**tET**	0.702	<0.001*
5	**Rtot**	0.467	0.011	**Rtot**	0.473	.01*	**Rtot**	0.621	<0.001*
6	**NHpk**	0.432	0.019	**NHpk**	0.409	0.03	**Qpk**	0.492	0.007*
7	**ERI**	0.408	0.028	**dQRL**	0.377	0.04	**EFR**	0.488	0.007*
8	**dQRL**	0.376	0.044				**Qr**	0.485	.008*
9	**dQFL**	0.368	0.049				**NHtot**	0.484	.008*
10							**NHpk**	0.434	0.019
Multiple									
1	**Qpk**	0.822	0.002*	**Qpk**	0.839	0.001*	**Qtot**	0.845	.001*
2	**Qr**	0.8	0.003*	**Qr**	0.806	0.003*	**tQFL**	0.736	.01*
3	**EFR**	0.607	0.047	**EFR**	0.637	0.04	**tE**	0.732	.01*
4							**tET**	0.719	0.013

(b)	Event	Single			Double			Multiple		
		Model	**Best r**	**% Best r**	**Model**	**Best r**	**% Best r**	**Model**	**Best r**	**% Best r**
Tupk (Qr)	**r**	0.757	0.5		0.709	0.548		0.838	0.8	
	R2	0.573	0.25	44	0.503	0.3	60	0.702	0.64	91
	Sig	0.016	0.009*		0.044	0.002*		0.029	0.003*	
Tur (Qr)	**r**	0.689	0.487		0.676	0.574		0.85	0.806	
	R2	0.475	0.237	50	0.457	0.33	72	0.723	0.65	90
	Sig	0.017	0.01*		0.047	0.001*		0.023	0.003*	
Tutot (Qtot)	**r**	0.842	0.677		0.91	0.855		0.878	0.845	
	R2	0.708	0.458	65	0.827	0.731	88	0.771	0.714	93
	Sig	0.012	0*		0*	0*		0.04	0.001*	

(c)	Stepwise Model			D/M
		1	**2**	**Added R^2**	**influence**
Tupk (Qr)	**r**	0.503	0.547		**MGr**
	R2	0.254	0.299	4.5	
	Sig	0	0		
Tur (Qr)	**r**	0.505	0.554		**MGr**
	R2	0.255	0.307	5.2	
	Sig	0	0		
Tutot (Qtot)	**r**	0.774	0.795		**MIn**
	R2	0.599	0.632	3.3	
	Sig	0	0		

Table 4.8: (a) Stepwise MLR output; (b) Rate of change of turbidity with respect to flow; (c) Ratios of gradient of multiple to single and double flow peak regression lines

(a)	Dependent Variable: Tupk					
Model		Unstandardized Coefficients		Standardized Coefficients	t	Sig.
		B	Std. Error	Beta		
1	(Constant)	2.033	0.074		27.66	<0.001
	Qr	0.325	0.07	0.503	4.662	<0.001
2	(Constant)	1.987	0.075		26.373	<0.001
	Qr	0.351	0.069	0.543	5.062	<0.001
	MGr	0.161	0.079	0.218	2.031	0.046
	Dependent Variable: Tur					
Model		Unstandardized Coefficients		Standardized Coefficients	t	Sig.
		B	Std. Error	Beta		
1	(Constant)	1.908	0.085		22.482	<0.001
	Qr	0.377	0.081	0.505	4.678	<0.001
2	(Constant)	1.85	0.087		21.378	<0.001
	Qr	0.408	0.08	0.547	5.127	<0.001
	MGr	0.199	0.091	0.233	2.182	0.033
	Dependent Variable: Tutot					
Model		Unstandardized Coefficients		Standardized Coefficients	t	Sig.
		B	Std. Error	Beta		
1	(Constant)	1.683	0.25		6.737	<0.001
	Qtot	0.798	0.082	0.774	9.782	<0.001
2	(Constant)	1.695	0.241		7.023	<0.001
	Qtot	0.786	0.079	0.763	9.958	<0.001
	MIn	0.143	0.061	0.181	2.367	0.021

(b)	Tupk	Qr	Tupk/Qr	Tur	Qr	Tur/Qr	Tutot	Qtot	Tutot/Qtot
Single	268.78	16.85	**16**	236	16.85	**14**	14580	1366	**11**
Double	242.15	13.68	**18**	209	13.68	**15**	15442.1	1407	**11**
Multiple	260.55	6.99	**37**	231	6.99	**33**	20811.5	1416	**15**

(c)	Multiple	Double	Gradient Ratio	Single	Gradient Ratio
Tupk	37	18	2.1	16	2.3
Tur	33	15	2.2	14	2.4
Tutot	15	11	1.4	11	1.4

Table 4.9: Logistic multiple regression output for event types effects on: (a) turbidity peak- and (b) turbidity range- attributes relationships. D (double), M (multiple), In (intercept) and Gr (gradient)

(a) Dep	Tupk						
Indep	**Statistics**	**r**	**R^2**	**Sig**	**B**	**Std. Err.**	**Sig**
Qr	**Model**	0.547	0.299	<0.001			
	Constant				1.987	0.075	<0.001
	Qr				0.351	0.069	<0.001
	MGr				0.161	0.079	0.046
Qpk	**Model**	0.48	0.23	<0.001			
	Constant				1.898	0.108	<0.001
	Qpk				0.394	0.09	<0.001
NHpk	**Model**	0.44	0.194	<0.001			
	Constant				2.279	0.032	<0.001
	NHpk				0.248	0.063	<0.001
Qtot	**Model**	0.428	0.184	<0.001			
	Constant				1.316	0.275	<0.001
	Qtot				0.341	0.09	<0.001
EFR	**Model**	0.415	0.172	0.001			
	Constant				1.647	0.196	<0.001
	EFR				0.478	0.131	0.001
Rtot	**Model**	0.395	0.156	0.001			
	Constant				2.116	0.074	<0.001
	Rtot				0.281	0.082	0.001
NHtot	**Model**	0.36	0.13	0.003			
	Constant				2.051	0.102	<0.001
	NHtot				0.161	0.052	0.003

(b) Dep	Tur						
Indep	**Statistics**	**r**	**R^2**	**Sig**	**B**	**Std. Err.**	**Sig**
Qr	**Model**	0.554	0.307	<0.001			
	Constant				1.85	0.087	<0.001
	Qr				0.408	0.08	<0.001
	MGr				0.199	0.091	0.033
Qpk	**Model**	0.521	0.272	<0.001			
	Constant				1.68	0.128	<0.001
	Qpk				0.494	0.104	<0.001
	MGr				0.158	0.076	0.043
Qtot	**Model**	0.439	0.193	<0.001			
	Constant				1.051	0.316	0.001
	Qtot				0.403	0.103	<0.001
NHpk	**Model**	0.426	0.181	<0.001			
	Constant				2.195	0.038	<0.001
	NHpk				0.277	0.074	<0.001
Rtot	**Model**	0.401	0.161	0.001			
	Constant				2.001	0.086	0
	Rtot				0.329	0.094	0.001
EFR	**Model**	0.394	0.155	0.001			
	Constant				1.505	0.229	<0.001
	EFR				0.524	0.153	0.001
NHtot	**Model**	0.355	0.126	0.003			
	Constant				1.933	0.119	<0.001
	NHtot				0.184	0.06	0.003

Table 4.10: Logistic multiple regression output for event types effects on total turbidity-attributes relationships. D (double), M (multiple), In (intercept) and Gr (gradient)

Dep Indep	Statistics	r	R^2	Tutot Sig	B	Std. Err.	Sig
Qtot	Model	0.795	0.632	<0.001			
	Constant				1.695	0.241	<0.001
	Qtot				0.786	0.079	<0.001
	MIn				0.143	0.061	0.021
tE	Model	0.698	0.488	<0.001			
	Constant				2.573	0.199	<0.001
	tE				0.984	0.126	<0.001
tQFL	Model	0.689	0.474	<0.001			
	Constant				2.774	0.179	<0.001
	tQFL				0.915	0.121	<0.001
tET	Model	0.685	0.469	<0.001			
	Constant				2.466	0.221	<0.001
	tET				1.027	0.137	<0.001
Rtot	Model	0.603	0.364	<0.001			
	Constant				3.641	0.084	<0.001
	Rtot				0.555	0.092	<0.001
Qr	Model	0.555	0.308	<0.001			
	Constant				3.635	0.099	<0.001
	Qr				0.437	0.091	<0.001
	MIn				0.284	0.086	0.002
Qpk	Model	0.551	0.303	<0.001			
	Constant				3.427	0.142	<0.001
	Qpk				0.55	0.116	<0.001
	MIn				0.287	0.086	0.001
tQRL	Model	0.518	0.269	<0.001			
	Constant				3.546	0.122	<0.001
	tQRL				0.3	0.062	<0.001
NHtot	Model	0.518	0.269	<0.001			
	Constant				3.546	0.122	<0.001
	NHtot				0.3	0.062	<0.001
NHpk	Model	0.49	0.24	<0.001			
	Constant				3.984	0.044	<0.001
	NHpk				0.316	0.08	<0.001
	MIn				0.19	0.087	0.033

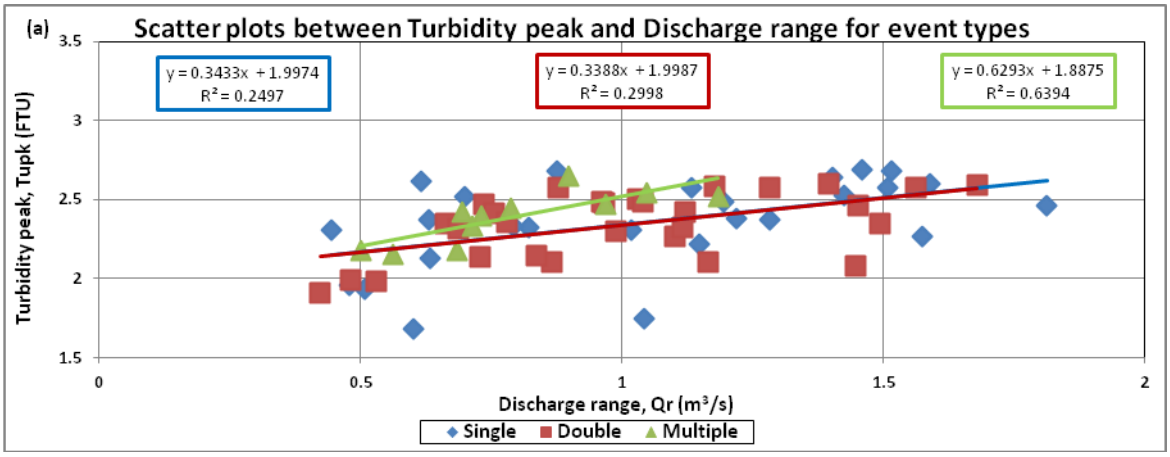

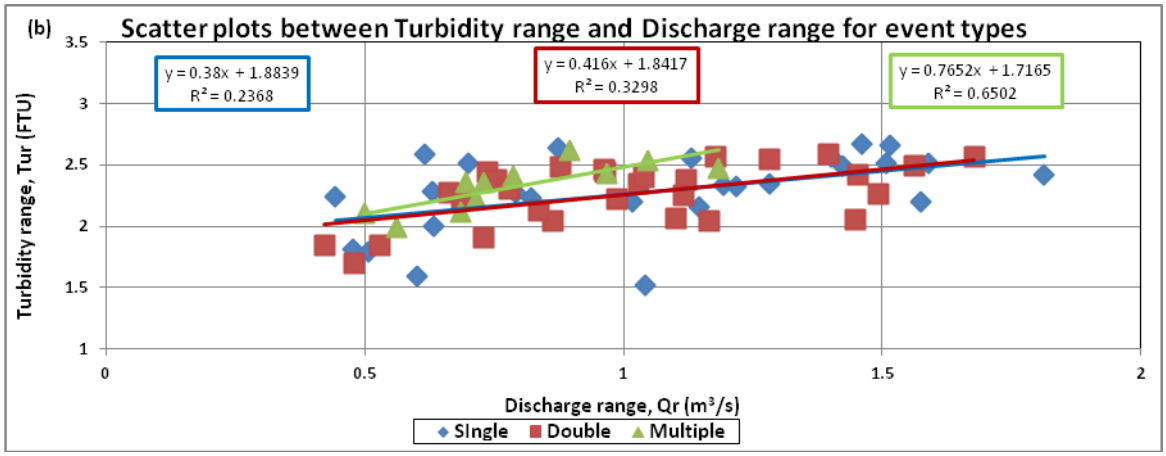

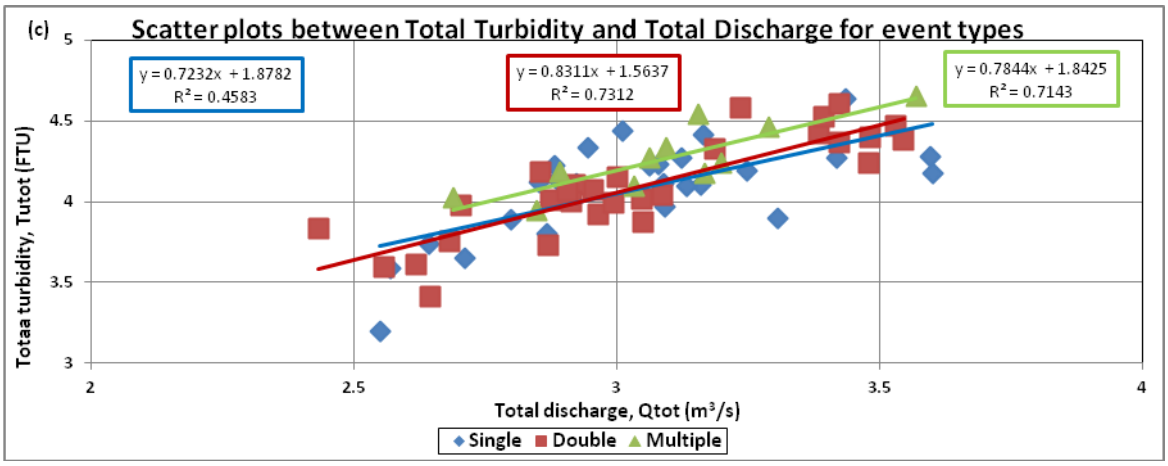

Figure 4.12: Scatter plot of turbidity attributes with event attributes for Single, Double and Multiple flow peak events respectively: (a) Tupk with Qr; (b) Tur with Qr; (c) Tutot with Qtot.

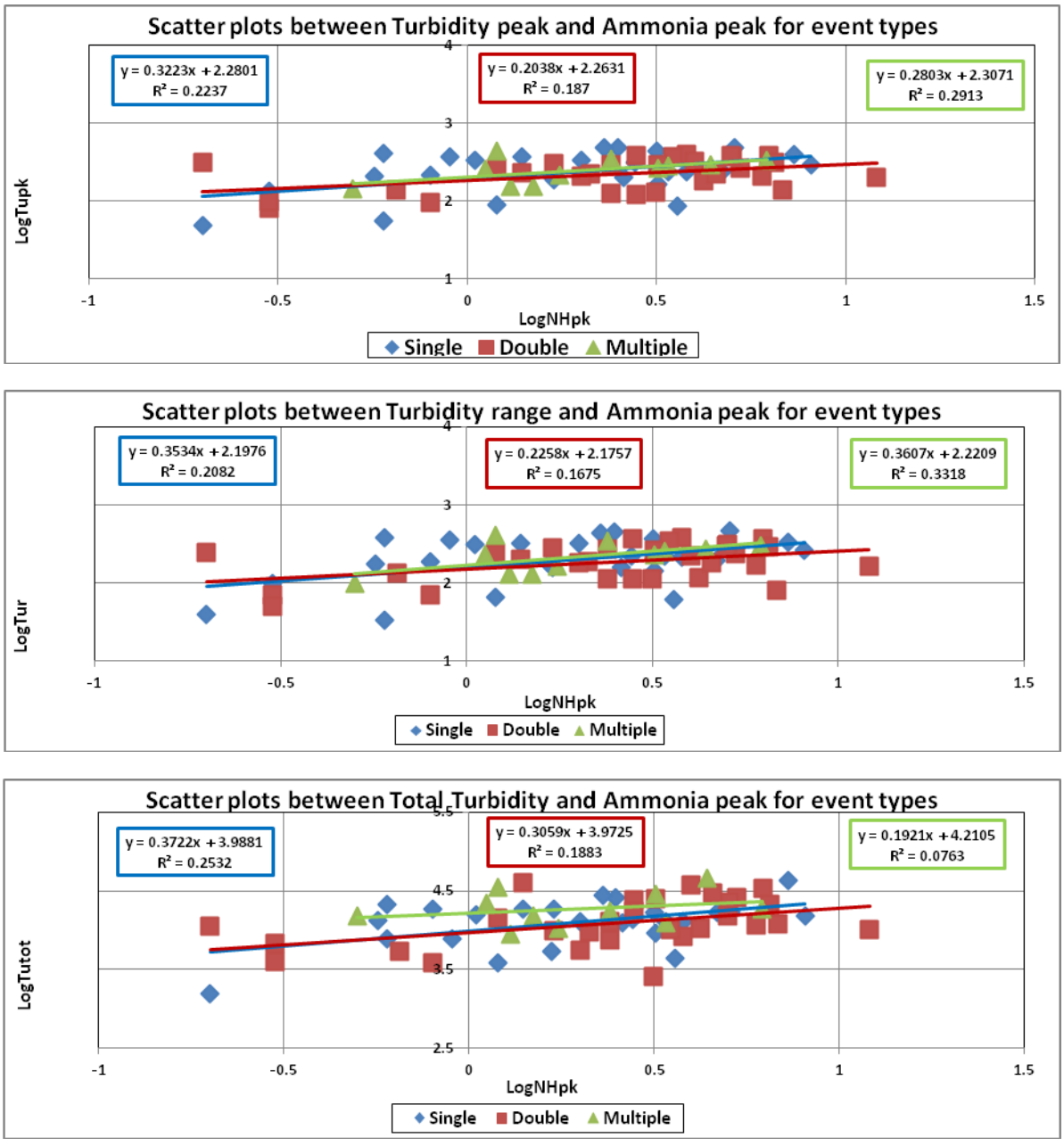

Figure 4.13: Scatter plot of turbidity attributes with ammonia peak for Single, Double and Multiple flow peak events respectively: (a) LogTupk with LogNHpk; (b) LogTur with LogNHpk; (c) LogTutot with LogNHpk.

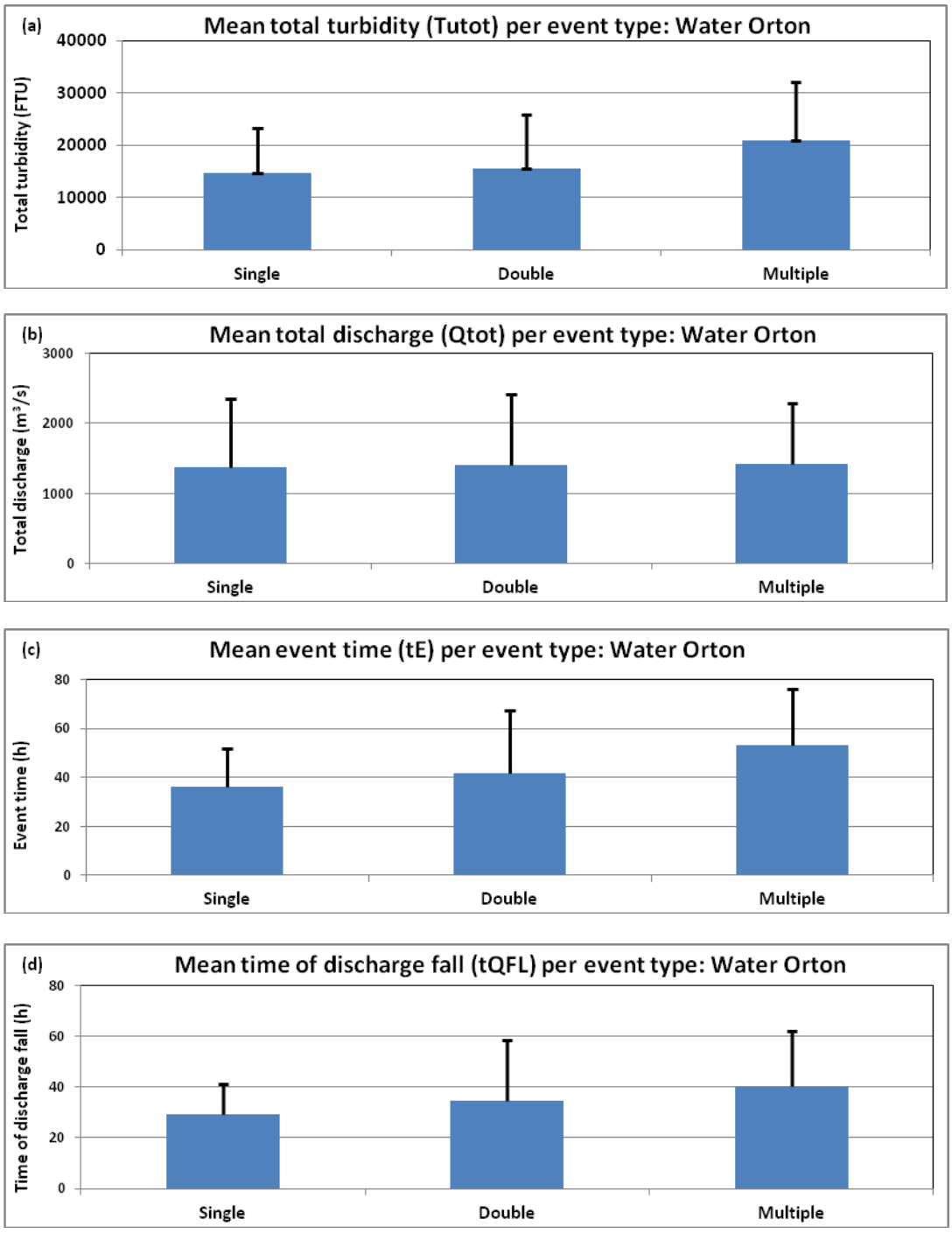

Figure 4.14: Means of events attributes for Single, Double and Multiple flow peak events: (a) Total turbidity; (b) Total discharge; (c) Event time; (d) Time of discharge recession showing error bars of standard deviation.

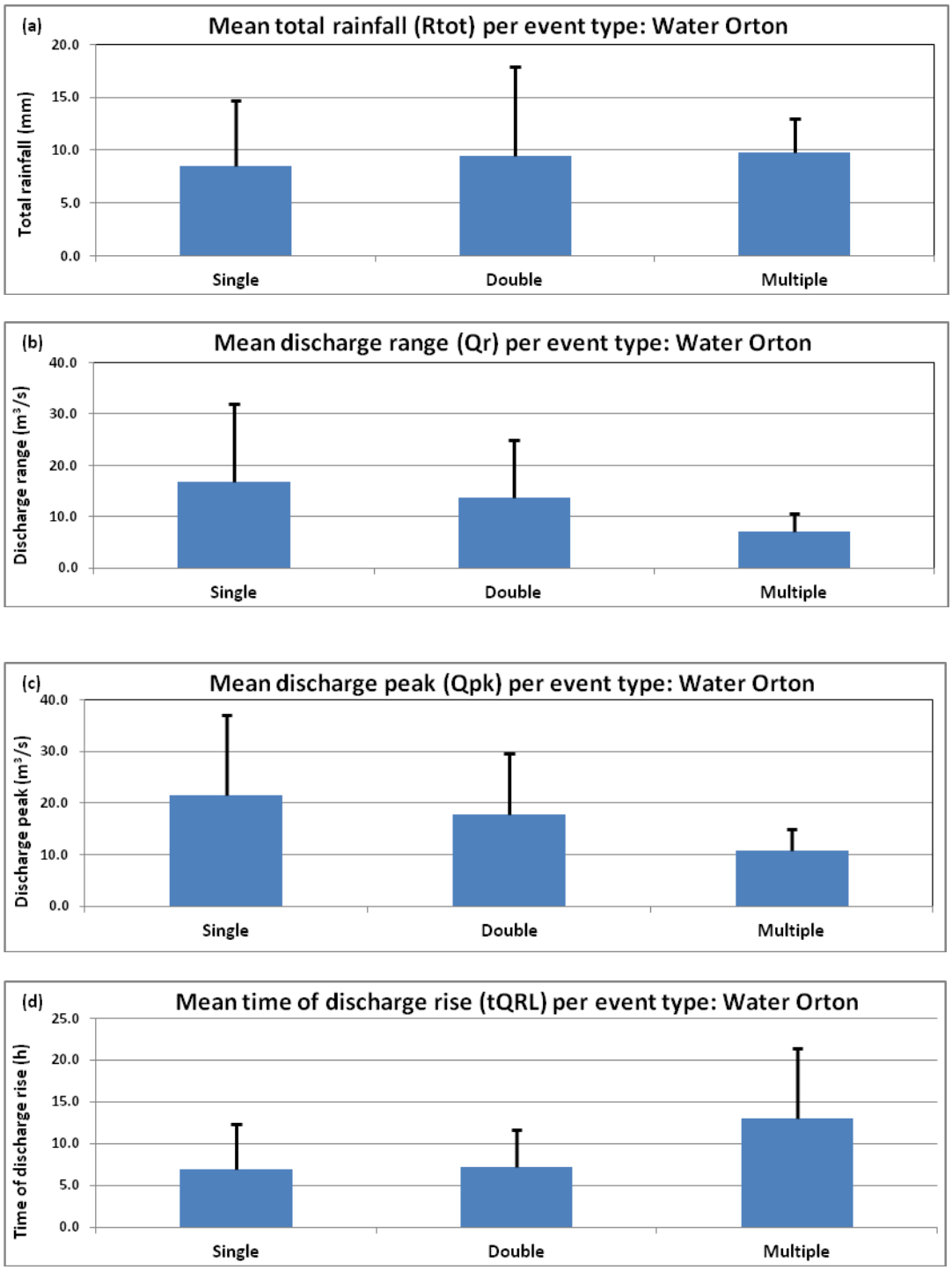

Figure 4.15: Means of events attributes for Single, Double and Multiple flow peak events: (a) Total rainfall; (b) Discharge range; (c) Discharge peak; (d) Time of discharge rise showing error bars of standard deviation.

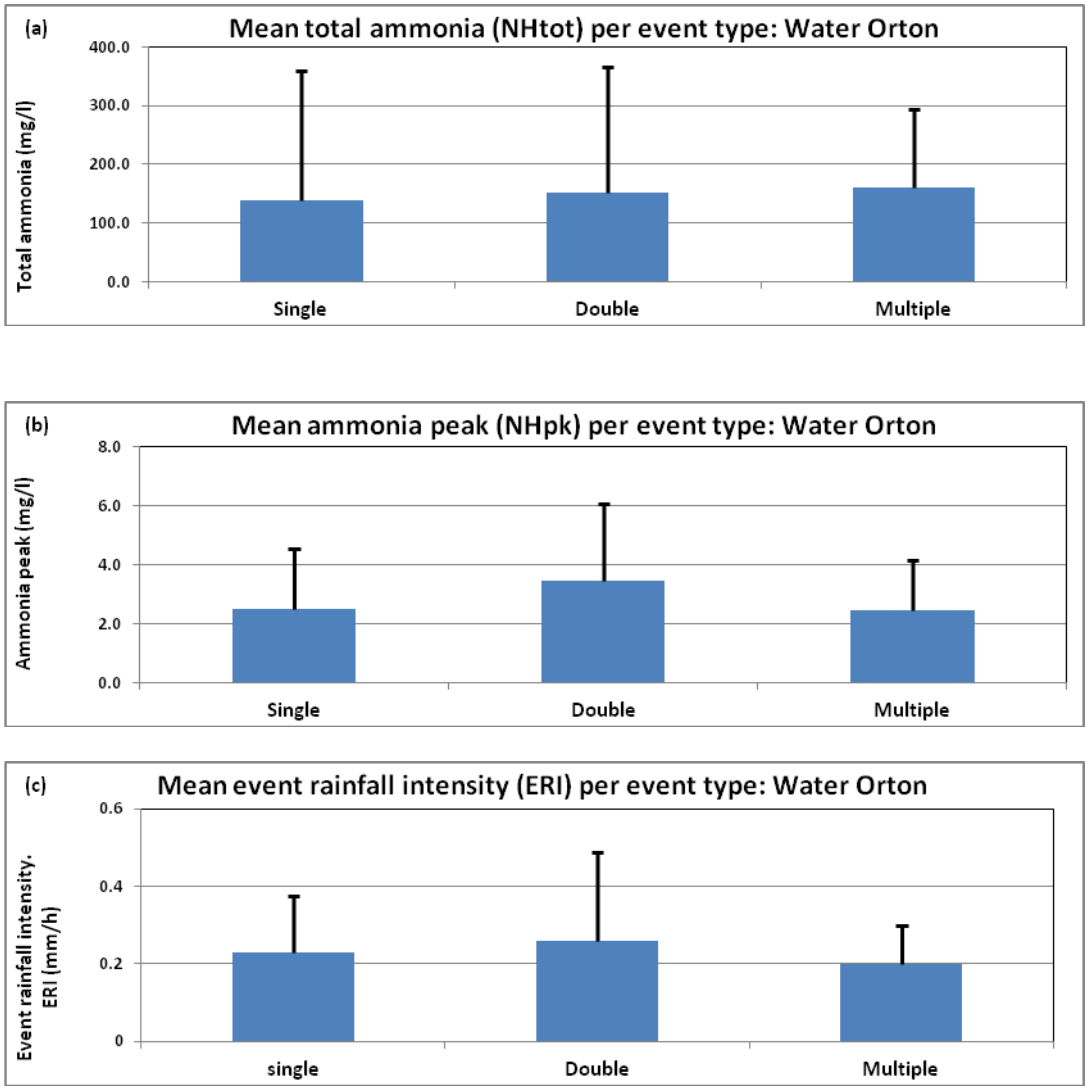

Figure 4.16: Means of events attributes for Single, Double and Multiple flow peak events: (a) Total ammonia; (b) ammonia peak; (c) Event rainfall intensity showing error bars of standard deviation.

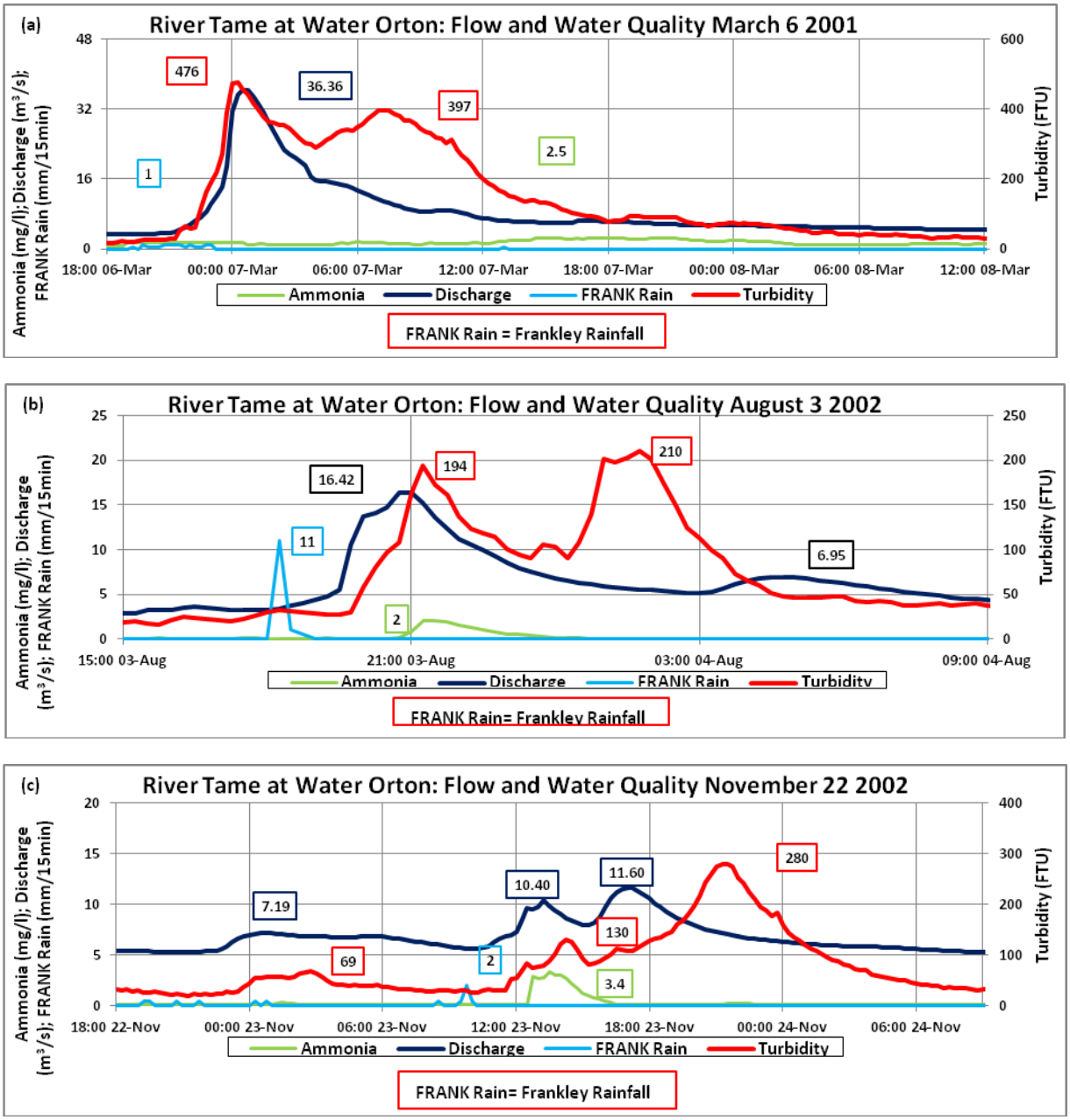

Figure 4.17: Time series of a (a) single flow peak with double turbidity peak, (b) double flow peak with double turbidity peak (c) multiple flow peak with multiple turbidity peak events.

4.5 Discussion

Generally, both flow and turbidity regimes are flashy with the mean rising times less than 12 hours for all event types. This is concurrent with past definitions of flashy catchments having a flow rise time of less than 24 hours (Lim, 2003), hydrograph recession times of between 1-3 days for River Tame (Rivett et al., 2011) or a short time to peak that may last only a matter of hours (Webster et al., 2001; Peters, 2009; Huey and Meyer, 2010). Among the numerous causes of flashiness given in Chapter 2.2.2, the possible cause within the studied catchment could include the high urban cover with high proportion of impervious surface and engineered catchment of higher drainage or channel density, leading to efficient routing of runoff during rain storm.

Single flow peak events are the norm in turbidity dynamics analysis.

Little has been published regarding the analysis of double and multiple flow peak events as distinct events in previous event-based turbidity/suspended sediment studies focused on single peak events (Jansson, 2002; Lefrançois et al., 2007; Duvert et al., 2010; Furusho et al., 2010). Such events are largely referred to with regard to the exhaustion of sediment in successive storms as given in Chapter 4.2 (Lawler et al., 2006; Herman et al., 2008; Horowitz, 2008; Duvert et al., 2010). However, the double and multiple flow peak events together constitute more than 60% of events within the studied catchment (Table 4.2 (a); Figure 4.5 (a)). As a result, the current focus on single 'textbook' storm events without characterising them could be missing key event attributes and result in an incomplete understanding of the primary control and processes that regulate urban river turbidity dynamics. Therefore, single events have been

found not to, and should not, be the only event type used in analysing urban catchment turbidity dynamics.

Single discharge peak events are considered to result principally due to the urbanised impervious surfaces contributing to runoff mostly during single rain storms (Furusho et al., 2010). Secondary discharge peaks (double/multiple) could be indicative of tributary contributions, associated with within-catchment storm unevenness and/or runoff from far sources and/or arrival of flow from more distal or less well-connected sediment reservoirs at different times (Rovira and Batalla, 2006; Reed et al., 2010).

Whilst differences were observed between attributes within single, double and multiple events (Figure 4.5 (b) and (c) and Figure 4.5), such differences were not significant (Table 4.2 (a)). However, the relationship between different event attributes did vary significantly between multiple events and both single and double events. There is a significant control of event type on the gradient of the relationships between turbidity peak and discharge, and turbidity range and discharge, as well as on the intercept of the relationship between total turbidity and discharge and ammonia peak. Further, the event type (notably multiple event type) had a significant effect on the gradient of the following relationships: turbidity peak-discharge range (significantly higher with $p<0.05$); turbidity range-discharge range and peak (significantly higher with $p<0.05$ respectively). It also impacted the intercept of the following relationships and on the intercept of total turbidity-discharge total, range, peak and ammonia peak regression lines (significantly higher with $p<0.05$ respectively) (Table 4.9 and Table 4.10; Figure 4.12 and Figure 4.13).

The gradient and intercept of suspended sediment-determinand regression lines represent the rate of change and availability of the suspended sediment with respect to the determinand respectively (Rovira and Batalla, 2006). Multiple flow peak events increase the rate of change of turbidity peak and range with respect to discharge peak, and availability of total turbidity with respect to total discharge and ammonia peaks. The results presented here therefore suggest that analysing suspended sediment or turbidity with single flow peak events alone could lead to underestimating the rate of change and material availability with respect to the determinands.

Rain events generate surface runoff and transport available suspended sediment into stream channels (BaČA, 2008). The area close to the stream channel starts contributing runoff first and increases from the time the hydrograph starts rising until it reaches the peak. The area contributing runoff is influenced by the event time (BaČA, 2008). Thus, by inference, the multiple flow peak events having highest mean event time likely have the largest area contributing runoff, thus highest total flow to the stream compared with single and double flow peak events (Figure 4.14). The main driving force of turbidity magnitude in temporal context is discharge (Conrad and Saunderson, 2000), with other attributing factors such as land use (urban imperviousness) and availability of erodible materials influencing magnitude of materials transported. In urban catchments, total stream flow results largely from total surface runoff (Lazaro, 1990) as subsurface runoff contribution from water storage is limited due to high imperviousness (Webster et al., 2001; Lawler et al., 2006). Therefore, for a given discharge, the availability of total turbidity sources is

significantly higher for multiple than for single and double flow peak events (Figure 4.12(c)).

The multiple flow events with the largest contributing area could have the highest total surface runoff and hence the highest potential turbidity source. The high material availability of multiple events, inferred from significant increase in the intercept of both the relationship between total turbidity and total discharge, and the relationship between total turbidity and ammonia peak, provides evidence for the above. Ammonia is important as a surrogate for organic pollution from point (domestic sewage, industrial waste) and/or non-point (fertilizer runoff) sources (Chapman, 1996). Such extended sources of sediment could explain the higher turbidity peak and range of multiple events at a given discharge. Thus, at the same discharge, sediment availability is significantly higher for multiple than single and double discharge peak events.

Urban river systems exhibit more clockwise events.

Relative peak occurrence was used to evaluate events with turbidity peaks leading (clockwise), lagging (anticlockwise) and coinciding with discharge peaks. The results show that the lag (anticlockwise) events are more frequent (52% for 34 events) than the lead events (clockwise; 42% for 28 events) in the studied catchment (Table 4.3(a); Figure 4.6(a)). However, the difference is not statistically significant (Table 4.3(b) and (c)). The percentage clockwise and coinciding peaks events increase from the lowest of 38 and 4% for the single events to the highest of 55 and 9% for the multiple events. In comparison, the anticlockwise events decrease from the highest of 58% for the single to the

lowest of 36% for the multiple flow peak events (Table 4.3(a); Figure 4.6(b), (d)). In spite of the insignificant differences due to low numbers per event types, this result is contrary to findings of many researches which report more clockwise than anticlockwise events (Goodwin et al., 2003; Rose, 2003; Rovira and Batalla, 2006; Lefrançois et al., 2007; Landers and Sturm, 2013). Few have reported anticlockwise events (Goodwin et al., 2003; Lefrançois et al., 2007). These could, thus, show that urban rivers do not always exhibit more clockwise events.

The lead lag of a single flow peak with single turbidity peak can be easily classified. However, the classification of an event which has multiple turbidity peaks for a single flow peak (Figure 4.17(a) to (c)) is more challenging. Here the highest peaks regarding both discharge and turbidity were used to determine the lead/lag/co events. For the March 6th 2001 event (Figure 4.17 (a)), the discharge peak lags the first and higher turbidity peak, which was taken to determine the event type, although it was followed by a lower turbidity peak. Thus the event was classified as a turbidity peak leading discharge peak (clockwise), with the net process effect of remobilisation and transport, without deposition, of in-channel deposited material whose amount is limited during the event and within the flow range involved (Jansson, 2002; Lefrançois et al., 2007). For the August 3 2002 double discharge peak event (Figure 4.17 (b)), the first and lower turbidity peak lags the first and higher discharge peak, while the second and higher turbidity peak leads the first and lower turbidity peak. Thus the event, as well as the November 22nd 2002 event (Figure 4.17 (c)), were classified as turbidity peak lagging discharge peak (anticlockwise) since

the major turbidity peak lags the major discharge peak, with the net process effect of in-channel deposition of material (Jansson, 2002; Lefrançois et al., 2007). Events in which the major turbidity peaks coincide with the major discharge peaks are classified as such with the net process effect of only mobilisation and transport without deposition, of materials whose amount is not limited during the event and within the flow range involved (Jansson, 2002; Lefrançois et al., 2007). As such, further developments are required to enhance the current systematic, quantitative approach of event classification to effectively characterise hysteresis in the complex multi-peak nature of urban storm events.

Despite limitation in the classification approach, the more anticlockwise than clockwise events identified could partly result from low discharge events. Single events with the highest percentage number of anticlockwise events (Table 4.3(a); Figure 4.6) had the lowest mean total discharge (Figure 4.14(b)). The number of anticlockwise events decreases as the mean total discharge increases from single to multiple events. Low energy conditions associated with low discharge could result in sediment deposition (Jansson, 2002; Lefrançois et al., 2007) as well as picking up of in-channel sediment and quick re-deposition in the upstream reaches (Estrany et al., 2011), and are mostly associated with anticlockwise events. The mean total discharge increases from single to multiple events (Figure 4.14(b)). Increasing total discharge could lead to increasing stream erosive/remobilisation and transport capacity (Lefrançois et al., 2007), and conversely result in decrease in stream deposition capacity. Dilution, a major hydrological process within all water bodies including rivers

(Bartram and Ballance, 1996), is described as a process in which concentration decreases with increasing flow (Moravcova et al., 2009). This could also be a potential cause of increasing number of clockwise events from single to multiple events, as many causes have been attributed to clockwise hysteresis including the later dilution with water from tributaries (Jansson, 2002). There are many tributaries feeding into the Water Orton monitoring station (Table 3.1; Figure 3.2). In addition to the factors discussed above, other catchment characteristics could result in the more anticlockwise events found. The zone of the river within which the monitoring site is located with its peculiar characteristics, as well as vegetation, could be possible factors. The downstream, lowland zones of rivers usually have gentle slopes and meandering stretches, both conducive for deposition of sediments (Gordon et al., 2013), possibly because of loss of energy. Also, vegetation growth observed in the catchment could trap sediment, result in reduced rate of runoff and total discharge (energy), possibly due to increased infiltration, thus favouring deposition of materials (Goodwin et al., 2003). The deposition of materials have been associated with anticlockwise events (Jansson, 2002; Lefrançois et al., 2007). Therefore, the gentle slope, meandering stretches and vegetation growth together favour deposition and could explain the more anticlockwise events observed.

Turbidity is influenced by the ability of a river for the transport and also on the availability of sediment (Lefrançois et al., 2007). For a given ability of a river to transport sediment which depends on its discharge, changes in turbidity is determined by sediment availability (Lefrançois et al., 2007). The ability of a river to transport sediment increases with increasing discharge, but if the

sediment amount is low then turbidity may decrease. Also, decreased discharge decreases the stream transport capacity, but turbidity may increase if availability of sediment increases (Lefrançois et al., 2007). These phenomena are referred to as supply-limited and transport- limited sediment dynamics (Holden, 2005). As transport and deposition of fine suspended sediment (wash load) depend in part on the availability of readily transportable sediment, changes in soil erosion, that could be caused by climatic change, may subsequently affect sediment transport and floodplain deposition rates (Asselman et al., 2003).

Clockwise events are mostly associated with high discharge possibly as a result of large storm events, with other possible causes as flushing and exhaustion of sediment, dilution of sediment with increased flow downstream or from tributary contribution and reduction in rainfall erosivity (Goodwin et al., 2003; Lefrançois et al., 2007; Stubblefield et al., 2007; Smith and Dragovich, 2009). Anticlockwise events are mostly associated with low discharge possibly as a result of small storm events, with other potential causes as lack of bed sediment supply, sediment from distal sources coming in late due to sediment peaks lagging flow peaks resulting from their different times of travel and sediments from distant, upper parts travelling a long distance without temporary deposition (Asselman et al., 2003; Lawler et al., 2006; Moravcova et al., 2009; Smith and Dragovich, 2009; Duvert et al., 2010).

Thus, some of the possible causes of the trend of less clockwise than anticlockwise events, with the clockwise and coinciding events increasing from single to multiple events are increasing discharge, dilution effects as well as turbidity/sediment availability. Also, some of the possible causes of the trend of

more anticlockwise than clockwise events, with the anticlockwise events decreasing from single to multiple events are decreasing/low discharge, late arrival of external sediment sources due to differences in relative travel times as well as distal sediment sources.

More of turbidity than discharge peaks is observed within a substantial proportion of events

More turbidity than discharge peaks were observed in 36% of total events (Figure 4.10). This constitutes more than a third of all events analysed and could, as such, be considered substantial. Events with the number of turbidity peaks greater than the number of discharge peak and those with number of turbidity peaks less than or equal to the number of discharge peaks respectively decreases and increases from single to multiple events (Table 4.6(a); Figure 4.9(a)). The pattern of events with turbidity peaks less than or equal to discharge peaks increasing from minimum with single to maximum with multiple flow peak events is similar to that of turbidity peaks leading and coinciding with discharge peaks (Table 4.3(a); Figure 4.6(b) to (d)) and the mean total discharge (Figure 4.14(b)). The increasing mean total discharge from single to multiple events, in addition to increasing the erosive and transport and decreasing deposition capacities of clockwise events and decreasing the erosive and transport and increasing deposition capacities of anticlockwise events respectively, could also lead to increasing discharge water for dilution. Thus, dilution by more water through tributary contributions of double and multiple events could partly be responsible for the decreasing number of more turbidity than discharge peaks by neutralising low turbid arriving late, resulting in

the less or equal number of turbidity peaks. Secondary sediment pulses independent of flow could possibly come from subsequent storms related to variability of rainfall across the catchment and/or arrival of flow from more distal or less well-connected sediment reservoirs at different times, and/or late sediment supply from tributaries (Rovira and Batalla, 2006; Reed et al., 2010).

On the average, more than half (59%, 39 events) of the total events had peak ammonia concentrations more than 2mg/l (Table 4.6(b); Figure 4.9(b)). This could indicate that effluent spillage is an issue in the catchment since ammonia concentrations could point to effluent spillage from CSOs, which are indicators of important and severe urban river water pollution (Lawler et al., 2006). Mostly, total ammonia concentrations for surface waters are less than 0.2mg/l but can be up to 2-3mg/l. Organic matter pollution found in domestic sewage or industrial waste, as well as distal erosion with exchangeable ammonia and/or fertilizer runoff, can lead to concentrations more than 2mg/l during wet-weather events (Chapman, 1996; Old et al., 2003b). Figure 4.11 has shown that, above the used ammonia peak threshold of 2 mg/l, total suspended sediment concentration significantly increased with increasing total ammonia within the Water Orton catchment. It is already proven that multiple events significantly increase the intercept of total turbidity-ammonia peak regression lines, which could be interpreted as significant increase in turbidity availability with respect to ammonia peak (Table 4.10; Figure 4.13(c)). Thus, effluent spillage is a significant issue with multiple flow peak events in the catchment. It is reported to receive significant discharge from sewage treatment plants (Rivett et al., 2011). There are 374 CSOs in the Tame catchment (Table 3.1) (Tame, 2010).

However, the pattern of the maximum with double and minimum with multiple events is similar to that of the event rainfall intensity (ERI, mm/h) defined as event total rainfall divided by event time (Figure 4.16(c)), which could also indicate that effluent spillage is based on rainfall intensity, and that the higher the intensity, the more frequent the spillage.

The distribution of events with higher number of turbidity than discharge peaks having peak ammonia concentration greater than or equal to 2mg/l also showed a similar pattern of maximum with double and minimum with multiple events. Thus, events with higher number of turbidity than discharge peaks could as well partly be due to effluent spillage, since on the average, 75% of such events were associated with peak ammonia concentration greater than or equal to 2mg/l (Table 4.6(c); Figure 4.9(c)). Spills could partly explain secondary turbidity peaks (Old et al., 2003b; Lawler et al., 2006). These spills may reach rivers if quantities of runoff resulting from rain event are higher than capacities the facilities are designed for providing substantial quantity of water and sediment when flows are high) (Old et al., 2006), probably getting to the tail end of the event after they have surcharged during long, high intensity rain events (Old et al., 2003b; Lawler et al., 2006).

4.6 Chapter summary

Single flow peak events have mostly been used in turbidity dynamics analysis. Results from this study showed more double and multiple together than single flow peak events within the catchment, thus implying analysing only single flow peak events or without characterising events could be missing key event processes. Double and multiple peaks have previously not been analysed

because they were deemed complex (Lefrançois et al., 2007). Multiple flow peak events showed significant increase in the rate of change of turbidity peak and range with respect to discharge peak, and availability of turbidity total with respect to discharge total and ammonia peaks respectively. This could mean analysing suspended sediment or turbidity with single flow peak events alone could lead to underestimating rate of change and material availability with respect to the various determinands. These could also be due to the multiple flow peak events having largest area contributing runoff as inferred from the event time. The study also showed more anticlockwise events within the catchment which is contrary to findings of many studies reporting more clockwise events. The gentle slope, meandering stretches and vegetation within the downstream river zone studied could support deposition and, thus partly explain this. The anticlockwise events decreased while the clockwise and coinciding events increased from single to multiple events. These could possibly be due to decreasing and increasing total discharge that could lead to decreasing and increasing dilution effects respectively. Also, more than a third of total events had more number of turbidity peaks than number of discharge peaks possibly due partly to dilution effects as well as effluent spillage which have been shown to be more frequent for higher intensity rain storms.

CHAPTER 5 SEASONALITY OF EVENTS DOWNSTREAM AN URBAN RIVER CATCHMENT

5.1 Chapter Introduction

This chapter examines the seasonality of turbidity responses to storm events downstream of an urban river. This second results chapter addresses the second research objective outlined in Chapter 1. The chapter consists of six main sections. It is first introduced and a brief literature background provided, leading to the objectives of the chapter. The methodological approach is then outlined. The study area, data (quantity and quality), quantification of event selection criteria and classification of events are the same as for Chapter 4. Methods used are described. The results section then gives the findings of the work, followed by the discussion and then the chapter summary.

5.2 Literature background

Drivers, controls and processes of turbidity dynamics in response to rain event events are not static but change with respect to different types of events as well as with time. Chapter 4 dealt with event characterisation and turbidity changes with respect to different attributes for the events types. It also looked at the effects of these event types on turbidity dynamics. It was seen that one particular event type (single, double, multiple) was not significantly more recurrent. Further, the event attribute means were not significantly different between event types. A number of events attributes had statistically significant correlations with turbidity attributes. The correlations between turbidity and key event attributes were shown to vary significantly between event types indicating

an alteration to the drivers, controls and/or processes between the different event types. However, such analysis took no account of the seasonal variation in the processes and controls on turbidity-discharge dynamics.

As has been confirmed by studies given below and summarised in Table 5.1, the discharge and other determinants as well as associated attributes change seasonally. Seasonal assessment of hydrologic responses gives more detailed information than mean annual flow values which tend to mask catchment dynamics (Hannaford and Buys, 2012). Changes during the seasons influence water parameters' quantity and quality. Evapotranspiration rate is highest in summer, a season during which base flow of rivers is lowest (Peters, 2009). Low streamflow during the dry season leads to increased point source pollution contaminants concentrations. This results from reduced diffuse sources during the dry season within urban catchments (Yunus and Nakagoshi, 2004). Further, during dry weather, pollutant level of gully pot liquor increase and impacts negatively on surface storm runoff during wet weather processes (Taylor and Owens, 2009). Highly contaminated sediment also accumulate in sewers during low flows and remobilised and transported during storm events (Goodwin et al., 2003).

Storm events with specific duration and intensity are normally not distributed evenly over a year, but are more frequent in some seasons than others (Mueller and Pfister, 2011). Rapid runoff generated from impervious areas by summer storms result in significant delivery of nutrients during ecologically sensitive periods (Edwards and Withers, 2008). Also strong seasonal changes for suspended sediment from urban road runoff with manifold mean concentration

increases during melt season being multiples of the corresponding concentrations during rainy season (Helmreich et al., 2010).

Seasonal variations in turbidity-discharge relationships have been observed within the Yangtze River. Both upstream and downstream parts of the Yangtze River show seasonality in flow and sediment transport during summer monsoons (Xu and Milliman, 2009). Seasonal SSC~Q hysteresis forms may be influenced by flow and erosion conditions which change seasonally (Landers and Sturm, 2013). Annual flow and sediment discharge were pronounced in the urbanised sections in summer, an indication of seasonal changes downstream (Old et al., 2006). High impervious cover and manmade drainage systems caused efficiently routing of rainfall during summer and winter (Old et al., 2006).

Examining the seasonal variation in discharge turbidity dynamics provides the opportunity to explore and examine the importance of specific sediment entrainment, transport and deposition processes at the catchment scale. This chapter, therefore, aims at exploring the seasonality in the characteristics of the storm events by analysing the following hypotheses.

1. High urban extent significantly influences catchment turbidity dynamics.
2. Seasons with varying discharge (hydrological conditions) cause significant variations in turbidity.
3. Effluent spillage significantly affects seasonal turbidity dynamics.
4. Significantly more anticlockwise events are associated with seasons with more low flows.

Table 5.1: Seasonal effects on variables and attributes in the literature

Variable/attribute	Effect	Reference
Hydrological responses	Seasonal assessment gives more detailed information than mean annual flow values	Hannaford and Buys, 2012
Stream quality and quantity	The concentrations of point source contaminants increase during dry seasons due to low flow resulting from low rainfall and runoff; wet season runoff increases pollution from non-point sources in urban catchments	Yunus and Nakagoshi, 2004
Storm runoff quality	Increased dry weather gully pot liquor pollutant level impacts negatively on surface storm runoff during wet weather processes	Taylor and Owens, 2009
Sewer sediment	Highly contaminated sediment could accumulate in sewers during low flows and remobilised and transported during storm events	Goodwin et al., 2003
Storm events	Storm events with specific duration and intensity are normally not distributed evenly over a year, but are more frequent in some seasons than others	Mueller and Pfister, 2011
Nutrient and SS quantity	Relative contributions of nutrient and suspended sediment sources are seasonal. Rapid runoff	Edwards and Withers,

	generated from impervious areas by summer storms could result in significant delivery of nutrients and suspended sediment during ecologically sensitive periods	2008
Urban road runoff	Strong seasonal changes for suspended sediment from urban road runoff with manifold mean concentration increases during melt season being multiples of the corresponding concentrations during rainy season	Helmreich et al., 2010
Turbidity and stream flow	Urbanization could cause increased concentrations of suspended sediment -related constituents such as turbidity and suspended sediment as well as nutrient with increasing stream flow	Peters, 2009

5.3 Methodology

5.3.1 Study area and data

The study area, data quantity and quality, event selection criteria and classification of events are the same as discussed in sections 4.3.1 through 4.3.3 (Chapter 4).

5.3.2 Analytical techniques

Monthly and seasonal mean attributes were determined for the 66 events characterised and classified in Chapter 3 and Chapter 4. These event characteristics were further subdivided into single, double and multiple flow peak events as well as events with turbidity peak leading, lagging and coinciding with discharge peaks. Chi-square tests, analysis of variance (ANOVA) and t-tests were applied to quantify the significance of observed differences in attributes between the seasons. Regressions between turbidity and discharge attributes were determined to identify a) significant relationships and b) those relationships that varied significantly between seasons. Logistic multiple linear regressions were performed between turbidity and the other significantly correlated attributes so as to identify the influence of the seasons on the turbidity attributes. The means of the significantly correlated attributes were determined to help unravel the emerged patterns. Column charts of attribute means with error bars of the standard deviations were prepared to show the variation in their distributions.

5.4 Results

5.4.1 Characteristics of general time series data (monthly and seasonal)

Seasonally, the highest and lowest mean turbidity, discharge, rainfall total, and ammonia were in winter and autumn, winter and summer, autumn and summer, and winter and spring respectively (Figure 5.2).

The highest average monthly turbidity was observed in January (Figure 5.1a). In subsequent months to May the average monthly turbidity decreased. It then increased till July and decreased to the lowest average monthly value in September. The average monthly turbidity subsequently increases again to the highest turbidity in January. The average month discharge shows a very similar pattern to turbidity (Figure 5.1b). Like turbidity, the average monthly discharge is at its lowest values in September and increases subsequently to its highest value in January, then decreasing till the lowest in September. Total rainfall is lowest in August (Figure 5.1c). Rainfall subsequently increases to the monthly high in October and fluctuates slightly within subsequent months (almost constant) till the lowest in August. Ammonia is lowest in June (Figure 5.1d), increases till August, the third monthly highest, and then decreasing till the second lowest in October. It then increases to the highest in December and then decreases till the lowest in June (Table 5.2; Figure 5.1).

Table 5.2: General mean turbidity (Tu), mean ammonia (NH_3), mean discharge (Q) and total rainfall for: (a) Monthly and (b) Seasonal time scales.

(a)	Tu (FTU)	NH_3 (mg/l)	Q (m^3/s)	R (mm)
March	54.33	0.49	4.83	147.5
April	58.52	0.42	5.04	207
May	42.43	0.35	4.36	198
June	49.20	0.30	3.74	172.5
July	57.78	0.43	4.17	222.5
August	48.91	0.98	3.15	98
September	28.16	0.49	2.94	118.5
October	45.08	0.34	5.01	311.5
November	41.97	0.81	4.85	206.4
December	54.58	1.24	5.46	212.9
January	82.82	1.01	5.91	226.6
February	65.32	0.65	5.52	157.6
Mean	**52.43**	**0.63**	**4.58**	**189.92**

(b)	Spring	Summer	Autumn	Winter	Mean (mm)
Turbidity	51.69	51.99	38.48	67.64	**52.45**
Ammonia	0.42	0.57	0.55	0.98	**0.63**
Discharge	4.74	3.69	4.28	5.64	**4.58**
Rainfall	552.5	493	636.4	597.1	**569.75**

5.4.2 Events type distribution

The seasonal distribution of the 66 events characterised and classified in Chapter 4 as single, double and multiple flow peak events are presented (Table 5.3 (a), Figure 5.3(a)). The highest number of observed events occurs in spring ~30%, with the lowest in summer ~20% (Table 5.3 (a), Figure 5.3(b)). Single events were highest in spring and winter, while double events were highest in summer and autumn (Figure 5.5). Within spring, 35% of events are single, 17% double and 55% multiple. In comparison, within summer, 12% of events are single, 34% double and only 9% of events are multiple.

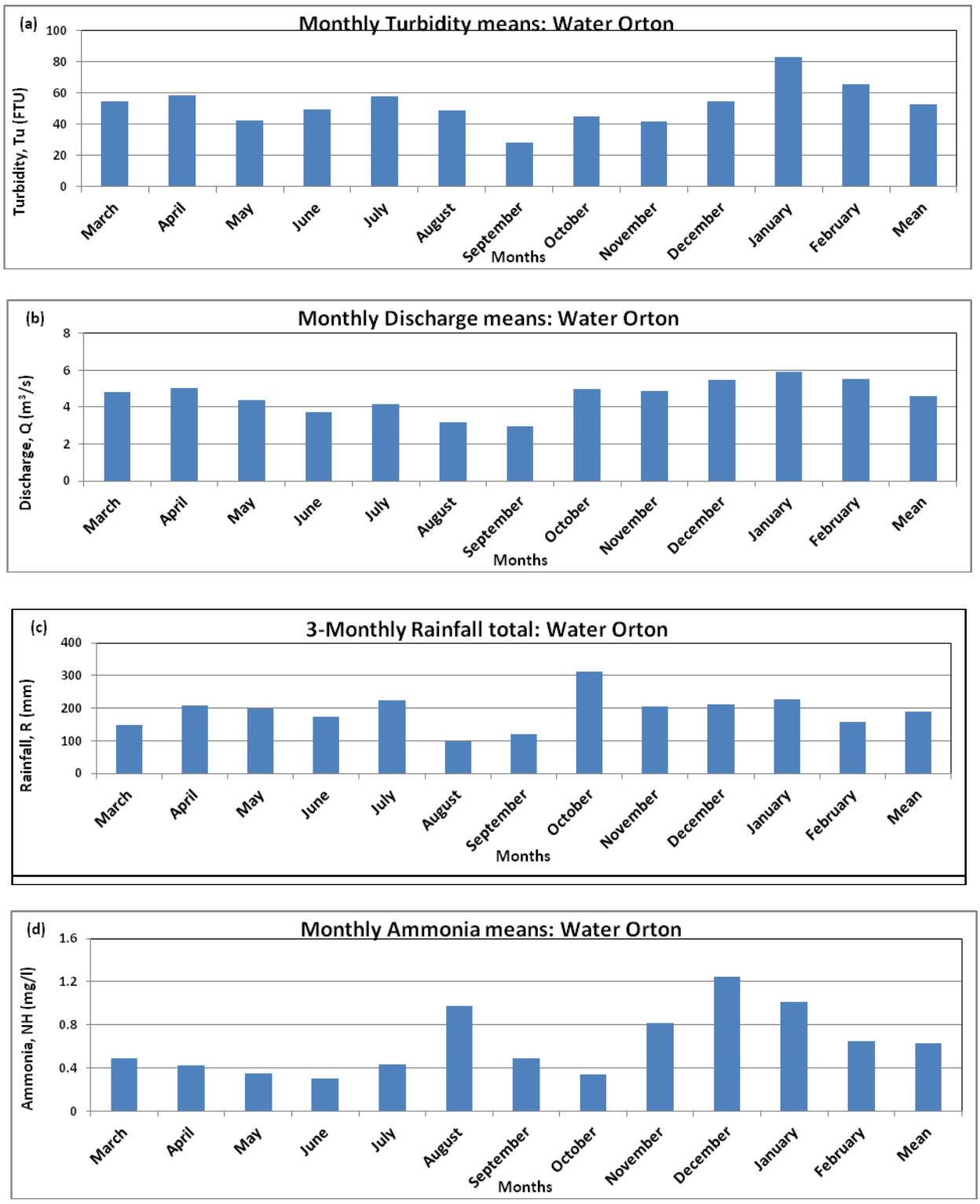

Figure 5.1: Monthly Means of instantaneous values of attributes for all data: (a) Turbidity; (b) Ammonia; (c) Discharge; (c) Rainfall. (d) Ammonia.

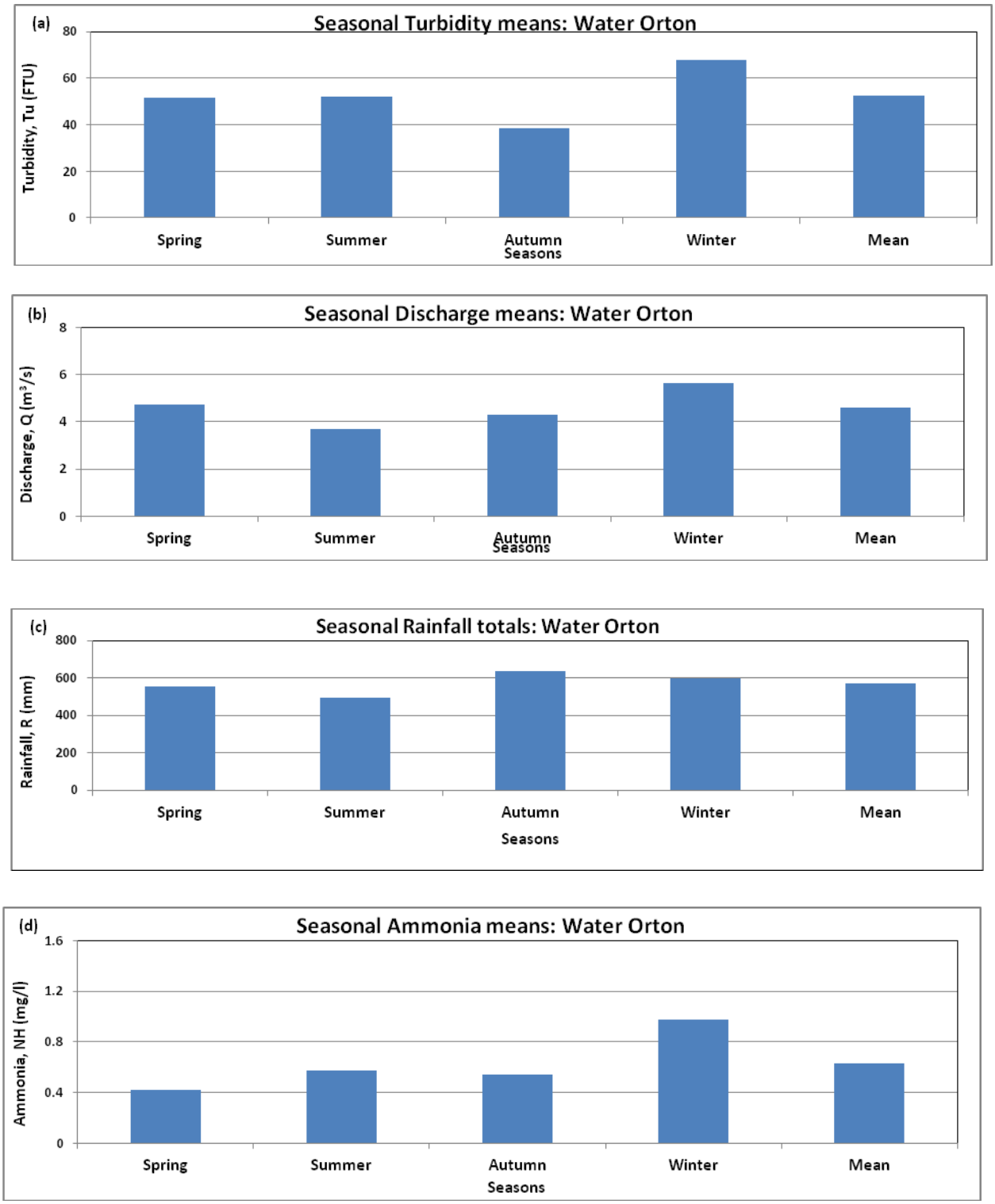

Figure 5.2: Seasonal Means of instantaneous values of attributes for all data:

(a) Turbidity; (b) Discharge; (c) Rainfall total; (d) Ammonia.

Table 5.4 (a) shows the seasonal distribution of single, double and multiple flow peak events. Due to the low number of events within the separate classes, Chi-square analysis was not valid to determine whether the occurrence of different event types as equally likely between seasons. Thus double and multiple events were combined. Results show that the distributions of events among the seasons did not differ significantly (p=0.46, n=66, df=3) (Table 5.4Table 5.4(b)).

5.4.3 Seasonal distribution of turbidity peaks

Turbidity peaks leading and coinciding with discharge peaks occur most frequently within spring. The least frequent occurrence of a leading and coinciding turbidity peak is within autumn and/or winter (Figure 5.6). Turbidity peak lagging discharge peak occurs most frequently within winter and least frequently within autumn (Table 5.5, Figure 5.6). Autumn has events with turbidity peak lagging discharge peak equal to those with turbidity peak leading and coinciding with discharge peak together (Table 5.5, Figure 5.7). Chi-square test with lead, lag and coincidence events as separate categories was not valid due to the low number of events within the different categories. However, when lead and coincidence events were combined (LdCo), it made test valid (Table 5.5(b)). Results show that the distributions of events did not differ significantly between seasons.

Table 5.3: Events type distribution: (a) Overall; (b) Seasonal; (c) Chi-square test for event type distribution within the seasons.

(a) Event	2001	%	2002	%	2003	%	Overal	%
Single	7	31.82	12	46.15	7	38.89	26	39
Double	11	50	12	46.15	6	33.33	29	44
Multiple	4	18.18	2	7.69	5	27.78	11	17
Total	22	100	26	100	18	100	66	100

(b) Event	Season	2001	%	2002	%	2003	%	Overall	%
Single	**Spring**	5	71.43	2	16.67	2	28.57	9	34.62
	Summer	1	14.29	1	8.33	1	14.29	3	11.54
	Autumn	0	0	5	41.67	1	14.29	6	23.08
	Winter	1	14.29	4	33.33	3	42.86	8	30.77
	Total	7		12		7		26	100
		2001	%	2002	%	2003	%	Overall	%
Double	**Spring**	5	45.45	0	0	0	0	5	17.24
	Summer	4	36.36	4	33.33	2	33.33	10	34.48
	Autumn	1	9.09	6	50	0	0	7	24.14
	Winter	1	9.09	2	16.67	4	66.67	7	24.14
	Total	11		12		6		29	100
		2001	%	2002	%	2003	%	Overall	%
Multiple	**Spring**	3	75	1	50	2	40	6	54.55
	Summer	1	25	0	0	0	0	1	9.09
	Autumn	0	0	1	50	1	20	2	18.18
	Winter	0	0	0	0	2	40	2	18.18
	Total	4		2		5		11	100
		2001	%	2002	%	2003	%	Overall	%
Overall	**Spring**	13	59.09	3	11.54	4	22.22	20	30.3
	Summer	6	27.27	5	19.23	3	16.67	14	21.21
	Autumn	1	4.55	12	46.15	2	11.11	15	22.73
	Winter	2	9.09	6	23.08	9	50	17	25.76
	Total	22	100	26	100	18	100	66	100

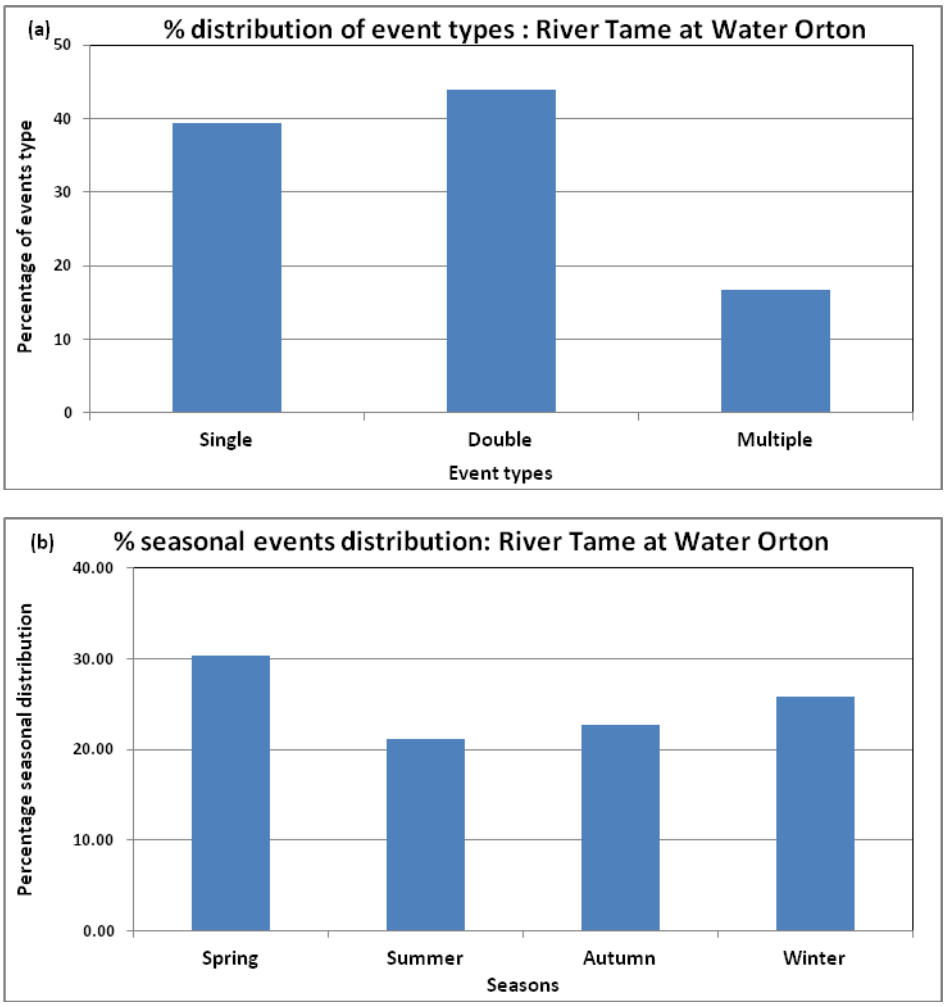

Figure 5.3: Overall percentage events distribution per: (a) types; (b) seasons.

Table 5.4: Seasonal distribution: (a) Single, Double and Multiple flow peak events; (b) Chi-square test for event type distribution within the seasons.

(a) Season	Single	%	Double	%	Multiple	%	Overall	%
Spring	9	35	5	17	6	55	20	**30**
Summer	3	12	10	34	1	9	14	**21**
Autumn	6	23	7	24	2	18	15	**23**
Winter	8	31	7	24	2	18	17	**26**
Overall	**26**	**39**	**29**	**44**	**11**	**17**	**66**	**100**

(b)			Cases					
			Valid		Missing		Total	
			N	Percent	N	Percent	N	Percent
Event * Season			66	100.00%	0	0.00%	66	100.00%
Event * Season Crosstabulation								
			Season					
			Autumn	Spring	Summer	Winter	Total	
Event	**DM**	**Count**	9	11	11	9	40	
		Expected Count	9.1	12.1	8.5	10.3	40	
	S	**Count**	6	9	3	8	26	
		Expected Count	5.9	7.9	5.5	6.7	26	
Total		**Count**	15	20	14	17	66	
		Expected Count	15	20	14	17	66	
Chi-Square Tests								
			Value	df	Asymp. Sig. (2-sided)			
Pearson Chi-Square			2.576[a]	3	0.462			
Likelihood Ratio			2.731	3	0.435			
N of Valid Cases			66					
a. 0 cells (.0%) have expected count less than 5. The minimum expected count is 5.52.								

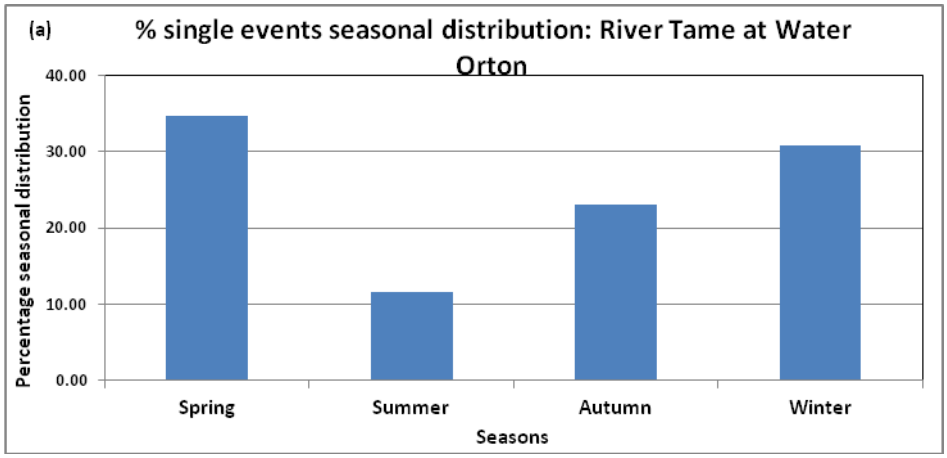

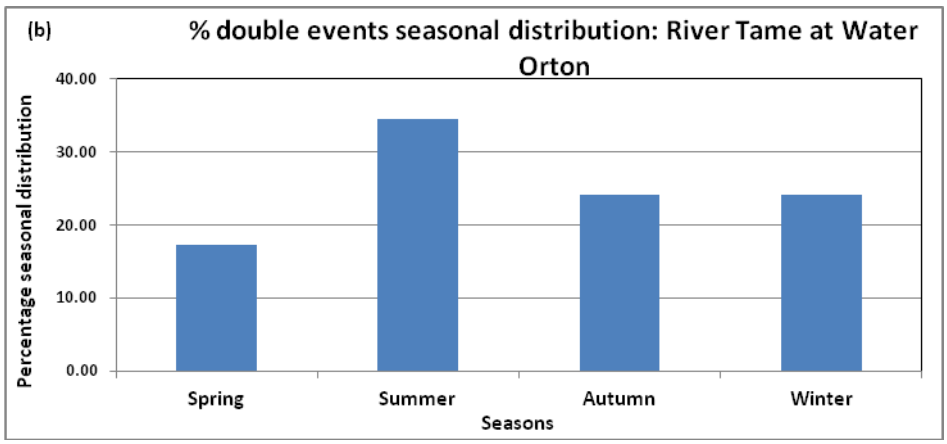

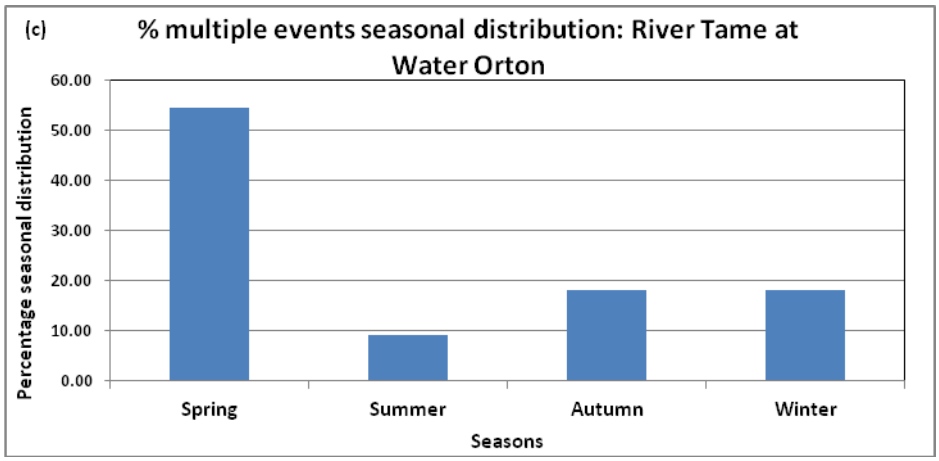

Figure 5.4: Percentage event type distribution between seasons for: (a) Single; (b) Double; (c) Multiple flow peak events.

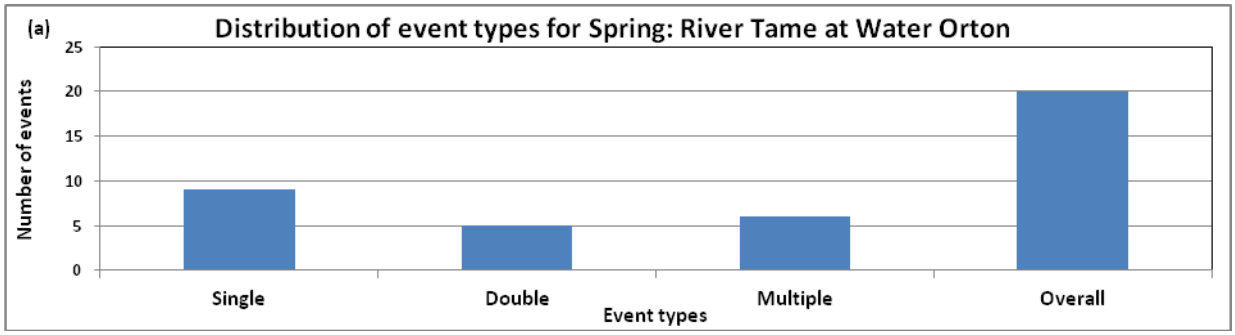

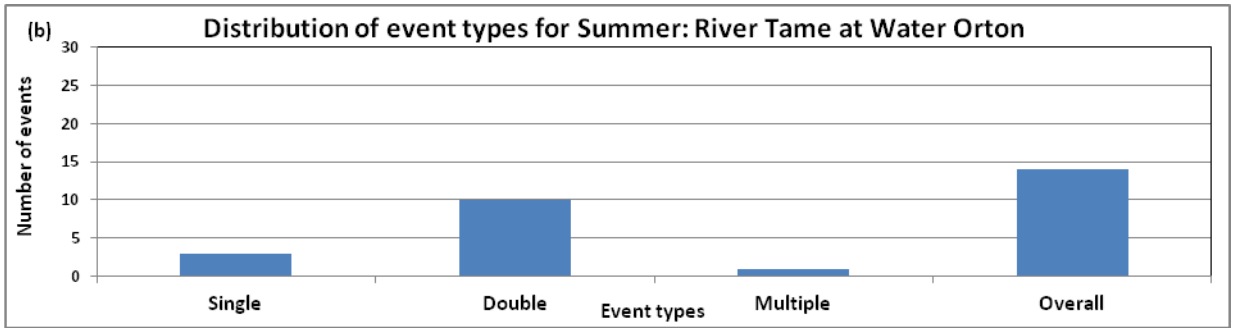

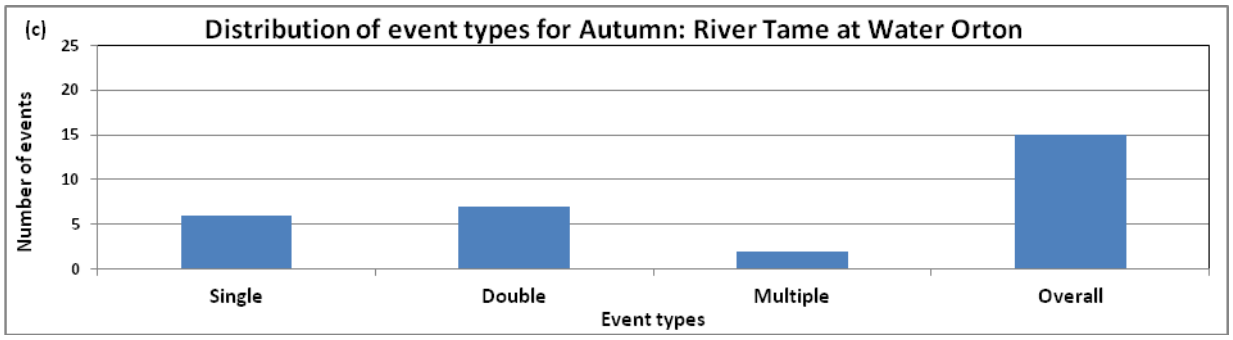

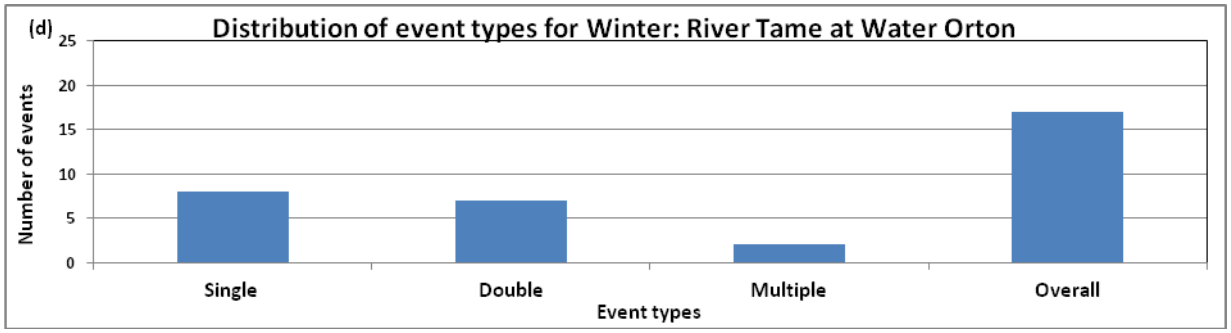

Figure 5.5: Event type distribution within seasons for: (a) Spring; (b) Summer; (c) Autumn; (d) Winter.

5.4.4 Characterisation of turbidity, discharge, rainfall, ammonia and time

Turbidity, discharge, rainfall and ammonia attributes per season are presented in Table 5.6(a), Figure 5.8 and Figure 5.9 . Means of total discharge do not differ substantially between spring, autumn and winter (Figure 5.8(b)), with spring and summer having the highest and lowest means respectively (Figure 5.9 (b)). Total turbidity, rainfall, ammonia, and event time and total event time have spring and summer, autumn and winter, winter and autumn and winter and summer with the highest and lowest means respectively (Figure 5.9). Analysis of variance test results indicate there are significant differences in the means of total turbidity, discharge, rainfall, ammonia, time of discharge recession, rainfall peak, event time and total event time between the seasons (Table 5.6(b)).

5.4.5 Turbidity relations with event attributes

Correlation coefficients of the regression analysis of turbidity attributes (Tupk, Tur, Tutot) with discharge and other events attributes are presented within Table 5.7. Turbidity peak and range correlates significantly with more attributes within the summer and less in autumn and winter. The strongest correlations are principally associated with discharge attributes. The exception being spring turbidity range and winter turbidity total which correlates strongly with rainfall total and total event time, respectively. Total turbidity does not correlate significantly with any attribute in autumn.

Table 5.5: Events Seasonal Means of Turbidity peak Ld/Lg/Co Discharge peak;

(b) Chi-square test for event type distribution within the seasons.

(a) Season	Ld	%	Lg	%	Co	%	Total	%
Spring	8	40	9	45	3	15	20	100
Summer	7	47	8	53	0	0	15	100
Autumn	6	43	7	50	1	7	14	100
Winter	6	35	11	65	0	0	17	100
Total	27	41	35	53	4	6	66	100

			Cases					
			Valid		Missing		Total	
(b)			N	Percent	N	Percent	N	Percent
Event * Season			66	100.00%	0	0.00%	66	100.00%
				Season				
				Autumn	Spring	Summer	Winter	Total
Event	LdCo	Count		7	11	7	6	31
		Expected Count		6.6	9.4	7	8	31
	Lg	Count		7	9	8	11	35
		Expected Count		7.4	10.6	8	9	35
Total		Count		14	20	15	17	66
		Expected Count		14	20	15	17	66

Chi-Square Tests			
	Value	df	Asymp. Sig. (2-sided)
Pearson Chi-Square	1.500a	3	0.682
Likelihood Ratio	1.517	3	0.678
N of Valid Cases	66		
a. 0 cells (.0%) have expected count less than 5. The minimum expected count is 6.58.			

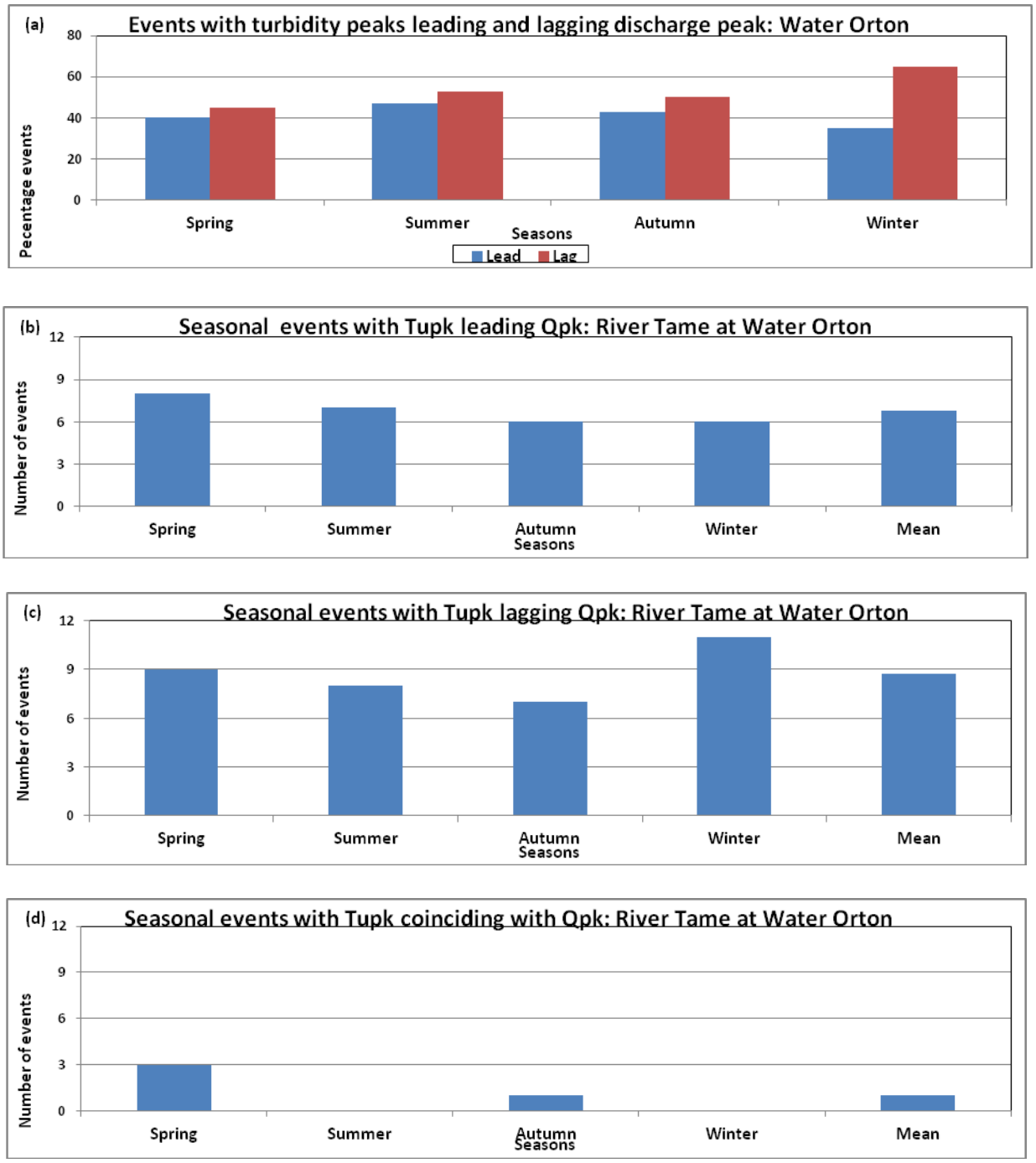

Figure 5.6: Distribution of Tu ld/lg/co Q peaks events between seasons for: (a) Tupk leading and lagging Qpk; (b) Tupk leading Qpk; (c) Tupk lagging Qpk; (d) Tupk coinciding with Qpk.

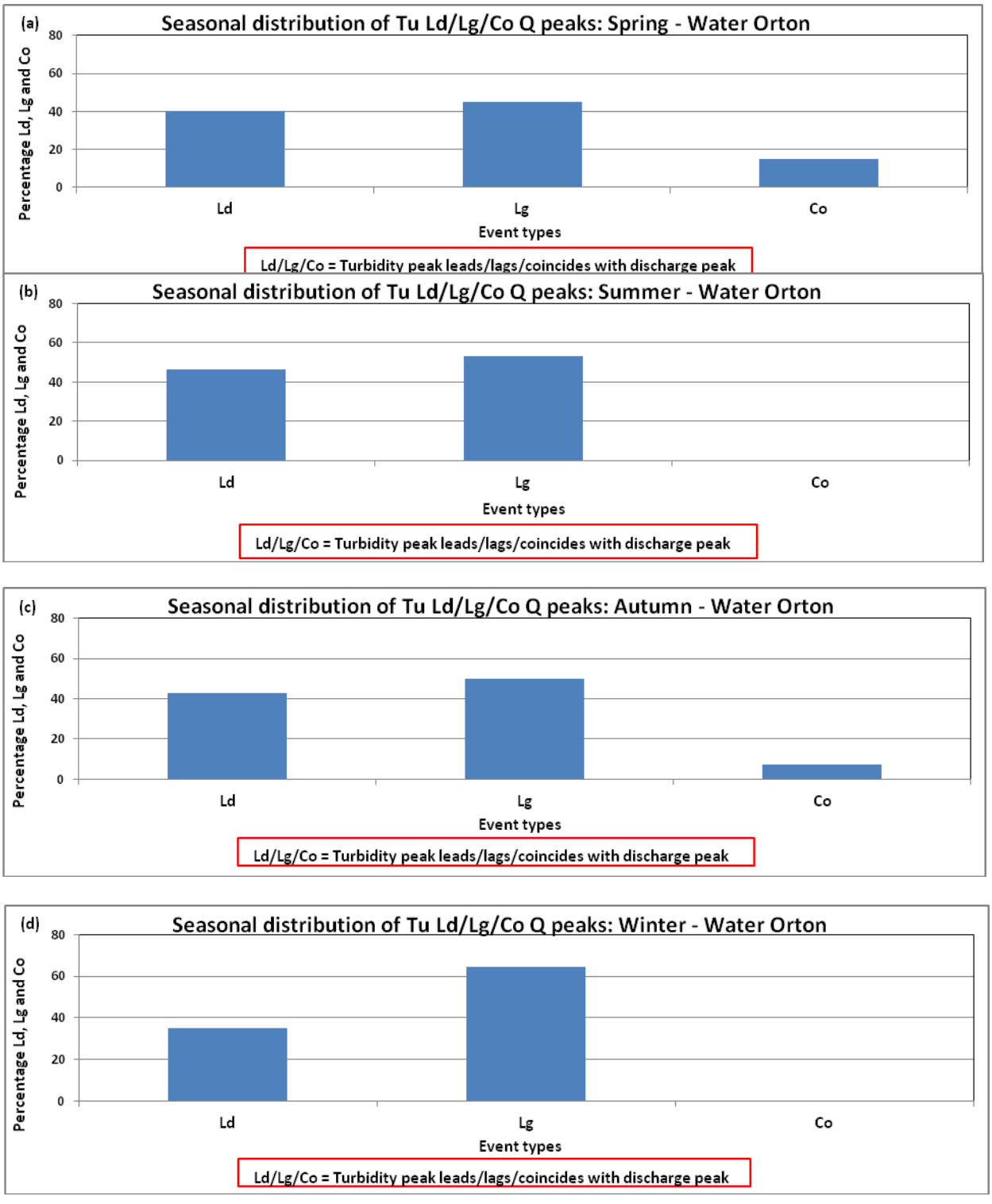

Figure 5.7: Distribution of Tu ld/lg/co Q peaks events within seasons: (a) Spring; (b) Summer; (c) Autumn; (d) Winter.

*Table 5.6: (a) Seasonal means of events attributes; (b) ANOVA results. * show statistically significant attribute means ($p \leq 0.05$).*

a)	Spring	Summer	Autumn	Winter
Tupk (FTU)	287.7	209.7	256.9	257.8
Tur (FTU)	254.2	178.6	233	217.3
Tutot (x10^2) (FTU	211.17	98.6	118.9	187.8
Qpk (m^3/s)	19.2	13.8	22.6	16.7
Qr (m^3/s)	14.45	10.9	18.1	12.1
Qtot(x10^2) (m^3/s)	15.9	7.8	15.5	15.6
EFR (m^3/s/h)	38.5	27	38.2	31.6
Rpk (mm)	1.3	2.7	1.7	0.88
Rant (mm)	1.6	1.1	0.7	1.0
Rtot (x 10) (mm)	1.0	0.8	1.1	0.76
ERI (mm/h)	2.5	2.9	2.6	1.6
NHpk (mg/l)	2.8	2.0	2.	4.0
NHtot (x10^2) (mg/	1.7	1.2	0.6	2.1
tE (h)	43.4	27.6	43.7	49.8
tET (h)	47.1	30	46.1	53.7

b)	Attribute	Sig	Ho	Ha	A IF Ha<95
1	**Tutot (FTU)**	<0.001*	0.0	100.0	R
2	**Qtot (m^3/s)**	0.001*	0.1	99.9	R
3	**NHtot (mg/l)**	0.002*	0.2	99.8	R
4	**tQFL (h)**	0.004*	0.4	99.6	R
5	**Rpk (mm)**	0.009*	0.9	99.1	R
6	**tE (h)**	0.011*	1.1	98.9	R
7	**tET (h)**	0.012*	1.2	98.8	R
8	**Rtot (mm)**	0.038*	3.8	96.2	R
9	**Tur (FTU)**	0.150	15.0	85.0	A
10	**Tupk (FTU)**	0.153	15.3	84.7	A
11	**Qpk (m^3/s)**	0.154	15.4	84.6	A
12	**NHpk (mg/l)**	0.162	16.2	83.8	A
13	**Qr (m^3/s)**	0.263	26.3	73.7	A
14	**dQFL (m^3/s/h)**	0.266	26.6	73.4	A
15	**LagTuQ (h)**	0.279	27.9	72.1	A
16	**tQRL (h)**	0.551	55.1	44.9	A
17	**LagTuNH (h)**	0.802	80.2	19.8	A
18	**dQRL (m^3/s/h)**	0.930	93.0	7.0	A

Definitions of attributes used in Table 5.6: Tu=turbidity, Q=discharge/flow, R=rainfall, NH=ammonia, pk=peak, r=range, tot=total, ant=antecedent, ERI=event rainfall intensity, EFR=event flow rate, dQRL=rate of flow rise, dQFL=rate of flow recession, tQRL, tQFL= flow rise and flow recession times, LagTuQ=turbidity-flow peaks lag time, LagTuNH=turbidity-ammonia peaks lag time, tE= event time, tET= total event time.

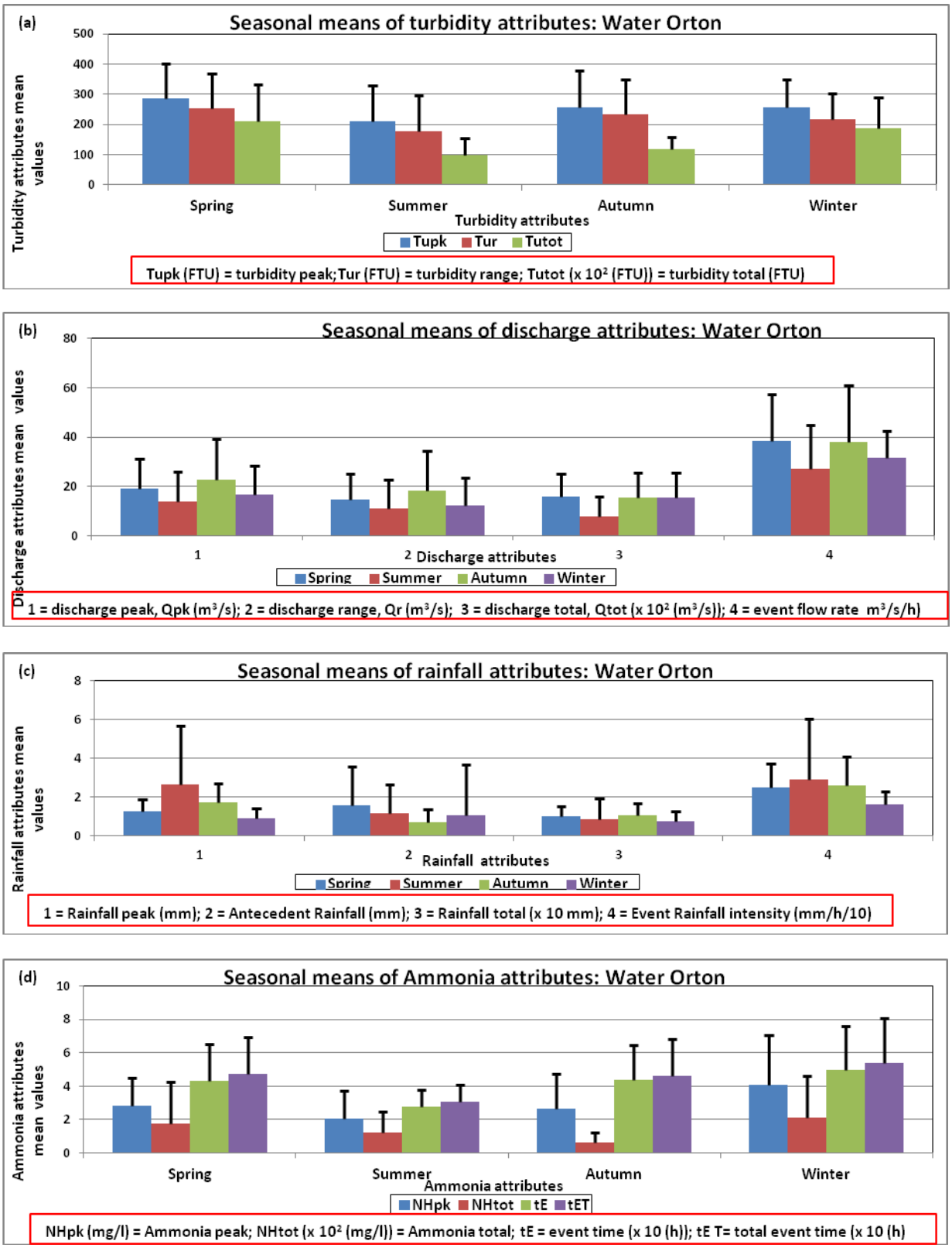

Figure 5.8: Seasonal means of attributes of: (a) turbidity; (b) discharge; (c) rainfall; (d) ammonia and time showing error bars of standard deviation.

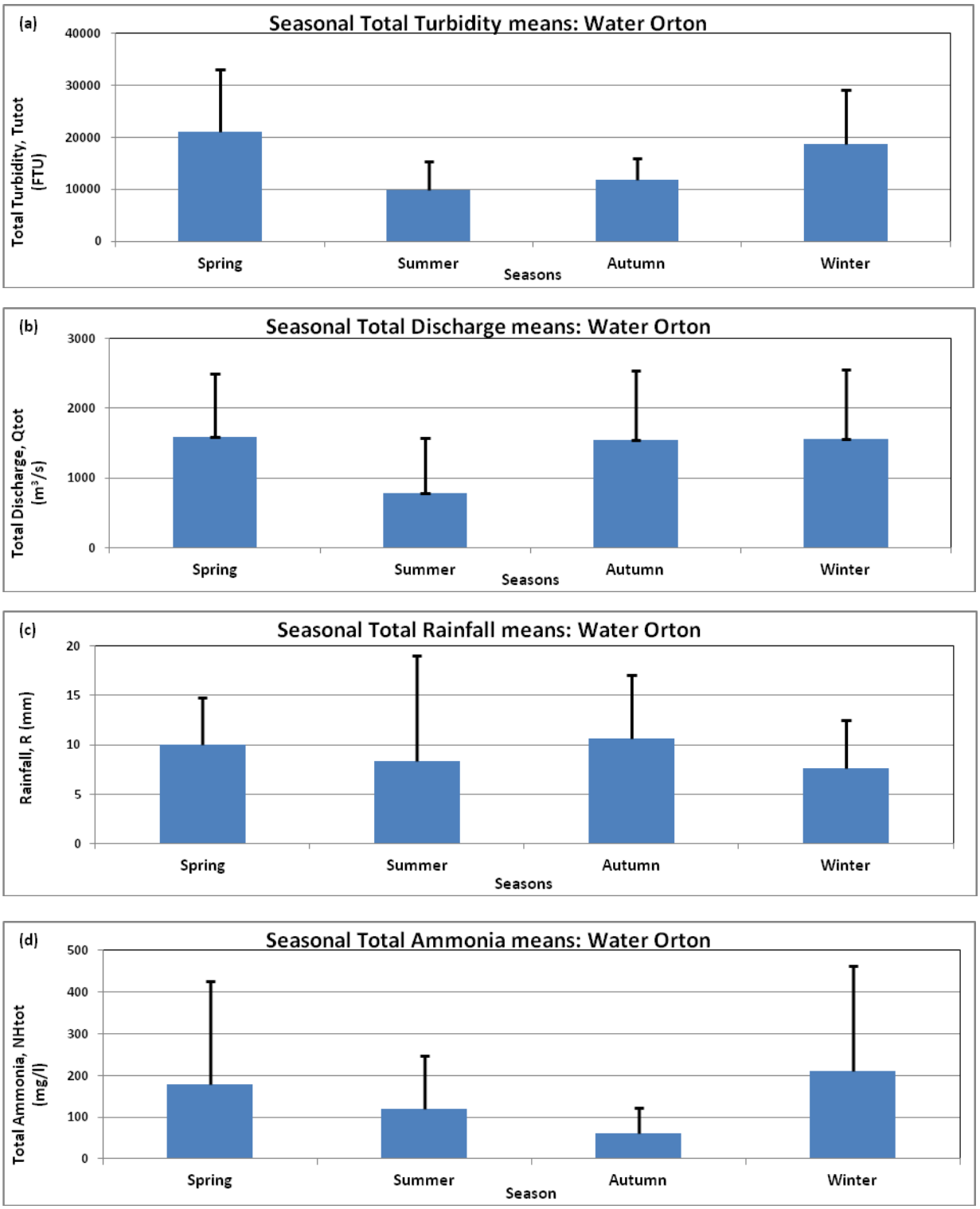

Figure 5.9: Events Seasonal Means of total values of attributes: (a) Turbidity; (b) Discharge; (c) Rainfall; (d) Ammonia showing error bars of standard deviation.

The correlations for turbidity peak, turbidity range and turbidity total with key variables discharge range and discharge total are presented within Figure 5.10 for the different seasons. As indicated within the regression analysis (Table 5.7 the linear relationship between turbidity peak and discharge range is strongest in summer and weakest within autumn. In comparison, the relationship between total turbidity and discharge is strongest within spring and weakest in autumn. General seasonal basic statistics comprising minimum, maximum, mean and standard deviation of the variables are summarised in Tables (b) and (c) in Appendix B; and presented within Figure 5.16 and Figure 5.17.

5.4.6 Turbidity relations with ammonia

Scatter plots of logarithms of total turbidity and ammonia and discharge attributes are presented within Figure 5.9 and Figure 5.10. The lowest and highest scatters are associated with summer and autumn for turbidity peak and range, and with spring and autumn for total turbidity – discharge range and total regressions respectively (Figure 5.10). Table 5.8 summarises the characteristics of these regression lines. The highest and lowest intercepts are in autumn and summer, and slopes in spring and autumn respectively for total turbidity – total discharge regression lines. For turbidity peak and range regressions, autumn and summer showed the highest and lowest intercepts, and slopes are summer and autumn respectively. Table 5.9 gives the seasonal mean times and rates of discharge rising and recession, with Figure 5.13 showing bar charts of the distributions. Summer has the lowest of both discharge rising and recession times. Winter also has the lowest of both discharge rising and recession rates. Table 5.10 gives the seasonal means of

lead and lag times between peaks of turbidity and discharge (a) for overall events and (b) for large discharge events (with total discharge greater than or equal to overall event total discharge mean of 1393 m^3/s). Results of t-test between the lead and lag times (c) show significantly different means between the lead and lag times for the overall events as well as for the seasons. Figure 5.14(a) and (b) show these distributions. Table 5.11 shows the distribution of lead and lag events within large events, overall events above (high flow) and below (low flow) mean Qtot of 1393 m^3/s and chi-square test results for overall events above and below mean Qtot. Overall and for all seasons except spring, there were significantly more number of low than high flows, with summer having the highest (Table 5.11(b); Figure 5.14(d)).

Table 5.7: Seasonal correlation of turbidity attributes with other attributes. All correlations are statistically significant at p ≤ 0.05.

	Tupk			Tur			Tutot		
(a)				**SPRING**					
No	**Attr**	**r**	**Sig**	**Attr**	**r**	**Sig**	**Attr**	**r**	**Sig**
1	**Qr**	0.616	0.004	**Rtot**	0.59	0.005	**Qtot**	0.829	<0.001
2	**Qpk**	0.567	0.009	**Qr**	0.58	0.007	**tE**	0.776	<0.001
3	**Rtot**	0.564	0.01	**Qpk**	0.52	0.018	**tET**	0.775	<0.001
4	**Qtot**	0.503	0.024	**Qtot**	0.51	0.021	**dQFL**	0.75	<0.001
5							**Rtot**	0.728	<0.001
6							**NHtot**	0.667	0.001
7							**tQRL**	0.495	0.026
8							**Qr**	0.459	0.042
(b)				**SUMMER**					
1	**Qr**	0.818	<0.001	**Qr**	0.83	<0.001	**Qtot**	0.735	0.002
2	**Qpk**	0.789	<0.001	**Qpk**	0.79	<0.001	**Rtot**	0.687	0.005
3	**Qtot**	0.683	0.005	**Qtot**	0.69	0.004	**tQFL**	0.676	0.006
4	**EFR**	0.659	0.008	**EFR**	0.68	0.005	**tE**	0.633	0.011
5	**NHpk**	0.657	0.008	**dQFL**	0.67	0.006	**NHpk**	0.687	0.022
6	**dQFL**	0.647	0.009	**NHpk**	0.60	0.017	**NHtot**	0.682	0.023
7	**Rtot**	0.553	0.032	**dQRL**	0.54	0.038	**tET**	0.555	0.032
8	**dQRL**	0.522	0.046				**Qpk**	0.546	0.035

9							Qr	0.551	0.033
(c)	**AUTUMN**								
1	**LagTuNH**	0.547	0.043	**LagTuNH**	0.54	0.046	**No significant correlation of any attribute**		
2									
(d)	**WINTER**								
1	**LagTuQ**	0.483	0.049	**LagTuQ**	0.48	0.048	**tET**	0.761	<0.001
2							**tE**	0.752	<0.001
3							**Qtot**	0.748	0.001
4							**tQFL**	0.679	0.003
5							**tQRL**	0.606	0.01
6							**LagTuNH**	0.587	0.013
7							**Rtot**	0.542	0.25
8							**LagTuQ**	0.513	0.035

Definitions of attributes used in Table 5.7: Tu=turbidity, Q=discharge/flow, R=rainfall, NH=ammonia, pk=peak, r=range, tot=total, ant=antecedent, ERI=event rainfall intensity, EFR=event flow rate, dQRL=rate of flow rise, dQFL=rate of flow recession, tQRL, tQFL= flow rise and flow recession times, LagTuQ=turbidity-flow peaks lag time, LagTuNH=turbidity-ammonia peaks lag time, tE= event time, tET= total event time.

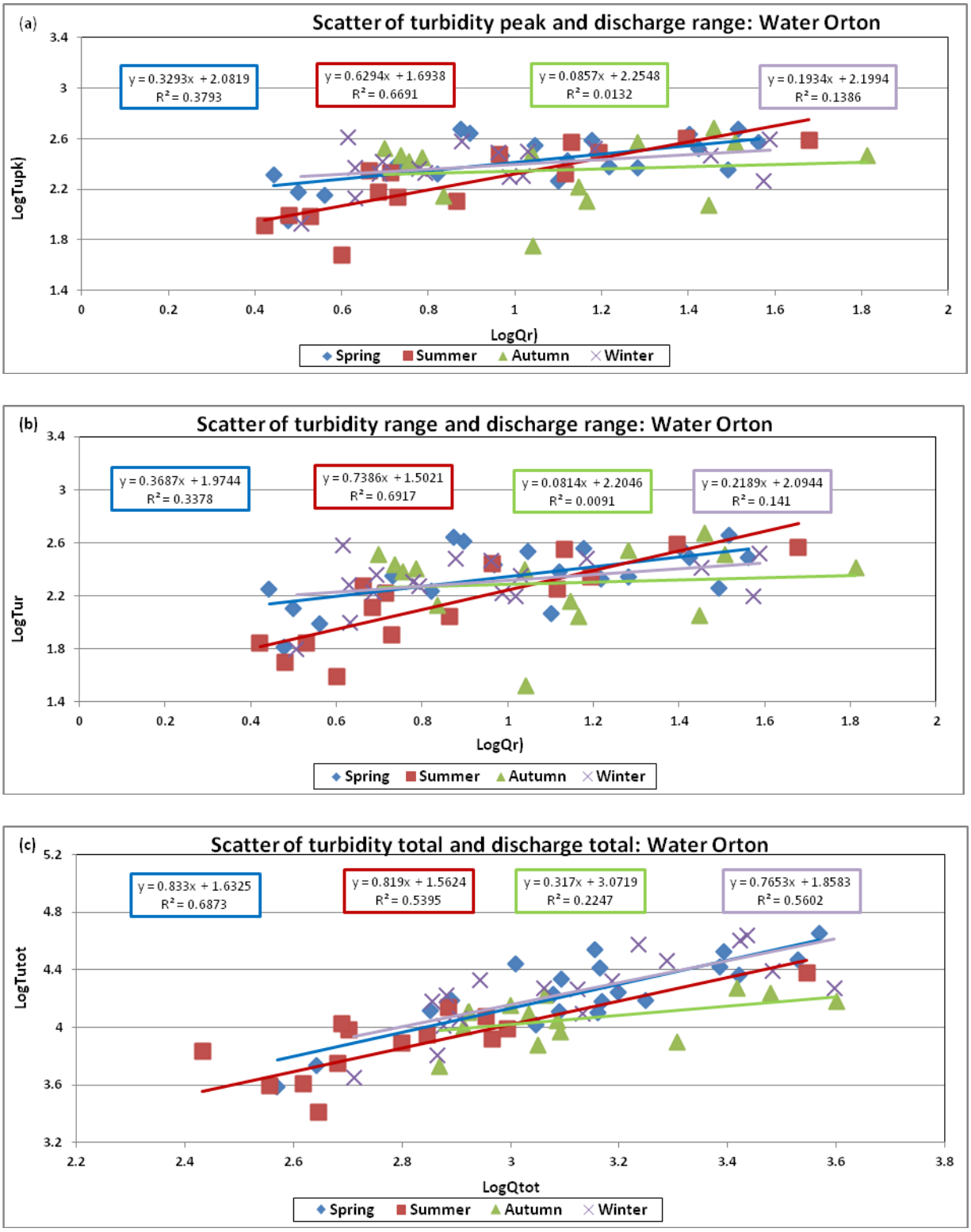

Figure 5.10: Seasonal regression of: (a) turbidity peak and discharge range; (a) turbidity range and discharge range; (c) turbidity total and discharge total.

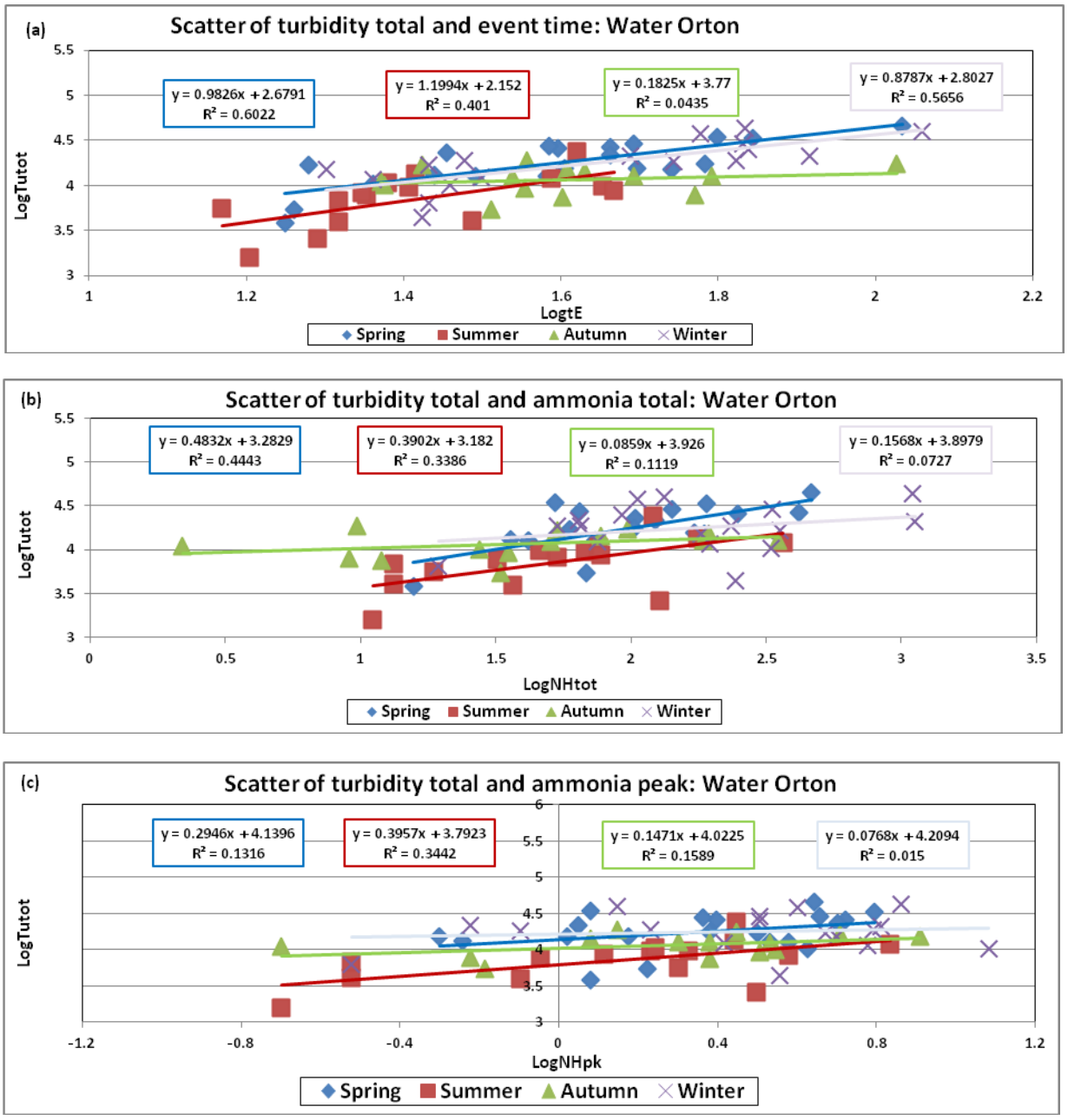

Figure 5.11: Seasonal regression of total turbidity with: (a) event time, (b) ammonia total, (c) ammonia peak.

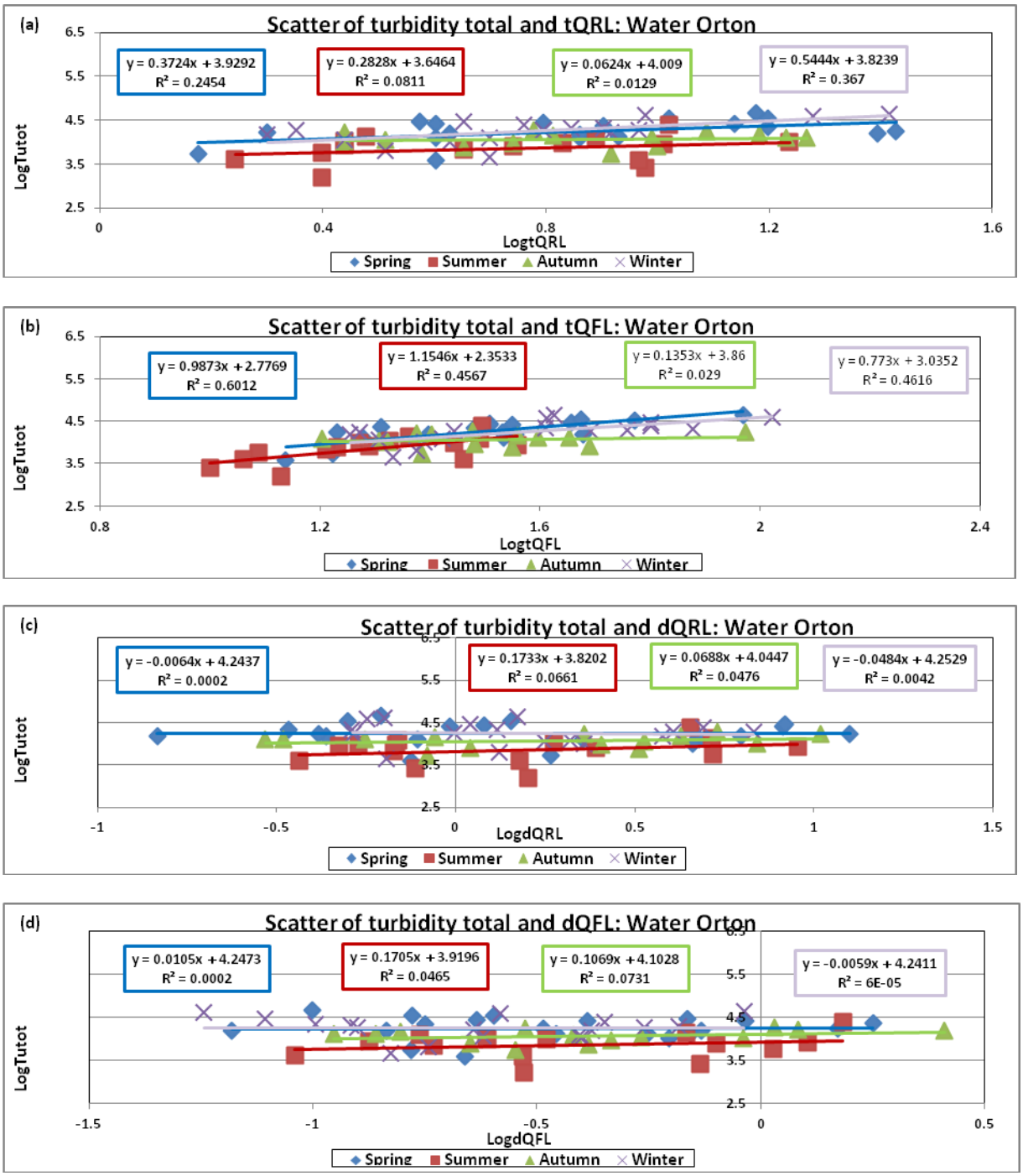

Figure 5.12: Seasonal regression of total turbidity with: (a) time of discharge rise, (b) time of discharge recession (c) rate of discharge rise, (d) rate of discharge recession.

*Table 5.8: Coefficients and statistics of seasonal rating curves for the downstream Water Orton catchment of River Tame, UK: (a) Turbidity peak-discharge range; (b) Turbidity range-discharge range; (c) Turbidity total-total discharge. * Not statistically significant*

Season	Intercept	Slope	R^2	Events
(a) Turbidity peak				
Spring	2.08	0.32	0.37	20
Summer	1.69	0.62	0.66	15
Autumn	2.23	0.08	0.013*	14
Winter	2.19	0.19	0.13*	17
(b) Turbidity range				
Spring	1.97	0.36	0.33	20
Summer	1.5	0.73	0.69	15
Autumn	2.2	0.081	0.00*	14
Winter	2.09	0.21	0.14*	17
(c) Turbidity total				
Spring	1.63	0.83	0.68	20
Summer	1.56	0.81	0.53	15
Autumn	3.07	0.31	0.22*	14
Winter	1.85	0.76	0.56	17

Table 5.9: Seasonal mean discharge rising and recession times and rates

Attribute	tQRL	tQFL	dQRL	dQFL
Season	(h)	(h)	$m^3/s/h$	$m^3/s/h$
Spring	9.3	34.2	3.1	0.5
Summer	6.4	21.2	2.4	0.5
Autumn	8.7	35.0	3.0	0.6
Winter	7.5	42.3	2.0	0.3

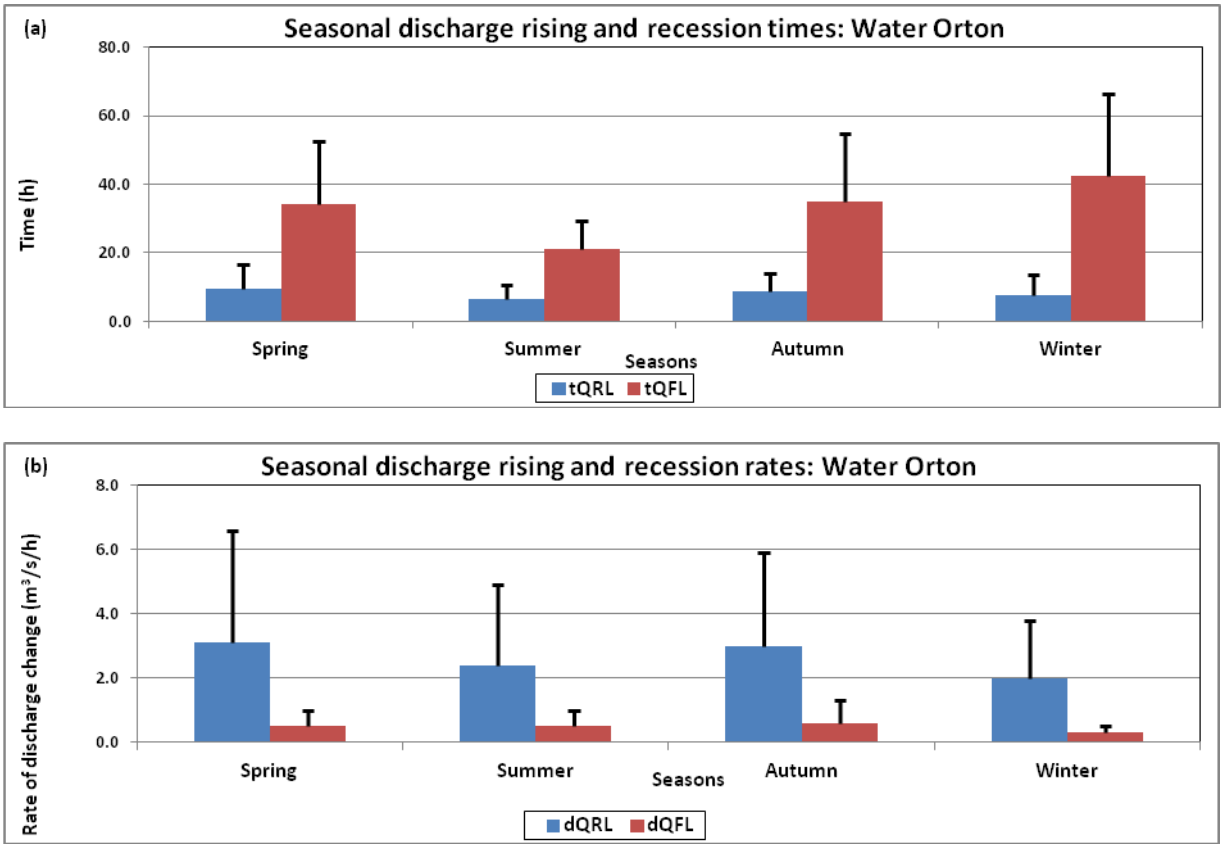

Figure 5.13: Distribution of seasonal mean discharge rising and recession (a) times (tQRL and tQFL), (b) rates (dQRL and dQFL) showing error bars of standard deviation.

Table 5.10: Lead and lag times between peaks of turbidity and discharge for: (a) all events, (b) large events, (c) Lead/lag time t-test results. (Large events are with total discharge ≥ overall event mean of 1393 m^3/s).

(a)	Lead time (h)			Lag time (h)		
Season	**Mean**	**Maximum**	**Minimum**	**Mean**	**Maximum**	**Minimum**
Spring	4.84	11.25	0.25	3.08	6.75	0.25
Summer	3.25	6.25	0.25	1.69	5	0.5
Autumn	1.79	5	0.25	1.64	4.5	0.25
Winter	1.25	4.25	0.25	2.55	5.25	0.5

(b)	Lead time (h)			Lag time (h)		
Season	**Mean**	**Maximum**	**Minimum**	**Mean**	**Maximum**	**Minimum**
Spring	3.93	10	0.25	6.25	6.75	0.25
Summer	0	0	0	1.5	5	0.5
Autumn	1.13	1.25	1	2.5	4.5	0.25
Winter	1.67	4.25	0.25	3.19	5.25	0.5

(c)	LagTuQ
Seasons	**Significance**
All	<0.001
Spring	<0.001
Summer	0.001
Autumn	0.009
Winter	0.001

Table 5.11: Distribution of: (a) lead and lag events within large events, (b) overall events above and below mean Qtot of 1393 m^3/s, (c) Chi-square test results for overall events above and below mean Qtot. (Large events are with total discharge ≥ overall event

(a)	Number of events with mean Qtot ≥ 1393 m^3/s					
Season	**Overall**	**events**	**Lead**	**%**	**Lag**	**%**
Spring	20	11	7	64	2	18
Summer	15	1	0	0	1	100
Autumn	14	4	2	50	2	50
Winter	17	7	3	43	4	57

(b)	Number of events above and below mean Qtot of 1393 m^3				
Season	**Overall**	**Above**	**%**	**Below**	**%**
Spring	20	11	17	9	14
Summer	15	1	2	14	21
Autumn	14	4	6	10	15
Winter	17	7	11	10	15
Total	66	23	35	43	65

(c)			Season				Total
			Autumn	**Spring**	**Summer**	**Winter**	
Event	**High**	**Count**	4	11	1	7	23
		Expected Count	4.9	7	5.2	5.9	23
	Low	**Count**	10	9	14	10	43
		Expected Count	9.1	13	9.8	11.1	43
Total		**Count**	14	20	15	17	66
		Expected Count	14	20	15	17	66

	Value	**df**	**Asymp. Sig. (2-sided)**
Pearson Chi-Square	9.367[a]	3	0.025
Likelihood Ratio	10.679	3	0.014
N of Valid Cases	66		

a. 1 cells (12.5%) have expected count less than 5.

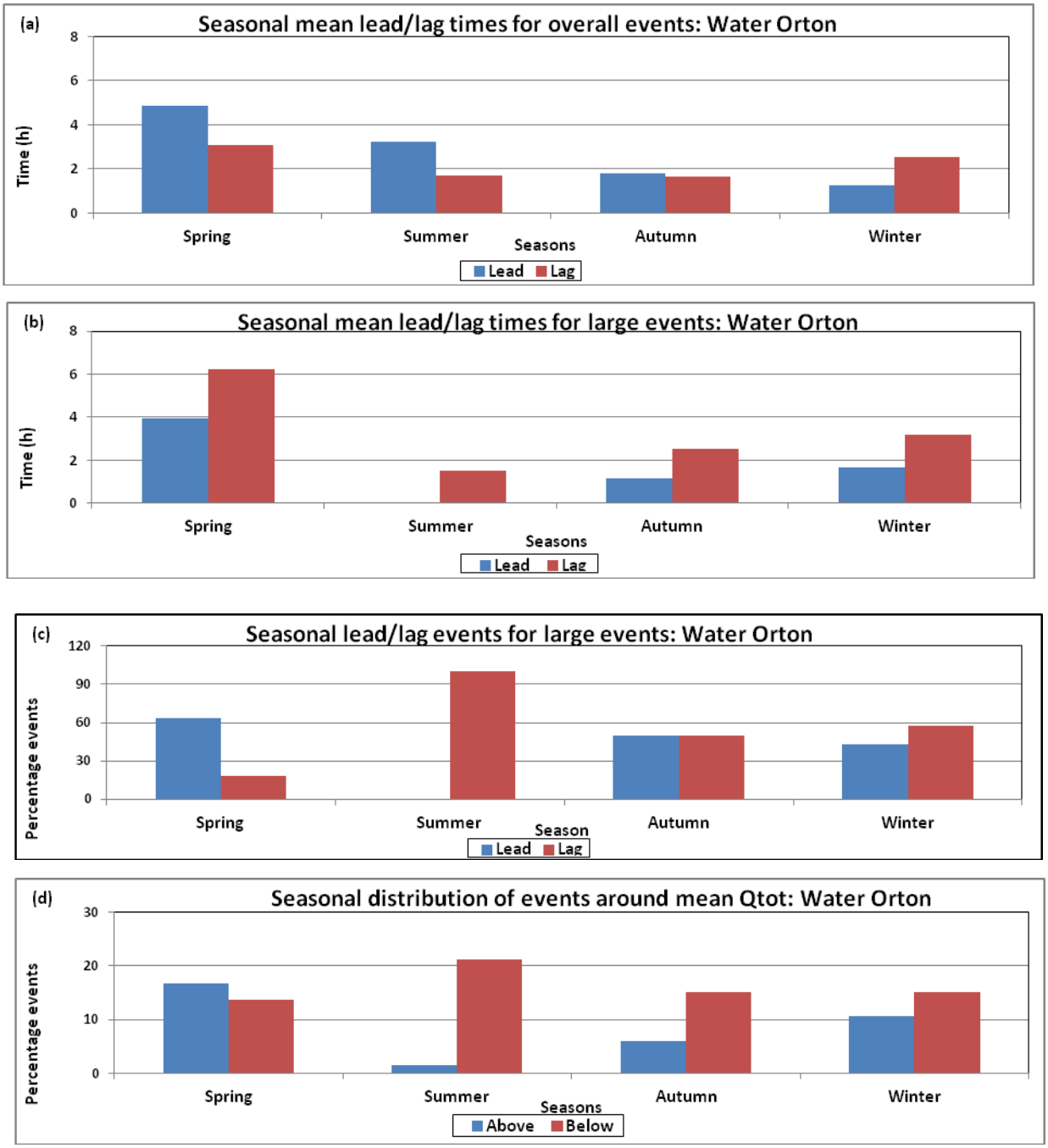

Figure 5.14: Lead and lag times between peaks of turbidity and discharge for: (a) all events, (b) large events; Distribution of: (c) lead and lag events within large events, (d) events above and below mean Qtot.

Table 5.12: Stepwise MLR output showing influence of seasons on turbidity – discharge regression. All significance is at 0.05 confidence level (CL) ($p \leq 0.05$).

	Dependent Variable: Tupk					
Model		**Unstandardized Coefficients**		**Standardized Coefficients**	**t**	**Sig.**
		B	**Std. Error**	**Beta**		
1	**(Constant)**	2.25	0.04		55.8	<0.001
	Qr	0.375	0.073	0.483	5.17	<0.001
	Dependent Variable: Tur					
Model		**Unstandardized Coefficients**		**Standardized Coefficients**	**t**	**Sig.**
		B	**Std. Error**	**Beta**		
1	**(Constant)**	2.161	0.05		43.647	<0.001
	Qr	0.384	0.089	0.418	4.31	<0.001
	Dependent Variable: Tutot					
Model		**Unstandardized Coefficients**		**Standardized Coefficients**	**t**	**Sig.**
		B	**Std. Error**	**Beta**		
1	**(Constant)**	1.683	0.25		6.737	<0.001
	Qtot	0.798	0.082	0.774	9.782	<0.001
2	**(Constant)**	1.603	0.239		6.721	<0.001
	Qtot	0.835	0.078	0.81	10.646	<0.001
	AGr	-0.05	0.018	-0.217	-2.858	0.006
3	**(Constant)**	1.953	0.267		7.305	<0.001
	Qtot	0.733	0.085	0.712	8.61	<0.001
	AGr	-0.06	0.017	-0.262	-3.485	0.001
	SuIn	-0.151	0.06	-0.215	-2.533	0.014

Table 5.13: Seasonal attributes effects on: (a) turbidity peak; (b) turbidity range. All significance is at 0.05 CL (p ≤ 0.05).

(a) Dep	Tupk					
Indep	**Statistics**	**R^2**	**Sig**	**B**	**Std. Err.**	**Sig**
dQFL	**Model**	0.257	<0.001			
	Constant			2.463	0.04	<0.001
	SuGr			0.345	0.104	<0.001
	dQFL			0.156	0.069	0.026
Qr	**Model**	0.254	<0.001			
	Constant			2.25	0.04	<0.001
	Qr			0.375	0.073	<0.001
Qpk	**Model**	0.23	<0.001			
	Constant			1.898	0.108	<0.001
	Qpk			0.394	0.09	<0.001
NHpk	**Model**	0.194	<0.001			
	Constant			2.279	0.032	<0.001
	NHpk			0.248	0.063	<0.001
Qtot	**Model**	0.184	<0.001			
	Constant			1.316	0.275	<0.001
	Qtot			0.341	0.09	<0.001
dQRL	**Model**	0.165	0.003			
	Constant			2.357	0.032	<0.001
	dQRL			0.155	0.058	0.009
	SuIn			-0.136	0.063	0.033
Rtot	**Model**	0.156	0.001			
	Constant			2.116	0.074	<0.001
	Rtot			0.281	0.082	0.001
LagTuNH	**Model**	0.084	0.018			
	Constant			2.378	0.029	<0.001
	SuGr			-0.196	0.081	0.018
LagTuQ	**Model**	0.069	0.034			
	Constant			2.389	0.031	<0.001
	SuIn			-0.142	0.066	0.034

(b) Dep	Tur					
Indep	**Statistics**	**R^2**	**Sig**	**B**	**Std. Err.**	**Sig**
dQFL	**Model**	0.261	<0.001			
	Constant			2.399	0.046	<0.001
	SuGr			0.423	0.12	0.001
	dQFL			0.163	0.079	0.043
Qr	**Model**	0.255	<0.001			
	Constant			2.161	0.05	<0.001
	Qr			0.384	0.089	<0.001
Qpk	**Model**	0.223	<0.001			
	Constant			1.761	0.125	<0.001
	Qpk			0.447	0.104	<0.001
Qtot	**Model**	0.193	<0.001			
	Constant			1.051	0.316	0.001
	Qtot			0.403	0.103	<0.001
NHpk	**Model**	0.181	<0.001			
	Constant			2.195	0.038	<0.001
	NHpk			0.277	0.074	<0.001
dQRL	**Model**	0.163	0.004			
	Constant			2.285	0.037	<0.001
	dQRL			0.173	0.066	0.011
	SuIn			-0.163	0.072	0.028
Rtot	**Model**	0.161	0.001			
	Constant			2.001	0.086	<0.001
	Rtot			0.329	0.094	0.001
LagTuNH	**Model**	0.149	0.006			
	Constant			2.265	0.039	<0.001
	SuGr			-0.291	0.094	0.003
	LagTuNH			0.09	0.044	0.046
LagTuQ	**Model**	0.073	0.028			
	Constant			3.23	0.036	<0.001
	SuIn			-0.17	0.076	0.028

Table 5.14: Seasonal effects of attributes on total turbidity. All significance is at 0.05 CL (p ≤ 0.05). Su (Summer), A (Autumn), W (Winter), In (intercept) and Gr (gradient).

Depth	Tutot					
Indep	**Statistics**	**R^2**	**Sig**	**B**	**Std. Err.**	**Sig**
Qtot	**Model**	0.678	<0.001			
	Constant			1.953	0.267	<0.001
	Qtot			0.733	0.085	<0.001
	AGr			-0.06	0.017	0.001
	SuIn			-0.151	0.06	0.014
tE	**Model**	0.632	<0.001			
	Constant			2.684	0.213	<0.001
	tE			0.966	0.131	<0.001
	SuIn			-0.202	0.063	0.002
	AGr			-0.784	0.319	0.017
	AIn			1.086	0.516	0.039
tQFL	**Model**	0.614	<0.001			
	Constant			2.863	0.199	<0.001
	tQFL			0.907	0.129	<0.001
	SuIn			-0.19	0.065	0.005
	AGr			-0.772	0.3	0.012
	AIn			0.997	0.455	0.032
tET	**Model**	0.584	<0.001			
	Constant			2.803	0.222	<0.001
	tET			0.874	0.133	<0.001
	SuIn			-0.235	0.065	0.001
	AGr			-0.107	0.037	0.006
Rtot	**Model**	0.561	<0.001			
	Constant			3.787	0.079	<0.001
	Rtot			0.517	0.083	<0.001
	SuIn			-0.288	0.064	<0.001
	AGr			-0.288	0.064	0.001
Qr	**Model**	0.461	<0.001			
	Constant			3.869	0.087	<0.001
	SuIn			-0.352	0.068	<0.001
	Qr			0.378	0.083	<0.001
	AGr			-0.205	0.062	0.001
tQRL	**Model**	0.436	<0.001			
	Constant			3.938	0.083	<0.001
	SuIn			-0.361	0.07	<0.001
	tQRL			0.38	0.094	<0.001
	AGr			-0.243	0.08	0.003
Qpk	**Model**	0.426	<0.001			
	Constant			3.746	0.131	<0.001
	SuIn			-0.337	0.072	<0.001
	Qpk			0.423	0.109	<0.001
	AGr			-0.174	0.057	0.003
NHtot	**Model**	0.424	<0.001			
	Constant			3.7	0.115	<0.001
	NHtot			0.253	0.057	<0.001
	SuIn			-0.283	0.069	<0.001
NHpk	**Model**	0.386	<0.001			
	Constant			4.155	0.049	<0.001
	SuIn			-0.338	0.076	<0.001
	NHpk			0.222	0.075	0.004
	AIn			-0.153	0.075	0.047
LagTuNH	**Model**	0.363	<0.001			
	Constant			4.178	0.048	<0.001
	SuIn			-0.382	0.074	<0.001
	LagTuNH			0.105	0.042	0.015
	AIn			-0.158	0.077	0.044
LagTuQ	**Model**	0.349	<0.001			
	Constant			4.225	0.041	<0.001
	SuIn			-0.376	0.076	<0.001
	WGr			0.295	0.135	0.033
	AIn			-0.162	0.078	0.041
dQRL dQFL	**Model**	0.299	<0.001			
	Constant			4.244	0.042	<0.001
	SuIn			-0.395	0.077	<0.001
	AIn			-0.181	0.079	0.026

Terms used in Table 5.12, to Table 5.14: Su (summer), A (autumn), W (winter), In (intercept) and Gr (gradient), Dep (dependent), Indep (independent), Tupk=turbidity peak Tur=turbidity range, Tutot=total turbidity, Qr=flow range, Qpk=flow peak, Qtot=total flow, Rpk=rainfall peak, Rtot=total rainfall, NHpk=ammonia peak, NHtot=total ammonia, tE=event time, tQRL=flow rise time, tQFL=flow recession time, dQRL=flow rise rate, dQFL=flow recession rate, LagTuNH=time between turbidity and ammonia peaks, , LagTuQ=time between turbidity and flow peaks.

5.4.7 Seasonal influence on total turbidity-event attribute regressions

The gradient and intercept of the relationship between turbidity peak and discharge varies significantly between seasons. Table 5.12 shows the output of the logistic multiple linear regressions identifying the influence of the various seasons on the regression relationship. Su, A, W, In and Gr represent summer, autumn, winter, intercept and gradient respectively. During summer a statistically significant decrease in the gradient in the relationship between total turbidity and discharge and a statistically significant increase in the intercept are observed. The relationship between total turbidity and total discharge also varies significantly between seasons, with a statistically significant decrease in the gradient during the autumn and in the intercept during the summer. Results with the other statistically significantly correlated attributes summarised in Table 5.13 and Table 5.14 mostly show similar seasonal influence stated above. Statistically significant decrease and increase in the intercept during autumn, and increase in the gradient during winter were also found associated with some attributes (Table 5.14).

5.4.8 Turbidity – ammonia relationship

Figure 5.11 shows the scatter plots of seasonal regression of total turbidity with event time, ammonia total and ammonia peak respectively. In all, summer regression lines seem to be lower than the others indicating lower intercept values. Table 5.15 and Figure 5.15 summarise the seasonal distribution of mean ammonia peaks and of events with NHpk values around 2mg/l. All seasons had mean NHpk values of more than or equal to 2mg/l (Figure 5.15(a)). Averagely, about 60% of total events have ammonia peak values more than or equal to 2mg/l, with maximum and minimum of 71 and 47% for winter and summer respectively. The seasonal distribution of ammonia peak events is however not significantly different according to chi-square test results (p=0.57) possibly due to small numbers.

Table 5.15: Seasonal distribution of events with NHpk values around 2mg/l of and mean ammonia peaks

Seasons	Number of events with NHpk around 2 mg/l Overall	MoE	%	Less	%	Mean NHpk (mg/l)
Spring	20	12	60	8	40	2.8
Summer	15	7	47	8	53	2.0
Autumn	14	9	64	5	36	2.6
Winter	17	12	71	5	29	4.1
Total	66	40	61	26	39	2.9

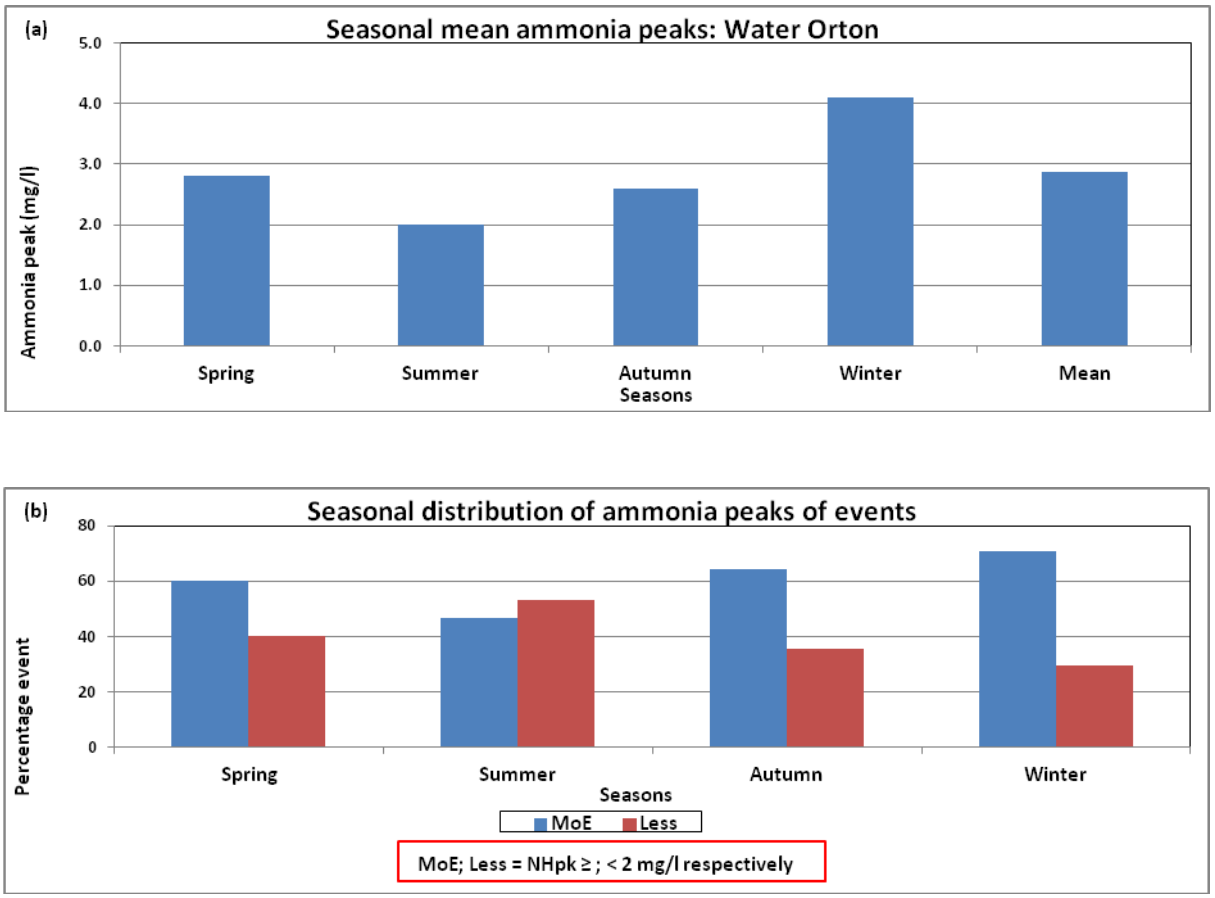

Figure 5.15: Seasonal distribution of: (a) mean ammonia peaks, (b) events with NHpk values around 2mg/l.

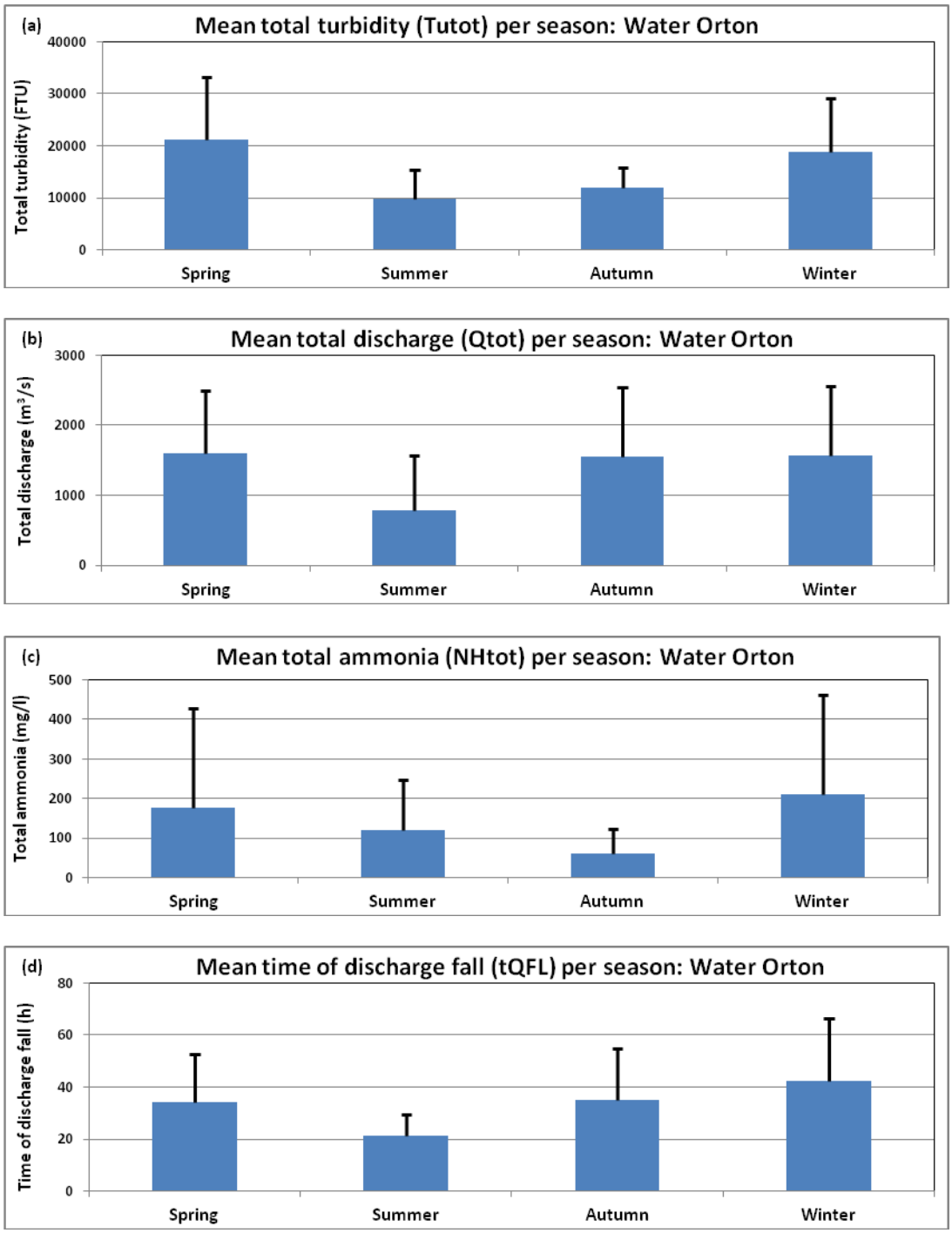

Figure 5.16: Means of events attributes for spring, autumn, winter and summer: (a) Total turbidity; (b) Total discharge; (c) Total ammonia; (d) Time of discharge recession showing error bars of standard deviation.

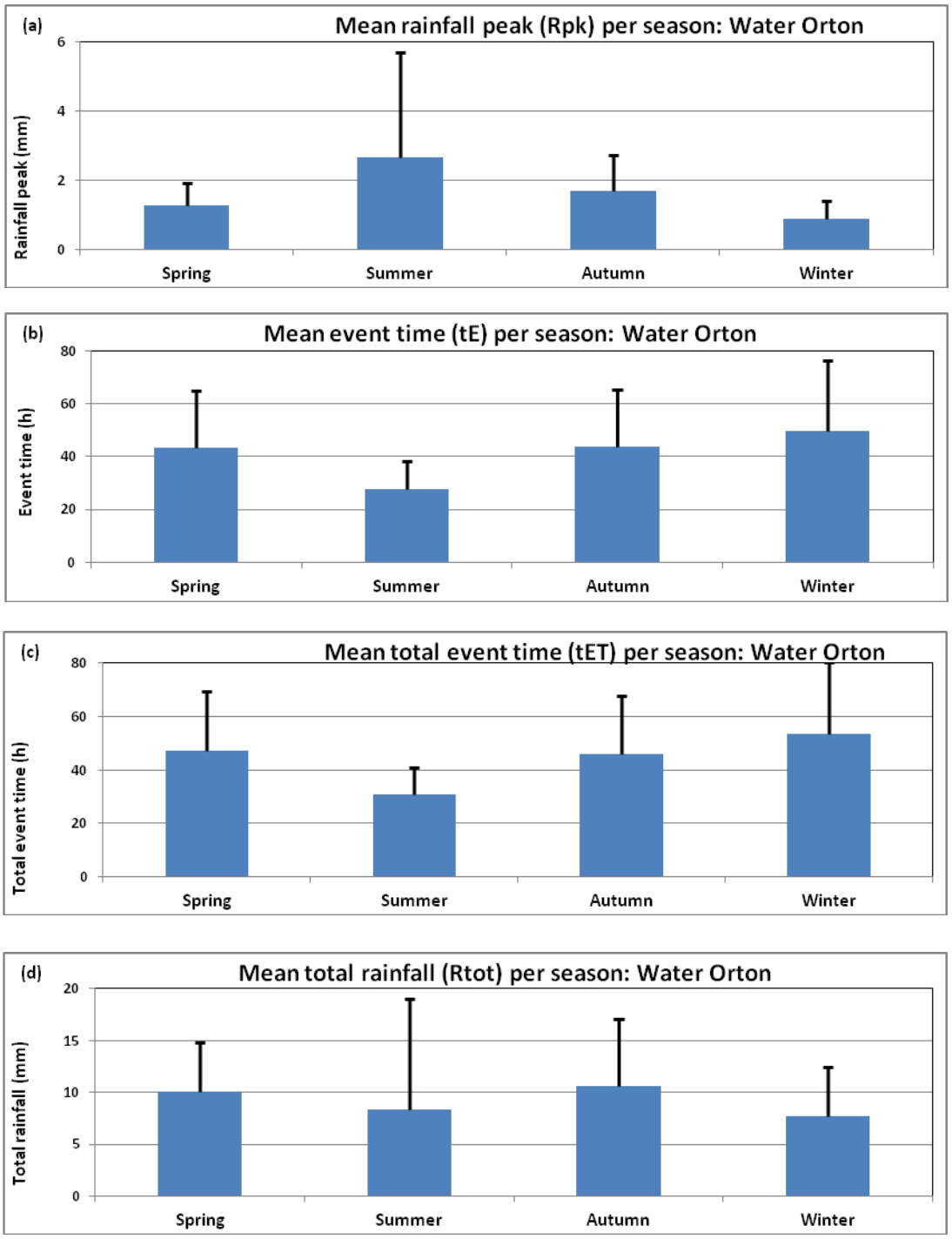

Figure 5.17: Means of events attributes for spring, autumn, winter and summer: (a) Rainfall peak; (b) Event time; (c) Total event time; (d) Total rainfall showing error bars of standard deviation.

5.5 Discussion

High urban extent significantly influences catchment turbidity dynamics

All four attributes, discharge rising and recession times (tQRL, tQFL), and rate of discharge rise and recession (dQRL, dQFL) that could measure flashiness, an indicator for urban extent (cover), had significant influence on total turbidity in summer and autumn (Table 5.14). This could confirm the significant influence of high urban extent/cover on catchment turbidity dynamics. The significant decrease in total turbidity during summer could result from significantly low summer flow (Table 5.14; Figure 5.16(b)). This likely results from the smaller contributing area of storm events, inferred from lower event time (Table 5.14; Figure 5.17(b)) (BaČA, 2008).

Recession occurs when deposition of suspended sediment, the major contributor of turbidity (Goransson et al., 2013), occurs due to reducing discharge. The lower or higher the discharge recession time, the equally shorter or longer time for the sediment to be deposited, and thus the lower or higher the turbidity, depending on availability. Summer and autumn were found to have the lowest and highest material availability respectively inferred from the intercept coefficients of total turbidity-total discharge regression (Table 5.8 (c); Figure 5.10(c)) (Rovira and Batalla, 2006). Although autumn showed the highest availability, it had the lowest rate of change of total turbidity with respect to total discharge and most of the other attributes. Also, the highest discharge recession rates (dQFL) occurred in autumn (Table 5.9; Figure 5.13(b)). These could lead to the significant decrease and increase in total turbidity during summer and autumn due to discharge recession time (tQFL) respectively. It

could thus be said that urban extent really had significant influence on the studied catchment turbidity dynamics.

Urbanisation adds impervious surfaces to the catchment and adds storm water drainage systems that are considered as key pathways for catchment runoff in response to quantity and spatial distribution of rainfall (Hall et al., 2003). Flashiness, measured with flow rise or recession times and rates, is linked with imperviousness and thus the extent of urban cover. The percentage imperviousness is highly and positively correlated with high flows and flashiness, with the greatest impact on flashiness (Nagy et al., 2012). Sediment delivery to rivers increases during highly flashy flows (Estrany et al., 2011). Thus, the effect of urbanisation with about 60% urban extent (Marsh and Hannaford, 2008; CEH, 2012) is evident in the catchment's highly flashy nature. Shorter times to peak and higher peaks result from higher imperviousness and good drainage network enhancing efficient and rapid routing (Goodwin et al., 2003). The amount of turbidity scatter is due to catchment area and flashy flow (Ferrier, 2001). Flashiness is the rate of flow change (dQRL) (McMahon et al., 2003), during which large quantity of flow occurs within a short time (Old et al., 2006). Sediment delivered to a river system is not only a function of erosion processes but also a function of the extent to which sediment movement pathways are connected to the river system (Naden and Cooper, 1999). More flow and sediment discharge are pronounced in the urbanised sections with high impervious cover and manmade drainage systems making efficient routing of runoff (Old et al., 2006). Such anthropogenic activities as river

channelisation, culverting and high impervious surfaces increase sediment yield (Holden, 2005).

Seasons with varying discharge (hydrological) conditions cause significant variations in turbidity

Summer and autumn were significantly different from spring and winter which are not significantly different from one another. This could indicate significant seasonal variations between discharge and turbidity, thus, confirming hypothesis. The occurrence of the greatest sediment increase in urban streams during season with highest flow has been reported (Nagy et al., 2012). High mean total discharge within spring is also widely noted (Richards et al., 2008). Transport pathways may be fully active in winter during high discharge (stream sediment transport capacity) events and less vegetation cover, resulting in more efficient sediment remobilisation and transfer processes (Estrany et al., 2011). Low mean total discharge in summer is also widely reported (Pavanelli and Pagliarani, 2002; Debels et al., 2005; Zabaleta et al., 2007; Bayram et al., 2012; Prudhomme et al., 2012), due, among other things, to high evapotranspiration as a result of high temperatures, lower humidity and higher leaf area indexes. Thus, the lowest mean total turbidity within summer likely results from the low discharges (stream sediment transport capacity). River suspended sediment concentration depend on the stream sediment transport capacity and sediment availability, with the stream sediment transport capacity changing with river discharge (Lefrançois et al., 2007). Low energy associated with low discharge events during summer and autumn could promote settling of sediment despite active transport pathways, whereas due to high discharge in spring and winter,

there will be increased transport capacity, resulting in more efficient sediment remobilisation and transfer processes (Estrany et al., 2011).

Variation in the intercept of the regression relationship between seasons could reflect the variations in sediment supply (Rovira and Batalla, 2006). The significantly lower summer intercept of the total turbidity-total discharge relationship (Table 5.8 (c) and Table 5.15; Figure 5.10(c)) may result from low availability of sediment in the channel during this period. In comparison, the significantly higher intercept within autumn likely indicates that there is higher sediment availability at the catchment scale during this period. Intercept values are similar within spring and winter (Table 5.8(c); Figure 5.10(c)).

The highest intercept coefficient in the relationship between total turbidity and total discharge occurs in autumn. This season also showed the lowest gradient coefficient and the lowest R value (Table 5.8 (c)). So although autumn showed the highest turbidity, it had the lowest rate of change of total turbidity with respect to total discharge and most of the other attributes. Autumn thus shows significantly lower rate of change of total turbidity with respect to total discharge inferred from its low gradient (Table 5.14). Turbidity-discharge regression lines intercept and gradient could reflect sediment availability and rate of change respectively (Rovira and Batalla, 2006). The variation in the relationship between total turbidity and discharge could result from the comparatively low discharge during this season. Significant decrease in summer intercept and autumn gradient for total turbidity due to total discharge could also be inferred from the event time. Analysis of variance test results showed significantly different event time means between the seasons (Table 5.6(b)). Logistic

multiple regression results also showed significantly lower summer intercept and autumn slope (Table 5.14). Event time influence the area contributing runoff (BaČA, 2008). The smaller the area contributing runoff, the smaller the quantity of runoff and turbidity could be. Thus, summer with the lowest total turbidity and autumn with lowest rate of change of total turbidity with respect to total discharge could also partly be due to smaller area contributing runoff inferred from low event time. Other factors that could as well contribute to the significant seasonal variations between discharge and turbidity are discussed as follows. The growth of dense bands of vegetation close to and along the banks of the river as observed in the studied catchment, especially during summer, could lead to formation of significant water infiltration areas (Cammeraat, 2002). The vegetation, among other factors affecting infiltration rate, could also cause rate of runoff to be highly variable both in time and space (Slattery et al., 2006). These could, among other things, result in reduced rate of runoff and thus total discharge (due to increased infiltration rate) and also reduced SSC, a major cause of turbidity, possibly due to trapping of suspended sediment with attached nutrients (e.g. ammonia), especially during big rainfalls (Goodwin et al., 2003). This could as well explain further the significantly lower levels of ammonia in summer, and significantly higher levels in winter found in the study, probably when there is erosion on fallow surfaces (Table 5.15).

Effluent spillages significantly affect seasonal turbidity dynamics

The number of events with ammonia peak values greater than 2mg/l does not vary significantly between seasons. Approximately 60% of the events have ammonia peak values greater than or equal to 2mg/l, with all seasonal mean

ammonia peak values above 2mg/l (Table 5.15; Figure 5.15(a)). Further, analysis of variance test results indicate that whilst means ammonia peaks are not significantly different between seasons, the total ammonia does vary significantly between seasons ($p=0.002$) (Table 5.6(b)). This could suggest there were effluent spillage, likely from CSOs, WwTWs and STWs in all seasons, with the highest spillage frequency occurring in winter and the lowest in summer (Table 5.15; Figure 5.15(b)). This could confirm the significant influence of effluent spillage and/or fertiliser runoff, as well as distal exchangeable ammonia on seasonal turbidity dynamics. Mostly, total ammonia concentrations for surface waters are less than 0.2mg/l but can be up to 2-3mg/l. Organic matter pollution found in domestic sewage or industrial waste can lead to concentrations of more than 2mg/l (Chapman, 1996).

The intercept in the relationship between total turbidity and ammonia total is significantly lower within the summer ($p<0.001$). Further, the intercept in the relationship between total turbidity and ammonia peak is significantly lower within the summer and autumn ($p<0.001$ and 0.047 respectively) (Table 5.14; Figure 5.11(b) and (c)). This could be due to the small amount of dilution resulting from the low discharges during summer and autumn. However, scatter in the turbidity discharge relationship indicates that other factors influence suspended sediment transport or turbidity dynamics (Hudson, 2003). In urbanised catchments, this considerable scatter, particularly at low flows, may result from the large number of point source inputs, notably sewage effluent and combined sewer overflows, and also to the variable degree of dilution by flow in the main stream (Naden and Cooper, 1999). The Tame River receives

significant discharge from sewage treatment plants (Rivett et al., 2011). Combined Sewer Overflows (CSOs) relieve sewerage systems of increased hydraulic pressure during heavy rains. 92 out of 374 CSOs found in the catchment were put under Unsatisfactory Intermittent Discharges (UIDs) and had adverse environmental effects on the receiving water body) (Salt, 2009) and which needed to be improved (Tame, 2010).

Significantly more anticlockwise events are associated with seasons with more 'low flows'

More anticlockwise events were observed than clockwise events, with all seasons except spring having anticlockwise events of more than 50% (Table 5.5(a); Figure 5.6(a)). Although such differences in numbers are not significant (Table 5.5(b)), the mean lead and lag times (times between turbidity peak leading and lagging discharge peaks) were significantly different in all seasons (Table 5.10(c)). There are significantly more events with low flows (with total discharge below the overall event mean of 1393m^3/s) for all seasons except spring (Table 5.11(b); Figure 5.14(d)). This pattern is similar to the seasonal distribution of clockwise and anticlockwise (lead and lag) events (Table 5.5(b)). Thus, the seasons with more than 50% anticlockwise could partly be due to more low flow events. However, summer with the highest number of low flows of 21% of overall events (Table 5.11(b); Figure 5.14(d)) did not have the highest number of anticlockwise events (Table 5.5(a); Figure 5.6(a)). This could mean low flow alone could not be the major cause of the anticlockwise events with turbidity peaks lagging discharge peaks. Anticlockwise are mostly related to sediment settling in stream channels as a result of low flow (Jansson, 2002;

Smith et al., 2003; Lefrançois et al., 2007; Doomen et al., 2008; Smith and Dragovich, 2009). River Tame catchment consists both of natural and modified portions mainly with natural in-channel deposits (Rivett et al., 2011). During anticlockwise events, catchment sediment supply is not limited, and erosive action during the initial part of the event opens up new supplies through the reach which are transported during the rising limb. However low flow events with low energy (stream sediment transport capacity) could not transport such large quantity of sediment from the reach and it is probable that net deposition occurs within the reach (Smith et al., 2003). Low energy conditions from low flow could result in picking and carrying channel sediment and for them to immediately be re-deposited within channel thereby promoting settling of sediment despite active transport pathways (Estrany et al., 2011). The vegetation in the catchment could also result in infiltration zones which could increase rate of infiltration and reduce rate of runoff and thus, reduce flow (Cammeraat, 2002; Goodwin et al., 2003; Slattery et al., 2006). The sediment already deposited in and that currently supplied to a channel or catchment determine its total availability (Lefrançois et al., 2007).

Anticlockwise events are also associated with sediment source mobilised slowly (Bowes et al., 2005) from a long, distal sources with difference in relative travel time (Jansson, 2002; Goodwin et al., 2003; Bowes et al., 2005; Smith and Dragovich, 2009). Significantly different means of times between turbidity peak leading and lagging discharge peak are found for all events and events for all seasons (Table 5.10 (c)). Lag times could be used to infer distal sources such that the highest lag time could mean runoff from the most distant source.

Seasonal mean lead and lag time distribution for overall events shows spring to have the highest mean lag time followed by winter (Table 5.9 (a); Figure 5.14(a)). Although, spring could be considered to show the most distant turbidity source, it also did not have the highest anticlockwise events. Thus, lag time alone could also not be the major cause of anticlockwise events. Winter with the highest anticlockwise events could thus be inferred to be due to a combined effect of low flow and distal turbidity source since it had the second highest mean lag time, possibly because of its wider areal rain event extent, and with the second highest number of low flows. This could suggest that seasons with more number of low flow events alone could not be enough criteria for more anticlockwise events. Suspended sediment concentration is controlled, in addition to discharge, by exhaustion and reprenishing of different sediment sources (Doomen et al., 2008), with the sediment source replenishing in the catchment attributed to the number of anticlockwise events. Anticlockwise events are generally indicative of large, continuously available catchment sediment supplies which do not show exhaustion (Smith et al., 2003).

5.6 Chapter summary

This chapter has confirmed that high urban extent significantly influences catchment turbidity dynamics. This is shown in the flashiness of the catchment as measured by, for example, the time of discharge recession which showed decrease in total turbidity during summer (shortest recession) and increase during autumn (second longest recession). The longer the discharge recession time, and with high availability, the more the turbidity would be in channel. The time of discharge recession also showed decrease in total turbidity during

autumn possibly due to low rate of change. It was also found that seasons with varying discharge conditions cause significant variations in turbidity. Significant decrease in total turbidity during summer due to low discharge and availability, and autumn due to low rate of change were found associated with total discharge. Effluent spillage also caused significant effects on seasonal turbidity dynamics. Total turbidity significantly decreased with total ammonia during summer and ammonia peak during autumn due to low availability and possibly low dilution. High vegetation trapping suspended sediment and attached nutrients e.g. ammonia, and low discharge (low water amount and energy) in summer discussed above could partly explain the above. Significantly more anticlockwise events were shown to be associated with seasons with more low flows. All events but spring with more anticlockwise events were associated with more low flows. Winter with the highest anticlockwise events was the season with the second most distance runoff source, possibly because of its wider areal rain event extent, and with the second highest number of low flows. Thus, low flows together with distal sources could be responsible for more anticlockwise events found.

CHAPTER 6 THE CONTROL OF SCALE ON CATCHMENT SEDIMENT DYNAMICS

6.1 Chapter Introduction

This third results chapter examines the scale effects of turbidity responses to storm events of an urban river, thus addressing the third research objective outlined in section 1.3 in Chapter 1. It consists of six main sections namely introduction, a brief literature background leading to the objectives of the chapter, outline of methodology including the study areas, data quantity, methods and analytical techniques, then the results section, followed by the discussion and then the chapter summary.

6.2 Literature background

In Chapter 4, events characterisation and turbidity changes with respect to different storm event attributes revealed the significant influence of events type on turbidity dynamics. It dealt with one temporal scale (short-events) (Stanfield and Jackson, 2011) within one spatial scale; the downstream Water Orton sub-catchment. Chapter 5 revealed a significant seasonal influence on event sediment dynamics and controls. These two result together thus considered the same temporal scale (events) within the same spatial scale.

The scatter in the turbidity-discharge relationship was found to differ among events and seasons. This scatter was attributed to factors controlling sediment processes in addition to discharge (Hudson, 2003), such as in-channel exhaustion or variations in sediment availability (Rovira and Batalla, 2006), point source input, discharge dilution (Naden and Cooper, 1999), flashiness and

catchment area (Ferrier, 2001). However, the scale dependence of these processes and controls has received little attention within the literature.

Of the small number of studies that examined the scale dependence of catchment sediment processes, most have concentrated on either a small number of variables or non-urban rivers (some given in Table 6.1). It is important to determine the controls on dynamics within urban rivers at different temporal and spatial scales (Yue, 2012). Between spatial scales, some types of rain event and flow events result in similar reactions that can be explained to show higher degree of consistency in erosion processes' temporal forms and/or sediment source contributions' size (Smith and Dragovich, 2009). Also, large-scale processes could be interpreted as a mix of small-scale processes (Merz and Blöschl, 2003).

Higher scatter and flashier flows have been associated with smaller catchment areas (Ferrier, 2001). The intercept of the suspended sediment-flow relationship is also strongly related to the percentage of urban area (Naden and Cooper, 1999) and smaller variation in turbidity for larger river catchment areas (Jiongxin, 2009). Further, higher specific sediment yields (SSY) are characteristic of small catchment areas (Gao and Puckett, 2012). As a result, negative relationships between mean suspended sediment and catchment area have been observed (Naden and Cooper, 1999) and lower maximum TSS is associated with storms within larger watersheds (Reed et al., 2010).

Higher sensitivity of turbidity to local sources in smaller drainage areas, with more homogeneous precipitation allowing a simpler explanation of rainfall data

and subsequent runoff and erosion drivers, are reported (Duvert et al., 2010). Problems of scale transference have been generally overlooked yet implications are fundamental to geomorphology. Increases in spatial scale involve increases in complexity and spatial dimensions, new variables, relationships and problems, and also comparison of event start times at the two spatial scales indicates that start of flow is delayed when catchment area increases (de Boer and Campbell, 1989).

This chapter thus examines the turbidity response for storm events at different spatial scales, comparing the smaller upstream James Bridge and larger downstream Water Orton sub-catchments. It aims to evaluate the control of scale on turbidity dynamics by investigating the following research statements.

1. There are more single discharge peak events with smaller catchments.
2. In larger catchments, multiple discharge peak events are more common.
3. First flush (clockwise) events are the most common for bigger catchments.
4. Downstream suspended sediment load is significantly affected by tributary inputs.

Table 6.1: Scale effects on turbidity dynamics given in the literature

Variable/attribute	*Effect of scale*	*Reference*
Tu – Q intercept	Strongly related to percentage urban cover	Naden and Cooper, 1999
Tu – Q scatter	Higher for small catchments	Ferrier, 2001
Flashiness	Higher for small catchments	Ferrier, 2001
Flashy storms	Significantly higher in number for smaller catchments	Merz and Bloschl, 2003
Lead time	Higher for large storms for bigger catchments	Hudson, 2003
Lag time	Higher for large storms for bigger catchments	Hudson, 2003
High magnitude localised storms	Response could be same pattern, though reduced, at the bigger as at smaller catchment	Smith and Dragovich, 2009
Moderate to high magnitude, high spatial storms	Bigger basin reaction is an enlarged scale of similar processes in smaller catchments	Smith and Dragovich, 2009
Small storm events	Bigger catchment flow and sediment is mostly derived from smaller areas and could be modified by main channel effects	Smith and Dragovich, 2009
Rainfall	More homogeneous for smaller catchments	Duvert et. al., 2010
Suspended sediment concentration	Higher sensitivity to local sources for smaller catchment	Duvert et. al., 2010

6.3 Methodology

6.3.1 Study area description

River Tame catchment has the highest urban cover in the UK (Lawler et al., 2006). Figure 6.1 shows the smaller James Bridge and bigger Water Orton sub-catchments studied. The study area, data quality, events selection criteria and classification are the same as discussed in sections **Error! Reference source not ound.** through 4.3.3 (Chapter 4) for the whole River Tame catchment and the Water Orton sub-catchment.

The James Bridge monitoring site is the headwaters of the River Tame. It has a sub-catchment of area 57 km^2 with an average altitude of 113.3 m A.O.D. The Black Country urban area is the source of the Wolverhampton branch, which flows through James Bridge gauging station with Darlaston, Waddens and Sneyd Brooks as tributaries (Figure 6.1) (Rivett et al., 2011). The Bescot station which is 2km downside the James Bridge station has mean annual rainfall, flow (mean and peak) of 712mm, 2.32 and 56.8 m^3s^{-1} respectively (Marsh and Hannaford, 2008; CEH, 2012). The altitude for Bescot is 107.3 m A.O.D. A major WwTW (Wastewater Treatment Works) is upstream of the James Bridge station at Willenhall and three additional WwTWs before Water Orton (Figure 6.1). Table 6.2 is a summary of some basic characteristics for the two studied sub-catchments as well as Bescot.

Table 6.2: Catchments characteristics

	Tame	James Bridge	Water Orton
Area (km^2)	1400	57	408
CSOs number	374		
Base flow index			0.61
Urban cover (%)			59.2
Grass-farm-woodland (%)			21.3
Station level (m AOD)		113.3	74.4
Tributaries number		3 (smaller)	7 (4 larger and 3 smaller)
Mean annual rainfall (mm)			725 (1961 - 1990)
Mean annual flow (m^3)			5.39
Peak flow - record (m^3)			128.33 (2006/7)
Peak flow - measured (m^3)		14.7	70.39
Peak flow rank			36
WwTW number		1	4

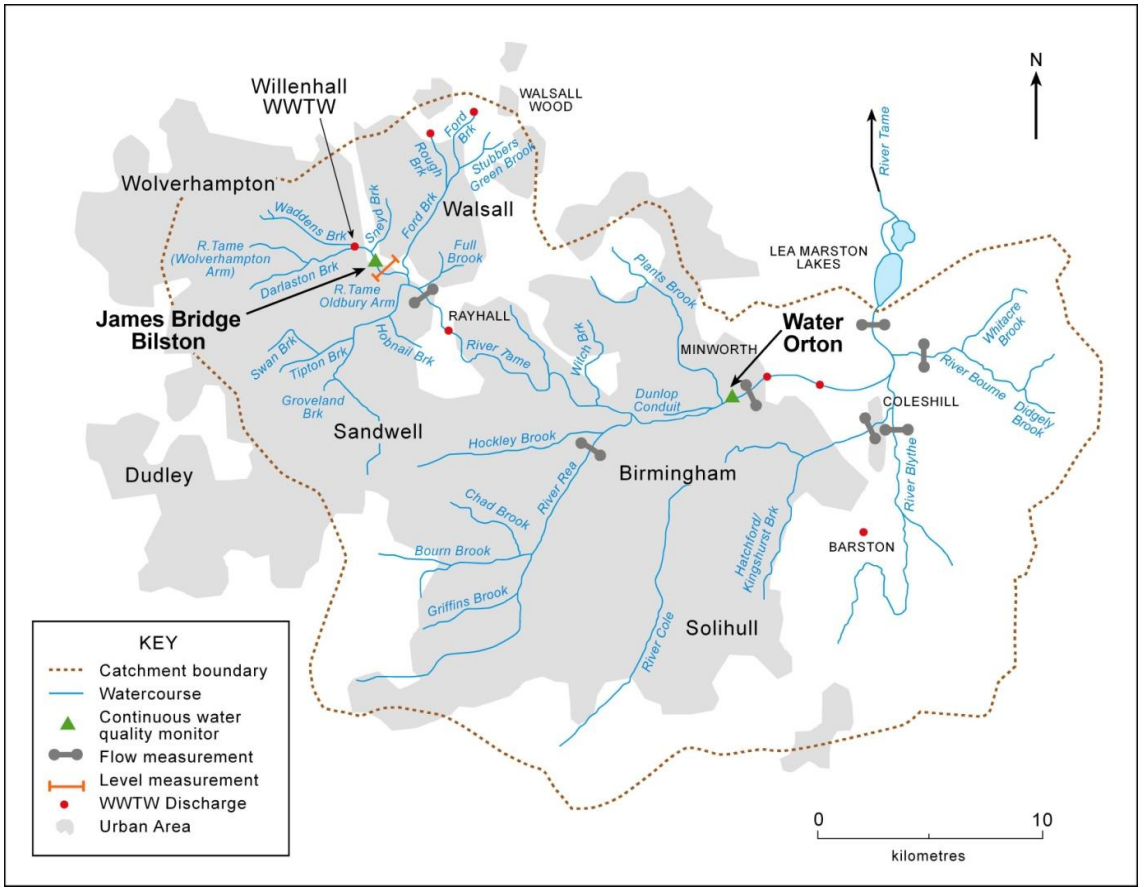

Figure 6.1: River Tame catchment showing the James Bridge and water Orton monitoring stations.

6.3.2 Data quantity

The period of study was from 15 March 2001 to 30 November 2003, comprising 3 seasons each for spring, summer and autumn and 2 seasons for winter due to limited data from the James Bridge monitoring station. Thus 33 continuous months (11 continuous seasons) of 15-minutes resolution turbidity (FTU), ammonia (mg/l), flow rate Q (m^3/s) and rainfall (mm) data were used. The James Bridge stations for automatic river flow and water quality monitoring (UK National Grid Reference SO, [Easting 9891, Northing 9751 for turbidity and ammonia; and Easting 9892, Northing 9750 for flow]); and Willenhall (UK National Grid Reference SO, [Easting 9786, Northing 9826 for rainfall]) were the sources of data. Station location description for Water Orton is given in section 3.3.

6.3.3 Analytical Techniques

Events attributes were analysed as outlined in detail within Chapter 4. The events identified independently within both the James Bridge and Water Orton catchments were cross referenced to determine which events within the upstream James Bridge catchment were subsequently identifiable within the downstream Water Orton monitoring station. Dates of upstream and downstream events were compared. Some upstream events did not have any connection downstream. Some upstream events were connected but did not qualify as events downstream because they were below event threshold and/or with turbidity data issues. One-to-one, two-to-one and three-to-one upstream-downstream events connections were found. Discharge and turbidity peak to peak times from the upstream to downstream monitoring stations were also

calculated to estimate the travel time of storm events. The attributes of the linked events were also compared, identifying the extent to which events maintained or transformed in nature as they increased in scale (progressed downstream). Chi-square tests determine the statistical significance of the number of events within each classification. Analyses of variance was also performed to determine attributes that differed significantly with event type and t-tests were conducted to identify attributes with significantly different means between the two scales. The statistical significant of relationships between turbidity and event attributes with Pearson's coefficients of correlation and logistic multiple regressions conducted establish the level of effects of the change of scale.

6.4 Results

6.4.1 Events types

A total of 90 and 53 events were identified for the James Bridge and Water Orton stations respectively, based on criteria described in chapter 4. Over 60 % of James Bridge events are single and over 60 % of Water Orton events are double and multiple (Table 6.3(a)). The event distribution differs significantly between the two sites (p=0.017; Chi-square; Table 6.3(b)). This suggests that a significant number of events are transformed in their nature as they propagate downstream.

The distribution of event types between the upstream and downstream monitoring stations is compared within Table 6.4(a). The smaller James Bridge sub-catchment shows a dominance of single events, compared with double and

multiple events. Within the larger Water Orton catchment, double events dominate the storm event types. Table 6.4(b) gives chi-square test results for the distribution in Table 6.4(a) and shows these difference are significant ($p<0.001$).

Whilst 143 discharge events were identified at the two scales over the extensive period of study, the strict data quality assessment imposed and the challenges of maintaining concurrent sensors over multiple years led to the majority of observed discharge events being discarded from scale dependent turbidity analysis (one of the two turbidity sensors was not effectively working during a given storm events). 56% have their corresponding downstream events not selected (without turbidity values) because of noisy turbidity and measured values that exceeded 500FTU. A further 10% are discarded because discharge range did not exceed the set threshold values to define an event. In the downstream catchment, 43 downstream events were disregarded due to above reasons (noisy turbidity or > 500FTU and discharge < threshold values).

Cross reference of the upstream and downstream events identified a total of 29 upstream events and 20 downstream events which occurred whilst both monitoring stations passed the rigorous data quality assessment. 98% of these selected upstream events connected to downstream events, with only about 2% not connected (Table 6.4(a); Figure 6.2 (a)). The 29 upstream events connect to 20 downstream events because two and three upstream events are connected to one downstream event on multiple occasions. There are 13 upstream events with one to one connections (Table 6.6).

6.4.2 Distribution of connected and lead-lag events

More lead events are observed at a larger scale and more lag events are observed at a small scale. Table 6.5(a) and Figure 6.2 (b) summarise the lead-lag events distributions for the 13 selected connected events. Table 6.5(b) summarise Chi-square test results for the distribution in Table 6.5(a), with lead and coinciding events put together, and shows this difference is significant at the 95% confidence level.

Table 6.3: Distribution of events: (a) overall; (b) Chi-square test results

(a)	James Bridge		Water Orton	
	No	**%**	**No**	**%**
Single	56	62	21	40
Double	30	33	25	47
Multiple	4	5	7	13
Total	**90**		**53**	

(b)	Value	df	Asymp. Sig. (2-sided)
Pearson Chi-Square	8.154[a]	2	**0.017**
Likelihood Ratio	8.109	2	0.017
N of Valid Cases	143		

a. 1 cells (16.7%) have expected count less than 5.

Table 6.4: Distribution of: (a) connection of events; (b) Chi-square test results.

(a) Connection	JB	%	WO	%
With Tu	29	32	20	19
Without Tu	50	56	43	41
Not	2	2	33	31
< threshold	9	10	9	9
Total	90		105	

(b)	Value	df	Asymp. Sig. (2-sided)
Pearson Chi-Square	28.653[a]	3	**<0.001**
Likelihood Ratio	34.223	3	<0.001
N of Valid Cases	195		

a. 0 cells (.0%) have expected count less than 5.

Table 6.5: Distribution of: (a) lead/lag/co events; (c) Chi-square test results for the 13 upstream events with one-to-one connection with 13 downstream events

(a)	JB	%	WO	%
Lead	3	23	8	61
Lag	9	69	4	31
Co	1	8	1	8
Total	**13**		**13**	

(b)	Value	df	Asymp. Sig. (2-sided)
Pearson Chi-Square	3.846[a]	1	**0.050**
Continuity Correction[b]	2.462	1	0.117
Likelihood Ratio	3.947	1	0.047
N of Valid Cases	26		

a. 0 cells (.0%) have expected count less than 5.

6.4.3 Discharge and turbidity peaks lead-lag and peak to peak times

Lead times are higher for the bigger Water Orton and lag times are higher for the smaller James Bridge catchments (Figure 6.3(b)). The difference in observed anti-first flush and first flush events within James Bridge and Water Orton is statistically significant (p=0.041; Figure 6.3 (a); Table 6.7 (a, b). The 13 one-to-one selected connected events have discharge and turbidity peaks lag time of 2.06 hours (h) (ranges 0.25 to 9 h) and 1.56 hours (ranges 1 to 2.5 h) for James Bridge and Water Orton respectively. In comparison, the lead time average 2.0 h (ranges 0.25 to 4.5) and 3.34 hours (ranges 0.5 to 6.75 h) (Table 6.7 (c)). The 13 one to one selected connected events have discharge and turbidity peak to peak time (h) ranges of 1.5 to 33.25 and 1 to 39 respectively (Table 6.6). Table 6.9 gives the range and mean values of the peak-to-peak times of both discharge and turbidity. **Error! Reference source not found.** shows the catter plots for discharge and turbidity peak-to-peak time and James Bridge and Water Orton lag times. The peak-to-peak scatter shows a higher correlation (R^2=0.337) than the lag time scatter (R^2=0.0151). Peak-to-peak times were

calculated by subtracting the time of peak at James Bridge from that at Water Orton. Negative times were obtained where peak at James Bridge comes after that at Water Orton, especially where Water Orton event was a multiple flow peak event which had started and peaked before its connected James Bridge event.

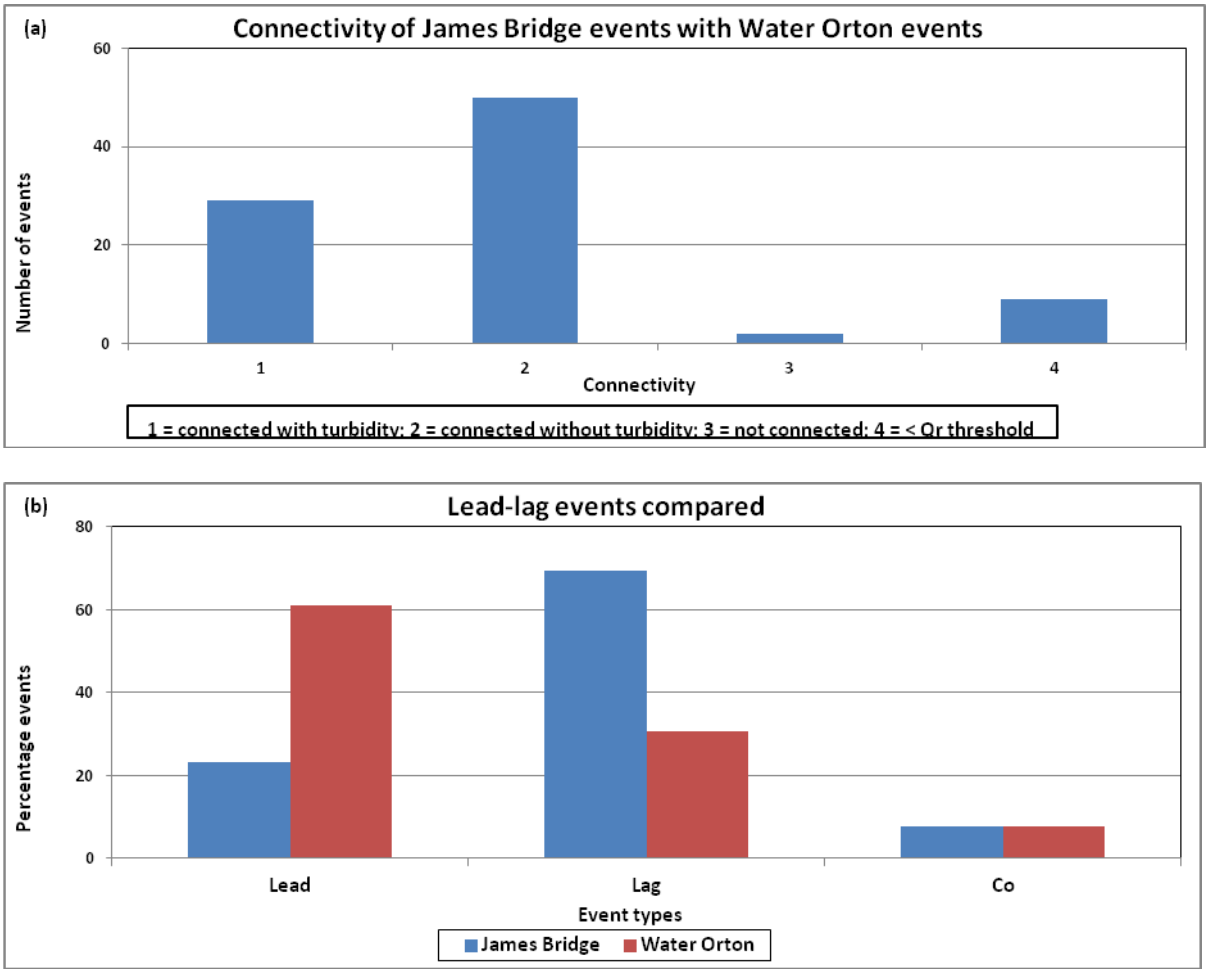

Figure 6.2: Distribution of (a) events connectivity; (b) Lead-lag events for the 13 upstream James Bridge events with one-to-one connection with 13 downstream Water Orton events.

Table 6.6: Peak to peak and lead/lag times for the 20 selected coinciding events

		Qpk Time			Tupk Time			Q - Tu Lag time (h)	
	Date	**JB**	**WO**	**Pk to pk (h)**	**JB**	**WO**	**Pk to pk (h)**	**JB**	**WO**
1	**27-Mar-01**	28(0130)	28 (0045)	(-)0.75	28 (0145)	27 (1800)	(-)7.75	(-)0.25	6.75
2	**03-Apr-01**	4 (0915)	5(1830)	33.25	4 (1815)	5(1830)	1.25	(-)9.00	0
3	**29-Jun-01**	29 (1615)	29 (2315)	7	29 (1600)	29 (2115)	5.25	0.25	2
4	**26-Sep-01**	26 (1915)	27 (0245)	7.5	26 (1930)	26 (2145)	2.25	(-)0.25	5
5	**30-Jul-02**	31 (0315)	31 (0445)	1.5	31 (1030)	31 (0615)	(-)4.25	(-)7.25	(-)1.50
6	**14-Oct-02**	14 (1500)	15 (2245)	31.75	14 (1545)	15 (2130)	5.75	(-)0.75	1.25
7	**01-Dec-02**	1 (0915)	1 (1045)	1.5	1 (0930)	1 (1145)	2.25	(-)0.25	(-)1.00
8	**23-Dec-02**	23(2000)	23(2130)	1.5	23 (1845)	23(2100)	2.25	1.25	0.5
9	**29-Dec-02**	29(0645)	29 (1445)	8	29(0700)	29 (1415)	7.25	(-)0.25	0.5
10	**16-May-03**	16 (1115)	17 (1915)	32	16 (0645)	17 (2145)	39	4.5	(-)2.50
11	**27-Jun-03**	27 (1715)	28(0030)	7.25	27 (1715)	27 (1815)	1	0	6.5
12	**28-Aug-03**	29(0030)	29 (0845)	8.25	29 (0045)	29(0430)	3.75	(-)0.25	4.25
13	**14-Nov-03**	14 (1545)	14(1800)	2.25	14(1600)	14 (1915)	3.25	(-)0.25	(-)1.25
14**	**22-Mar-01**	22(2130)	22(0200)	4.5	22(2100)	21 (1415)	(-)30.75	0.5	11.75
15**	**20-Nov-02**	20 (1045)	23(1700)	6.25	20 (1145)	23(2130)	81.75	(-)1.00	(-)4.50
16**	**26-Dec-02**	26 (1015)	26 (1145)	1.5	26 (1030)	26 (1630)	6	(-)0.25	(-)4.75
17**	**18-May-03**	18(2200)	19 (0345)	5.75	18 (2130)	19 (0315)	6.75	0.5	0.5
18**	**16-Jul-03**	17(1430)	17(2200)	7.5	17 (1415)	17 (2145)	7.5	0.25	0.25
19***	**06-Nov-02**	6(0830)	10(1100)	98.5	6(0800)	10(1130)	99.5	0.5	(-)0.50
20***	**11-Nov-02**	14 (0445)	14(0600)	1.25	14(0230)	14(1030)	8	2.25	(-)4.50

, * = 2, 3 upstream events results in 1 downstream events respectively.

6.4.4 Coinciding events Pearson's rank correlation and basic statistics

Table 6.9 summarises the correlation coefficients of turbidity range (Tur) and total (Tutot) with the other storm attributes for James Bridge and Water Orton for the 13 events. Scale is shown to have a critical impact on the related attributes to the turbidity range and total turbidity. A significant correlation is evident between turbidity range on only one single event attribute (discharge range) at the James Bridge monitoring station.

Table 6.7: (a) (Anti-) first flush distribution; (b) Chi-square results of distribution; (c) Lead-lag times statistics; (d) Chi-square results of range values.

(a) Station	FF	%	AFF	%
James Bridge	3	25	9	75
Water Orton	8	67	4	33

(b)	Value	df	Asymp. Sig. (2-sided)
Pearson Chi-Square	4.196[a]	1	**0.041**
Continuity Correction[b]	2.685	1	0.101
Likelihood Ratio	4.332	1	0.037
N of Valid Cases	24		
a. 0 cells (.0%) have expected count less than 5.			

(c) Lag times (h)	First Flush (FF)		Anti - First Flush (AFF)	
Station	**Range**	**Mean**	**Range**	**Mean**
James Bridge	4.25	**2.00**	8.75	**2.06**
Water Orton	6.25	**3.34**	1.5	**1.56**

(d)	Value	df	Asymp. Sig. (2-sided)
Pearson Chi-Square	3.884[a]	1	**0.049**
Continuity Correction[b]	2.313	1	0.128
Likelihood Ratio	4.019	1	0.045
N of Valid Cases	21		
a. 2 cells (50.0%) have expected count less than 5.			

Table 6.8: (a) Peak to peak times statistics; Chi-square results for (b) number of events; (c) ranges; (d) means.

(a)	Peak to peak time (h)			
Attribute	**Discharge (Q)**		**Turbidity (Tu)**	
Statistic	**Range**	**Mean**	**Range**	**Mean**
Positive	31.75	11.81	6.25	6.66
Negative	0.75	0.75	3.50	6.00

(b) Numbers	Value	df	Asymp. Sig. (2-sided)
Pearson Chi-Square	.003[a]	1	0.953
Continuity Correction[b]	0	1	1
Likelihood Ratio	0.003	1	0.953
N of Valid Cases	25		
a. 2 cells (50.0%) have expected count less than 5.			

(c) Range	Value	df	Asymp. Sig. (2-sided)
Pearson Chi-Square	10.208[a]	1	**0.001**
Continuity Correction[b]	6.927	1	0.008
Likelihood Ratio	8.49	1	0.004
N of Valid Cases	43		
a. 2 cells (50.0%) have expected count less than 5.			

(d) Mean	Value	df	Asymp. Sig. (2-sided)
Pearson Chi-Square	4.887[a]	1	**0.027**
Continuity Correction[b]	3.128	1	0.077
Likelihood Ratio	5.294	1	0.021
N of Valid Cases	26		
a. 2 cells (50.0%) have expected count less than 5.			

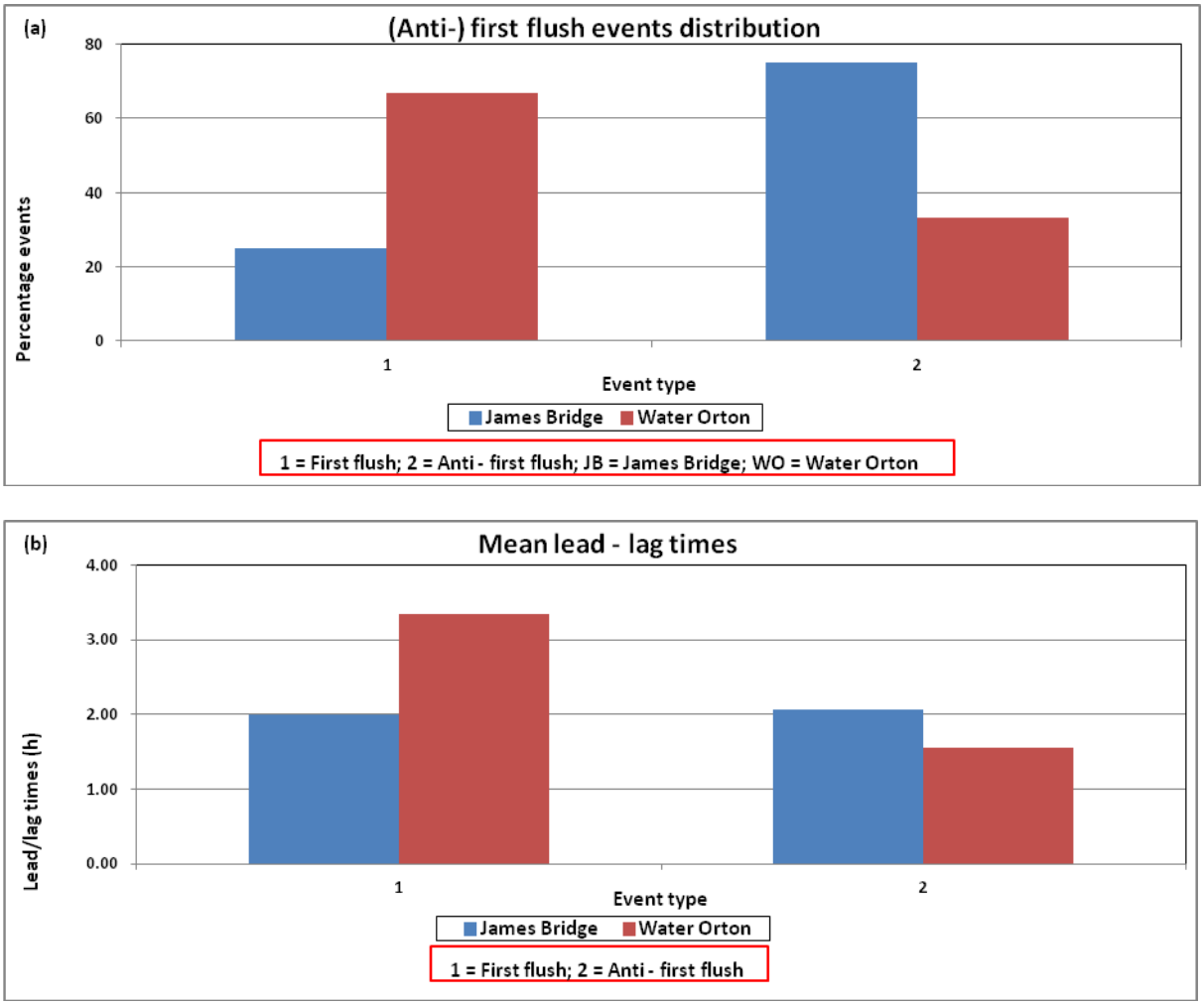

Figure 6.3: (a) Distribution of (anti-) first flush events; (b) Mean lead-lag times for James Bridge and Water Orton.

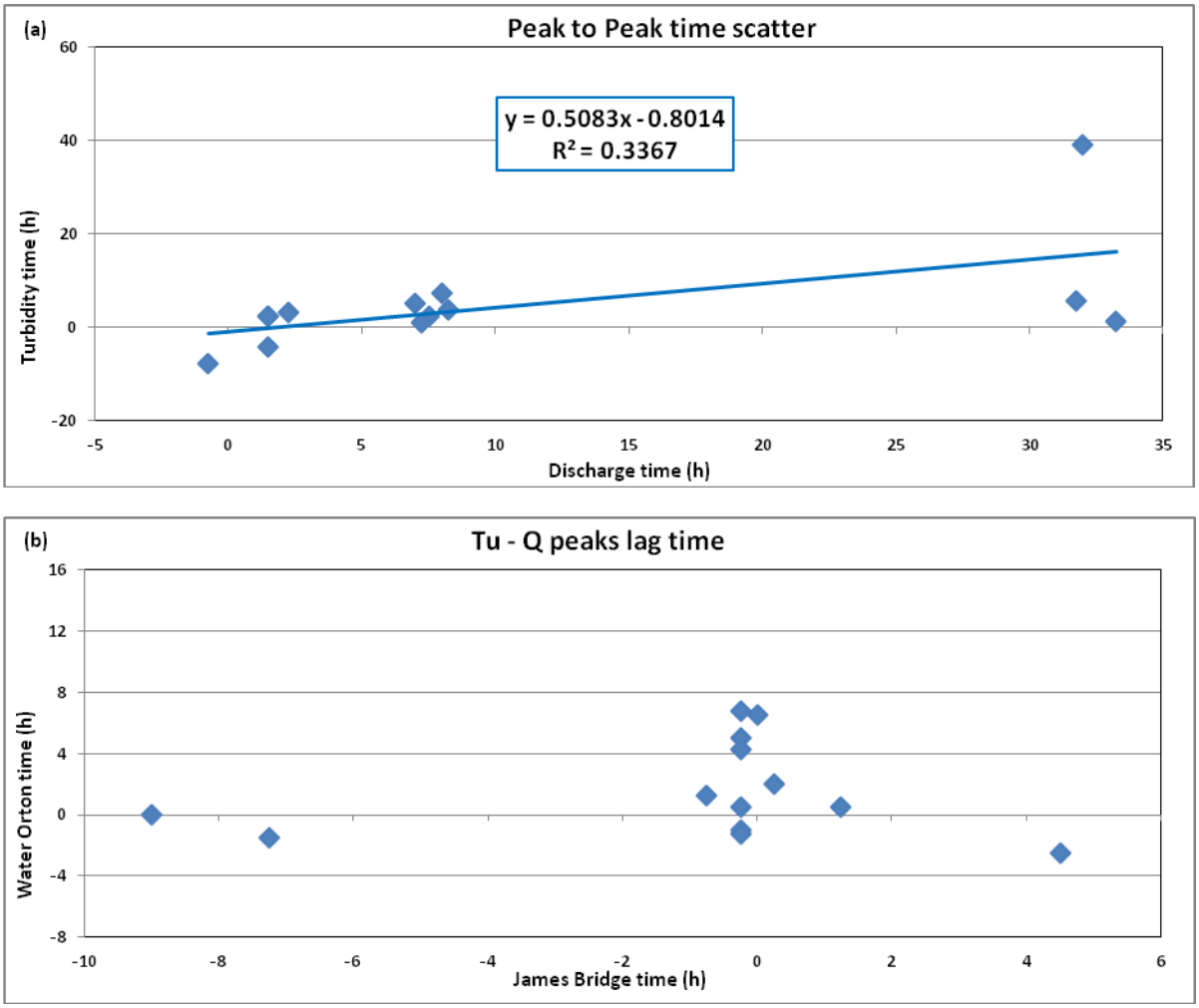

Figure 6.4: Scatter plots for (a) discharge and turbidity peak to peak times; (b) James Bridge and Water Orton discharge-turbidity peak lag times.

Table 6.9: Pearson's rank correlation coefficient of turbidity range (Tur) and total (Tutot) with the other attributes for: (a) James Bridge; (b) Water Orton.

(a)		Tur			Tutot	
No	**Attr**	**r**	**Sig**	**Attr**	**r**	**Sig**
1	**Qr**	0.567	0.043	**Qtot**	0.911	<0.001
2				**Rtot**	0.8	0.001
3				**tE**	0.747	0.003
4				**Qr**	0.697	0.008
5				**tET**	0.695	0.008
6				**Qpk**	0.674	0.011
7				**tQFL**	0.616	0.025

(b)		Tur			Tutot	
1	**NHpk**	0.75	0.003	**NHtot**	0.79	0.001
2	**Qtot**	0.725	0.005			
3	**Rtot**	0.677	0.011			
4	**Qr**	0.672	0.012			
5	**tE**	0.665	0.013			
6	**tET**	0.643	0.018			
7	**Qpk**	0.619	0.024			
8	**tQRL**	0.612	0.026			
9	**tQFL**	0.605	0.028			

In comparison, a total of nine attributes are significantly correlated within turbidity range at the Water Orton monitoring station, with the discharge range providing only the fourth strongest relationship with turbidity range. This pattern is reversed for the determination of the turbidity total. Only one attribute is significantly related to the turbidity total within the Water Orton catchment, whilst seven are significant within the James Bridge catchment.

Descriptive statistics, t-test analysis and scatter plots for the selected coinciding events for same attributes are presented. Table 6.10(a) summarises the basic statistics of attributes means while Table 6.10(b) shows the t-test results. Significant differences in means between the two catchments are found in 7 attributes. Figure 6.5 to Figure 6.8 show the scatter plots for the same attributes at the two catchments, and their characteristics summarised in Table 6.10 (c).

R^2 values ranged from the lowest of 0.001 for NHtot to the highest of 0.56 for rainfall peak.

Table 6.10: (a) Basic attributes statistics; (b) T-test results; (c) characteristics of scatter between same attributes at the two catchments for the 13 one to one events. Values in bold are significant at p ≤ 0.05

(a)	JB (29 event)		WO (20 event)	
	Mean	**Std. Dev.**	**Mean**	**Std. Dev.**
tE (h)	19.59	9.73	45.14	22.75
tET (h)	21.52	9.76	47.85	23.15
Qpk (m^3/s)	4.58	2.96	22.06	18.26
Qr (m^3/s)	3.63	2.93	17.62	17.52
tQRL (h)	4.88	3.66	9.69	4.50
dQRL (h)	1.42	2.54	2.05	1.83
tQFL (h)	14.70	8.18	35.45	20.94
dQFL (h)	0.27	0.23	0.59	0.66
Qtot (m^3/s)	161.69	119.27	1834.98	1292.60
Tupk (FTU)	315.34	107.46	254.52	117.11
Tur (FTU)	277.24	106.34	226.07	115.17
tTuRL (h)	5.01	4.77	9.01	5.38
dTuRL (FTU/h)	104.90	116.11	30.52	20.90
tTuFL (h)	14.58	8.56	36.13	22.08
dTuFL (FTU/h)	22.52	11.64	8.06	5.88
LagTuQ (h)	1.50	2.25	2.73	2.36
Rpk (mm)	1.48	1.97	1.74	1.42
Rtot (mm)	8.36	7.00	11.72	9.91
NHpk (mg/l)	1.50	1.65	2.50	2.07
Tutot (FTU)	8465.36	4482.34	19504.92	12163.43
NHtot (mg/l)	58.68	81.59	161.66	249.72

(b)	Attribute	Sig
1	**Tutot**	**<0.001**
2	**tE**	**<0.001**
3	**Qtot**	**<0.001**
4	**Qr**	**<0.001**
5	**tQRL**	**<0.001**
6	**NHtot**	**0.005**
7	**LagTuQ**	**0.014**
8	**dQRL**	0.064
9	**NHpk**	0.078
10	**Tur**	0.096
11	**Rpk**	0.131
12	**Rtot**	0.183

(c)	Attribute	R^2	Intercept	Slope
1	**Tutot**	0.101	2.238	0.484
2	**tE**	0.059	1.265	0.222
3	**Qtot**	0.418	1.14	0.917
4	**Qr**	0.547	0.401	1.396
5	**tQRL**	0.022	0.97	-0.09
6	**NHtot**	0.001	1.859	0.025
7	**LagTuQ**	0.034	0.247	-0.118
8	**NHpk**	0.368	0.359	-0.664
9	**Tur**	0.117	1.093	0.472
10	**Rpk**	0.56	0.113	0.57
11	**Rtot**	0.305	0.353	0.663

Definitions of attributes used in Table 6.10: Tu=turbidity, Q=discharge/flow, R=rainfall, NH=ammonia, pk=peak, r=range, tot=total, ERI=event rainfall intensity, EFR=event flow rate, dQRL=rate of flow rise, dQFL=rate of flow recession, tQRL, tQFL= flow rise and flow recession times, dTuRL=rate of turbidity rise, dTuFL=rate of turbidity recession, tTuRL, tTuFL= turbidity rise and turbidity recession times, LagTuQ=turbidity-flow peaks lag time, LagTuNH=turbidity-ammonia peaks lag time, tE= event time, tET= total event time.

6.4.5 Regression analysis for turbidity and other attributes

Regression analysis for turbidity range and total with the other attributes are given in Figure 6.9 to Figure 6.12 showing the scatter plots for the 13 selected coinciding events. Generally, higher scatter were found with the smaller James Bridge catchment for turbidity range, and with the bigger Water Orton catchment for turbidity total regression lines except for total ammonia in both cases where the reverse is the case.

Table 6.11(a) and (b) show results of logistic regression for turbidity range and total with other event attributes using Water Orton (W) data as dummies variables. More attributes have statistically significant effects due to both James Bridge and Water Orton data (both spatial scales) on turbidity range than for turbidity total dynamics with only one attribute, a pattern similar to the correlation table for Water Orton (Table 6.9(b)).

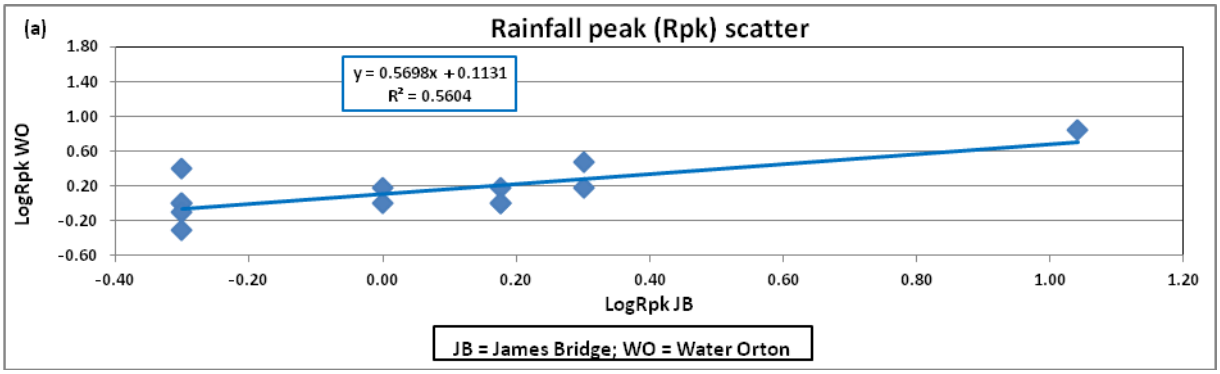

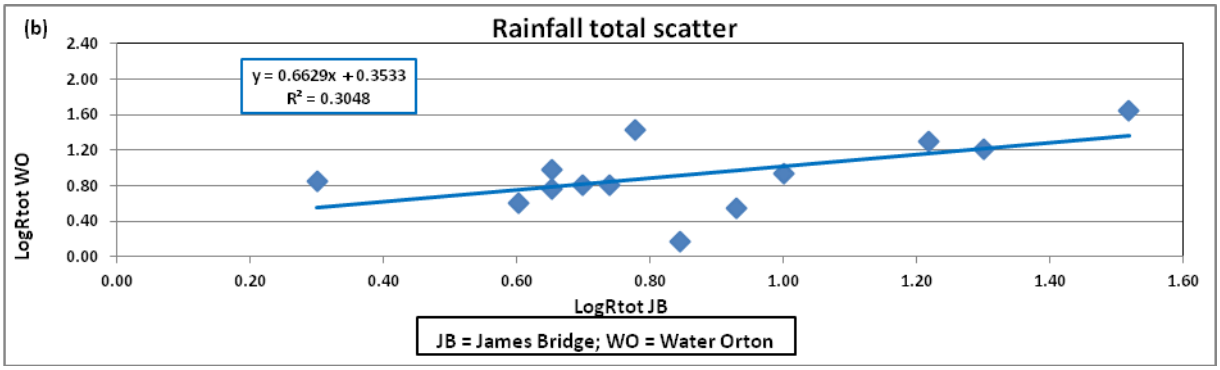

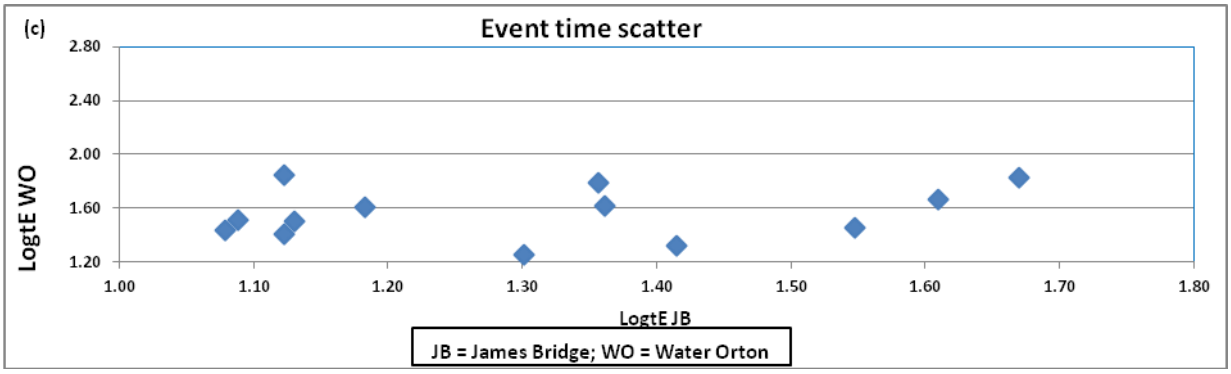

Figure 6.5: Scatter between the two catchments for (a) rainfall peak; (b) total rainfall; (c) event time.

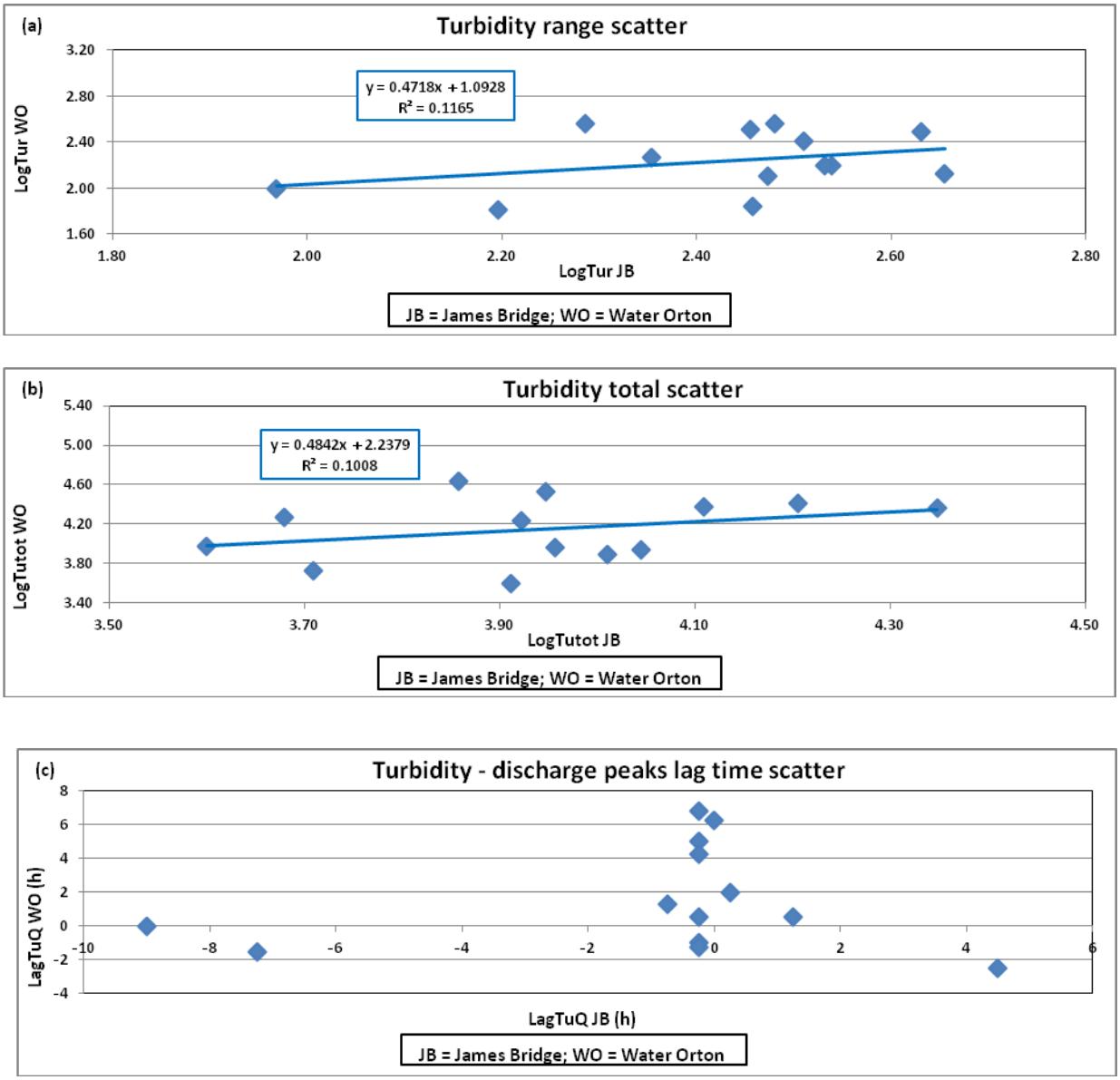

Figure 6.6: Scatter between the two catchments for (a) turbidity range; (b) total turbidity; (c) turbidity – discharge peaks lag time.

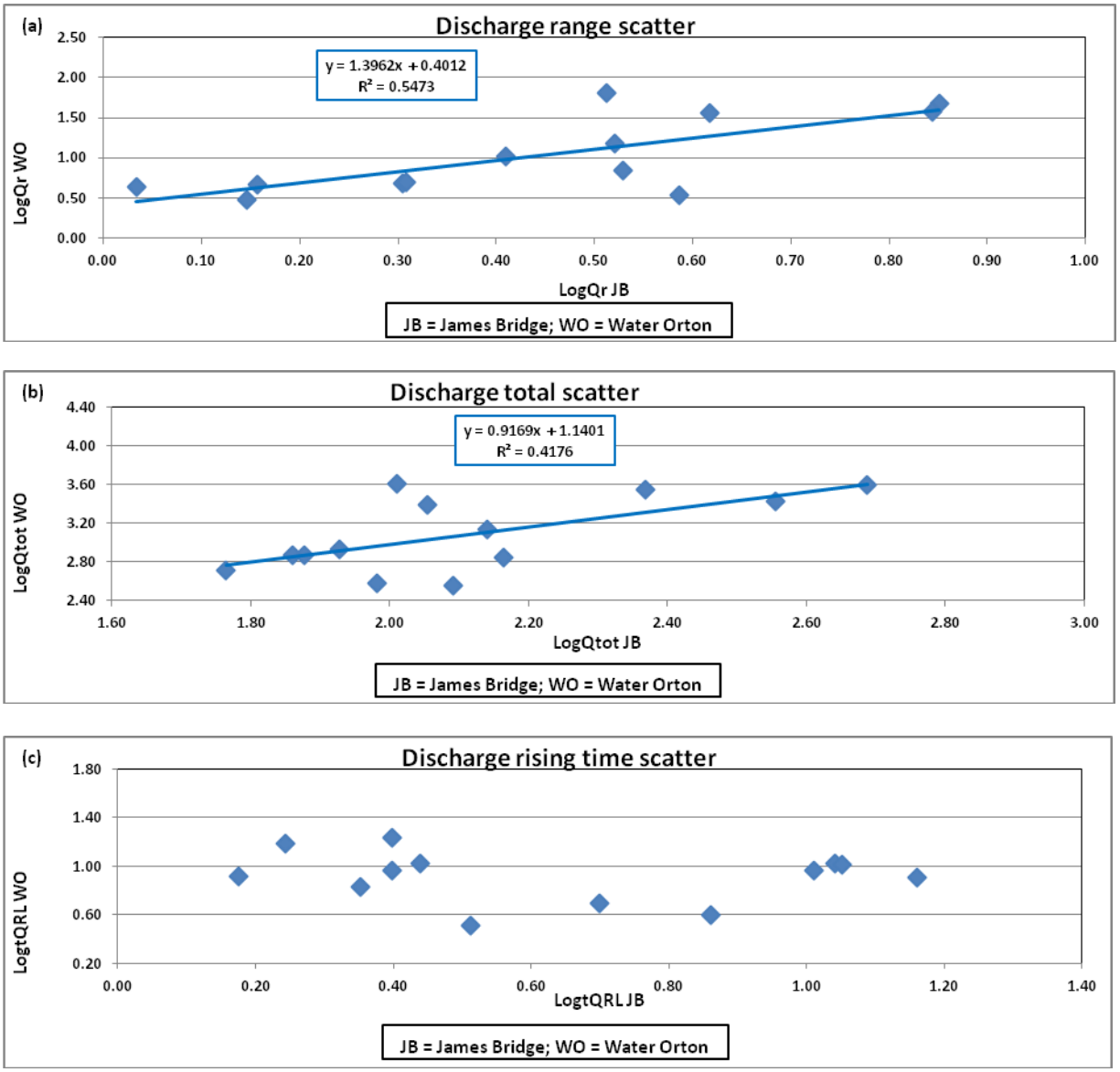

Figure 6.7: Scatter between same attributes for the two catchments with selected events downstream for (a) discharge range; (b) total discharge; (c) discharge rising time.

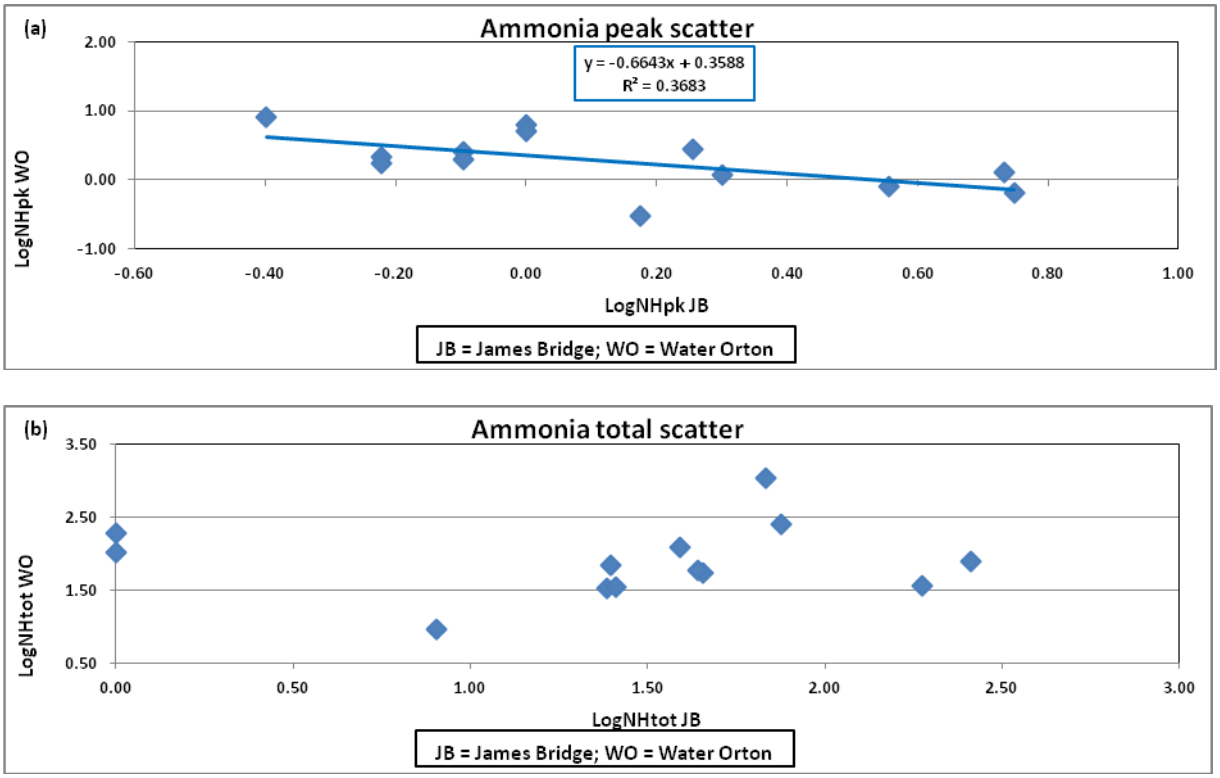

Figure 6.8: Scatter between same attributes for the two catchments with selected events downstream for (a) ammonia peak; (b) total ammonia.

6.4.6 Upstream events coinciding with unselected downstream events

From Table 6.4(a), it is shown that there are 50 selected upstream events coinciding with 43 downstream events unselected due to reasons given. Table 6.12 summarises the discharge peak to peak times between the two catchments, consisting of 37 one-to-one, 5 two-to-one, and 1 three-to-one upstream-to-downstream events. This is calculated by finding the difference between the times of peak for the upstream and the connected downstream

events. The range is from 0.5 to 99.25 (98.75) h and the mean is 11.7 h for the positive and 26.3 for the negative. Basic statistics, t-test analysis and scatter plots for the upstream events coinciding with unselected coinciding events for same attributes are presented. Table 6.13(a) summarises the basic statistics of attributes means while Table 6.13(b) shows the t-test results. Significant differences in means between the two catchments are found in 6 attributes. The characteristics of scatter plots, most of which are not significant, for the same attributes at the two catchments are summarised in Table 6.13(c). R^2 values ranged from the lowest of 0.0001 for rainfall peak (Rpk) to the highest of 0.157 for ammonia total (NHtot).

6.4.7 Coinciding events types

From Table 6.4(a), 29 upstream selected events coincided with 20 downstream selected events, out of which 13 were one to one connections (Table 6.6). Further, 50 upstream selected events coincided with 43 downstream unselected events in which reliable turbidity measurements were not available; out of which 37 were one to one connections (Table 6.12). To maximize the sample numbers, analysis focuses here on the transition of the discharge event type (single, double, multiple) from upstream to downstream of all 50 one-to-one events including those without reliable turbidity measurements. As indicated earlier, the numbers of events are not uniformly distributed between event types within the different catchments.

Table 6.11: Logistic regression for attributes' scale effect on turbidity (a) range, (b) total.

(a) Dep	Tur					
Indep	**Statistics**	**R^2**	**Sig**	**B**	**Std. Err.**	**Sig**
Qr (m^3/s)	**Model**	0.5	<0.001			
	Constant			1.853	0.109	<0.001
	Qr			0.375	0.095	0.001
	WIn			0.405	0.088	<0.001
NHpk (mg/l)	**Model**	0.469	0.001			
	Constant			2.109	0.062	<0.001
	WIn			0.318	0.08	0.001
	JGr			0.478	0.13	0.001
Rtot (mm)	**Model**	0.402	0.003			
	Constant			2.057	0.109	<0.001
	Rtot			0.334	0.109	0.006
	JIn			-0.209	0.076	0.012
Qtot (m^3/s)	**Model**	0.399	0.003			
	Constant			1.346	0.312	<0.001
	WGr			0.507	0.148	0.002
	JGr			0.292	0.101	0.008
tQRL (h)	**Model**	0.369	0.005			
	Constant			1.542	0.257	<0.001
	WIn			0.887	0.263	0.003
	JGr			0.762	0.275	0.011
Qpk (m^3/s)	**Model**	0.361	0.006			
	Constant			1.992	0.122	<0.001
	WGr			0.51	0.143	0.002
	Qpk			0.224	0.103	0.04
tE (h)	**Model**	0.177	0.032			
	Constant			2.235	0.061	<0.001
	WGr			0.149	0.065	0.032
NHtot (mg/l)	**Model**	0.175	0.033			
	Constant			2.425	0.06	<0.001
	JGr			-0.098	0.043	0.033
LagTuQ (h)	**Model**	0.16	0.043			
	Constant			2.238	0.062	<0.001
	WIn			0.188	0.088	0.043
Rpk (mm)	**Model**	0.16	0.043			
	Constant			2.238	0.062	<0.001
	WIn			0.188	0.088	0.043

(b) Dep	Tutot					
Indep	**Statistics**	**R^2**	**Sig**	**B**	**Std. Err.**	**Sig**
NHtot (mg/l)	**Model**	0.511	<0.001			
	Constant			3.201	0.232	<0.001
	JGr			0.5	0.118	<0.001
	WIn			0.745	0.239	0.005
Qtot (m^3/s)	**Model**	0.324	0.002			
	Constant			3.339	0.214	<0.001
	Qtot			0.273	0.08	0.002
tE (h)	**Model**	0.29	0.005			
	Constant			3.105	0.305	<0.001
	tE			0.659	0.211	0.005
Rtot (mm)	**Model**	0.257	0.008			
	Constant			3.686	0.135	<0.001
	Rtot			0.404	0.14	0.008
Qr (m^3/s)	**Model**	0.229	0.013			
	Constant			3.837	0.093	<0.001
	Qr			0.285	0.107	0.013

Definition of terms in Table 6.11: J, W, In and Gr are James Bridge, Water Orton, intercept and slope respectively, Qr=flow range, Qpk=flow peak,

Qtot=total flow, Rpk=rainfall peak, Rtot=total rainfall, NHpk=ammonia peak, NHtot=total ammonia, tE=event time, tQRL=flow rise time.

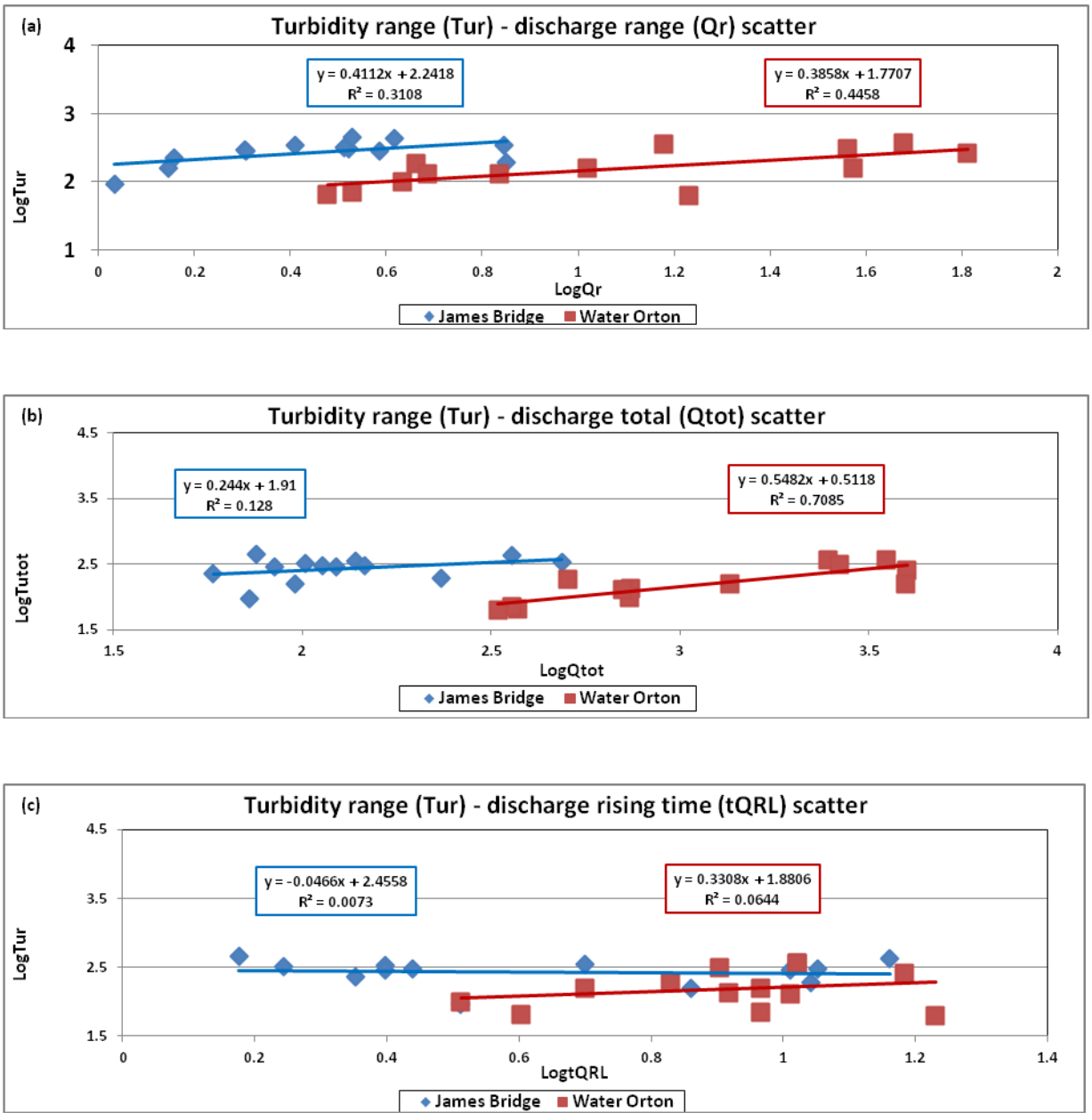

Figure 6.9: Scatter plots of turbidity range with (a) discharge range; (b) total discharge; (c) discharge rising time.

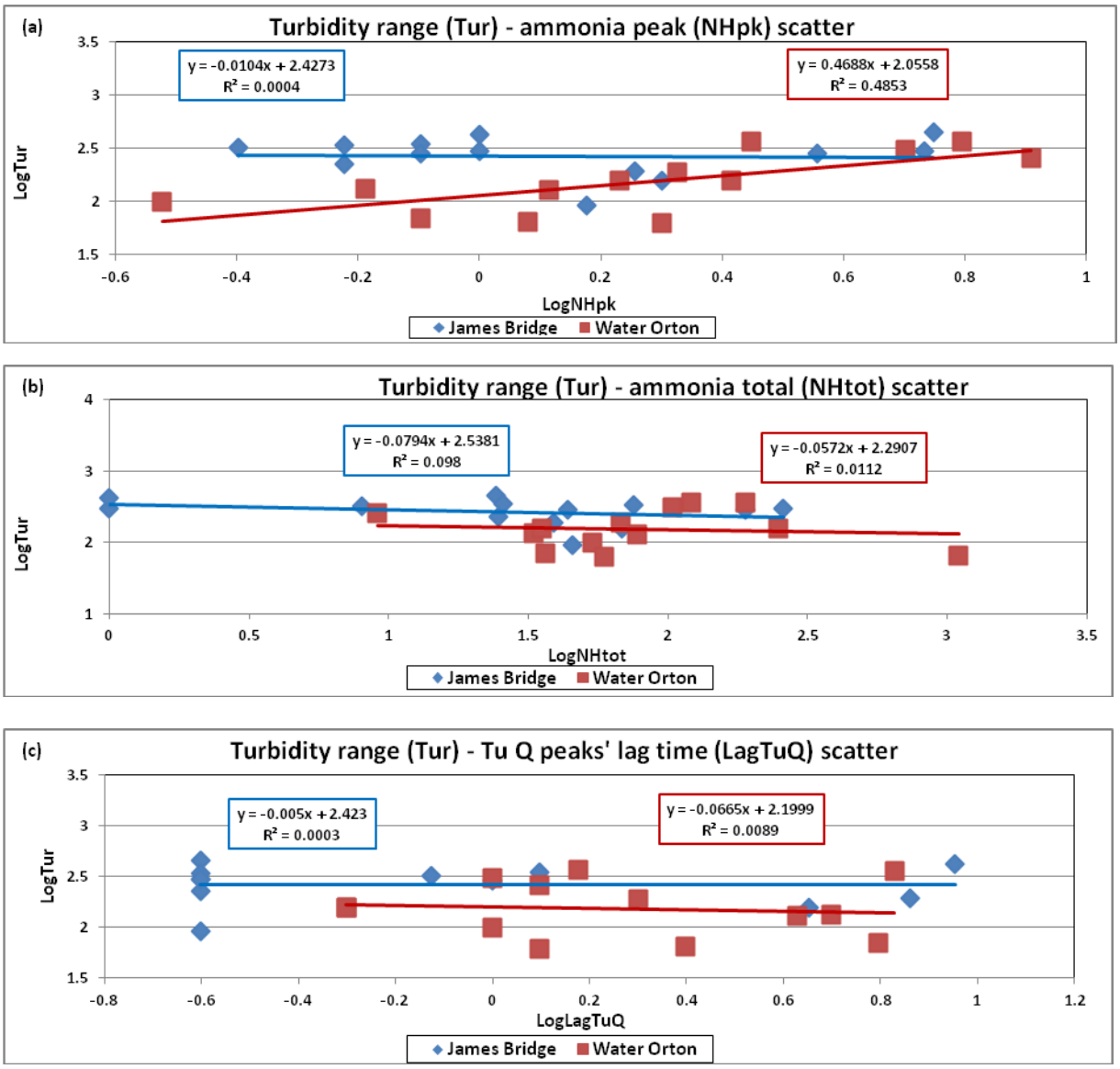

Figure 6.10: Scatter plots of turbidity range with (a) ammonia peak; (b) total ammonia; (c) turbidity-discharge peaks lag time.

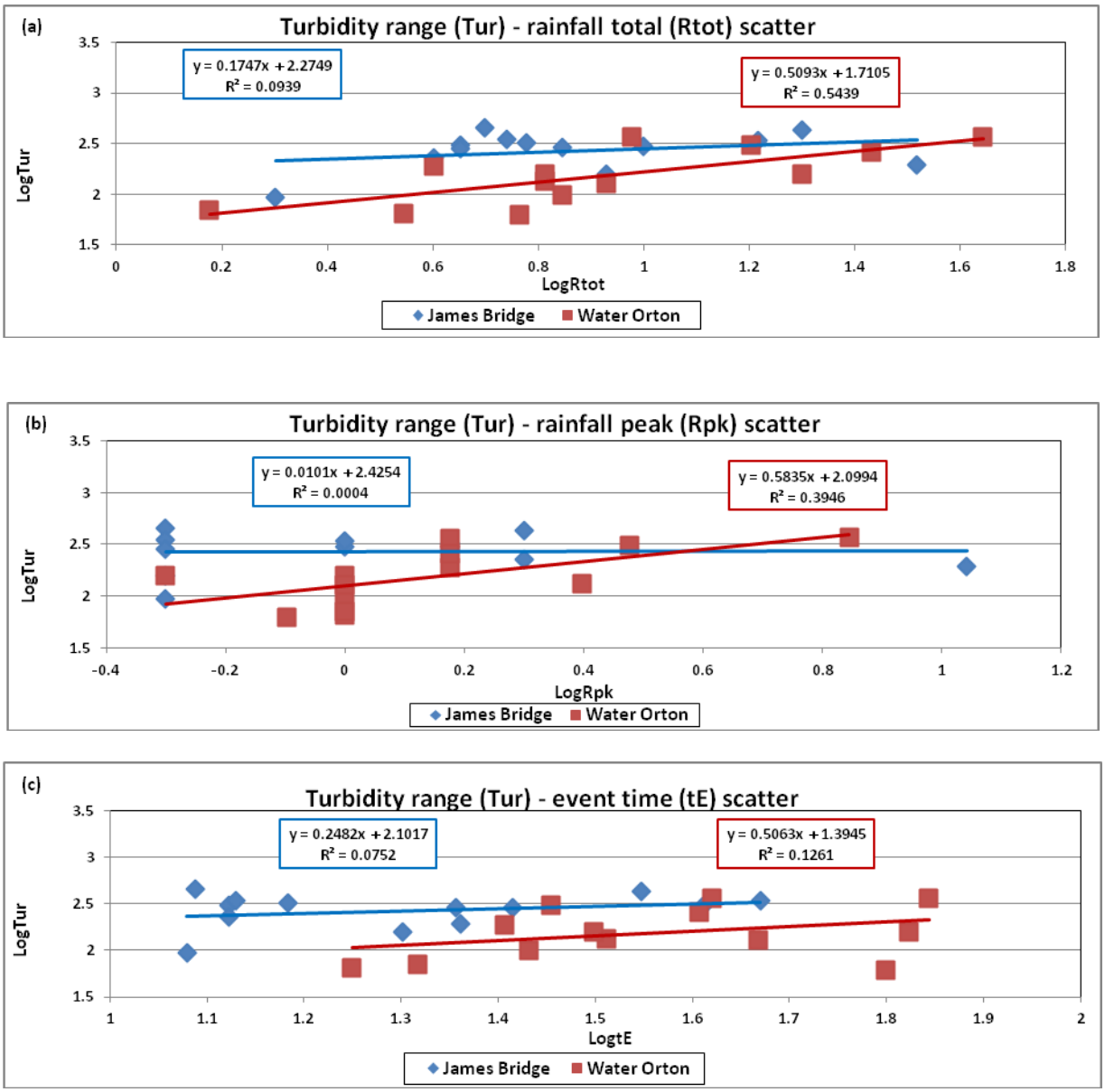

Figure 6.11: Scatter plots of turbidity range with (a) rainfall total; (b) rainfall peak; (c) event time.

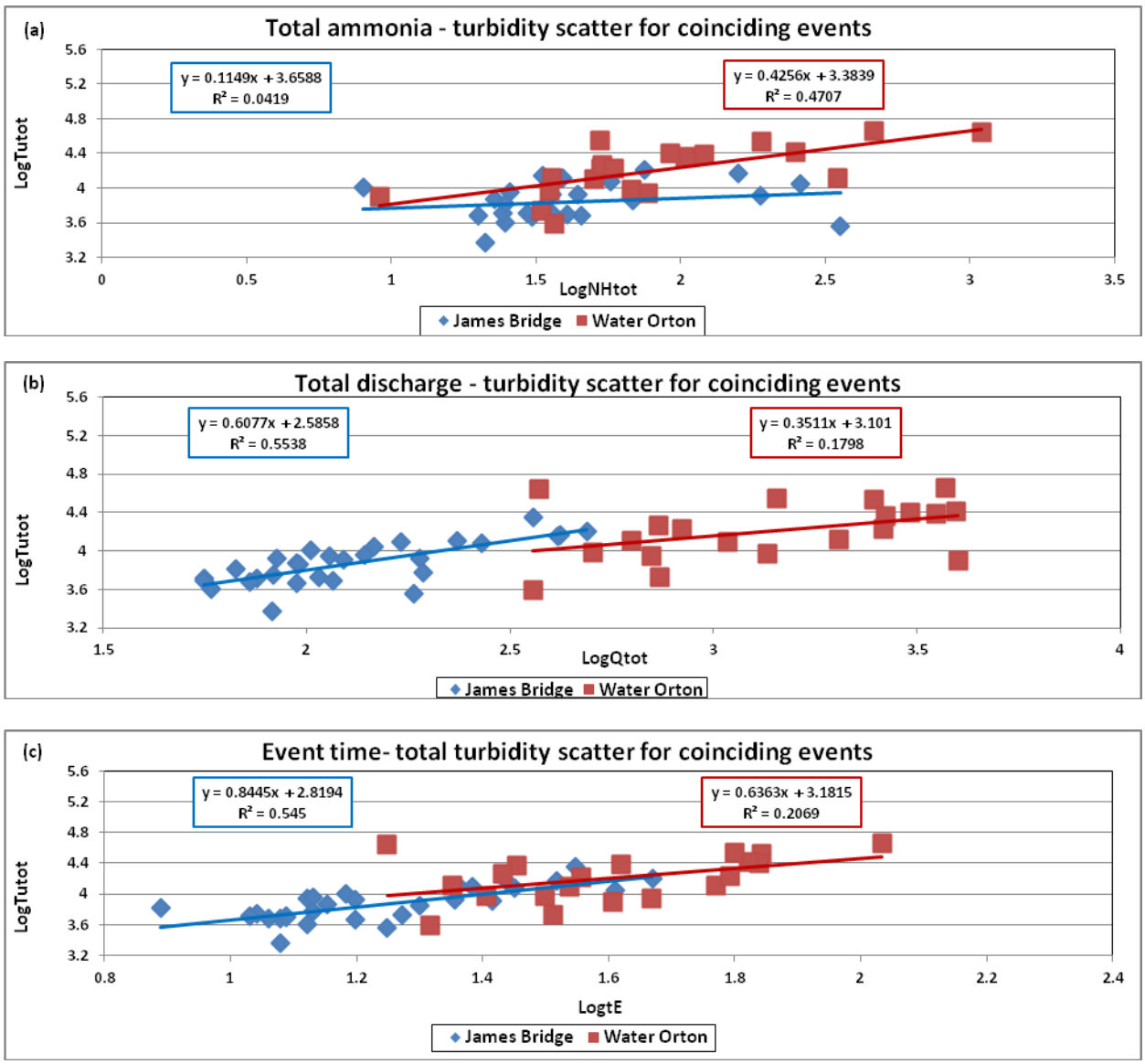

Figure 6.12: Scatter plots of total turbidity with (a) total ammonia; (b) total discharge; (c) event time.

Table 6.12: Discharge peak to peak times.

		Qpk Time		
	Date	**JB**	**WO**	**Pk to pk (h)**
1	**27-Apr-01**	28 (0145)	28(0730)	5.75
2	**28-Apr-01**	29 (0615)	29(1230)	6.25
3	**17-May-01**	17(1430)	17(1645)	2.25
4	**16-Aug-01**	16 (0700)	16(0730)	0.5
5	**13-Sep-01**	13(1930)	12(2200)	(-)21.5
6	**20-Sep-01**	20 (1800)	20(2100)	3
7	**05-Oct-01**	6(0030)	6(1445)	14.25
8	**07-Oct-01**	7 (1700)	7(1815)	1.25
9	**15-Oct-01**	15 (1615)	15(1645)	0.5
10	**18-Oct-01**	18(0700)	20(0645)	43.75
11	**24-Oct-01**	24 (0615)	23(0215)	(-)28
12	**30-Oct-01**	31 (0745)	31(0815)	0.5
13	**12-Nov-01**	12 (0815)	12(1645)	8.5
14	**30-Nov-01**	30 (0715)	1(1130)	28.5
15	**05-Dec-01**	5(0630)	4(0400)	(-)26.5
16	**27-Jan-02**	28 (0915)	26(1330)	(-)43.75
17	**22-Feb-02**	23 (0300)	26(0515)	74.25
18	**24-May-02**	24(0530)	24(0630)	1
19	**26-May-02**	26 (1715)	26(1015)	(-)7
20	**03-Jun-02**	3 (1215)	3(1315)	1
21	**04-Aug-02**	5(0130)	5(0245)	1.25
22	**08-Aug-02**	9 (0000)	9(2030)	20.5
23	**12-Oct-02**	12 (0545)	12(0645)	1
24	**01-Jan-03**	1(0530)	1(0715)	1.75
25	**02-Jan-03**	2(2330)	3(1000)	10.5
26	**17-Jan-03**	17(1330)	17(1445)	1.25
27	**10-Feb-03**	11(0130)	11(0630)	5
28	**01-Mar-03**	1(1900)	5(2215)	99.25
29	**21-Apr-03**	21 (0215)	21(0745)	6.5
30	**22-Jun-03**	23 (0515)	23(0630)	1.25
31	**25-Jul-03**	25 (1315)	25(1415)	1
32	**22-Sep-03**	22(1330)	22(1530)	2
33	**29-Oct-03**	29(2100)	29(0830)	(-)12.5
34	**01-Nov-03**	2 (0115)	31(0430)	(-)44.75
35	**17-Nov-03**	17(1630)	17(2345)	7.25
36	**25-Nov-03**	26(1000)	26(1030)	0.5
37	**29-Nov-03**	29(1200)	29(1345)	1.75
38**	**07-Nov-01**	7 (1045)	8(0500)	6.5
39**	**21-May-02**	21 (0715)	20(2300)	(-)8.25
40**	**09-Jun-02**	9 (1615)	9(2245)	21.5
41**	**21-May-03**	21 (2015)	22(2345)	6.25
42**	**09-Sep-03**	10 (0345)	10(1545)	12
43***	**01-Feb-02**	3 (0615)	2(1815)	(-)12

, * = 2, 3 upstream events results in 1 downstream event respectively.

Table 6.13: (a) Basic statistics of attributes of upstream events coinciding with unselected events downstream; (b) T-test results; (c) Characteristics of scatter between same attributes at the two catchments. Values in bold are significant at $p \leq 0.05$

(a)	JB (57 km^2)		WO (408 km^2)	
	Mean	**Std. Dev.**	**Mean**	**Std. Dev.**
tE (h)	19.18	8.94	48.12	47.17
tQpk (h)	17.12	8.10	32.57	26.43
Qpk (m^3/s)	3.59	2.34	22.28	19.43
Qr (m^3/s)	2.78	2.33	18.70	19.18
Qtot (m^3/s)	105.50	53.76	1893.70	1966.22
sQtot (m^3/s/km^2)	1.85		4.64	
tQRL (h)	3.78	3.08	15.71	25.63
tQFL (h)	15.40	8.50	32.42	28.35
dQRL (m^3/s/h)	1.15	1.11	3.06	4.50
dQFL (m^3/s/h)	0.23	0.18	1.84	5.88
Rpk (mm)	1.10	0.60	1.76	1.33
Rtot (mm)	5.83	3.70	13.96	10.83
NHpk (mg/l)	1.29	1.35	3.47	3.36
NHtot (mg/l)	42.71	40.60	142.24	175.43

(b)	Attribute	Sig
1	**Rtot**	**<0.001**
2	**tE**	**<0.001**
3	**Qtot**	**<0.001**
4	**Qr**	**<0.001**
5	**tQRL**	**<0.001**
6	**NHtot**	**<0.001**

(c)	Attribute	R^2	Intercept	Slope
1	**tE**	0.001	1.602	-0.05
2	**Qtot**	0.016	2.738	0.201
3	**Qr**	0.023	1.162	-0.244
4	**Qpk**	0.021	1.332	-0.226
5	**tQRL**	0.001	0.95	-0.039
6	**NHpk**	0.023	0.346	0.197
7	**NHtot**	0.157	1.492	0.326
8	**Rpk**	0.0001	0.154	0.009
9	**Rtot**	0.01	1.132	-0.16

Definition of terms in Table 6.13: Qr=flow range, Qpk=flow peak, Qtot=total flow, sQtot=total flow/unit catchment area, Rpk=rainfall peak, Rtot=total rainfall, NHpk=ammonia peak, NHtot=total ammonia, tE=event time, tQRL=flow rise time, tQFL=flow recession time, dQRL=rate of flow rise, dQFL= rate of flow recession.

Table 6.15 (a) indicates how the upstream event type coincides with the downstream event type. In total, 23 upstream events (12 single, 9 double and 2 multiple discharge peaks) are maintained as they propagate through the catchment. In comparison, the majority, a total of 27, are transformed in nature.

Figure 6.13 (a) shows the distribution of upstream coinciding event types downstream. It could be seen, for instance, that out of the 3 multiple discharge peak events upstream, 1 was transformed to double and 2 remained multiple discharge peak events at the downstream Water Orton catchment. The difference between number of events maintaining and transforming their nature is not significant (Table 6.15 (b)). Table 6.16 shows the overall transformation of upstream (US) events downstream (DS).

Table 6.14: (a) Distribution of coinciding events; (b) Chi-square test results.

(a) Event	JB	%	WO	%
Single	32	64	17	34
Double	15	30	27	54
Multiple	3	6	6	12
Total	50		50	

(b)	Value	df	Asymp. Sig.
Pearson Chi-Square	9.004[a]	1	**0.003**
Continuity Correction[b]	7.843	1	0.005
Likelihood Ratio	9.144	1	0.002
N of Valid Cases	100		
a. 0 cells (.0%) have expected count less than 5.			

Table 6.15: (a) Distribution of upstream coinciding events downstream; (b) Chi-square test results.

(a) Event	WO Single	%	WO Double	%	WO Multiple	%
JB Single	12	38	17	53	3	9
JB Double	5	33	9	60	1	7
JB Multiple	0	0	1	33	2	67

(b)	Value	df	Asymp. Sig.
Pearson Chi-Square	.485[a]	1	0.486
Continuity Correction[b]	0.149	1	0.7
Likelihood Ratio	0.493	1	0.483
N of Valid Cases	50		

a. 0 cells (.0%) have expected count less than 5.

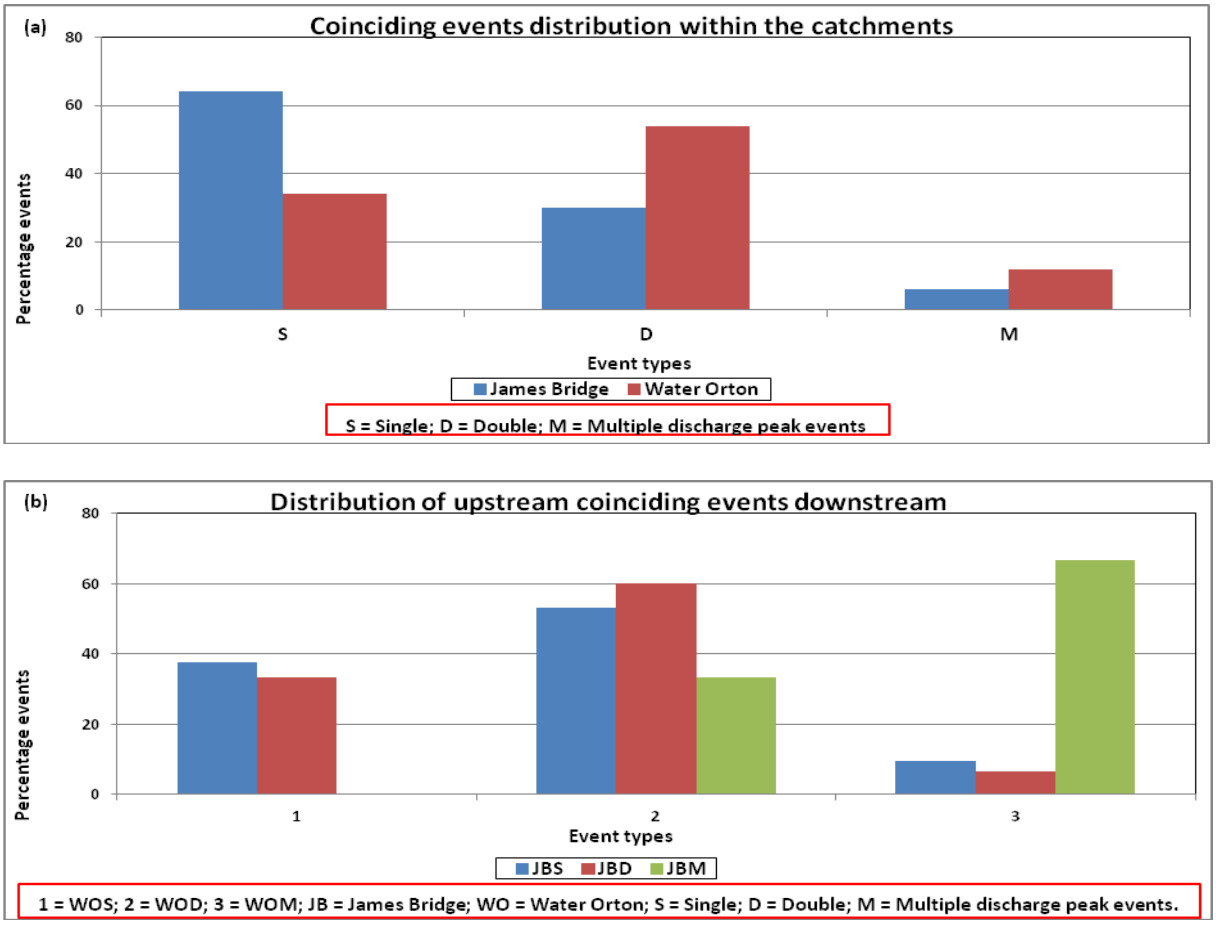

Figure 6.13: Distribution of coinciding events (a) between the catchments; (b) of upstream types downstream

Table 6.16: Transformation of upstream events downstream

	James Bridge (US)		Water Orton (DS)	
Number	**Date**	**Type**	**Date**	**Type**
1	27-Mar-01	S	27-Mar-01	D
2	03-Apr-01	D	05-Apr-01	D
3	27-Apr-01	S	27-Apr-01	D
4	28-Apr-01	D	28-Apr-01	D
5	17-May-01	M	17-May-01	M
6	29-Jun-01	S	29-Jun-01	D
7	16-Aug-01	S	16-Aug-01	M
8	13-Sep-01	S	12-Sep-01	D
9	20-Sep-01	S	19-Sep-01	M
10	26-Sep-01	S	26-Sep-01	D
11	05-Oct-01	S	05-Oct-01	S
12	07-Oct-01	S	07-Oct-01	S
13	15-Oct-01	S	15-Oct-01	S
14	18-Oct-01	S	17-Oct-01	M
15	24-Oct-01	S	22-Oct-01	S
16	30-Oct-01	D	30-Oct-01	D
17	12-Nov-01	S	12-Nov-01	D
18	30-Nov-01	D	29-Nov-01	M
19	05-Dec-01	S	03-Dec-01	D
20	27-Jan-02	D	25-Jan-02	S
21	22-Feb-02	M	22-Feb-02	D
22	24-May-02	S	24-May-02	D
23	26-May-02	D	25-May-02	D
24	03-Jun-02	S	03-Jun-02	D
25	30-Jul-02	D	30-Jul-02	D
26	04-Aug-02	S	04-Aug-02	D
27	08-Aug-02	D	07-Aug-02	D
28	12-Oct-02	S	11-Oct-02	D
29	14-Oct-02	S	15-Oct-02	S
30	01-Dec-02	S	01-Dec-02	S
31	23-Dec-02	D	23-Dec-02	S
32	29-Dec-02	D	29-Dec-02	S
33	01-Jan-03	S	01-Jan-03	D
34	02-Jan-03	D	02-Jan-03	D
35	17-Jan-03	S	17-Jan-03	D
36	10-Feb-03	S	10-Feb-03	S
37	01-Mar-03	S	01-Mar-03	D
38	21-Apr-03	D	20-Apr-03	D
39	16-May-03	D	17-May-03	S
40	22-Jun-03	S	22-Jun-03	S
41	27-Jun-03	D	27-Jun-03	D
42	25-Jul-03	S	25-Jul-03	S
43	28-Aug-03	M	28-Aug-03	M
44	22-Sep-03	S	22-Sep-03	D
45	29-Oct-03	S	29-Oct-03	D
46	01-Nov-03	S	01-Nov-03	S
47	14-Nov-03	S	14-Nov-03	S
48	17-Nov-03	S	17-Nov-03	S
49	25-Nov-03	D	25-Nov-03	S
50	29-Nov-03	S	29-Nov-03	D

S = single, D = double, M = multiple discharge peak events, US, DS = upstream, downstream.

6.4.8 Suspended sediment concentration – turbidity rating curves

Significant relationship between LogTu and LogSSC was found in the James Bridge catchment (R^2=0.100, p=0.024, n=51), with significant intercept as well (p<0.001), but not in the Water Orton catchment (Table 6.17). However, both catchments show substantial scatter (Figure 6.14 (a) and (b)) and therefore large uncertainty in the relationships. Despite the high scatter, the relations as shown in equations below were used for the determination of SSC from the turbidity values and, together with the discharge values determine SSL. This is because literature has already established strong relationships between turbidity and SSC.

$$SSC = 0.65 \times Tu^{0.177} \text{ (James Bridge)} \quad (1)$$

$$SSC = 0.798 \times Tu^{0.116} \text{ (Water Orton)} \quad (2)$$

$$SSL = SSC \times Q \quad (3)$$

where SSL is suspended sediment load (g/s), SSC is suspended sediment concentration (mg/l) and Q is discharge (m^3/s). The coefficient and exponent values of turbidity in the above equations respectively represent the intercept and gradient values of LogSSC-LogTu mean lines of best shown (Figure 6.14 and Table 6.17).

The regression relationships are applied within this study (Table 6.17 and Figure 6.14 (a) and (b)). However, because of the high scatter, we account for the uncertainty in the relationship and its impact on the calculated sediment loads. The green lines represent the maximum gradients between SSC and turbidity. The lower bounds, the red lines, assume no relationship between the

two. Slope/gradient bounds could as well be used. Figure 6.15 compares James Bridge SSL for the maximum and mean gradients. It is evident that for the same discharge, the maximum gradient line gives slightly higher SSL than the mean gradient beyond a discharge of about 50 m^3/s, and keeps increasing with discharge.

Table 6.17: Model characteristics of the Suspended Sediment Concentration (SSC) – Turbidity (Tu) rating curves for James Bridge and Water Orton catchments. Significant relationships are indicated in bold.

Dep	**Site**	**LogTu**						**95% CI for B**	
Indep		**Statistics**	**R^2**	**Sig**	**B**	**Std. Err**	**Sig**	**Lower Bound**	**Upper Bound**
LogSSC	**James Bridge (JB)**	**Model**	0.100	**0.024**					
		Constant			0.650	0.143	**<0.001**	0.367	0.941
		LogTu			0.177	0.076	**0.024**	0.024	0.330
	Water Orton (WO)	**Model**	0.029	0.204					
		Constant			0.798	0.169	**<0.001**	0.459	1.137
		LogTu			0.116	0.09	0.204	-0.065	0.297

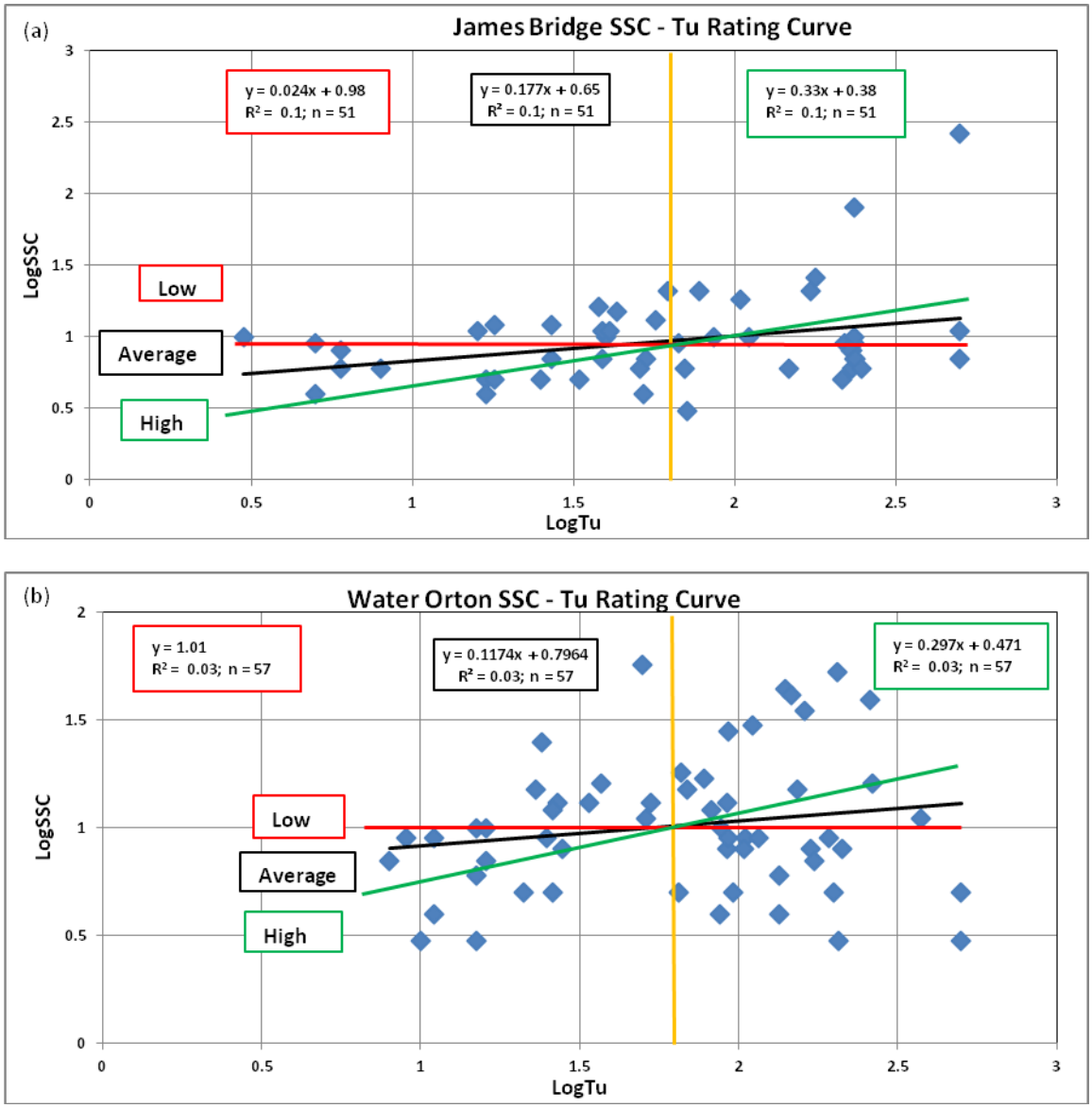

Figure 6.14: Log of Suspended Sediment Concentration (SSC) – Turbidity (Tu) Rating Curves for: (a) James Bridge, and (b) Water Orton catchments and also showing the lower and higher bounds.

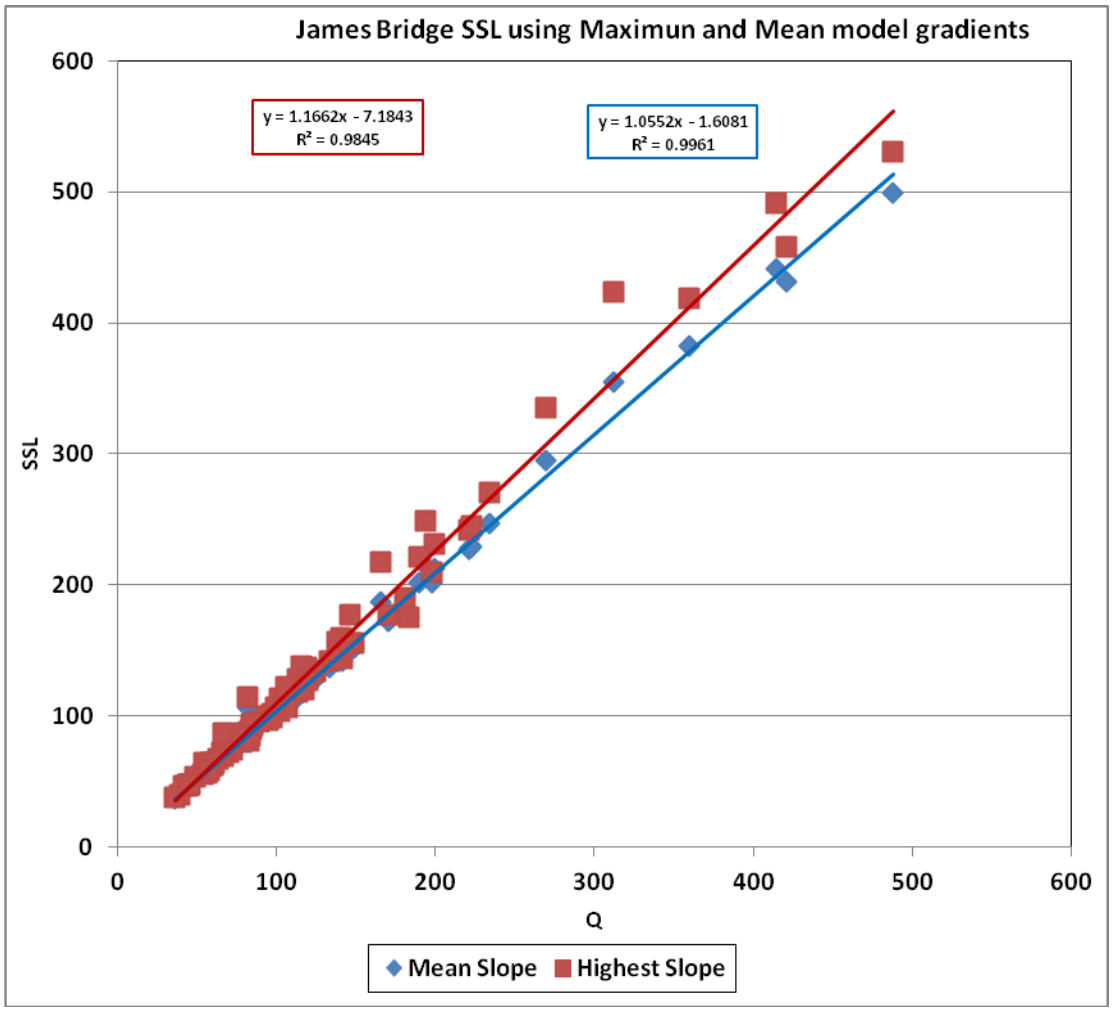

Figure 6.15: James Bridge Suspended Sediment Loads (SSL) – Discharge (Q) using Maximum and Mean model gradients.

6.4.9 Suspended sediment loads (SSL) determination

Table 6.18 indicates some basic statistics and the analysis of variance (ANOVA) of SSL between single, double and multiple events. Significantly different means between single, double and multiple events for total discharge, turbidity and suspended sediment load are found ($F=9.260$; $p<0.001$, $n=90$), ($F=16.652$; $p<0.001$, $n=90$) and ($F=8.417$; $p<0.001$, $n=90$) in the James Bridge catchment but not in the Water Orton catchment (Table 6.18 (a)).

Also, means of SSL were significantly different between single, double and multiple ($F=8.417$; $p<0.001$, $n=90$) (Table 6.18 (b)) as well as between Anti First Flush and First Flush events ($F=4.290$; $p=0.042$, $n=90$) (Table 6.18 (c)) in the James Bridge catchment but not in the Water Orton catchment. These are shown in the Box and Whiskers plots in Figure 6.16 and Figure 6.17.

The overall event means per unit area of total discharge, suspended sediment load and turbidity for James Bridge are approximately 0.6, 0.63 and 3.6 times those for Water Orton respectively (Table 6.18 (a)). The means per unit area of suspended sediment load for single, double and multiple events for James Bridge are about 0.48, 0.87 and 0.88 times those for Water Orton respectively (Table 6.18 (b)), while those for anti-first flush and first flush events for James Bridge are about 0.66 and 0.64 times those for Water Orton respectively (Table 6.18 (c)).

Table 6.18: ANOVA for: (a) Qtot, Tutot and SSLtot, (b) SSL (Suspended Sediment Loads (g/s)) for Single, Double and Multiple; and (c) SSL for Anti First Flush and First Flush events; and (d) t-test results for SSL of River Tame at James Bridge and Water Orton monitoring sites. Significant mean differences are indicated in bold.

(a) ANOVA with all events									
(a) Site	**Event Attribute**	**n**	**ANOVA**		**Basic Statistics**			**% JB of WO**	
			F	**Sig**	**Mean**	**Std Dev**	**Mean/Area**	**Mn/A**	**Mean**
James Bridge (JB) (Area, 57km^2)	**Q_{tot} (m^3/s)**	90	9.26	**<0.001**	120.1	85	2.11	59.66	8.33
	Tu_{tot} (FTU)	90	16.652	**<0.001**	8094.2	4294	142	357.79	49.99
	SSL_{tot} (g/s)	90	8.417	**<0.001**	125.1	89.9	2.19	62.7	8.76
Water Orton (WO) (Area, 408 km^2)	**Q_{tot} (m^3/s)**	53	0.034	0.967	1440.96	1021.8	3.53		
	Tu_{tot} (FTU)	53	0.696	0.503	16192.95	10669	39.69		
	SSL_{tot} (g/s)	53	0.018	0.982	1428.21	1115.8	3.5		
(b) ANOVA of SSL with Single, Double and Multiple events									
Site	**Event Type**	**n**	**ANOVA**		**Basic Statistics**				
			F	**Sig**	**Mean**	**Std Dev**			
James Bridge	**Single**	56	8.417	**<0.001**	97.14	59.7	1.7	47.83	6.68
	Double	30			169.96	117.61	2.98	87.09	12.17
	Multiple	4			180.65	40.65	3.17	88.35	12.34
Water Orton	**Single**	21	0.018	0.982	1453.59	1185.76	3.56		
	Double	25			1396.96	1085.68	3.42		
	Multiple	7			1463.63	1175	3.59		
(c) ANOVA of SSL with First flush and Anti First Flush events									
(c) Site	**Event Type**	**n**	**ANOVA**		**Basic Statistics**				
			F	**Sig**	**Mean**	**Std Dev**			
James Bridge	**Anti First Flush**	49	4.29	**0.042**	110.3	84.01	1.94	65.75	9.19
	First Flush	30			154.63	104.59	2.71	64.18	8.97
Water Orton	**Anti First Flush**	28	2.65	0.11	1200.86	952.1	2.94		
	First Flush	28			1724.58	1322.92	4.23		
(d) t-test of SSL for James Bridge and Water Orton									
	Equality of	**Variances**			**Means**				
					t	**df**			
	Variance assumed	**F**	**Sig**				**Sig (2-tail)**		
SSL	**Equal**	103.01	**<0.001**	-11.05	141.00	**<0.001**			
	Non-equal			-8.49	52.40	**<0.001**			

Definition of terms: Qtot = total flow, SSLtot = suspended sediment load, Tutot = total turbidity.

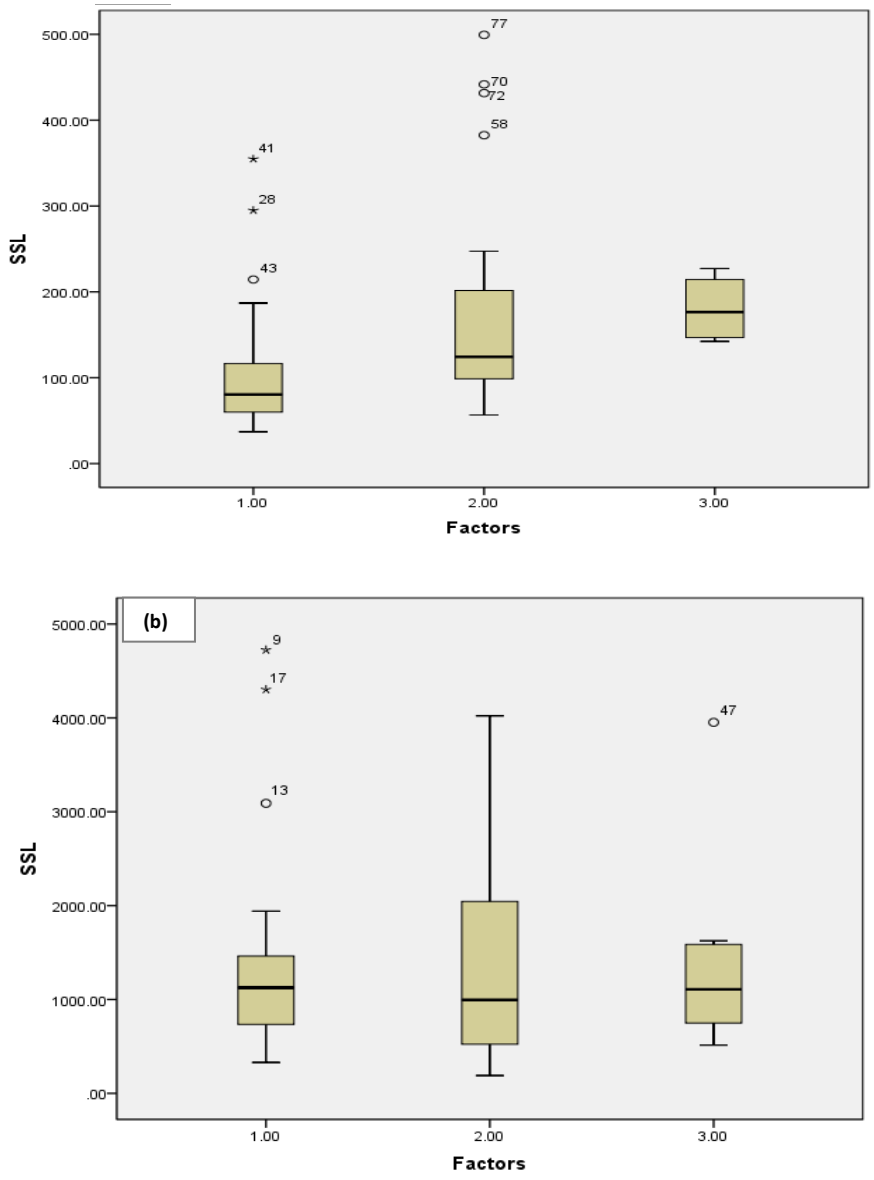

Figure 6.16: Box and whiskers plots for SSL (Suspended Sediment Loads (g/s)) for River Tame at (a) James Bridge and (b) Water Orton monitoring sites.

1, 2 and 3 = Single, Double and Multiple events; SSL = Suspended Sediment Load (g/s).

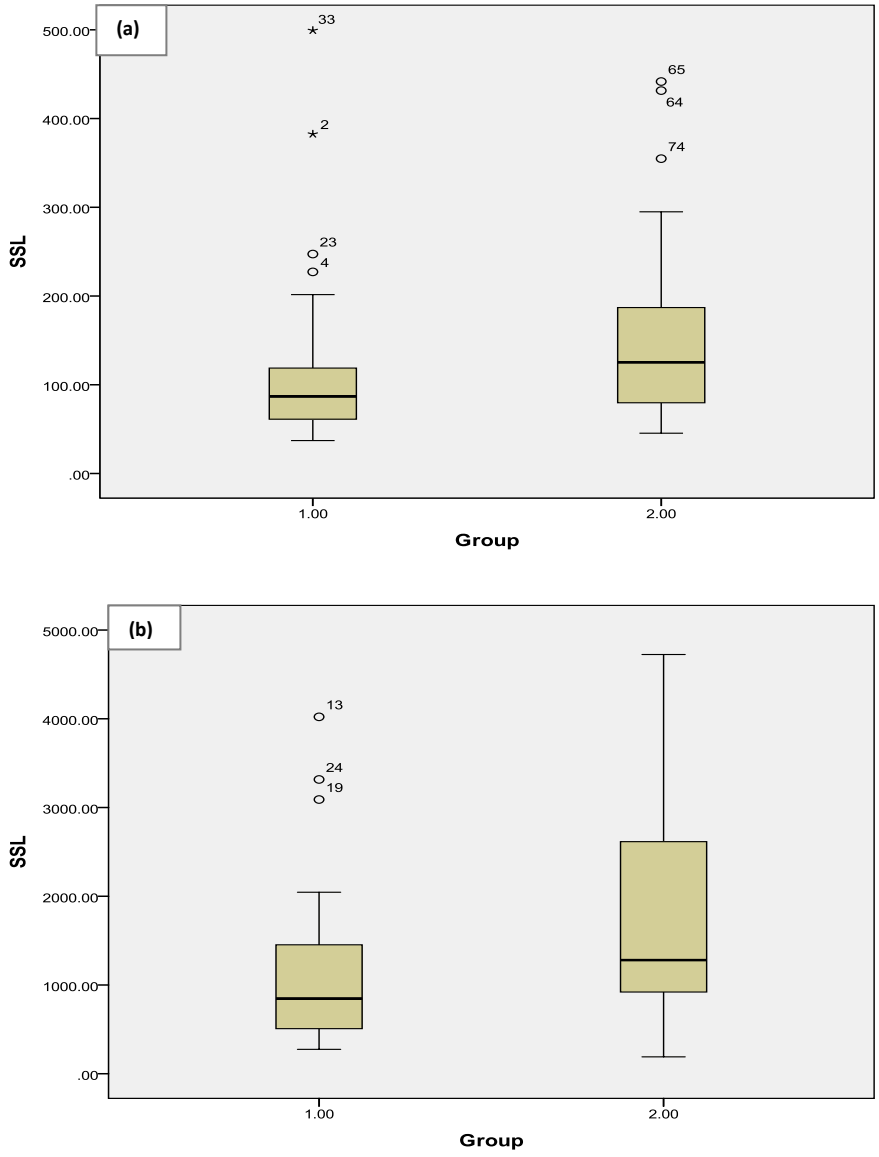

Figure 6.17: Box and whiskers plots for SSL (Suspended Sediment Loads) (g/s) for River Tame at (a) James Bridge and (b) Water Orton monitoring sites. 1 and 2 = Anti First Flush and First Flush events; SSL = Suspended Sediment Load (g/s).

6.4.10 Tributary effects on turbidity dynamics

Table 6.19 shows catchment areas, percentage urban covers (UC %) and daily mean statistics for discharge and turbidity for monitoring sites on River Tame and tributaries. Also, daily mean discharge and turbidity per unit area values were computed for 20 days of 15-minutes resolution data for January from 9th (11:45) to 28th (22:45). Both Water Orton (the downstream, lowland stretch) and James Bridge (the upstream, headwaters stretch) data were in 2003, while Bourne Brook (a tributary) data were in 2014, since this was the only period of turbidity data for a tributary of River Tame. Bourne Brook has the highest percentage urban cover (Table 6.19 (a)) and the highest Tu-Q intercept value as well, with James Bridge having the highest Tu-Q slope/gradient (Table 6.20 (b); Figure 6.18). Bourne Brook intercept BB(In) and James Bridge slope JB(Gr) of the Tu-Q regression line are both significantly higher than their corresponding Water Orton values (Table 6.20 (b)), showing that the differences in the intercept of James Bridge and slope of Bourne Brook seen in Figure 6.18 are not significantly different from their corresponding values of Water Orton.

Table 6.19: River Tame and tributaries data from monitoring stations showing (a) catchment areas, percentage urban covers (UC); daily mean statistics for (b) discharge and (c) turbidity; daily mean per catchment are statistics for (d) discharge and (e) turbidity. Mean values are indicated in bold.

(a) Description					
Site	**Area (km^2)**	**UC (%)**			
Bourn Brook	27.9	80			
Rea Carthope	74	45			
James Bridge	57	65			
Water Orton	408	59			
(b) Discharge (m^3s^{-1})					
Site	**Min**	**Max**	**Mean**	**Std Dev**	**Total**
Bourn Brook	0.17	1.90	0.43	0.26	803.13
Rea Carthope	0.41	9.38	0.90	0.96	1676.02
James Bridge	0.64	6.81	1.08	0.51	2018.86
Water Orton	3.31	27.90	5.51	2.84	10043.38
(c) Turbidity (FTU)					
Site	**Min**	**Max**	**Mean**	**Std Dev**	**Total**
Bourn Brook	3	490	38	52	70503
Rea Carthope	Not Available				
James Bridge	1	495	49	73	89872
Water Orton	21	496	75	81	140447
(d) Discharge per unit area ($m^3s^{-1}km^{-2}$)					
Site	**Minimum**	**Maximum**	**Mean**		
Bourn Brook	0.008	0.025	0.014		
Rea Carthope	0.006	0.045	0.012		
James Bridge	0.014	0.045	0.019		
Water Orton	0.009	0.031	0.013		
(e) Turbidity per unit area (FTU km^{-2})					
Site	Min	Max	Mean		
Bourn Brook	0.334	2.995	1.260		
Rea Carthope	**Not Available**				
James Bridge	0.209	2.554	0.086		
Water Orton	0.073	0.582	0.180		

Table 6.20: Characteristics of: (a) scatter plots (Figure 6), and (b) Logistic regression model for daily means of turbidity and discharge per unit catchment area for Water Orton, James Bridge and Bourne Brook. Significant values are indicated in bold.

(a) Scatter plots characteristics						
Site	**Intercept (In)**	**Slope (Gr)**	**R^2**	**Days**		
Water Orton (WO)	-13.57	2.43	0.83	20		
James Bridge (JB)	-98.25	9.77	0.57	20		
Bourne Brook (BB)	-8.97	9.25	0.58	20		
(b) Model characteristics						
Dep	**Tumean/area**					
Indep	**Statistics**	**R^2**	**Sig**	**B**	**Std. Err.**	**Sig**
Qmean/area	Model	0.651	**0.015**			
	Constant			-66.07	16.21	**<0.001**
	Qmean/area			6.23	1.12	**<0.001**
	BB(In)			101.12	13.31	**<0.001**
	JB(Gr)			1.99	0.80	**0.015**

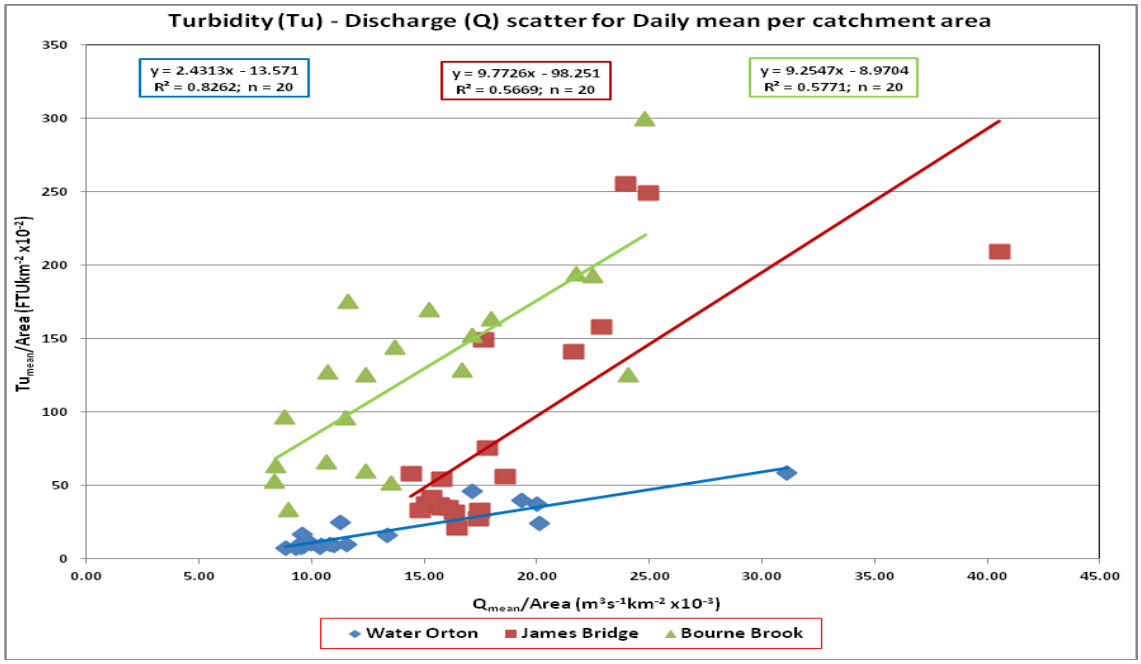

Figure 6.18: Characteristics of scatter plots for daily means of turbidity and discharge per unit catchment area for Water Orton, James Bridge and Bourne Brook.

6.5 Discussions

There are more single discharge peak events from smaller catchments.

It has been argued that single discharge peak events are due to urbanised impervious surfaces contributing to runoff mostly during single rain storms (Furusho et al., 2010). With a similar urban covers between the two catchments (Table 6.2), the difference in event type distribution likely results from increased rainfall variability at increasing scales. A poor correlation between peak and total rainfall between the catchments was observed (Table 6.13(c), implying uneven spatial distribution throughout the catchment.

Single rain storms with low rainfall totals, occurring in the smaller catchment, could result in events at the small scale that are too small to be designated as an event when they propagate to the downstream catchment. For example, 1 August 2002 and 4 February 2003 events were designated as single events upstream. However, at the larger scale an event was not identified because of lower catchment discharge threshold. Such a loss of event between the different scales will be most prevalent within single event types. This results from the single flow peak events having the lowest mean discharge total (Figure 4.14(b)).

Large magnitude, single rainfall in the smaller catchment likely results in single discharge peak events in both catchments because discharge values exceeded the set discharge threshold within both catchments. For example, 7 October 2002 and 22 June 2003 among many others were qualified as single events both upstream and downstream. In smaller catchments, the precipitation could

be more homogeneous (Duvert et al., 2010) and could result in single discharge peak events allowing a simpler explanation of rainfall data and subsequent runoff and erosion drivers.

Secondary discharge peaks (double/multiple) could be indicative of tributary contributions, associated with within-catchment storm unevenness and/or runoff from far sources (Rovira and Batalla, 2006). Also, many smaller catchments could be part of a bigger catchment, since large catchment-scale processes could be interpreted as a mix of small-scale processes (Merz and Blöschl, 2003). They could also be due to secondary rain events, with lower/higher secondary discharge peaks possibly due to lower/higher rainfall intensities (Jansson, 2002). The tributaries are lower in number and smaller in size at the smaller catchment (Table 6.2). Spatial variability of rainfall (not analysed due to unavailability of data) across the catchment and distal runoff sources could both be less pronounced for smaller catchments. These could have resulted in more single discharge peaks for the smaller catchment and, therefore, supports the hypothesis that smaller catchments exhibit more single events.

In larger catchments, multiple discharge peak events are more common

There were significantly more single peak events in the smaller catchment and significantly more double and multiple peak events in the larger catchments (Table 6.3(a) and (b), as well as Table 6.14(a) and (b)). This could also support the fact that larger catchments could exhibit more double and multiple events. Some events transformed and others maintained their nature downstream in the study (Table 6.16). Events transforming in nature could result from within-

catchment storm changing spatially and temporally. Larger scale response to events could be having prevailing influence mainly from smaller areas' contribution of discharge and sediment of the catchment and altered in stream channel until it gets to the outlet) (Smith and Dragovich, 2009). Such modifications could include transmission losses and tributary inputs magnitude and timing. While transmission losses and low energy conditions upstream due to low discharge could result in more single events, large stormflow and input from tributaries controlling downstream flow dynamics could result in more double and multiple discharge peak events (Estrany et al., 2011). Secondary discharge peaks (double/multiple) could be indicative of tributary contributions, associated with within-catchment storm unevenness and/or runoff from far sources (Rovira and Batalla, 2006). Also, larger catchments may consist of many smaller catchments, since large catchment-scale processes could be interpreted as a mix of small-scale processes (Merz and Blöschl, 2003). They could also be due to secondary rain events, with lower/higher secondary discharge peaks possibly due to lower/higher rainfall intensities (Jansson, 2002).

The tributaries are higher in number and larger in size within the larger catchment (Table 6.2). Spatial variability of rainfall (not analysed due to unavailability of data) across the catchment and distal runoff sources are likely more pronounced for larger catchments. These could result in more double and multiple discharge peaks within the larger catchment. Differing event times could as well result in more multiple peak events in bigger catchments.

First flush (clockwise) events are most common for larger catchments.

The study showed a significantly higher number of first flush events (p=0.041) for the larger catchment (65% of events) and a higher number of anti-first flush events (75% of events) for the smaller catchments (Table 6.7(a) and (b); Figure 6.3(a)). The mean turbidity-discharge peaks lead/lag times also differed significantly between the two spatial scales (Table 6.10(b); p=0.014), with greater lead times observed in the larger catchment (Table 6.7(c), Figure 6.3(b)). These could confirm more clockwise events for larger catchments.

Rivers more commonly exhibit clockwise hysteresis, especially for larger catchments where wash load constitutes a huge part of carried suspended sediment (Hudson, 2003). Many causes have been attributed to clockwise hysteresis such as re-suspension and transport of in-channel deposited sediment (Walling et al., 1997; Jansson, 2002; Hudson, 2003; Bowes et al., 2005; Gao and Pasternack, 2007; Moravcova et al., 2009; Smith and Dragovich, 2009); flushing and exhaustion of sediment (Jansson, 2002; Goodwin et al., 2003; Gao and Pasternack, 2007; Kleinhans et al., 2007; Lefrançois et al., 2007; Stubblefield et al., 2007; Doomen et al., 2008; Smith and Dragovich, 2009; Duvert et al., 2010), with limited availability (Lefrançois et al., 2007); reduction in rainfall erosivity (Smith and Dragovich, 2009); increased base flow during recession (Lawler et al., 2006; Rovira and Batalla, 2006); and later dilution with water from tributaries (Jansson, 2002).

Dilution from increased base flow during recession could not be a cause of the observed hysteresis because it is associated with significant water storage,

normally limited in highly impervious urbanised catchment (Webster et al., 2001; Lawler et al., 2006) such as the studied catchment. Reduction in rainfall erosivity as a cause could also not be confirmed in this study because no such analysis was made of rainfall spatial patterns or within-storm rainfall variability (Vivoni et al., 2007) due to the unavailability of data on the unevenness of storm events spatially and temporally within the catchments (Smith and Dragovich, 2009).

Flushing and exhaustion of sediment could be a cause for the more clockwise events for the larger catchment. Flushing is a process in which increasing flow is associated with increasing concentration (Moravcova et al., 2009). A greater mean lead time found in the larger catchment (Table 6.7(c); Figure 6.3(b)), is consistent with higher wash load or finer sediment component with scale, resulting in exhaustion of sediment. It also indicates a change in the nature of sediment transported by the river, as the relative amount of sand from bed material increases. More than 66% ($R > 0.8$) of the variability in lead times was accounted for by drainage area (Hudson, 2003).

Another possible cause for the clockwise events in the catchment could be re-suspension or remobilisation and transport of channel bed deposited materials. About 33% events in the bigger catchment are anticlockwise events (Table 6.7(a); Figure 6.3(a)), which could result in overall in-stream settling of sediment (Jansson, 2002; Lefrançois et al., 2007), as the discharge reduces during recession (Lane et al., 1996; Lefrançois et al., 2007; Estrany et al., 2011). Just a small portion of the sediment from upstream catchment actually reaches the bigger catchment outlet because of local deposition of sediment within

catchment and channel (Cammeraat, 2002; Goodwin et al., 2003; Estrany et al., 2011). During major rainfall events of higher discharge (high erosion and transport capacity), these deposited sediment are flushed out, remobilised and transported (Jansson, 2002; Lefrançois et al., 2007; Estrany et al., 2011).

Dilution, a major hydrological process within all water bodies including rivers (Bartram and Ballance, 1996), described as a process in which concentration decreases with increasing flow (Moravcova et al., 2009), is another potential cause of more clockwise events in the bigger catchment. Less and smaller tributaries at the smaller catchment but more and bigger at the larger catchment found in the study (Table 6.2), could mean more flow at the bigger catchment for higher dilution. This could explain why total turbidity has significant correlation with more (7) attributes for the smaller James Bridge catchment and less (1) for the bigger Water Orton catchment (Table 6.9). The mean total turbidity per unit catchment area for James Bridge is more than three times that of Water Orton. High suspended sediment/turbidity from James Bridge could be diluted by water from other downstream tributaries with lower suspended sediment/turbidity. Higher specific sediment yield is associated with smaller catchments, and could possibly be due among other things, to higher SSC responsiveness to proximal sources (Duvert et al., 2010). It is seen that there are 4 wastewater treatment plants before the bigger Water Orton catchments (Table 6.2). It also shows 374 combined sewer overflows within the whole Tame catchment (EA, 2009). The relative position of the Willenhall WWTW with respect to the James Bridge monitoring station could suggest inadequate dilution from flow downstream Willenhall, either from main stream or tributary,

before James Bridge. On the contrary, the relative positions of the Willenhall and the 3 additional WWTWs with respect to the Water Orton monitoring station could suggest much more than adequate dilution from flow downstream the last Rayhall, both from main stream and tributaries before Water Orton (Figure 6.1). This could confirm that there is much more discharge from Water Orton to dilute the point source inputs.

Downstream SSL is significantly affected by tributary inputs

The significant mean differences between single, double and multiple events at the smaller James Bridge catchment (Table 6.18(a)) could mean that SSL in this catchment depends on, among other factors, both total discharge and total turbidity. This could mean that significantly more suspended sediment loads associated with the double and multiple events would not have been analysed if only single events had been used in the James Bridge catchment. This could have resulted in severe underestimation of SSL with the wider implications of, among other things, detrimental ecological impacts on aquatic lives that are sensitive to such higher suspended sediment loads. This shows the significance of, and further justifies the relevance and need for the events characterisation and classification exercises carried out. The non-significant differences between events SSL means at the larger Water Orton (Table 6.18 (a)) could mean that SSL in this catchment has no significant relationship with both total discharge and total turbidity. Thus, if analysis of SSL has been done at this larger catchment alone, it could have hidden the significant differences found at the smaller James Bridge catchment, with the wider implications of, among other things, tremendous detrimental ecological impacts on aquatic lives at the

smaller James Bridge. This also shows the significance of, and further justifies the relevance and need for the spatial scale effect studies. Some of the possible factors that could explain the non-significant mean SSL differences at the larger Water Orton catchment are discussed below. The observed meandering, downstream Water Orton stretches (Figure 3.7 to Figure 3.10) could be indicative of the lowland reach of the studied River Tame, a zone normally associated with increased suspended sediment deposition (Gordon et al., 2013). The increased deposition could possibly be due to reduced rate of runoff and, thus, reduced flow energy needed for material re-suspension and transport, likely as a result of the curved sections and reduced slope. Also, the observed growth of dense vegetation close to and along the banks of the river and within the catchment, especially during summer, could have much more cumulative effect for the larger catchment than the smaller one. These dense bands of vegetation could lead to formation of significant water infiltration areas (Cammeraat, 2002). Vegetation could cause highly variable rate of runoff (Slattery et al., 2006) such as reduced runoff and total, and could reduce total SSL (due to trapping of suspended sediment and attached nutrients) (Goodwin et al., 2003). This could as well explain further the significantly lower levels of ammonia in summer found in the study.

Tributary influence on urban turbidity dynamics was inferred from the effect of Bourn Brook turbidity within the catchment. Bourne Brook, with significantly higher intercept (higher material availability), (Rovira and Batalla, 2006) than that of Water Orton (Table 6.20(b)), has the highest percentage urban content, (Table 6.19(a)) and also the highest mean turbidity per unit area (Table 6.19

(e)). This could imply that the highest turbid flow from the Bourn Brook stretch with the highest percentage urban cover could have been diluted by the least turbid flow from the James Bridge stretch with the lowest percentage urban cover, therefore resulting in the significantly lower mean turbidity per unit area at the lower percentage urban cover Water Orton stretch than Bourn Brook. Again, this could further explain the effect of dilution resulting in the lower downstream turbidity, suspended sediment load and ammonia found in the studied urban catchment. Decreased levels of downstream nutrients effluents (e.g. ammonia) due probably to dilution from less polluted tributaries is published (Bayram et al., 2012). Studies have reported highest turbidity and total suspended sediment (Huey and Meyer, 2010) as well as suspended sediment concentration and loads, which could be due, among other things, to short concentration times and more CSOs (Goodwin et al., 2003) for highly urbanised sites. This could signify the importance of tributary effect on urban turbidity dynamics. The significantly higher James Bridge slope JB(Gr) (rate of change), (Rovira and Batalla, 2006) than that of Water Orton (Table 6.20 (b)) could be due to the fact that James Bridge is the upstream, headwaters stretch of the river. Such zones are noted for, among other things, their steep slopes which could lead to faster runoff and thus turbidity per unit discharge (Gordon et al., 2013). The combined effects of the above could have led to the relatively lower suspended sediment load as compared to that of the turbidity per catchment area and subsequently contributed to the non-significant relationships found at the larger Water Orton catchment (Table 6.18 (a) to (c)).

6.6 Chapter summary

More single events were observed within the smaller upstream catchment. Upstream-downstream transmission losses resulting from low discharge and energy, evident by the lower specific mean total discharge for the smaller upstream catchment, leads to less single events downstream due to low event threshold. The higher number of more single events occurring within smaller catchments could also result from the smaller number of tributaries and their reduced size, more homogeneous precipitation; less pronounced rainfall spatial variability and distal runoff sources could also be responsible. Also, more multiple events were found for the larger catchments. More and larger tributaries leading to higher specific mean total discharge could be partly responsible. Other possible causes could be more pronounced rainfall spatial variability and distal runoff sources for larger catchments, and differing event timings for larger catchments. The significantly higher number of single events in the smaller catchment and the higher number of double and multiple events in the larger catchments indicates a flipping behaviour in event type distribution with scale. Again, significantly more clockwise (first flush) events in the larger downstream catchment were found. Flushing and exhaustion of sediment as shown in greater mean lead time, remobilisation and transport of channel bed deposited materials during higher discharge and higher dilution from higher total discharge are likely causes. Thus, within the studied catchment, significantly more clockwise (first flush) events in the larger downstream and anticlockwise (anti-first flush) events in the smaller upstream catchments found also shows flipping behaviour in clockwise-anticlockwise events distribution with scale. The

effect of vegetation growth especially in summer (conducive for sediment and ammonia trapping), the lowland river zone with meandering sections and lower slope (both conducive for sediment and attached ammonia deposition) as well as tributary input (possible dilution with less turbid headwaters flow), could have resulted in lower downstream turbidity, SSL and ammonia. These, among other factors discussed earlier, could have led to the significant SSL mean differences at James Bridge found in the study. This could mean that if analysis of SSL has been done at the larger Water Orton catchment with non-significant SSL mean differences alone, it could have hidden the significant differences found at the smaller James Bridge catchment. This could result in such wider implications as tremendous detrimental ecological impacts on aquatic lives at the smaller James Bridge catchment. Also, the possible effects of river zones and tributary contributions found could have led to incomplete story regarding turbidity and suspended sediment dynamics in the studied catchment if they were included in the study. These could also show the significance of, and further justify the relevance and need for the spatial scale effect studies including tributary catchments. These findings could be very important for monitoring, policy and decision making.

CHAPTER 7 SYNTHESIS AND CONCLUSION

7.1 Chapter introduction

The suspended sediment dynamics of urban rivers during storm events using continuously monitored, high resolution turbidity data were explored in this project. It aimed at contributing knowledge and novel methods to improve understanding of fluvial turbidity and thus, suspended sediment dynamics at smaller headwaters and bigger downstream sub-catchments of an urban river through individual and sequenced storm events. These novel methods include quantified events selection criteria, quantified event classification based on number of hydrograph peaks and quantified complex event classification based on lead-lag of the highest peaks of both discharge and turbidity. The specific objectives as given in Chapter 1 were to:

1. To characterise events and examine their influence to unravel the interaction of factors influencing the turbidity dynamics;

2. To assess inter- and intra- seasonal variability to identify their distribution and examine their influence on the turbidity patterns;

3. To evaluate the scale effect on turbidity dynamics by comparing the upstream and downstream sub-catchments; and

4. To identify key controls, drivers and processes that determine space-time patterns in storm event turbidity dynamics in urban river catchments.

Review of relevant literature (given in Chapter 2 and Chapter 4 to Chapter 6) led to the identification of the following research gaps:

1. Turbidity dynamics in storm events are not systematically characterised in the research literature leading to limits in our process understanding.

2. Most studies of storm events turbidity dynamics have formed on short time periods (days or weeks); therefore, there is the need to explore seasonal and inter-annual patterns and processes.

3. Previous studies have formed on single gauges in urban environments; hence, there is a need to assess the importance of space-time patterns of event dynamics.

4. There is a paucity of understanding the key controls, drivers and processes that determine space-time patterns in storm event turbidity dynamics in urban river catchments.

The work proceeded with events characterisation (Chapter 3), followed by assessing the turbidity dynamics with the classified events (Chapter 4), their seasonality (Chapter 5), and their spatial scale effects (Chapter 6), with their synthesis and conclusion given in this section (Chapter 7).

7.2 Event characterisation

The study sites used for the subsequent assessment of urban sediment dynamics were described. Diverse and mostly qualitative methods for hydrological events selection criteria were observed through the review of literature. Examples include rainfall event whose start and end times are considered to be the first measured rainfall and when SSC get back to near starting values (Goodwin et al., 2003); flow event as one in which the sampling is made in a way that the hydrograph contains both rising and recession parts

(Smith and Dragovich, 2009). Few definitions which gave quantitative selection criteria were specific to site or context which could not be generalised. For example, storm event with rain event equalling and exceeding a total of 5mm and with sufficiently large areal coverage (Stanfield and Jackson, 2011); and hydrological event with rising limb beginning at flow rise of over 3l/s per 10min or rise in SSC of over 10mg/l per 10min and recession limb ending at flow and SSC values lower than 3l/s and 10mg/l per 10min (Lefrançois et al., 2007). Also, mostly qualitative methods for hydrological events classifications were observed through the review of literature. Notably, peaks and troughs were visually identified within the storm hydrograph, with continuous storms resulting in multi-peaked flows separated by defined troughs considered separately (Smith and Dragovich, 2009). These led to the development of a systematic approach to define individual storm events and to classify and characterise their form. For the first time, the quantification of robust, universally adaptable hydrological events selection and classification criteria were developed. The availability of continuously monitored, high resolution data enabled and facilitated these. These methodologies were applied to determine the primary controls on sediment dynamics within urban catchments and their dependence on events, seasons and scale. Aside their use in this study, these useful, robust methodologies could be used as standardised events selection and classification criteria that could be applicable within different catchments, contexts and for different purposes.

7.3 Events turbidity dynamics

Hitherto, single flow peak events were mostly used in turbidity dynamics analysis. Events were required to be single-peaked as much as possible so that rotational direction could be determinable (Evans and Davies, 1998). Probable reasons for the use of single flow peak events mostly, aside its simplicity, could be as follow. Hydrograph forms depend on occurrences in nature which mostly make them multi-rise often resulting in a given stream flow value having irregular and complicated concentration (Moravcova et al., 2009). There are instances where events cannot be put in a known class due to their complicated forms as a result of irregular rainfall patterns (Lefrançois et al., 2007). Also, noisy simulated runoff occurred especially in the case of multi-peaks rainfall events due to the highly noisy rainfall time series used as input (Talei et al., 2010). Those studies that do discuss double and/or multiple flow peak events (Rovira and Batalla, 2006; Furusho et al., 2010; Talei et al., 2010) treat them as a succession of peaks that are used, for example, to explain sediment exhaustion within the catchment, thus, making their analysis is severely limited.

The developed methods enabled the classification of single, double and multiple flow peak events as distinct, separate events. This classification revealed that the double and multiple flow peak events together constituted over 60% of the overall downstream Water Orton catchment events. Thus analysing only single events could be missing key dynamics involving these double and multiple flow peak events. Notably, an enhanced sensitivity of observed turbidity varying with discharges and ammonia inputs was observed. Multiple events showed increased rate of change as shown in the increased gradient of regression lines

of turbidity peak and range with discharge peak and range. They also showed increased availability as shown in the increased intercept of regression lines of total turbidity with discharge peak, range, and total as well as ammonia peak. Single peak events did not show any significant effect of the variables on turbidity attributes. Thus, if only single peak events were used for such analysis in the studied catchment, a possible underestimation of effects on turbidity dynamics leading to incorrect conclusion might have been made. These could lead to inappropriate policies, strategies, interventions and/or other decisions that might rely or be based on such findings regarding the urban catchment.

The events classified with the developed methods were used to analyse hysteresis resulting from turbidity peaks leading, lagging or coinciding with discharge peaks. More anticlockwise (with turbidity peaks lagging discharge peaks) events were observed within the catchment that could partly result from more low discharge events. These findings are contrary to most published research. Many researchers reported a dominance of clockwise events. There were challenges involved in determining the lead lag of multiple events since they are often complex (Moravcova et al., 2009), with a few events not classified because of their complex patterns (Lefrançois et al., 2007). Using the highest peaks regarding both discharge and turbidity for the double and multiple peak events made it possible for this to be done. Thus, these have enhanced the effective characterization of the complex multi-peak hysteresis in urban storm events. This is significant since the accompanying net processes of remobilisation and transport, and deposition associated with lead and lag events within the double and multiple peak events might have been missed if

they were not analysed. Here again, resultant catchment processes that might be the bases for management and/or policy decisions might be partial but not holistic and thus, leading to inappropriate actions regarding the urban catchment.

Further, a pattern of anticlockwise events decreasing while the clockwise and coinciding events increased from single to multiple events was observed. This may result from a decreasing and increasing total discharge that could lead to decreasing and increasing dilution effects respectively. These give further explanation and thus enhancing understanding of patterns of processes regarding events types' effect on clockwise and anticlockwise events.

The study also found more than a third of total events with more turbidity than discharge peaks which might possibly be due to dilution effects and effluent spillage which has been shown to be more frequent for higher intensity rain storms. The association of more turbidity than discharge peaks with effluent spillage also gives further explanation and thus enhancing understanding of turbidity dynamics.

7.4 Events seasonality

Significant seasonal effects during summer and autumn were observed. Changes in seasonal turbidity during summer and autumn resulted from reduced discharge and low dilution of available sediment. Significant effects on seasonal turbidity dynamics were also observed, likely due to the result of variations in effluent spillage into the river system. Significant effects associated with total and peak ammonia during summer and autumn possibly due to low

availability and low dilution were also observed in the studied catchment. All seasons but spring having more anticlockwise than clockwise events were associated with more low flows. Winter with the highest anticlockwise events was the season with the second most distance runoff source, possibly because of its wider areal rain event extent, and with the second highest number of low flows. Thus, both low flows and distal runoff sources might be the main causes for anticlockwise events.

7.5 Spatial scale effect

There was a flipping behaviour in event type distribution with scale with more single events in the smaller and more multiple events in the larger catchments. These findings might have been possible because of the effective characterisation of events into single, double and multiple peaks within the studied catchment. These might be due to transmission losses, low discharge and energy shown in lower specific mean total discharge and less tributaries for the smaller upstream catchment. Also, more and larger tributaries, higher specific mean total discharge, more pronounced rainfall spatial variability, distal runoff sources and differing event timings might account for more multiple events in the larger catchments. The significant implication of this is that if double and multiple events were not analysed, about 40 and 60% of events with respect to the smaller and the larger catchments would have been left out. As such, the associated characteristics of discharge (total and specific), transmission losses, rainfall spatial variability and tributary effects and accompanying processes might not have been analysed.

Again, a flipping behaviour in clockwise-anticlockwise events distribution with scale was found in the catchment. Higher discharge resulting in flushing and exhaustion of sediment as shown in greater mean lead time, remobilisation and transport of channel bed deposited materials during higher discharge and higher dilution from the bigger and more tributaries might be some of the possible causes of more clockwise than anticlockwise events in the larger catchment. Conversely, lower discharge, transmission losses, less dilution from the smaller and less tributaries and late arrival of runoff might be some of the possible causes of more anticlockwise than clockwise events in the smaller catchment. These findings might have been possible because of the effective characterisation of the complex multi-peak urban storm events hysteresis by use of the highest peaks regarding both discharge and turbidity, thus enabling complete analysis of total classified events.

7.6 Wider implication

Management and monitoring

Monitoring and management of river flow and downstream transport of sediment in large watersheds requires adequate understanding of the importance of urbanisation (Old et al., 2006). Impervious cover induces stream responses of increased sediment (with associated contaminants) and flashy hydrology (Nagy et al., 2012). At the beginning of rainy seasons, previously stored sediment is mostly re-suspended by the early rains. This first-flush effect results in high sediment and pollutant concentrations, thus, leading to water management challenges. (Estrany et al., 2011).

Findings from the study could thus be useful for hydrologists, hydro ecologists, water quality experts and other policy makers regarding timing of monitoring schedules and other management practices within urban catchments. The quantification of robust, universally adaptable hydrological events selection and classification criteria developed could be used as standardised methods that could be applicable within different catchments, contexts and for different purposes. The classification revealed that the double and multiple events together constituted more than 60% of the total events which could have been missed together with key dynamics involving them if only single events were analysed. Such key dynamics include significant effects of increased turbidity found with multiple events. Thus, a possible underestimation of effects on turbidity dynamics that might lead to inappropriate policies, strategies, interventions and/or other decisions that might rely or be based on such findings regarding the urban catchment might be made.

The different zones of the studied river (headwaters and lowland) with their different characteristics such as gradients, depth, width and riparian vegetation significantly affected turbidity and SSL dynamics as well. Therefore, there is the need to include the analyses of these different zones that may be part of a study or monitoring programme, with their uniquely different characteristics since they could have ecologically harmful effects. If analysis of SSL has been done at the larger Water Orton catchment alone where no significant differences in means of SSL between event types were found, it could have hidden the significant differences found at the smaller James Bridge catchment, with such wider implications as, tremendous detrimental ecological impacts on

aquatic lives at the smaller catchment. Also, tributary inputs which significantly affected downstream turbidity values could have led to less accurate loads with detrimental ecological and other effects if it was not analysed.

Knowledge and understanding

The developed novel, robust and universally adaptable quantitative methods for determining start and end times for single hydrological events provides a framework for any future examination of rivers sediment dynamics. It provides a quantitative, repeatable approach that will permit the inter-comparison and transferability of knowledge between studies undertaken across catchments within a range of climatic regions, across the broad range of landscapes and at a range of spatial scales. Similarly, the quantitative methods for characterising events into single, double and multiple discharge peaks with distinct characteristics could solve the challenge of possible underestimations with the mostly used single peak events analysis. These could promote more or further event-based studies of various flow-related attributes, thereby improving understanding of their dynamics.

The classification revealed that the double and multiple flow peak events together constituted more than 40 and 60% of the total events for the smaller and larger catchments. Multiple events had significant effects on turbidity-ammonia/discharge regression. Analyzing only single events could have missed key dynamics involving these double and multiple flow peak events such as the associated characteristics of discharge, transmission losses, rainfall spatial

variability, which could not be assessed due to patchy data, and tributary effects and accompanying processes.

Turbidity was significantly affected mostly in summer and autumn, making the two seasons critical for the catchment. Urban extent and effluent spillage had significant effect on turbidity dynamics in summer and autumn. Also, three out of four seasons had more anticlockwise than clockwise events with all three associated with more low flows as well. Winter with the highest anticlockwise events had both high number of low flows and lag times indicative of distant runoff source, possibly because of its wider areal rain event extent as a result of the rainfall being synoptic or frontal in nature. Findings associated with events seasonality are important since they have revealed many other determinands and attributes with significant effects on turbidity which were not found with event types' analysis.

A flipping behaviour in event types and in clockwise-anticlockwise events distribution with scale was found. Also, the means of turbidity, SSC and SSL significantly changed with event types in the smaller but not in the larger spatial scale. These are significant since it could mean analysing only one spatial scale might not have provided the holistic processes and controls prevailing in the catchment.

7.7 Further works and conclusion

Future research

The following are recommended for future research.

1. The novel methods developed should be used for various catchment sizes or spatial scales (small, medium and big), types (rural and urban), combinations (smaller/bigger/nested, rural/urban/mixed). Also, they should be used for longer periods than used in this study to cover more events and seasons.

2. There were more anticlockwise than clockwise events. The anticlockwise and clockwise events mostly lead to net material deposition and remobilisation and transport respectively. Actual field measurements regarding deposition, remobilisation and transport in the catchment could provide more knowledge to improve understanding.

3. Effluent spillage which significantly affected turbidity in summer and autumn was found as a major cause of more number of turbidity peaks than discharge peaks per events. Further study on this to find other causes is recommended.

4. Urban extent was found to have significant effect on turbidity dynamics in summer and autumn. Other land cover or use patterns should be studied for holistic information in land use effects on urban catchment turbidity.

5. Seasonal effects of individual types of the characterised event on turbidity could be studied for their individual effects to be identified, since that could add on to what is found in this work.

6. The study concentrated on only two monitoring sites, and might not be able to capture, for instance, the processes between and beyond the two sites. It is recommended that further studies with finer and coarser spatial scale resolutions be carried out to capture details in smaller and larger scale effects. Also, total rainfall was mostly used. The use of other such rainfall characteristics as intensity and duration is recommended so as to improve analysis with rainfall.

7. Data from only two rain gauge stations were used, one per monitoring site, and as such not allowing for proper analysis of spatio-temporal variability of rainfall across the catchment. This was needed for better analysis of catchment processes and controls for better understanding. Further study using more rain gauge stations could provide more and accurate insight into what actually happens across the catchment.

8. Natural and anthropogenic activities within the urban catchment result in complex hydrographs. Analysis of the complex events hysteresis have, thus, not been done. Analysis of these complex hysteresis could now be carried out with the method developed to add to what has been found.

Concluding remarks

Event-based study of turbidity dynamics has been conducted successfully by characterising events hydrologically leading to a novel, robust, universally

adaptable events selection and classification criteria. Use of the single, double and multiple events classified has identified possible significant underestimation of turbidity or suspended sediment availability and rate of change with respect to discharge and other determinands using only single events for analysis. A flipping behaviour in events types distribution with scale, with significantly more single events in the smaller and multiple events in the larger catchments was observed. It has also found that the first-flush phenomenon assumed to be more dominant for river systems is not always the case. Anticlockwise events dominate the catchment, with three out of four seasons having more anticlockwise than clockwise events. Summer and autumn showed significant effects of some determinands on turbidity. However, spatial scale study again showed a flipping behaviour in clockwise – anticlockwise events distribution with scale, with significantly more clockwise events in the larger downstream and anticlockwise events in the smaller upstream catchments Again, significant effluent spillage found in the urban catchment which has significant effects on seasonal turbidity dynamics, occur mostly during high intensity rain event events and might be the main cause of events with more turbidity peaks than discharge peaks. The significant changes in turbidity found both with event types and seasonality were mainly controlled by discharge, material availability (inferred from intercept of turbidity-discharge line of best fit) and rate of change with respect to determinands. The effect of vegetation growth especially in summer (conducive for sediment and ammonia trapping), the lowland river zone with meandering and lower slope (both conducive for sediment and ammonia deposition) as well as tributary input (possible dilution with less turbid

headwaters flow), could have resulted in lower downstream turbidity, SSL and ammonia. These, among other factors discussed earlier, could have led to the respective significant SSL mean differences at James Bridge but not at Water Orton found in the study. This could mean that if analysis of SSL has been done at the larger Water Orton catchment alone, it could have hidden the significant differences found at the smaller James Bridge catchment. This could result in such wider implications as tremendous detrimental ecological impacts on aquatic lives at the smaller James Bridge catchment. Also, the possible effects of river zones and tributary contributions found could have led to incomplete story regarding turbidity and suspended sediment dynamics in the studied catchment. These could also show the significance of, and could further justify the relevance and need for the spatial scale effect studies. These findings could be very important for monitoring, policy and decision making.

Appendix A

List of Abbreviations

SS	Suspended sediment
SSC	Suspended sediment concentrations
SSY	Suspended sediment yield
SSL	Suspended sediment load
Tu	Turbidity
Q	Discharge
STW	Sewage treatment works
CSS	Combined sewer system
CSO	Combined sewer overflow
Pb	Lead
r	Pearson's rank correlation coefficient
R	Rainfall
R^2	Coefficient of determination
F8	Figure-of-eight
C	Clockwise

AC	Anti-clockwise
C3	Concave loops with clockwise rotation
A3	Concave loops with anti-clockwise rotation
Lead/Ld	Events with turbidity peak leading discharge peak
Lag/Lg	Events with turbidity peak lagging discharge peak
Co	Events with turbidity and discharge peaking together
UK	United Kingdom
EA	Environment Agency
U/S	Upstream
D/S	Downstream
UIDs	Unsatisfactory Intermittent Discharges
WwTW	Wastewater Treatment Works
FTU	Formazin Turbidity Units
CEH	Centre for Ecology and Hydrology
t_{STS}	Starting time of time series
t_{ETS}	Ending time of time series
t_o	Rain start time
t_c	Rain centroid time

t_{eo}	Event start time
t_{ee}	Event end time
t_E	Event time
t_{ET}	Total event time
t_r	Event response time
Q_{pk}	Flow peak
Q_o	Minimum flow at event start time
Q_{ee}	Minimum flow at event end time
Q_r	Flow range
Q_{tot}	Event total flow
EFR	Event flow rate
t_{Qpk}	Flow peak time
t_{QRL}	Flow rise time
t_{QFL}	Flow recession time
dQ_{RL}	Rate of flow rise
dQ_{FL}	Rate of flow recession
Lag_{RQ}	Rainfall-low lag time
Tu_{pk}	Turbidity peak

Tu_o	Minimum turbidity at event start time
Tu_{ee}	Minimum turbidity at event end time
Tu_r	Turbidity range
t_{Tupk}	Turbidity peak time
t_{TuRL}	Turbidity rise time
t_{TuFL}	Turbidity recession time
dTu_{RL}	Rate of turbidity rise
dTu_{FL}	Rate of turbidity recession
Lag_{TuQ}	Turbidity-flow peaks lag time
R_{pk}	Rainfall peak
R_{ant}	24 - hour antecedent rain
R_{tot}	Event total rainfall
ERI	Event rainfall intensity
NH_{pk}	Ammonia peak
t_{NHpk}	Ammonia peak time
Lag_{TuNH}	Turbidity-ammonia lag time
ANOVA	Analysis of variance
D	Double events

M	Multiple events
Su	Summer
A	Autumn
W	Winter
Gr	Gradient of regression lines
In	Intercept of regression lines
MLR	Multiple Linear Regression
NHpk	Ammonia peak
NHtot	Ammonia total
p	Statistical significance
CL	Confidence level
N/n	Number of events
df	Degrees of freedom
LEDs	Light emitting diodes
LDRs	Light Dependent Resistors
PDs	Photodiodes
PTs	Photo transmitters
ISEs	Ion-selective electrodes

Appendix B

More Tables

(a) Event types basic statistics

Event	Attribute	Min	Max	Mean	Std. Dev.
Single	**Tutot (FTU)**	1581	43289	14580	8728
	Qtot (m^3/l)	354.86	3988.25	1366	979.7
	tE (h)	16	68.25	36	15.35
	tET (h)	19.5	72	39.75	15.31
	tQFL (h)	13.5	57.25	29	12
	Rtot (mm)	1.5	27	8.5	6.2
	Rpk (mm)	0.2	4.5	1.2	0.814
	ERI (mm/h)	0.08	0.67	0.23	0.145
	Qr (m^3/l)	2.77	64.9	16.8	15.2
	tQRL (h)	1.5	26	6.9	5.4
	NHtot (mg/l)	9.1	1098.4	139.4	220.3
	NHpk (mg/l)	0.2	8.1	2.5	2
Double	**Tutot (FTU)**	2567	40166	15442	10407
	Qtot (m^3/l)	270.55	3512.97	1407	1006.1
	tE (h)	14.75	114.75	42	25.6
	tET (h)	18	120	44.59	25.97
	tQFL (h)	10	105.25	35	23.8
	Rtot (mm)	1	44	9.5	8.4
	Rpk (mm)	0.4	11	1.91	2.23
	ERI (mm/h)	0.03	1.05	0.26	0.228
	Qr (m^3/l)	2.64	47.69	13.7	11.2
	tQRL (h)	1.75	19	7.2	4.5
	NHtot (mg/l)	2.2	1121.2	151.2	214.3
	NHpk (mg/l)	0.2	12.1	3.5	2.6
Multiple	**Tutot (FTU)**	8785	45214	20811	11215
	Qtot (m^3/l)	488.01	3706.5	1416	868.5
	tE (h)	24	108.25	53	22.9
	tET (h)	24	114	57.82	24.04
	tQFL (h)	16	93.25	40	22.2
	Rtot (mm)	5	14.5	9.8	3.2
	Rpk (mm)	0.6	5.5	1.6	1.4
	ERI (mm/h)	0.1	0.48	0.2	0.1
	Qr (m^3/l)	3.16	15.27	7	3.6
	tQRL (h)	2.25	26.75	13	8.4
	NHtot (mg/l)	50.3	465.09	159.4	135
	NHpk (mg/l)	0.5	6.2	2.5	1.7

(b) Seasonal basic statistics (spring and summer)

	Attribute	Min	Max	Mean	Std. Dev.
Spring	**Tutot (FTU)**	1581	45214	21115	12002
	Tupk (FTU)	90	476	288	115
	Tur (FTU)	65	451	254	115
	Qtot (m^3/s)	371.76	3706.50	1594.75	906.02
	Qr (m^3/s	2.77	36.51	14.46	10.71
	Qpk (m^3/s)	6.12	44.49	19.22	11.86
	tE (h)	17.8	108.3	43.5	21.5
	tET (h)	19.5	114.0	47.1	22.4
	tQRL (h)	1.5	26.8	9.3	7.2
	tQFL (h)	13.8	93.3	34.2	18.4
	dQRL (m^3/s/h)	0.2	12.6	3.1	3.5
	dQFL (m^3/s/h)	0.1	1.8	0.5	0.5
	Rtot (mm)	3.5	17.0	10.0	4.8
	Rpk (mm)	0.5	3.0	1.3	0.6
	NHtot (mg/l)	9.7	1098.4	177.5	249.3
	NHpk (mg/l)	0.5	6.3	2.8	1.7
	LagTuQ (h)	0.0	11.3	3.3	3.5
	LagTuNH (h)	0.0	24.5	8.5	8.1
Summer	**Tutot (FTU)**	2567	24034	9852	5487
	Tupk (FTU)	48	397	210	118
	Tur (FTU)	39	384	179	119
	Qtot (m^3/s)	270.55	3512.97	782.93	787.86
	Qr (m^3/s)	2.64	47.69	10.96	11.87
	Qpk (m^3/s)	5.06	49.98	13.87	11.97
	tE (h)	14.8	46.5	27.7	10.4
	tET (h)	18.0	51.0	30.7	10.3
	tQRL (h)	1.8	17.3	6.4	4.3
	tQFL (h)	10.0	36.3	21.2	8.2
	dQRL (m^3/s/h)	0.4	9.0	2.4	2.5
	dQFL (m^3/s/h)	0.1	1.5	0.5	0.5
	Rtot (mm)	1.0	44.0	8.3	10.7
	Rpk (mm)	0.5	11.0	2.7	3.0
	NHtot (mg/l)	13.3	365.1	119.9	127.4
	NHpk (mg/l)	0.2	6.8	2.0	1.7
	LagTuQ (h)	0.3	6.3	2.4	2.2
	LagTuNH (h)	0.3	23.5	6.1	6.7

(c) Seasonal basic statistics (autumn and winter)

	Attribute	Min	Max	Mean	Std. Dev.
Autumn	**Tutot (FTU)**	5370.0	17281.4	11890.0	3993.7
	Tupk (FTU)	56	486	257	120
	Tur (FTU)	33	466	233	116
	Qtot (m^3/s)	739.97	3988.25	1549.61	989.67
	Qr (m^3/s)	5.00	64.90	18.06	16.38
	Qpk (m^3/s)	7.37	70.39	22.59	16.78
	tE (h)	23.50	106.50	43.75	21.49
	tET (h)	24.0	111.0	46.2	21.7
	tQRL (h)	2.8	18.5	8.7	5.3
	tQFL (h)	16.0	94.3	35.0	19.6
	dQRL (m^3/s/h)	0.3	10.5	3.0	2.9
	dQFL (m^3/s/h)	0.1	2.6	0.6	0.7
	Rtot (mm)	4.0	27.0	10.6	6.4
	Rpk (mm)	0.5	4.5	1.7	1.0
	NHtot (mg/l)	2.2	194.3	61.1	60.6
	NHpk (mg/l)	0.2	8.1	2.6	2.1
	LagTuQ (h)	0.0	5.0	1.6	1.8
	LagTuNH (h)	0.0	42.3	7.9	12.2
Winter	**Tutot (FTU)**	3837	40166	18782	10268
	Tupk (FTU)	85	410	258	91
	Tur (FTU)	62	382	217	84
	Qtot (m^3/s)	513.76	3946.39	1562.64	989.39
	Qr (m^3/s)	3.21	38.76	12.08	11.47
	Qpk (m^3/s)	7.16	43.60	16.72	11.73
	tE (h)	20.0	114.8	49.8	26.3
	tET (h)	24.0	120.0	53.7	26.8
	tQRL (h)	2.0	26.0	7.5	6.2
	tQFL (h)	18.0	105.3	42.3	24.2
	dQRL (m^3/s/h)	0.5	6.8	2.0	1.8
	dQFL (m^3/s/h)	0.1	0.9	0.3	0.2
	Rtot (mm)	2.8	20.0	7.7	4.8
	Rpk (mm)	0.2	2.0	0.9	0.5
	NHtot (mg/l)	15.7	1121.2	209.5	253.7
	NHpk (mg/l)	0.3	12.1	4.1	3.0
	LagTuQ (h)	0.3	5.3	2.1	1.7
	LagTuNH (h)	0.3	104.3	18.7	27.9

List of References

Andjelkovic I. 2001. GUIDELINESO ON NON-STRUCTURAL MEASURES IN URBAN FLOOD MANAGEMENT. In: INTERNATIONAL HYDROLOGICAL PROGRAMME. Paris: UNESCO. p 1-87.

Asselman NEM, Middelkoop H, Van Dijk PM. 2003. The impact of changes in climate and land use on soil erosion, transport and deposition of suspended sediment in the River Rhine. Hydrological Processes 17:3225-3244.

Astaraie-Imani M, Kapelan Z, Fu G, Butler D. 2012. Assessing the combined effects of urbanisation and climate change on the river water quality in an integrated urban wastewater system in the UK. Journal of Environmental Management 112:1-9.

BaČA P. 2008. Hysteresis effect in suspended sediment concentration in the Rybárik basin, Slovakia / Effet d'hystérèse dans la concentration des sédiments en suspension dans le bassin versant de Rybárik (Slovaquie). Hydrological Sciences Journal 53:224-235.

Bartram J, Ballance R, editors. 1996. Water Quality Monitoring-A Practical Guide to the Design and Implementation of Freshwater Quality Studies and Monitoring Programmes: on behalf of United Nations Environment Programme and the World Health Organization (UNEP/WHO).

Bayram A, Önsoy H, Bulut VN, Akinci G. 2012. Influences of urban wastewaters on the stream water quality: a case study from Gumushane Province, Turkey. Environmental Monitoring and Assessment:1-19.

Beck MB. 2005. Vulnerability of water quality in intensively developing urban watersheds. Environmental Modelling & Software 20:381-400.

Bejankiwar R. 2009. Water Quality Status Report.

Bilotta G, Brazier R. 2008. Understanding the influence of suspended solids on water quality and aquatic biota. Water Research 42:2849-2861.

Bizzi S, Lerner DN. 2012. Characterizing physical habitats in rivers using map-derived drivers of fluvial geomorphic processes. Geomorphology 169:64-73.

Bowes MJ, House WA, Hodgkinson RA, Leach DV. 2005. Phosphorus-discharge hysteresis during storm events along a river catchment: the River Swale, UK. Water Research 39:751-762.

Brakebill JW, Ator SW, Schwarz GE. 2010. Sources of Suspended-Sediment Flux in Streams of the Chesapeake Bay Watershed: A Regional Application of the SPARROW Model1. JAWRA Journal of the American Water Resources Association 46:757-776.

Cammeraat LH. 2002. A review of two strongly contrasting geomorphological systems within the context of scale. Earth Surface Processes and Landforms 27:1201-1222.

Carpenter B, Jackson S, Taylor-Guevara H. 2002. A River in Jeopardy.

Carter J, Walling DE, Owens PN, Leeks GJL. 2006. Spatial and temporal variability in the concentration and speciation of metals in suspended

sediment transported by the River Aire, Yorkshire, UK. Hydrological Processes 20:3007-3027.

CEH. 2012. River Tame Catchment Information In: Centre for Ecology and Hydrology.

Chapman DV. 1996. Water quality assessments: a guide to the use of biota, sediments, and water in environmental monitoring: E & Fn Spon.

Chelsea Nagy R, Graeme Lockaby B, Kalin L, Anderson C. 2012. Effects of urbanization on stream hydrology and water quality: the Florida Gulf Coast. Hydrological Processes 26:2019-2030.

Choubey V. 1992. Correlation of turbidity with Indian Remote Sensing Satellite-1A data. Hydrological Sciences Journal 37:129-140.

Choy ML. 2004. A comparison of the effects of regulated and not regulated hydrologic regimes on fine sediment deposition and benthic macroinvertebrate distributions. University of California, Berkeley.

Codd GA. 2000. Cyanobacterial toxins, the perception of water quality, and the prioritisation of eutrophication control. Ecological Engineering 16:51-60.

Collins AL, Naden PS, Sear DA, Jones JI, Foster IDL, K M. 2011a. Sediment Targets for informing river catchment management: international experience and prospects. Hydrological Processes.

Collins AL, Naden PS, Sear DA, Jones JI, Foster IDL, Morrow K. 2011b. Sediment targets for informing river catchment management: international experience and prospects. Hydrological Processes:n/a-n/a.

Conrad C, Saunderson H. 2000. Temporal and spatial patterns of suspended sediment yields for selected rivers in eastern United States: implications

for nutrient and contaminant transfer In: The role of erosion and sediment transport in nutrient and contaminant transfer Waterloo, Canada: IAHS. p 37-46.

Crabtree B, Hickman M, Martin D. 1999. Integrated water quality and environmental cost-benefit modelling for the management of the River Tame. Water Science and Technology 39:213-220.

de Boer DH, Campbell IA. 1989. Spatial scale dependence of sediment dynamics in a semi-arid badland drainage basin. CATENA 16:277-290.

De Carlo EH, Beltran VL, Tomlinson MS. 2004. Composition of Water and Suspendes sediment in strems of urbanised subtropical watersheds in Hawaii. Applied Geochemistry 19:1011-1037.

Debels P, Figueroa R, Urrutia R, Barra R, Niell X. 2005. Evaluation of water quality in the Chillán river (Central Chile) using physicochemical parameters and a modified water quality index. Environmental Monitoring and Assessment 110:301-322.

Devereux OH, Prestegaard KL, Needelman BA, Gellis AC. 2010. Suspended-sediment sources in an urban watershed, Northeast Branch Anacostia River, Maryland. Hydrological Processes 24:1391-1403.

Doomen AMC, Wijma E, Zwolsman JJG, Middelkoop H. 2008. Predicting suspended sediment concentrations in the Meuse river using a supply-based rating curve. Hydrological Processes 22:1846-1856.

Duvert C, Gratiot N, Evrard O, Navratil O, Némery J, Prat C, Esteves M. 2010. Drivers of erosion and suspended sediment transport in three headwater

catchments of the Mexican Central Highlands. Geomorphology 123:243-256.

EA U. 2009. River Tame Flood Risk Management Strategy: Environmental Report - Non Technical Summary May 2009. In.

Edwards AC, Withers PJA. 2008. Transport and delivery of suspended solids, nitrogen and phosphorus from various sources to freshwaters in the UK. Journal of Hydrology 350:144-153.

Ellis PA, Mackay R, Rivett MO. 2007. Quantifying urban river–aquifer fluid exchange processes: A multi-scale problem. Journal of Contaminant Hydrology 91:58-80.

Estrany J, Garcia C, Walling DE, Ferrer L. 2011. Fluxes and storage of fine-grained sediment and associated contaminants in the Na Borges River (Mallorca, Spain). CATENA 87:291-305.

Evans C, Davies TD. 1998. Causes of concentration/discharge hysteresis and its potential as a tool for analysis of episode hydrochemistry. Water Resources Research 34:129-137.

Ferrier RC, Edwards, Anthony C., Hirst, David, Littlewood, Ian G., Watts, Carol, D., Morris, Rob. 2001. Water quality of Scottish rivers: spatial and temporal trends. Science of The Total Environment 16.

Furusho C, Chancibault K, Andrieu H. 2010. Analysis of the hydrological functioning of an Urbanizing River. In: World Wide Workshop for Young Environmental Scientists: 2010 proceedings.

Gao P, Pasternack G. 2007. Dynamics of suspended sediment transport at field-scale drain channels of irrigation-dominated watersheds in the

Sonoran Desert, southeastern California. Hydrological Processes 21:2081-2092.

Gao P, Puckett J. 2012. A new approach for linking event-based upland sediment sources to downstream suspended sediment transport. Earth Surface Processes and Landforms 37:169-179.

Gippel CJ. 1995. Potential of turbidity monitoring for measuring the transport of suspended solids in streams. Hydrological Processes 9:83-97.

Goodwin TH, Young AR, Holmes MGR, Old GH, Hewitt N, Leeks GJL, Packman JC, Smith BPG. 2003. The temporal and spatial variability of sediment transport and yields within the Bradford Beck catchment, West Yorkshire. The Science of The Total Environment 314-316:475-494.

Google. 2013. Google Earth. In: www.earth.google.co.uk.

Goransson G, Larson M, Bendz D. 2013. Variation in turbidity with precipitation and flow in a regulated river system–River GotaAlv, SW Sweden. Hydrol Earth Syst Sci Discuss 10:255-293.

Gordon ND, McMahon TA, Finlayson BL, Gippel CJ, Nathan RJ. 2013. Stream hydrology: an introduction for ecologists: John Wiley & Sons.

Gray JR, Gartner JW. 2009. Technological advances in suspended-sediment surrogate monitoring. Water Resour Res 45:W00D29.

Gray SR, Gartner JW, Anderson CW, Fisk GG, Douglas Glysson G, Gooding DJ, Hornewer NJ, Larsen MC, Macey JP, Rasmussen PP, Wright SA, C. ZA. 2010. Surrogate technologies for monitoring suspended-sediment transport in rivers. In: Poleto C, Charlesworth S, editors. Sedimentology

of Aqueous Systems, First edition ed: United States Geological Survey, USA. p 3-45.

Gurnell A, Lee M, Souch C. 2007. Urban Rivers: Hydrology, Geomorphology, Ecology and Opportunitied for Change. Geography Compass 1:1118-1137.

HACH. 2008. NH4D sc Ammonium Sensor USER MANUAL- Edition 2. In. Germany: Hach Company.

Hall JW, Evans EP, Penning-Rowsell EC, Sayers PB, Thorne CR, Saul AJ. 2003. Quantified scenarios analysis of drivers and impacts of changing flood risk in England and Wales: 2030–2100. Global Environmental Change Part B: Environmental Hazards 5:51-65.

Hannaford J, Buys G. 2012. Trends in seasonal river flow regimes in the UK. Journal of Hydrology 475:158-174.

Helmreich B, Hilliges R, Schriewer A, Horn H. 2010. Runoff pollutants of a highly trafficked urban road – Correlation analysis and seasonal influences. Chemosphere 80:991-997.

Herman EK, Toran L, White WB. 2008. Threshold events in spring discharge: Evidence from sediment and continuous water level measurement. Journal of Hydrology 351:98-106.

Holden J. 2005. An introduction to physical geography and the environment: Pearson Education.

Horowitz A. 2009. Monitoring suspended sediments and associated chemical constituents in urban environments: lessons from the city of Atlanta,

Georgia, USA Water Quality Monitoring Program. Journal of Soils and Sediments 9:342-363.

Horowitz A, Elrick KA, Smith JJ. 2007. Mesuring the fluxes of suspended sediment, trace elements, and Nutrients for the city of Atlanta, U. S. A.: Insightd on the global water quality impacts of increasing urbanisation. In. Atlanta, GA: United States Geological Survey.

Horowitz AJ. 2008. Determining annual suspended sediment and sediment-associated trace element and nutrient fluxes. Science of The Total Environment 400:315-343.

Horowitz AJ, Elrick KA, Smith JJ. 2008. Monitoring urban impacts on suspended sediment, trace element, and nutrient fluxes within the City of Atlanta, Georgia, USA: program design, methodological considerations, and initial results. Hydrological Processes 22:1473-1496.

Horowitz AJ, Stephens VC, Elrick KA, Smith JJ. 2012. Concentrations and annual fluxes of sediment-associated chemical constituents from conterminous US coastal rivers using bed sediment data. Hydrological Processes 26:1090-1114.

Huang J-l, Du P-f, Ao C-t, Lei M-h, Zhao D-q, Ho M-h, Wang Z-s. 2007. Characterization of surface runoff from a subtropics urban catchment. Journal of Environmental Sciences 19:148-152.

Hudson PF. 2003. Event sequence and sediment exhaustion in the lower Panuco Basin, Mexico. CATENA 52:57-76.

Huey GM, Meyer ML. 2010. Turbidity as an Indicator of Water Quality in Diverse Watersheds of the Upper Pecos River Basin. Water 2:273-284.

Hupp CR, Noe GB, Schenk ER, Benthem AJ. 2013. Recent and historic sediment dynamics along Difficult Run, a suburban Virginia Piedmont stream. Geomorphology 180–181:156-169.

Jansson MB. 2002. Determining sediment source areas in a tropical river basin, Costa Rica. CATENA 47:63-84.

Jiongxin X. 2009. Plausible causes of temporal variation in suspended sediment concentration in the upper Changjiang River and major tributaries during the second half of the 20th century. Quaternary International 208:85-92.

Kleinhans MG, Wilbers AWE, ten Brinke WBM. 2007. Opposite hysteresis of sand and gravel transport upstream and downstream of a bifurcation during a flood in the River Rhine, the Netherlands. Netherlands Journal of Geosciences 86:273-285.

Landers MN. 2010. Review of methods to estimate fluvial suspended sediment characteristics from acoustic surrogated metrics. In: Second Joint Federal Interagency Conference, Las Vegas, NV, June 27-July 1, 2010. Atlanta, GA: United States Geological Survey.

Landers MN, Sturm T. 2013. Hysteresis in suspended sediment to turbidity relations due to changing particle size distributions. Water Resources Research:n/a-n/a.

Lane S, Thorne C. 2004. Fluvial Systems and Processes. An update of the Foresight Future Flooding:83-92.

Lane SN, Richards KS, Chandler JH. 1996. Discharge and sediment supply controls on erosion and deposition in a dynamic alluvial channel. Geomorphology 15:1-15.

Lawler DM. 2005. The importance of high-resolution monitoring in erosion and deposition dynamics studies: examples from estuarine and fluvial systems. Geomorphology 64:1-23.

Lawler DM, Petts GE, Foster IDL, Harper S. 2006. Turbidity dynamics during spring storm events in an urban headwater river system: The Upper Tame, West Midlands, UK. Science of The Total Environment 360:109-126.

Lazaro TR. 1990. Urban hydrology: a multidisciplinary perspective: CRC Press.

Lefrançois J, Grimaldi C, Gascuel-Odoux C, Gilliet N. 2007. Suspended sediment and discharge relationships to identify bank degradation as a main sediment source on small agricultural catchments. Hydrological Processes 21:2923-2933.

Lenhart CF, Brooks KN, Heneley D, Magner JA. 2010. Spatial and temporal variation in suspended sediment, organic matter, and turbidity in a Minnesota prairie river: implications for TMDLs. Environmental Monitoring and Assessment 165:435-447.

Lewis DL, Tate, K. W., Dahlgren, R. A., Newell, J. 2002. Turbidity and Toal Suspended Solid Concentration Dynamics in Streamflow from California Oak Woodland Watersheds. In: USDA Forest Service Gen. Tech. Rep. PSW-GTR-184. California: USDA Forest Service p107-118.

Lim HS. 2003. Variations in the water quality of a small urban tropical catchment: implications for load estimation and water quality monitoring. Hydrobiologia 494:57-63.

Liu X, Wang W, Ren H, Li W, Zhang C, Han D, Liang K, Yang R. 2009. Quality monitoring of flowing water using colorimetric method based on a semiconductor optical wavelength sensor. Measurement 42:51-56.

López-Tarazón JA, Batalla RJ, Vericat D, Francke T. 2009. Suspended sediment transport in a highly erodible catchment: The River Isábena (Southern Pyrenees). Geomorphology 109:210-221.

Marsh TJ, Hannaford J. 2008. UK Hydrometric Register, Hydrological Data UK series. Centre for Ecology and Hydrology. Hydrological Data UK series:1-214.

Massei N, Dupont JP, Mahler BJ, Laignel B, Fournier M, Valdes D, Ogier S. 2006. Investigating transport properties and turbidity dynamics of a karst aquifer using correlation, spectral, and wavelet analyses. Journal of Hydrology 329:244-257.

McMahon G, Bales JD, Coles JF, Giddings EM, Zappia H. 2003. USE OF STAGE DATA TO CHARACTERIZE HYDROLOGIC CONDITIONS IN AN URBANIZING ENVIRONMENT1. JAWRA Journal of the American Water Resources Association 39:1529-1546.

Merz R, Blöschl G. 2003. A process typology of regional floods. Water Resources Research 39:1340.

Minella JPG, Merten GH, Reichert JM, Clarke RT. 2008. Estimating suspended sediment concentrations from turbidity measurements and the calibration problem. Hydrological Processes 22:1819-1830.

Moravcova J, Pavlicek T, Koupilova M, Ondr P, Vachalova R, Vachal J. 2009. Behaviour of selected c-q hysteresis parameters by extreme rainfall-

runoff events in artificially drained localities. Journal of Landscape Studies 2:77-88.

Mueller EN, Pfister A. 2011. Increasing occurrence of high-intensity rainstorm events relevant for the generation of soil erosion in a temperate lowland region in Central Europe. Journal of Hydrology 411:266-278.

Naden PS, Cooper DM. 1999. Development of a sediment delivery model for application in large river basins. Hydrological Processes 13:1011-1034.

Nagy RC, Graeme Lockaby B, Kalin L, Anderson C. 2012. Effects of urbanization on stream hydrology and water quality: the Florida Gulf Coast. Hydrological Processes 26:2019-2030.

O'Toole M, Diamond D. 2008. Absorbance based light emitting diode optical sensors and sensing devices. Sensors 8:2453-2479.

Old GH, Leeks GJ, Packman JC, Smith BP, Lewis S, Hewitt EJ, Holmes M, Young A. 2003a. The impact of a convectional summer rainfall event on river flow and fine sediment transport in a highly urbanised catchment: Bradford, West Yorkshire. Science of The Total Environment 314:495-512.

Old GH, Leeks GJL, Packman JC, Smith BPG, Lewis S, Hewitt EJ. 2006. River flow and associated transport of sediments and solutes through a highly urbanised catchment, Bradford, West Yorkshire. Science of The Total Environment 360:98-108.

Old GH, Leeks GJL, Packman JC, Smith BPG, Lewis S, Hewitt EJ, Holmes M, Young A. 2003b. The impact of a convectional summer rainfall event on river flow and fine sediment transport in a highly urbanised catchment:

Bradford, West Yorkshire. The Science of The Total Environment 314-316:495-512.

Owens P, Batalla R, Collins A, Gomez B, Hicks D, Horowitz A, Kondolf G, Marden M, Page M, Peacock D. 2005. Fine-grained sediment in river systems: environmental significance and management issues. River Research and Applications 21:693-717.

Papoutsa C, Hadjimitsis DG. 2013. Remote Sensing for Water Quality Surveillance in Inland Waters: The Case Study of Asprokremmos Dam in Cyprus. Remote Sensing of Environment: Integrated Approaches.

Pavanelli D, Pagliarani A. 2002. SW—Soil and Water: Monitoring Water Flow, Turbidity and Suspended Sediment Load, from an Apennine Catchment Basin, Italy. Biosystems engineering 83:463-468.

Peters NE. 2009. Effects of urbanization on stream water quality in the city of Atlanta, Georgia, USA. Hydrological Processes 23:2860-2878.

Prudhomme C, Young A, Watts G, Haxton T, Crooks S, Williamson J, Davies H, Dadson S, Allen S. 2012. The drying up of Britain? A national estimate of changes in seasonal river flows from 11 Regional Climate Model simulations. Hydrological Processes 26:1115-1118.

Rasmussen PP, Gray JR, Douglas Glysson G, C. Z. 2009. Guidelines and procedures for computing time-series suspended-sediment concentrations and loads from in-stream turbidity-sensor and streamflow data: U. S. Geological Survey Techniques and Methods.

Reed TM, Todd McFarland J, Fryar AE, Fogle AW, Taraba JL. 2010. Sediment discharges during storm flow from proximal urban and rural karst springs, central Kentucky, USA. Journal of Hydrology 383:280-290.

Richards RP, Baker DB, Crumirine JP, Kramer JW, Ewing DE, Merryfield BJ. 2008. Thirty-year trends in suspended sediment in seven Lake Erie tributaries. Journal of Environmental Quality 37:1894-1908.

Rivett MO, Ellis PA, Mackay R. 2011. Urban groundwater baseflow influence upon inorganic river-water quality: The River Tame headwaters catchment in the City of Birmingham, UK. Journal of Hydrology 400:206-222.

Rose S. 2003. Comparative solute–discharge hysteresis analysis for an urbanized and a 'control basin' in the Georgia (USA) Piedmont. Journal of Hydrology 284:45-56.

Rovira A, Batalla RJ. 2006. Temporal distribution of suspended sediment transport in a Mediterranean basin: The Lower Tordera (NE SPAIN). Geomorphology 79:58-71.

Salt A. 2009. United Utilities UIDs case study detailing the work at Princess Parkway UIDs, Rossendale UID and Wyre Estuary UIDs, Wastewater Treatment & Sewerage. In. p 79-82.

Schwarzenbach PR, Egli T, Hofstetter TB, Gunten Uv, Wehrli B. 2010. Global Water Pollution and Human Health. Environmental Resources:109-136.

Seeger M, Errea MP, Beguerıa S, Arnáez J, Martı C, Garcıa-Ruiz J. 2004. Catchment soil moisture and rainfall characteristics as determinant factors for discharge/suspended sediment hysteretic loops in a small

headwater catchment in the Spanish Pyrenees. Journal of Hydrology 288:299-311.

Slattery MC, Gares PA, Phillips JD. 2006. Multiple modes of storm runoff generation in a North Carolina coastal plain watershed. Hydrological Processes 20:2953-2969.

Smith BPG, Naden PS, Leeks GJL, Wass PD. 2003. Characterising the fine sediment budget of a reach of the River Swale, Yorkshire, U.K. during the 1994 to 1995 winter season. Hydrobiologia 494:135-143.

Smith HG, Dragovich D. 2009. Interpreting sediment delivery processes using suspended sediment-discharge hysteresis patterns from nested upland catchments, south-eastern Australia. Hydrological Processes 23:2415-2426.

Song J, Xu Z, Hui Y, Li H, Li Q. 2010. Instream flow requirements for sediment transport in the lower Weihe River. Hydrological Processes 24:3547-3557.

Stanfield LW, Jackson DA. 2011. Understanding the Factors That Influence Headwater Stream Flows in Response to Storm Events1. JAWRA Journal of the American Water Resources Association 47:315-336.

Stubblefield AP, Reuter JE, Dahlgren RA, Goldman CR. 2007. Use of turbidimetry to characterise suspended solids snd phosphorous fluxes in the Lake Tahoe basin, Califonia, USA. Hydrological Processes 21:281-291.

Sun H, Cornish P, Daniell TM. 2001. Turbidity-based erosion estimation in a catchment in South Australia. Journal of Hydrology 253:227-238.

Susfalk RB, Fitzgerald B, Knust AM. 2008. Characterization of Turbidity and Total Suspended Solids in the Upper Carson River, Nevada. In. Nevada: Prepared by: Desert Research Institute, Nevada System of Higher Education; for: Nevada Division of Environmental Protection.

Talei A, Chua LHC, Quek C. 2010. A novel application of a neuro-fuzzy computational technique in event-based rainfall–runoff modeling. Expert Systems with Applications 37:7456-7468.

Tame. 2010. Tame Urban Pollution Management - Water Projects Online In: www.waterprojectsonline.com/case.../Severn_Trent_Tame_2010.pdf

Taylor K, Owens P. 2009. Sediments in urban river basins: a review of sediment–contaminant dynamics in an environmental system conditioned by human activities. Journal of Soils and Sediments 9:281-303.

Topping D, Wright S, Melis T, Rubin D. 2007. High-resolution measurements of suspended-sediment concentration and grain size in the Colorado River in Grand Canyon using a multi-frequency acoustic system. In: Proceedings of the 10th International Symposium on River Sedimentation.

Viglione A, Chirico GB, Woods R, Blöschl G. 2010. Generalised synthesis of space–time variability in flood response: An analytical framework. Journal of Hydrology 394:198-212.

Vivoni E, Entekhabi D, Bras R, Ivanov V. 2007. Controls on runoff generation and scale-dependence in a distributed hydrologic model. Hydrology & Earth System Sciences 11.

Walling D, Webb B, Russell M. 1997. Sediment-associated nutrient transport in UK rivers. IAHS Publications-Series of Proceedings and Reports-Intern Assoc Hydrological Sciences 243:69-84.

Walling DE, Owens PN, Carter J, Leeks GJL, Lewis S, Meharg AA, Wright J. 2003. Storage of sediment-associated nutrients and contaminants in river channel and floodplain systems. Applied Geochemistry 18:195-220.

Wass P, Marks S, Finch J, Leeks G, Ingram J. 1997. Monitoring and preliminary interpretation of in-river turbidity and remote sensed imagery for suspended sediment transport studies in the Humber catchment. Science of The Total Environment 194:263-283.

Webster P, West JR, Gurnell AM, Petts GE, Sadler JP, Forster CF. 2001. Development, Flood Risk and the Urban Environment: Experiences from the River Tame. Water and Environment Journal 15:167-173.

Wenger SJ, Roy AH, Jackson CR, Bernhardt ES, Carter TL, Filoso S, Gibson CA, Hession WC, Kaushal SS, Martí E. 2009. Twenty-six key research questions in urban stream ecology: an assessment of the state of the science. Journal of the North American Benthological Society 28:1080-1098.

Wood PA. 1977. Controls of variation in suspended sediment concentration in the River Rother, West Sussex, England. Sedimentology 24:437-445.

Xu J. 2008. The behavior of specific sediment yield in different grain size fractions in the tributaries of the middle Yellow River as influenced by eolian and fluvial processes. Earth Surface Processes and Landforms 33:1157-1173.

Xu K, Milliman JD. 2009. Seasonal variations of sediment discharge from the Yangtze River before and after impoundment of the Three Gorges Dam. Geomorphology 104:276-283.

YSI Inc. 2015. Ammonia, Ammonium. In. 1700/1725 Brannum Lane, Yellow Springs, OH 45387 USA: YSI Incorporated.

Yue J. 2012. Urban Rivers: A Landscape Ecological Perspective. Hydrol Current Res 3:2.

Yunus A, Nakagoshi N. 2004. Effects of seasonality on streamflow and water quality of the Pinang River in Penang Island, Malaysia. Chinese Geographical Science 14:153-161.

Zabaleta A, Martínez M, Uriarte JA, Antigüedad I. 2007. Factors controlling suspended sediment yield during runoff events in small headwater catchments of the Basque Country. CATENA 71:179-190.

Ziegler AC. 2002. Issues related to use of turbidity measurements as a surrogate for suspended sediment. In: Turbidity and Other Sediment Surrogates Workshop, Reno, NV.